UNIVERSITÉ DE LILLE
UNITÉ DE MÉCANIQUE DE LILLE
ÉCOLE DOCTORALE SCIENCES POUR L'INGÉNIEUR (SPI)

Rapport de thèse pour l'obtention du grade de
Docteur de l'Université de Lille
Spécialité : Mécanique, énergétique, génie des procédés, génie civil
Présentée par : Muhammad **Ayub ASGHAR**

Etude expérimentale des propriétés mécaniques des composites Fibres de Jute/Polypropylène fabriqués à partir des fils co-torsadés et par la technique de thermoformage

An experimental study of the mechanical properties of jute / polypropylene composites manufactured by the commingled yarn and thermoforming

Thèse soutenue publiquement le 9 décembre 2021
Devant le jury composé de :

M. Toufik KANIT	Professeur, Université de Lille	Président
Mme Nadia BAHLOULI	Professeure, Université de Strasbourg	Rapporteure
M. Bruno CASTANIE	Professeur, INSA Toulouse	Rapporteur
M. Abdelghani SAOUAB	Professeur, Université du Havre	Examinateur
M. Yasir NAWAB	Associate Professor, National Textile University, Pakistan	Co-Directeur de thèse
M. Abdellatif IMAD	Professeur, Université de Lille	Directeur de thèse

Acknowledgment

First of all, I would like to thank Almighty, who made me able to accomplish this thesis. Then I would like to express my deep and sincere gratitude to my thesis director Prof. Abdellatif IMAD, co-director Dr. Yasir NAWAB. With their enthusiasm, inspiration, and great efforts to explain things clearly and simply, they helped to make this complicated subject very easy for me. Their guidance and encouragement have helped me in all the time of research and writing of this thesis.

My sincere thanks are due to the referees, Mme Nadia BAHLOULI, M. Bruno CASTANIE, for their detailed reviews, constructive criticism, and excellent advice during the preparation of this thesis. I would also like to thank the president of jury M. Toufik KANIT and jury member M. Abdelghani SAOUAB to judge my thesis and for very interesting discussions.

Besides my advisors, I would like to thank all the colleagues. Especially, I also thank my fellow M. Muzzamal HUSSAIN for his great support.

Last but not the least, I would like to thank my beloved parents and my siblings, who enabled and motivated me to perform and successfully complete this research work. I also want to pay special thanks to my wife, daughter and son who kept me motivated throughout this journey.

I am thankful to Unité de Mécanique de Lille, Université de Lille for giving me Opportunity to do my PhD research. I also express my gratitude to National Textile University, Faisalabad and thankful to the Pakistan - France collaboration in the domain of natural fiber reinforced composites.

Dedication

To my parents and teachers

Table of Contents

List of Figures

List of Tables

List of Abbreviations

FRC: Fiber reinforced composites

NFRC: Natural fiber-reinforced composites

GFRC: Glass fiber-reinforced composites

3D: Three dimensional

2D: Two dimensional

TT: Through the thickness

PEG: Polyethylene glycol

PLA: Polylactic acid

MJ/kg: Mega Joules per kilogram

Ne: linear density of yarn as hanks per pound (English system, 1 hank: 840 yards)

Tex: linear density of yarn as grams per kilometer (g/km)

CNG: Compressed natural gas

UD: Unidirectional

Uster: A textile instrument manufacturing company, head office Uster, Switzerland

FVF: Fiber volume fraction

PBT: Polybutylene terephthalate

PP: Polypropylene

PEEK: Polyether ether ketone

TPI: Twist per inch

LDPE: Low density polyethylene

HDPE: High density polyethylene

HIPS: High impact polystyrene

MD: Machine direction

CD: Cross direction

SEM: Scanning electron microscope

SBS: Short beam strength

PEI: Polyetherimide

Context of Study

Composites materials are replacing conventional materials in every walk of life due to its easy manufacturing, higher mechanical properties and machineability. Composite materials comprised of reinforcement and matrix. Recently a lot of emphasis is laid on using the materials with least environmental effect, therefore, there is a lot of focus of biocomposites e.g., composites made using one or both constituents from natural origin.

Currently, biocomposites made from natural fibers and thermoplastic matrix have gained considerable attention. Among natural fibers the bast fibers are best candidates to be used in composites materials due to better mechanical performance. These fibers include hemp, flax, jute etc. Jute is also a bast fiber and found in abundance, while polypropylene is low-cost thermoplastic material which is found easily. Its melting point is 160 ^{o}C, which is well below 200 ^{o}C, the degradation temperature of cellulose.

Despite the advantages of recyclability, biodegradability, low cost and availability, there are issues associated with natural fiber composites. The market share of natural fiber composites is limited due to limited number and quantities of natural fibers available for composites, diversity in fiber's structure, poor mechanical properties of fibers as well as composites, susceptibility to microbial attacks, cellulose degradation temperature around 200° C, which hinders development of natural fiber reinforced thermoplastic composites using thermoforming and resin transfer molding at high temperatures.

The fabrication of thermoplastic matrix is a difficult job due to high viscosity factor. The major problem in the fabrication of natural fibers is their hairiness which hinders the closer packing of fibers constituents to have higher fiber volume fraction (FVF). The close packing of natural fibers is worse than the filament yarns. In order to overcome this this issue certain chemical treatments are normally used. Yet another problem associated with the natural fibers is their poor wettability with the matrix, especially with thermoplastic matrices.

The area of applications of natural fiber thermoplastic composites can increase many folds subject to addressing above issues of low fiber-matrix interface, poor wettability, hairiness of natural fibers and low mechanical properties. In order to cover this hairiness, in order to increase the weavability of natural fibers on weaving machines normally the technique of yarn sizing (yarn coating) have been reported in the literature, however in order to increase the weavability, there is no literature found on the reduction of natural fiber hairiness through the singeing process which involves the burning of protruding fibers.

As per the best knowledge of the author 3D commingled weaving technique has not been used for natural fiber composites to date. The major issue is the poor melting-out of thermoplastic material in the thick inner layers, which do not directly contact the hot-plates/heating system. This is a major problem to be addressed, especially for thick 3D structures. Few works existed on the development prepregs based on natural fibers and associated composites. The use of prepreg, especially the dry commingled prepregs, may result in the development of more homogenous and high-quality natural fiber composites with rapid fabrication. As per the best knowledge of the author, there is no detailed study available regarding the manufacturing of thermoplastic composites through the application of gradual loading technique during thermoforming process.

Objectives of Thesis:

Based on the research gap identified in the literature the following objectives have been set in this study:

I. To check the effect of jute yarn singeing on the physical and mechanical properties of associated composites

II. To develop and optimize commingling technique for fabrication of 1D and 2D natural fiber reinforced thermoplastic composites and its comparison with composites made with conventional fabrication techniques.

III. To develop and evaluate natural fiber reinforced 3D woven thermoplastic composites by yarn commingling technique.

IV. To study the effect of instant and gradual loading during fabrication of thermoplastic composite on physical and mechanical properties.

Structure of thesis:

This thesis comprised of 6 chapters.

Chapter 1:

In this chapter the literature review is presented, and this further divided in several sections. First of all a brief introduction about composite, Natural Fibers Composite (NFC) and its applications are presented. Subsequently, the fibers, yarns and reinforcements used in the natural fiber composites are discussed in detail. The effect matrix used for the NFC are described and techniques used for the thermoplastic composites making is also discussed in detail, in addition, the pros and cons of various molding techniques are also presented. The

effect of fabrication parameters such as, time, temperature and pressure on composite making using compression hot has also been discussed. Finally, the research gaps and objectives are discussed.

Chapter 2:

This chapter discuss the details of materials, reinforcement manufacturing techniques, composite fabrication methods and testing methods used in this thesis. The jute yarn used to make all type of reinforcement and singed at flame to remove protruding fibers before reinforcement weaving. After singeing the reinforcement was made either with the jute commingled or non-commingled yarn. The commingled yarn was prepared by twisting jute/PP yarn at simplex frame. The 1D (unidirectional), 2D and 3D reinforcement was prepared. The composites were made at compression hot press using instant and gradual loading techniques to check the effect of both the techniques. The tensile, flexural, short beam shear and Charpy impact tests were conducted as per standards to compare the mechanical properties of difference composites, later on the tested samples were checked microscopely.

Chapter 3:

This chapter entails the mechanical properties of four layered UD commingled and non-commingled composites made using gradual loading. The tensile, flexural, short beam shear and Charpy impact test were conducted to compare the properties of both type of composites. The results show that the tensile strength of commingled composites was higher as compared to non-commingled composites; similar results were observed for flexural, SBS and Charpy impact. The overall failure strain is also higher for commingled composites. The microscopic images of tested samples suggest that the fiber in the commingled composites are following more wavy path which leads to higher strain values. The commingled technique, overall improves the mechanical properties with better fiber-matrix interface.

Chapter 4:

In this chapter the mechanical properties of non-commingled jute/polypropylene composites made through conventional thermoforming technique have been compared to those of commingled composite. The commingling technique shortens and simplifies the composite manufacturing process.

The cross-section of samples shows that the commingling technique improves the overall distribution and impregnation of reinforcement. Both types of composites were tested against the tensile, flexural, and Charpy impact properties using standard testing methods. The commingled composites showed better tensile, flexural, SBS and Charpy impact properties.

Chapter 5:

This chapter concerns about the investigation of the effect of instant and gradual loading on the physical and mechanical properties of the commingled thermoplastic composites. The microstructure study was carried out up to fibril level in order to observe the physical effect of instant and gradual loading on the cellulosic structure of jute. The tensile, flexural, SBS and Charpy impact tests were conducted to check the mechanical properties of both composites. The microstructure of fibers of composites made using instant loading showed significant damage as compared to samples which were made with gradual loading. The fibers of composite made using gradual loading had a very healthy fibers with even polygonal boundary. The tensile, flexural, SBS and Charpy impact results showed superior mechanical performance of gradual loaded samples.

Chapter 6:

In this chapter the mechanical properties of 3D woven commingled thermoplastic composites has been discussed. The 3D woven commingled composites were developed for the first time and composites samples were made with compression hot press using gradual loading technique. The samples were tested at 0° and 90°. The tensile, flexural, short beam shear and Charpy impact tests were conducted to analyze the mechanical properties of 3D woven commingled composites. The results showed higher mechanical properties at 90° direction due to higher number of reinforcing yarns, whereas in 0° the fewer number of reinforcing yarn result into poor mechanical performance. The crossection of samples shows that reinforcing yarns are placed in layers with through the thickness binder yarns with even fiber-matrix distribution.

Chapter 1. Bibliography

In this chapter the literature review is presented, and this further divided in several sections. First, a brief introduction about composite, Natural Fibers Composite (NFC) and its applications are presented. Subsequently, the fibers, yarns and reinforcements used in the natural fiber composites are discussed in detail. The matrices used for the NFC are described and techniques used for the thermoplastic composites making is also discussed in detail, in addition, the pros and cons of various molding techniques are also presented. The effect of fabrication parameters such as, time, temperature and pressure on composite fabrication using compression molding technique has also been discussed. Finally, the research gaps and objectives are discussed.

1.1 Composites materials generalities

Composites are defined as a combination of two or more materials having improved properties over the individual constituent materials [1,2]. Tailoring of the unprecedented physical and mechanical characteristics of composites makes them ideal multifunctional materials to meet specific requirements. A composite material is mainly composed of two components, the matrix and the reinforcement. The reinforcement acts as the dispersed phase and helps in load-carrying while the matrix is usually in the continuous phase and assists in keeping the preferred arrangements of the reinforcement component, transferring the load to the reinforcement and protecting the reinforcement from environmental damages. Composite materials are being used for centuries in various forms, i.e., bricks, concrete, wood, bone, paper, etc.[3]. Composite materials are widely used in automobiles, aerospace, sports, marine, medical, construction and packaging industries. There are various ways to classify the composite materials, but mainly categorized based on the type of reinforcement (Figure 1-1) and matrix.
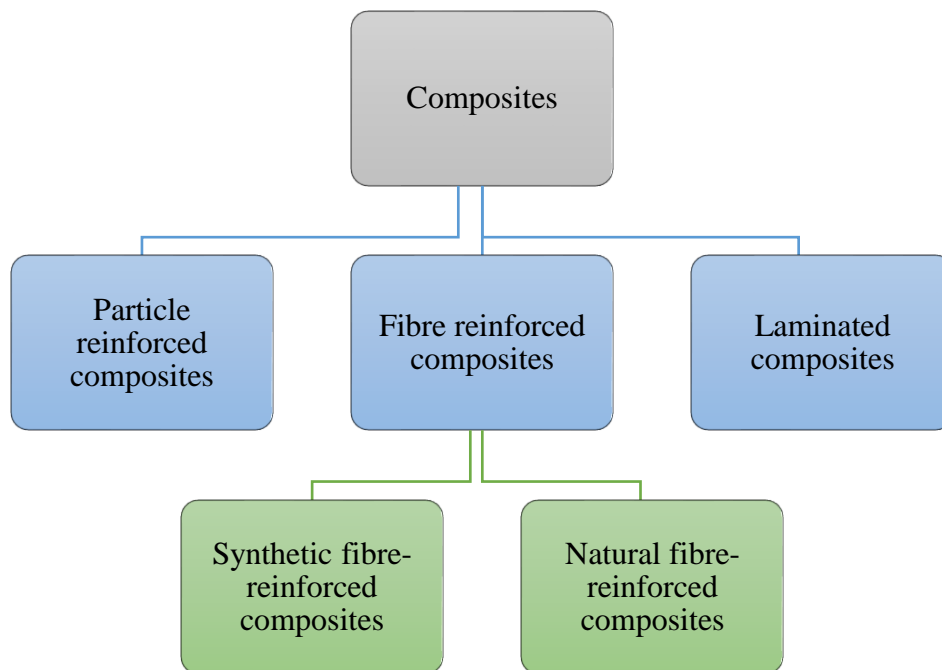
Figure 1-1. Classification of composites according to the reinforcement types

Particle-reinforced composites are developed by incorporating one or more metallic or non-metallic particles in a matrix. Particles are added to improve the micro-scale strength and hardness of fabricated composite. Laminated composites are fabricated by the bonding of layers using heat, pressure, or adhesive. The layer sequence and orientation assist in

achieving better properties of laminated composites compared to the monolithic materials. Synthetic or natural fibers in the form of fiber, yarn, or fabric are mainly embedded in a matrix to fabricate the fiber reinforced composites (FRC).

The main advantages of the FRC are [2] higher specific modulus, high specific strength, excellent fatigue properties and lower density than metals. The fibers act as reinforcement, whereas the resin or matrix acts as an adhesive. The matrix can be of the following types:

I.   Thermoplastic matrix (polypropylene, polyphenylene, polyamide, etc.)

II.   Thermoset matrix (polyesters, melamines, phenolics, epoxies, polyurethanes, etc.)

III.   Elastomeric matrix (rubber)

IV.   Mineral matrix: silicon carbide, carbon.

V.   Metal matrix: aluminum alloys, titanium alloys [4].

Thermoplastic resins do not react chemically; their molecules are, instead attached to each other by van-der-Waals forces (Figure 1-2(a)). These are the reversible form of a matrix which melts back upon heating. Thermoset resins form cross-linking into a rigid three-dimensional structure after curing. These are the irreversible resins, i.e., when the matrix is once cured, it cannot be melted down again (Figure 1-2(b)).

(a)   (b)
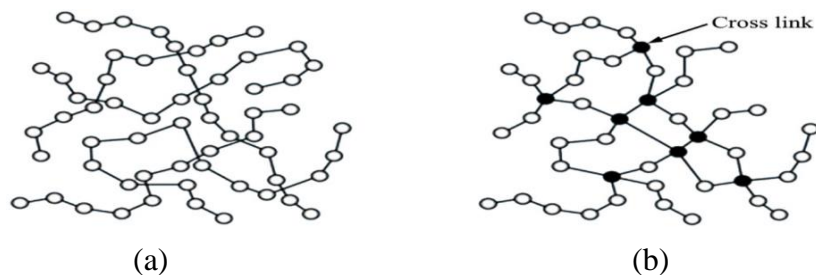
Figure 1-2. Polymer matrices (a) Thermoplastic and (b) Thermoset [4]

Fibers are mainly used as reinforcement for FRC materials either in the form of fibers, yarns or fabrics. The fibers are superior in mechanical properties as they have high length to width ratio as compared to particles and other reinforcements. Fibers may be in filament or staple form depending on applications and manufacturing process [5]. Some properties of reinforcements are mentioned in Table 1-1.

Table 1-1. Properties of some of the reinforcements used for the fabrication of composites

[2]

Reinforcements	Fiber Diameter (mm)	Density (g/cm^3)	Modulus of Elasticity (GPa)	Tensile Strength (MPa)	Elongation (%)
"R" glass, high performance	10	2.5	86	3200	4
"E" glass, Common	16	2.6	74	2500	3.5
Kevlar 49	12	1.45	130	2900	2.3
Graphite, high strength	7	1.75	230	3200	1.3
Graphite, high modulus	6.5	1.8	390	2500	0.6
Boron	100	2.6	400	3400	0.8
Aluminum	20	3.7	380	1400	0.4
Aluminum Silicate	10	2.6	200	3000	1.5
Silicon carbide	14	2.55	200	2800	1.3
Polyethylene	-	0.96	100	3000	-

1.2   Natural Fiber Reinforced Composites (NFRC)

Natural fiber-reinforced composite (NFRC) are more sustainable for the environment because the amount of CO_2 released by the natural fibers, at the end of their life cycle, is the same as consumed by these fibers during their growth [6].

On the other hand, Glass fibers have an adverse impact on the environment related to energy consumption as compared to natural fibers. Moreover, the major disadvantage of glass fiber is its end life disposal, where approximately up to 50% of volume remains unburned residues [7].

The natural fibers have least environmental impact in term of energy requirement during different production cycles. Table 1-2 shows a comparison between Flax fiber mat and Glass fiber mat. Flax fiber are superior to glass fiber with respect to environmental impact [8]. The flax fiber required around 82.5% less energy.

Table 1-2. A comparison of the non-renewable energy requirements for the production of glass and flax fibers [8]

Glass fiber mat	MJ/kg*	Flax fiber mat	MJ/kg
Raw materials	1.7	Seed production	0.05
Mixture	1.0	Fertilizers	1.0
Transport	1.6	Transport	0.9
Melting	21.5	Cultivation	2.0
Spinning	5.9	Fiber separation	2.7
Mat production	23.0	Mat production	2.9
Total	54.7	Total	9.55

*MJ/kg: Mega Joules per kilogram

The consumption of natural fibers composites is continuously increasing as compared to man-made fiber composites. Figure 1-3 shows tentative European natural fiber composites market revenue, by application, 2013 - 2024 in million USD [9]. NFRC share their major part in civil and automobile applications.
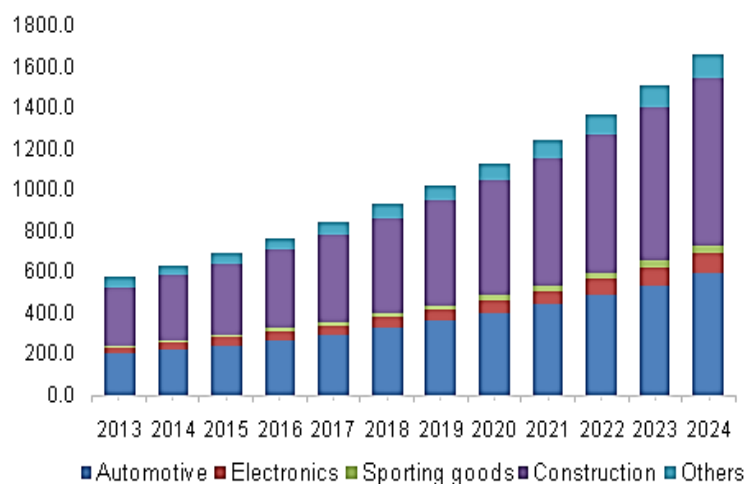
Figure 1-3. European natural fiber composites market revenue, by application, 2013 - 2024 in USD Million [9]

There are different types of Natural fiber composites (NFC), but Eco composites made with natural fibers are the most important. Although biodegradable polymeric materials have been used, but there are two main problems linked to their use, one is cost and the other is their availability in large quantities. Now a days the most suitable way for making the environment friendly composites is the use of natural fiber as reinforcements [10–15]. This can lead to lesser ecological and environmental issues [16,17]. There are certain problems associated with the Natural fiber composites e.g., poor fiber-matrix interface, the most important one. Hasham et al., [18] worked on problem of poor interface between hydrophilic reinforcement and hydrophobic matrix. This study focused on the mercerization treatments to improve the mechanical properties. Zhu et al., [19] studied the different treatments of flax fibers, such as mercerization, silane coupling agent treatments, acylation, peroxide treatment and Nano coatings for improving the fiber-matrix interface. Zafeiropoulos et al., [20] studied the crystallinity and its effects on the interface in flax fiber reinforced composites. The testing results showed that interfacial adhesion improved with the treatments of these flax fiber reinforced composites. Chabba et al., [21] investigated the interface development results of the composite made with the flax reinforcement and modified soy protein concentrate (MSPC-G). Anderson et al., [22] also worked on the unidirectional flax fiber as reinforcement in composites. They developed a statistical model to predict the upper limit of tensile strength of these composites. It was investigated that the experimental strength of unidirectional flax fiber composites, made from roving or manually aligned fibers reaches the theoretical limit only at relatively lower fiber volume fraction. Notta et al., [23] reported the mechanical modelling of short fiber flax composite having complex distribution of fiber orientation. Oksman et al., [24] studied the mechanical behaviour of poly lactic acid (PLA) and flax fiber composites. They compared mechanical properties of PLA/Flax composite to the PP/Flax composites. The results showed that the tensile strength of PLA/Flax composite is better than the PP/Flax composite by 50%.
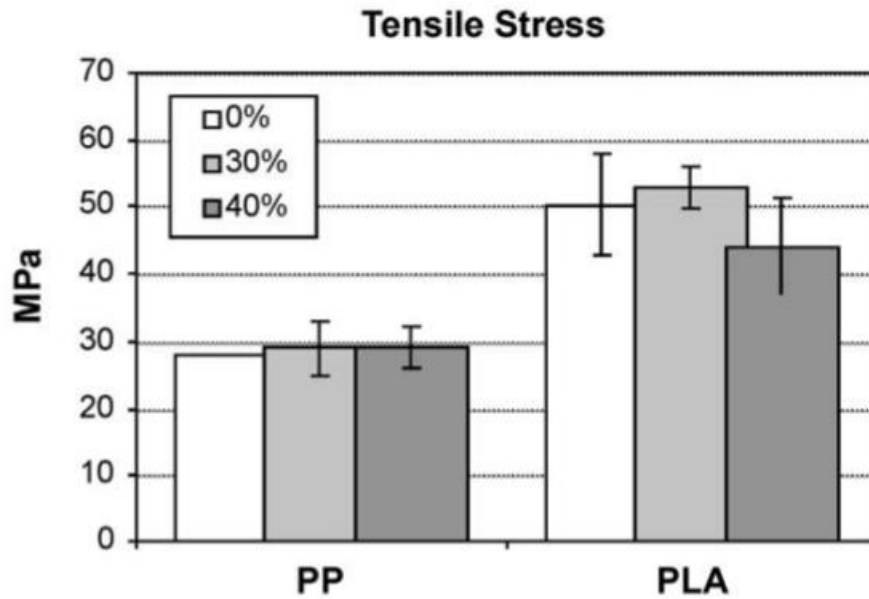
Tensile Stress

Figure 1-4. Tensile stress of PLA/flax composite compared to PP/flax[24]

Kumar et al., [25] made a composite of woven flax as reinforcement and poly lactic acid (PLA) as a matrix. They used Montmorillonite clay (MMT) to enhance the composite mechanical properties. The increase in modulus has been reposted by the use of MMT. Assarar et al., [26] studied the mechanical and ageing properties of flax and glass fiber reinforced composites. Water absorption of flax fiber composite was found to be 12 times higher than the glass composites. Ageing also affects the mechanical properties of glass reinforced composites with decrease in the modulus and failure strain of the composite. Paynel et al., [27] developed by bio-composites in which they used flax fibers as reinforcement and mucilage-polysaccharides as a matrix. Mucilage-polysaccharides was extracted from the flax seeds. The values of tensile strength, modulus and strain were found to be 300-400 MPa, 7-10 GPa and 4-5% respectively. Several research works are available on jute reinforced thermoset composites [28–34], however, some work is also reported on the jute reinforced thermoplastic composites. Placket et al., [35] worked on jute fiber reinforced biodegradable Polylactic acid composites. Using SEM images they studied the composite fracture surface and tensile properties. The behaviour of the composites was found to be brittle for tensile specimens and fiber pullout was also observed. Some void formation was also observed at the interface of fiber-matrix as shown in Figure 1-5.
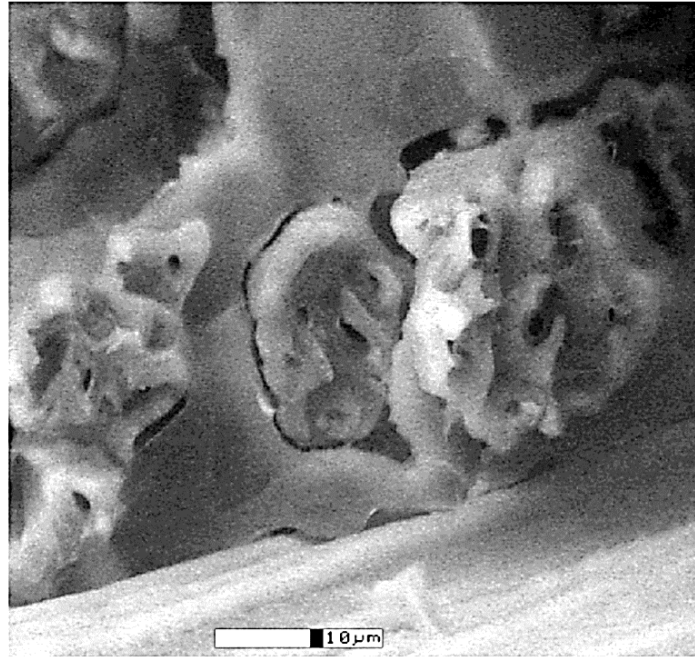
Figure 1-5. ESEM photomicrograph of a PLA/jute composite tensile fracture surface showing void spaces between fiber bundles and the PLA matrix [35]

Rana et al., [36] developed jute/polypropylene composite by using high speed thermo-kinetic mixer. Different researcher also worked on the ramie reinforced composites [37–39]. Hong et al., [40] used ramie fiber and Polylactic acid for making biodegradable composites. They used coupling agent on ramie fiber for making a better interface with the PLA. Lodha et al., [41] made composites using unidirectional ramie fiber reinforcement with soy protein isolate base resin as matrix. They investigated the mechanical, thermal and moisture regain properties of biodegradable composites. Pavia junior et al., [42] made a cotton-ramie hybrid plain-woven reinforced composite using polyester matrix. The effect of orientation of fiber and different fiber volume fractions on tensile properties of composites was observed. The results revealed higher fiber orientation in the direction of tensile force shows highest tensile strength as shown in Figure 1-6.
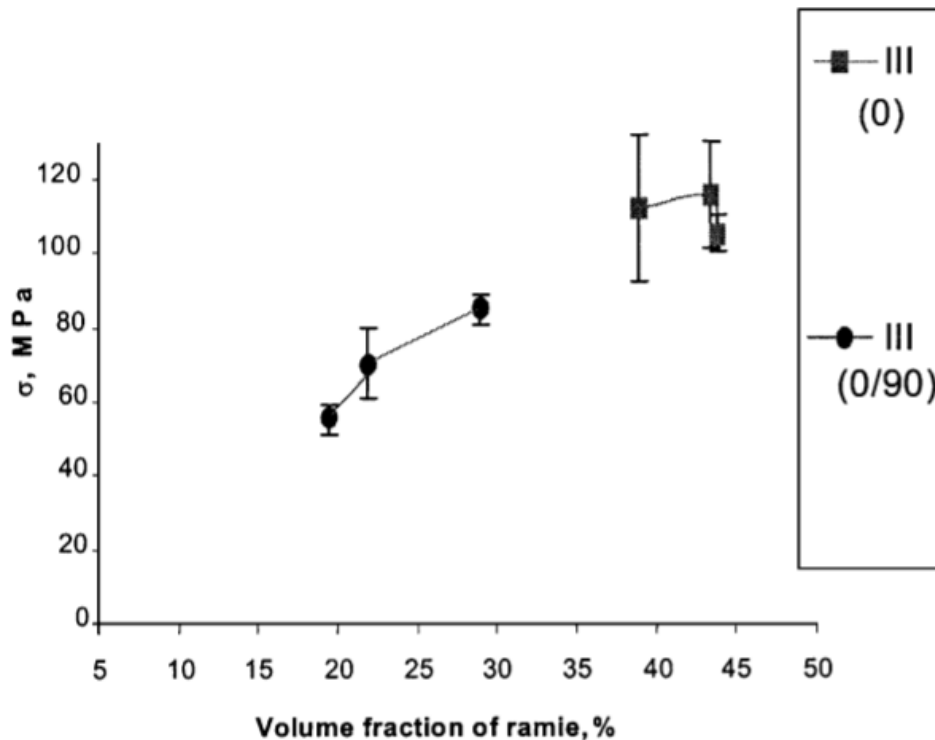
Figure 1-6. Effect of the volume fraction of ramie fibers parallel

to the tensile axis [42].

Gehring et al., [43] developed short hemp fiber-polypropylene composites and studied the mechanical behavior using different fiber weight fractions. The non-linear behavior was observed in all experiments. Moethew et al., [44] developed hybrid bamboo/glass fiber reinforced polypropylene composites using compression molding technique. They revealed that the mechanical properties of the composites can be enhanced by the use of additional glass fibers. Conzatti et al., [45] developed a non-woven web composite with dispersed wool fibers and polypropylene matrix at a 60 wt% of wool fibers. The maleinized polypropylene was used for creating a better interface with the fibers. Composite morphology, thermal properties and mechanical properties were studied. The effect of fiber length, orientation and distribution was observed on composite fiber-matrix interface. Franco et al., [46] made short henequen fibers-polyethylene composites and studied the fiber-matrix interface and mechanical properties. The fibers were treated with silane coupling agents and alkaline material. Improved mechanical properties, especially the flexural properties were observed in the results due to these surface treatments.

1.3   Applications of Natural Fiber Composites

Natural fibers are replacing man-made synthetic fibers in numerous composite applications (Figure 1-7). These composites can effectively be used as a substitute of wood and in other technical applications e.g., automotive parts.

Airplane seats and fuel tanks were developed with natural fibers in 1996 due to lower density values of these composites. The biodegradable property of natural fibers has found its applications in the medical field. 3D scaffolds for tissue culture of human's body organs have successfully been made by biodegradable regenerated natural fibers using electro-spinning technology. For this purpose polyethylene glycol (PEG) and polylactic acid (PLA) fibers are mostly used [47].

The textile waste has been used for years in the automotive industry for the reinforcement of thermoplastics in automobiles. In the German automotive industries a number of automobile components made of flax and hemp fibers composites have successfully replaced glass fibers composites (Figure 1-8) [48]. Sisal is a preferred fiber in interior applications as it causes lower level of smell as compared to flax fiber. Flax is likely to cause smell at higher molding temperatures. For fabricating many non-load-bearing components natural fiber composites are being used in the automotive sectors. Car manufactures are now attempting to develop biodegradable, sustainable and recyclable components of their vehicles [48]. Hurricane-resistant structures and houses are also being developed in United States by natural fiber reinforced composites [49].

Figure 1-7. Some applications of natural fiber composites [50]

Natural fibers have comparative advantages over glass fiber due to low energy consumption, weight, price and recyclability. However, the glass fiber strength is relatively higher as compared to natural fibers (Figure 1-8).
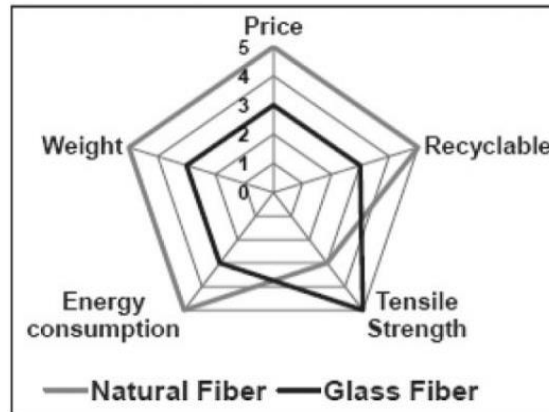
Figure 1-8. Comparison between natural fiber and glass fiber [51]

The mechanical properties of natural fiber reinforced composites are on the lower side as compared to glass fiber reinforced composites. However, by making the hybrid composites (i.e., the combination of natural fibers and synthetic fibers), the mechanical properties can be enhanced [52]. Natural fiber composites have also found their applications in anti-ballistics. Flax, hemp, coir and jute reinforced polypropylene composites have been studied for ballistic applications. Wambua et al., [53] studied Flax, hemp, and jute fabric reinforced polypropylene composites against ballistic tests by using fragment simulating projectiles. Fernanda et al., [54] tested Coir fiber reinforced epoxy composites against the ballistic impact. They found that the use of 30% volume of coir fiber in the ballistic composite exhibits same ballistic properties as compared to 100% Kevlar composite with marginal economic benefit due to lower cost of the natural fiber.

The use of natural fiber composites is roughly 5 to 10 kg per car (80,000 to 160,000 tons in Western Europe) [55]. Because of the shortcomings of natural fiber composites in mechanical properties as compared to glass, carbon, kevlar etc., their use is mainly restricted to car interiors and non-load-bearing components like rear shelves and door casings [56].

1.4 Natural fibers used in composites

The most common classification of natural fibers is based on the type of their botanical origin. There are three main classifications of natural fibers on the bases of their botanical

source i.e., animal, vegetable and mineral [57,58]. A classification on these bases is shown in Figure 1-9.
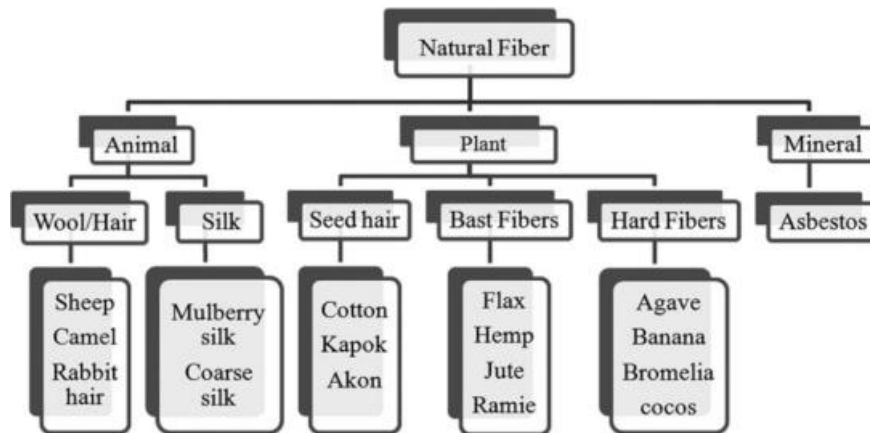
Figure 1-9: Classification of natural fibers [59]

There are, in general, six basic types of natural fibers with respect to origin which are hair, seed, leaf, bast, core, grass and other fibers. Flax, hemp, jute, kenaf and ramie fibers belong to bast fiber category while banana, pineapple, agave and sisal are leaf fiber class. Coir, cotton, and kapok fiber fall in seed fiber class, while rice, wheat and corn fall in grass type fibers. Wood and some roots are also the class of natural fibers.

Natural vegetable based fibers mainly contain varying combinations of cellulose, hemicellulose, lignin, and pectin. Chemical compositions of some cellulosic fibers are given in Table 1-3.

Table 1-3: Chemical compositions of natural cellulosic fibers [60]

Fiber	Cellulose (wt %)	Hemicellulose (wt %)	Lignin (wt %)
Cotton	82.7 - 90	5 - 7	2
Bamboo	26 - 43	30	21-31
Flax	71	18.6 - 20.6	2.2
Kenaf	72	20.3	9
Jute	61-71	14 - 20	12.5 - 13
Hemp	68	15	10
Ramie	68.6 - 91	5 -16	0.6 - 0.7

In spite of number of advantages of natural fibers they have certain demerits, which limit their applications. They have low mechanical properties as compared to synthetic fibers and high moisture regain. They are also affected by ageing so cannot be used for extreme

applications. Some of the merits and demerits of natural and synthetic fibers are given in Table 1-4.

Table 1-4. Merits and demerits of natural and synthetic fibers [61]

Fibers	Merits	Demerits
Synthetic fibers	1. Moisture resistance 2. Good mechanical properties	1. Difficult in recycling 2. Toxic 3. Not renewable 4. Relative high price
Natural fibers	1. Environment friendly 2. Low density 3. Biodegradability 4. Ease of availability/low cost 5. Annually renewable 6. Less respiratory irritation	1. Inhomogeneous quality 2. Swelling due to moisture regain 3. Incompatibility with resin 4. Inhomogeneous quality

Some properties of natural fibers are given in Table 1-5, which is clearly showing that bast fibers have better mechanical properties as compared to other fibers and also have high stiffness due to high lignin content. The bast fibers are long fibers and can be used easily as reinforcement for composite fabrication.

Table 1-5: Properties of natural fibers [62]

Plant fiber	Tensile strength (MPa)	Young's modulus (GPa)	Specific modulus (GPa)	Failure strain (%)	Density (kg/m^3)	Moisture content (%)
Cotton	300-700	6-10	4-6.5	6-8	1550	8.5
Kapok	93.3	4	12.9	1.2	311-384	10.9
Bamboo	575	27	18	3.3-4	1500	11
Flax	500-900	50-70	34-48	1.3-3.3	1400-1500	12
Hemp	310-750	30-60	20-41	2-4	1400-1500	12
Jute	200-450	20-55	14-39	2-3	1300-1500	12
Ramie	915	23	15	3.7	1550	8.5
Banana	529-914	27-32	20-24	1-3	1300-1350	13
Pineapple	413-1627	60-82	42-57	0-1.6	1440-1560	13

| Sisal | 80-840 | 9-22 | 6-15 | 2-14 | 1300-1500 | 11 |
| Coir | 106-175 | 6 | 5.2 | 15-40 | 1150-1250 | 13 |

1.4.1 Natural bast fibers (jute, flax and ramie)

jute, flax and ramie etc., (Figure 1-10) are the natural fibers which are mostly used in natural fiber composites for their better mechanical properties [63,64]. Jute is one of the most commonly used natural fibers because of its lower price. Jute is produced from plants of the genus Corchorus. It is the second largest natural fiber produced in the world [65]. Bangladesh, India and China provide one of the best conditions for jute plant growth [66]. It has a wide range of usage as shown in Table 1-6.

| Jute | Flax | Ramie |

Figure 1-10: Plant and fiber of jute, flax and ramie[67]

Over the 5000 years the flax fiber has been used to make the linen fabric. Flax belongs to the Linaceae family. Due to higher cellulosic content flax fiber is more crystalline having higher strength and stiffness. The average staple length and diameter of flax fiber is 42 ± 2 mm and 14 ± 2 µm respectively with 1.5 g/cm^3 density[68].

Ramie is a type of bast fiber similar to jute and flax fiber [69]. The length of the plant of ramie is 1 ± 2.5 m [70]. The plant and fiber of jute flax and ramie are shown in Figure 1-10. Ramie fiber provides better heat resistance, superior tensile strength and modulus than other bast fiber such as jute, flax, hemp and sisal fiber [60].

Table 1-6. Applications and advantages of jute reinforced composites [71]

Application areas	Advantages
Automobile industries 1. Door panels 2. Seat backs 3. Headliners 4. Dash boards 5. Trunk liners	1. Lighter in weight 2. Lesser raw material 3. Cost economic 4. Serviceable mechanical properties 5. Use of renewable resource
Building Component 1. Door 2. Window 3. Wall partition 4. Ceiling 5. Floor	1. Better physical properties 2. Fire, termite & better moisture resistance properties 3. Available at semi-finished / finished state, i.e., reduced labor & finishing cost
Transport Sector (railway coach & vehicle) 1. Flooring 2. Ceiling 3. Seat & Backrest	1. Better physical properties 2. Fire, termite & better moisture resistance properties 3. Available at semi-finished / finished state, i.e., reduced labor & finishing cost
Furniture 1. Table 2. Chair 3. Kitchen cabinet etc.	1. Better physical properties 2. Fire, termite & better moisture resistance properties 3. Available at semi-finished / finished state, i.e., reduced labor & finishing cost

Jute is mainly composed of cellulose, hemicellulose, and lignin. The length of jute fibers is generally from one to four meters. Jute is an abundant natural biodegradable plant fiber used as reinforcement in bio-composites [72,73]. Jute has two main types which are used commercially **a.** C. capsularis and **b.** C. olitorius. The chemical composition of both the types is shown in Table 1-7.

Table 1-7. Chemical composition of Jute fibers in % age of bone dry weight of the fibers [74]

Constituents	White Jute C. capsularis	Brown Jute C. olitorius
Alphacellulose	60.0-63.0	58.0-59.0
Hemicellulose	21.0-24.0	22.0-25.0
Lignin	12.0-13.0	13.0-14.0
Fats and waxes	0.4-1.0	0.4-0.9
Pectin	0.2-1.5	0.2-0.5
Proteins/nitrogenous matter, etc	0.80-1.9	0.8-1.6
Ash	0.7-1.2	0.5-1.2

The jute fiber is multicellular fiber unlike cotton and other fibers, a single jute fiber is composed of bundle of ultimate cells which are joined with the help of middle lamella. The jute fiber has high percentage of lignin which makes it stiff. The lumen of jute cells go all the way to fiber length with slight variation in the tube diameter [74].
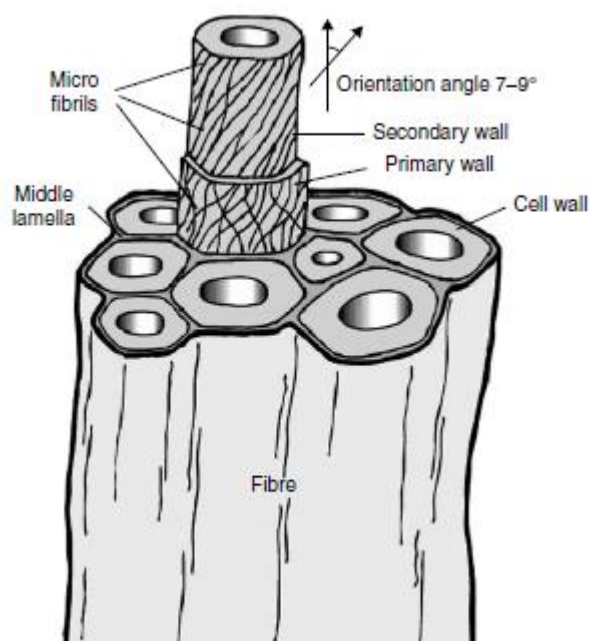
Figure 1-11. Morphology of Jute fiber microstructure [74]

Figure 1-12 [75] shows the TGA curves of jute, hemp and flax fibers within the range of 25^0C–500^0C with a heating rate of 10^0C per minute. The curves show more stability of Flax fiber then the rest two, while the jute has the least stability with higher degradation. This degradation is mainly due to different chemical compositions of the fibers regarding the

variation in the amount of hemicellulose, cellulose, lignin, pectin etc. The initial decrease in the weight of natural fibers up to 100^0C is due to evaporation of moisture form the biomass material. At 155^0C to 169^0C temperature range thermal degradation of lignin occurs, then comes the hemicellulose for which the degradation is in the range of 230^0C to 307^0C, and finally the decomposition of cellulose occurs in the temperature range of 323^0C to 392^0C. In general lignin is the first part of natural fibers which decomposes in a lower temperature range (106^0C to 170^0C) [76].
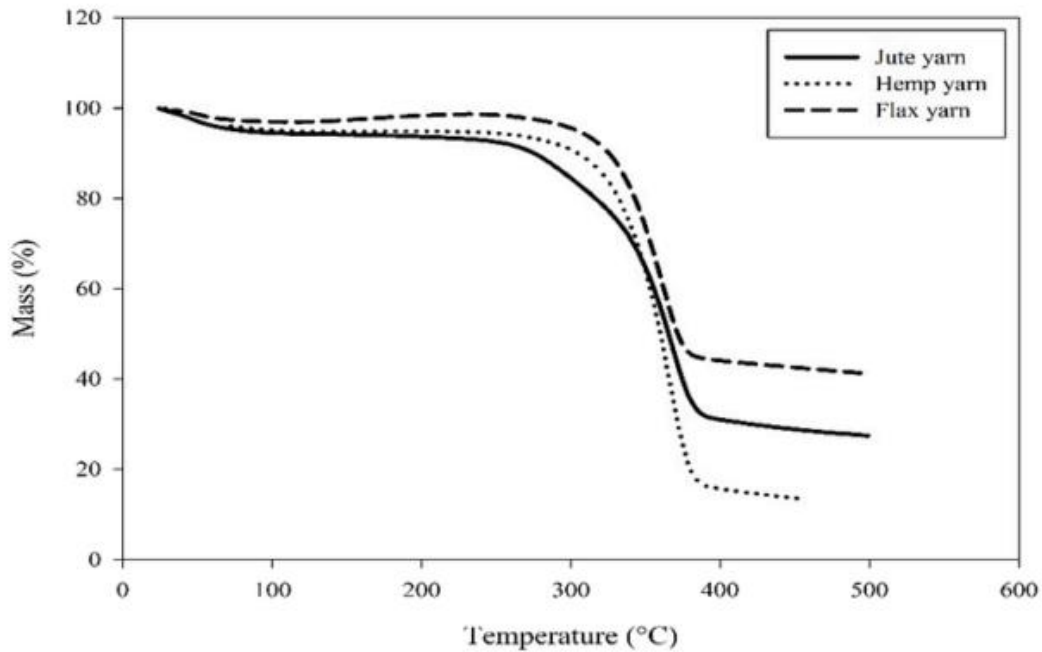
Figure 1-12. TGA curve for hemp, jute and flax fibers showing stability of these fibers upto200 °C, initial weight loss under 100^0C is due to moisture evaporation[75]

1.5 Yarns used in natural fiber composites

Reinforcement is prepared using yarn of different type and variety. The yarn manufacturing technique depends upon the type of material being used, intended applications and process being used for manufacturing.

Normally three types of yarns are used for the reinforcement fabrications as shown in Figure 1-14, however for the natural fibers the staple yarn is produced since it is short in length so twisted together to make the long length of yarn. The high performance yarn is mostly used in the form of filament and sometimes as staple yarn. The composite yarn is used when there is need to combine the properties of two or more yarns in a single yarn. The two most used types of yarn manufacturing for the composite reinforcement are staple and filament yarn.
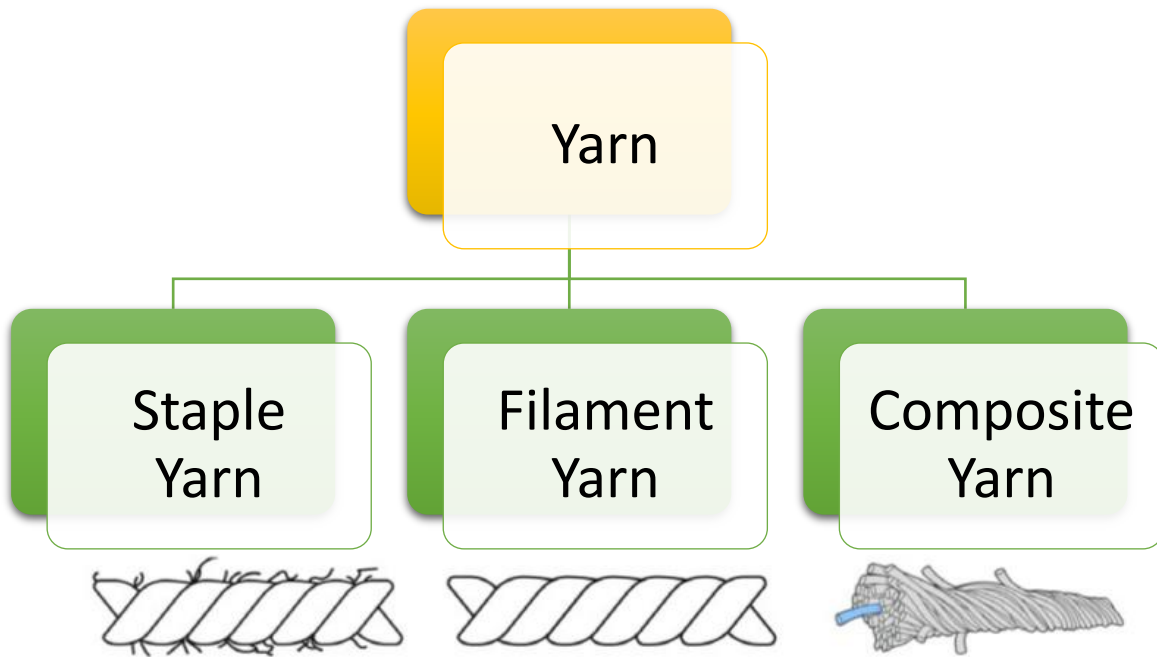
Figure 1-14. Yarn types used for the reinforcement

All types of reinforcements are made with certain materials. A textile yarn must possess some properties based on which type of material being used. There are various parameters which are considered for yarn to be used for reinforcement fabrication as shown in the Table 1-8 [78]

Table 1-8. Important yarn parameters[78]

Parameter	
Dimensional parameters	Linear density (i.e., g/m)
	Diameter
	Number of filaments in crossection
Structural parameters	Thread density (i.e., threads/inch)
	Core[a] content
	Core–sheath[b] ratio
Fiber parameters	Length, Linear density
	Crimp (waviness)
	Cross-section shape

[a]Core: inner part of the yarn, [b]Sheath: outer part of the yarn

The filament yarns are mostly made with synthetic fibers which are used in composite fabrication. The natural filament yarns are used for composites fabrication such as silk, viscose and rayon [78].

As mentioned earlier the filament yarn used in the composite fabrication are made of synthetic material so it can be further classified as the mono and multifilament. The filament yarns are made with the melt, dry and wet spinning depending upon the nature of base materials. For high performance applications mostly carbon, Kevlar and Ultra high molecular weight polyethylene are used, while for conventional applications PP, PE, nylon and glass yarn are used[79]. Figure 1-15 shows the types of filament yarns used for reinforcement fabrication.
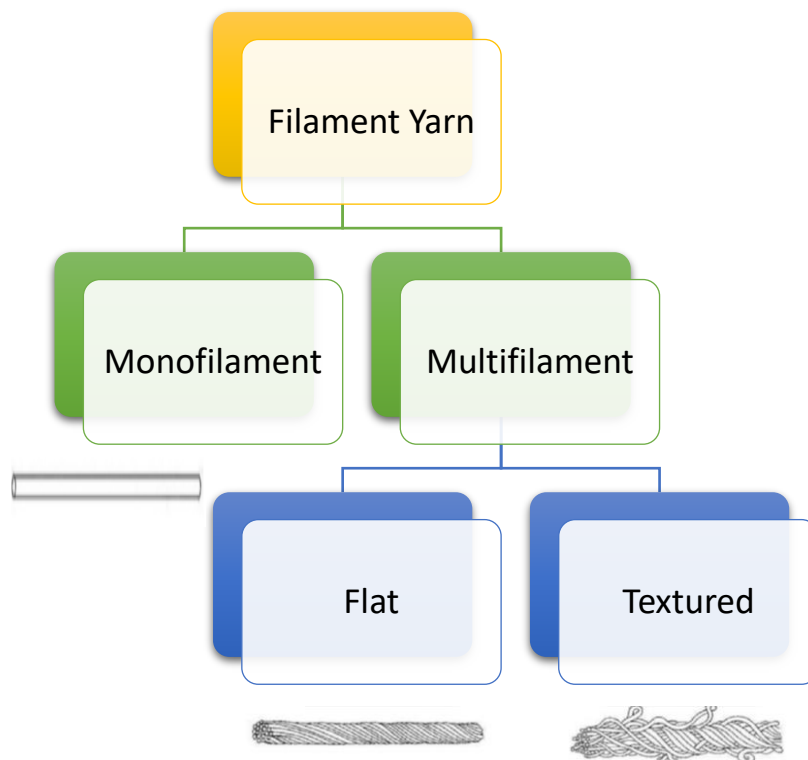
Figure 1-15. Classification of filament yarn [77]

The spun yarns are used from prehistoric times for the clothing and made with different type of short staple fibers. Mostly the spun yarns are made with the natural fibers but sometimes the synthetic filaments are cut into to small fibers to make spun yarn as per end applications. Different types of spinning techniques are used to make the spun yarn including; rotor, ring, open end and air vortex *etc.* [80]. Classification of spun yarns is shown in Figure 1-16
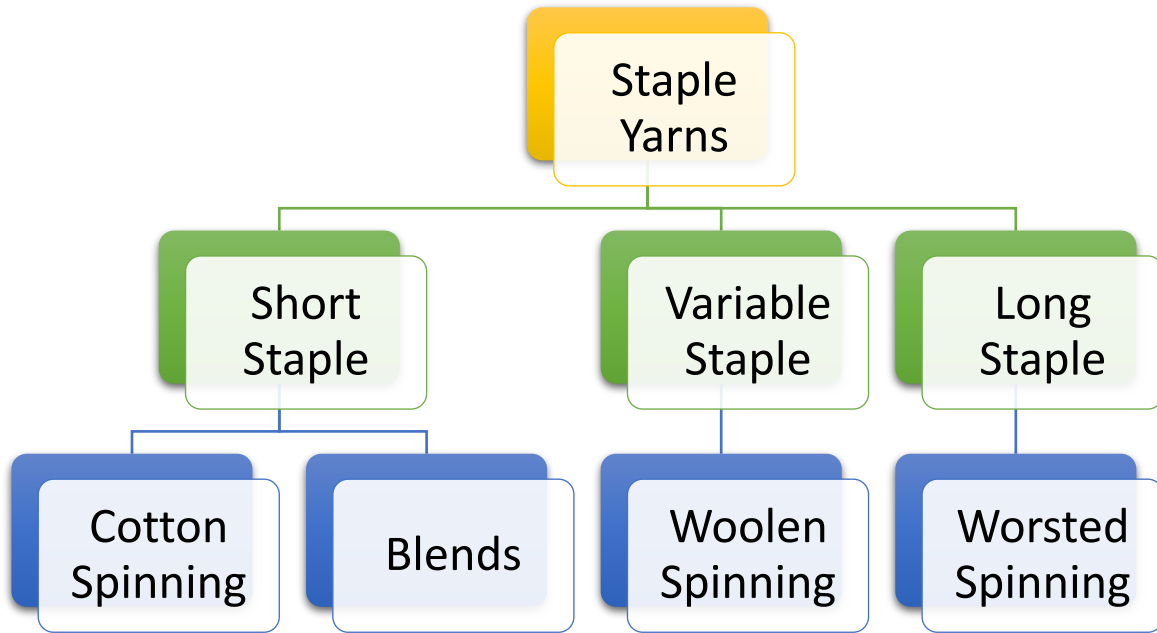
Figure 1-16. Classification of staple yarns [77]

The natural fibers used in the composite fabrication are mostly coarser and not very easy to spin due to high stiffness, so the coarser yarns are mostly made from those fibers. One of the problems arises while spinning the yarn with the coarser fibers, is the high amount of protruding fibers as they have high amount of fibers with variable lengths. These variable length fibers are likely to protrude beyond the surface of the spun yarn resulting in to hairiness which cause problems in subsequent weaving process. Figure 1-17 shows the longitudinal view of different fibers[74,81].
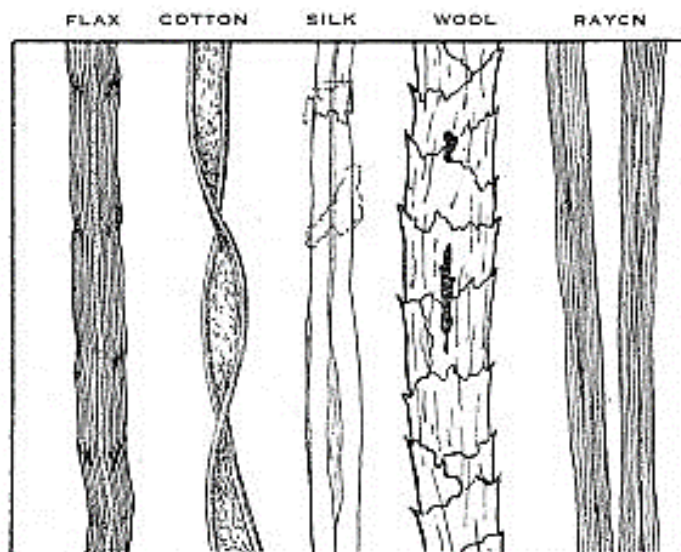
Figure 1-17. Longitudinal view of different natural fibers[82]

The problem in weaving due to hairiness can be avoided by applying starch on the yarn but this must be removed subsequently before composite fabrication to avoid interface problem. So one of the most suitable solutions to avoid the complications of applying starch and remove hairiness is singeing of yarn which will burn the protruding fibers along with smooth texture. The details are given in below section.

1.5.1 Singeing of spun yarns

Singeing is a process of removal of protruding fibers from spun yarns or fabrics by burning. This process is commonly used in textiles. The process is mostly used for sewing thread for its smoother appearance and better resistance to abrasion of the sewing process [83].

The yarn to be singed is passed through concentrated flame at a constant speed for which the air fuel mixture is carefully adjusted in order to remove unwanted hairiness without damaging the yarn core.

Jute yarn, like cotton, has a larger amount of hairiness which needs size coating prior to weaving process. The sizing process upon the yarn is followed by the desizing process; it is very unlikely to remove the sizing material completely. During the composite fabrication process such size coating works as an obstacle hindering to have a good interface between the fiber and the matrix. There are quite a few papers in the literature, mentioning the singeing technique for spun cotton yarn. Zhigang Xia et al., [84] have reported removal of cotton yarn hairiness to 80% by the singeing process. But their main emphasize was to enhance yarn quality with lesser hairiness and better evenness, the effect of reduction of yarn hairiness on the improved weave-ability was not targeted.

Current literature review shows no research on the singeing process of jute yarns for improving quality with better evenness; in spite they have high hairiness content.

The hairiness increases the abrasion among the warp yarns during shedding resulting into to frequent warp breakage and reduced weaving efficiency. Singeing of the jute yarn has been found to be a two-in-one process, as it not only reduces the hairiness, which helps to reduce abrasion for forming a clear shed for weft insertion, without the need of time taking sizing and desizing process, but also increases the strength of jute yarns up to 10% as reported by Asghar et al., [85]. Singeing of the bast fibers is proved to be more viable option than sizing.

1.6 Matrices used in natural fiber composites

In composite materials, mostly polymeric matrix (thermoset and thermoplastics) are used. Thermoplastics resins have their advantage over the thermosets due to their recyclability. As already mentioned, in thermoplastics the molecules are held together by weaker intermolecular forces such as the van-der-waals or hydrogen bonds. When the temperature is applied, these secondary bonds break temporarily, and after re-cooling, these molecules are rearranged into a new configuration, resulting in a new solid [86]. Table 1-9 shows a comparison between some of the thermoset and thermoplastic resins.

Table 1-9. Comparison of the properties of thermoset and thermoplastic resins [2]

Type of resin	Density (kg/m^3)	Elastic modulus (MPa)	Tensile strength (MPa)	Elongation (%)	Thermal expansion coefficient (°C^{-1})
Thermosets					
Epoxy	1200	4500	130	2	11 x 10^{-5}
Phenolic	1300	3000	70	2.5	1 x 10^{-5}
Polyester	1200	4000	80	2.5	8 x 10^{-5}
Vinyl ester	1150	3300	75	4	5 x 10^{-5}
Thermoplastics					
Polypropylene (PP)	900	1200	30	20-400	9 x 10^{-5}
Polyethylene (PE)	910-925	1150	20-30	20-100	---
Polyphenylene	1300	4000	65	100	5 x 10^{-5}
Polyamide (PA)	1100	2000	70	200	8 x 10^{-5}
Polyether sulfone	1350	3000	85	60	6 x 10^{-5}
Polyetherimide (PEI)	1250	3500	105	60	6 x 10^{-5}
Polyether-ether-ketone (PEEK)	1300	4000	90	50	5 x 10^{-5}

Polyethylene is the mostly used thermoplastic polymer and its consumption is up to 70 % of all polymers [87]. Polypropylene is the second most commonly used thermoplastic polymer after polyethylene [88] due to its intermediate properties between polyethylene and polyvinyl chloride and its easy processing [89],[90–92]. Due to low price, easy recycling, low density and high toughness, polypropylene has found various applications. Density of polypropylene is in the range of 900-910 kg/m^3. It has melting point in the range of 130 -171°C depending on the material crystallinity. Polypropylene is used abundantly for composite fabrication as it is easy to use and handle.

Thermoplastic resins can be further classified as engineered plastics like polyamide (PA), polyetherimide (PEI) polyether-ether-ketone (PEEK)) and general plastics like polypropylene (PP), polyethylene (PE) and acrylonitrile butadiene styrene (ABS) [92,93].

1.7 Natural fiber reinforced thermoplastic composites

Thermoplastic composites have an advantage over the thermoset composites due to their recyclability, sustainability and low cost hence they are more environmentally friendly, especially when they are coupled with natural fibers. The market share of natural fiber-reinforced composites are increasing day by day [12,66,94]. Jute is one of the most abundant natural fibers grown in South Asia [66]. Being inexpensive, it is among the preferred natural fibers for natural fiber composites (NFC). Several studies can be found in literature on the use of jute fiber, and investigation of properties of the associated composites [72,73,95–97].

1.8 Thermoplastic composite fabrication techniques

Various techniques have been reported in the literature to fabricate the natural fiber reinforced thermoplastic composite materials, such as injection moulding, thermoforming, thermoplastic RTM (resin transfer molding), and commingling. The brief details of these techniques are as follow;

1.8.1 Injection molding technique

Injection molding technique is mostly used for thermoplastic materials. The thermoplastic materials which are normally in the form of pellets are fed into the injection molding machine and advance towards the closed mold through screw pressure by the injection unit. The material is melted by heat and pressure during the process. As the thermoplastic material cools, it solidifies adopting the shape of the mold (Figure 1-18).
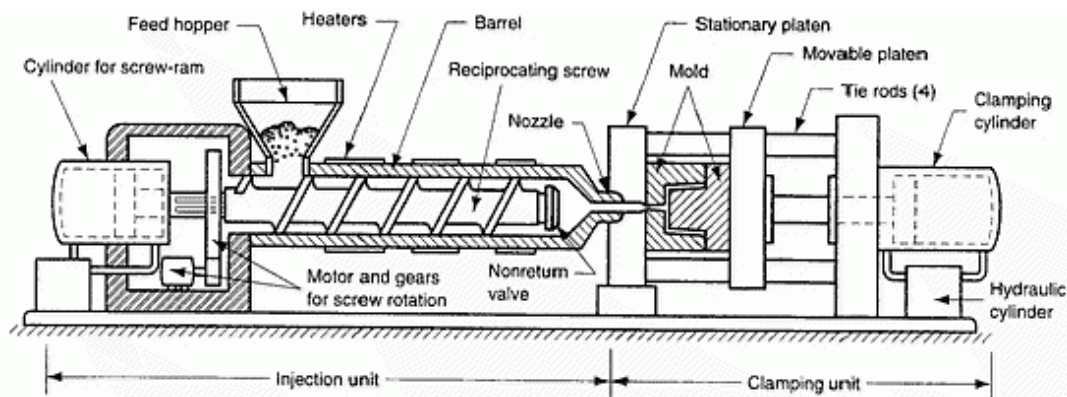
Figure 1-18. Injection molding technique [98]

The process span of injection molding is from 2 seconds to 2 minutes depending upon various factors, for the reason the injection molding is one of the fastest processes for making plastic products. Injection molding mainly have four steps clamping, injection, cooling and ejection [99]. Clamping helps for the proper closing of the mold for desired dimensions of the finished part. Molds are usually in two halves, one mold part is fixed to the machine and other is moved to close the mold cavity. In the injection process the thermoplastic resin in pallet form is fed into to the machine via gravity feeding though hopper, their melting is carried out in the long screw barrel of machine. The resin is gradually heated in the barrel in different heating zones in the range of 120^0C to 320^0C mainly depending upon the thermoplastic melting temperature, it may be as low as 120^0C for thermoplastic rubber to as high as 320^0C for polycarbonate. The mold is then cooled down through numerous water channels provided inside the mold metallic body. Cooling of thermoplastic parts is also associated with shrinkage which can be compensated by designing the mold at a slightly larger size depending upon the shrinkage of material. When the part is cooled down at about 20^0C below the melting point of the thermoplastic resin, the part is ejected with help of ejector pins mechanism. The thermoplastic product is likely to stick to the mold inner walls, for the reason the mold inside is coated with mold releasing agents such as PVA or Silicon spray. As the thermoplastic part is dropped down into the dispensing tray, the extra material is trimmed from the part for final finishing. The extra plastic material is then chopped, mixed with the fresh plastic granules and reused for injection molding. In general, there are four variables to be controlled in injection molding process; these are temperature, pressure, time and distance. For making composites, chopped fibers are used along with the thermoplastic resin. The staple lengths of these chopped fibers are from few millimeters to around 12mm [100].

A vast range of fibers can be used in injection molding like natural fibers (hemp, jute, flax, kenaf, sisal, abaca, fruit hair fibers like coir etc.,) or higher performance fibers (glass carbon etc.,) [101], [102]. A wide injection pressure is used for injection molding, 800 to 1500 psi (50 to 100 bars), depending upon various parameters of the process. The pressure must be high enough to fill >99% of the mold cavity. Too much pressure may result into part sticking inside the mold, part burning or warpage [103].

Bajracharya et al., [104] studied the mechanical properties of the composite made off 4mm long chopped glass with plastic solid waste (PSW) matrix. The glass fiber weight proportion was used in the range of 30, 20, 10 and 0%. They found that the values of tensile strength and

modulus of the composite were 74 and 238%, 50 and 155% and 20 and 67% better for 30, 20 and 10% glass weight ratio as compared to pure thermoplastic (0%) solid waste.

The strength of these short fiber composites depend upon the fiber orientation inside the mold during injection process. Kenny el at., studied the mechanical properties of short glass fiber polypropylene injection molded composite and found that the strength of the finished part is 40% higher in the outer part of the mold than the inner part due to much higher glass fibers orientation in the outer part [104]. The bottleneck of injection molded composites comes from the lack of control of fiber orientation as they freely flow in the molten thermoplastic resin during injection process.

Injection molding is a simple one-go process, which is normally used for high production. The product price is cheaper (for cheaper thermoplastic resin used). The process can make complex shapes. As two-sided mold is used so both side finished parts are made. Thermoplastic composites cannot be used for higher temperature application due to lower melting temperatures. Product is weaker in strength if reinforcement is not used. Even with the use of chopped fibers the strength is not compatible of longer strands preforms used in RTM, VARTM (vacuum assisted resin transfer molding), prepregs and pultrusion. The process needs expensive two-sided mold with heating arrangements. In addition, injection molding machine needs high capital investment.

One of the limitations however with the injection molding process is that only short fibers can be used with it and when longer reinforcement strands are to be used like woven or knitted, it is impossible to apply as the viscosity of thermoplastic matrices is too high to flow through their dense skeletons. So for reinforcement made with woven or knitted fabrics the hot press compression molding technique is employed.

1.8.2 Thermoforming / Compression molding

Thermoforming technique is used for both thermoplastic and thermoset composites. For thermoplastic composites the technique uses commingled or non-commingled thermoplastic sheets subjected to high pressure and heat in a two-sided mold (Figure 1-19). The mold is heated at some 25 °C above the melting temperature of the matrix material with the specimen inside the mold. The cured part is then removed from the mold after cooled to below 50-100°C of the melting point. Surface films or textures can be added for enhancing the surface aspect. The temperature range in the thermoforming of thermoplastics and thermoplastic composites is quite comparable to injection molding process and in the range of 120^0 to 370^0C [105]. Like injection molding the optimum temperature depends upon the type of

plastic used. The thermoforming pressure has a wide range and mainly dependent upon the type of matrix, types of reinforcement and end use of the product.
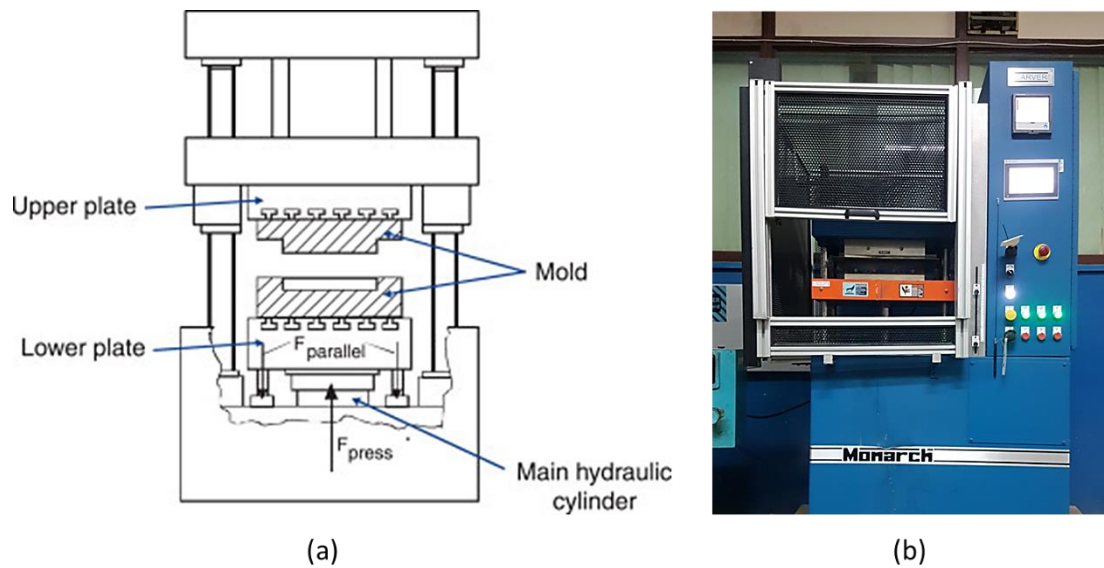
Figure 1-19. (a) Schematic presentation of compression molding (b) compression hot press machine [98]

Compression molding is a simple one go process with high production. The product price is cheaper (for cheaper thermoplastic resin used). Complex shapes can be made. As two-sided mold is used, so both side finished parts are made. It is one of the most commonly used techniques for thermoplastics/thermoset composite manufacturing. However, thermoplastic composites cannot be used for high-temperature applications. An expensive two-sided mold is required with the heating arrangement, which requires a high capital investment. Higher compression pressure is likely to bleed out excessive amount of thermoplastic resin and hence increasing the fiber volume fraction, but the thermoforming pressure beyond a certain limit is likely to damage the fiber reinforcement.

Fabrication parameters of natural fiber reinforced thermoplastic composites are the key factors for the development and reproduction of composite laminates. The main fabrication parameters for compression molding are shown in Figure 1-20.
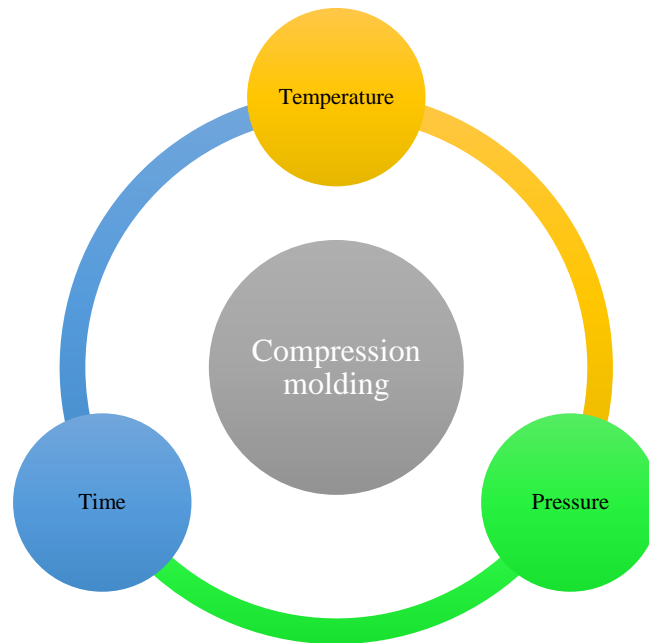
Figure 1-20. Process parameters of compression molding technique [106]

1.8.2.1 *Effect of molding temperature on the fabrication of composites*

Temperature is considered as an important process parameter of compression molding. Temperature is associated with the amount of heat required to melt the polymer matrices. An increase in the temperature reduced the viscosity of the matrix, improved the impregnation between the reinforcement and matrix, which ultimately enhanced the composite properties. The selection of molding temperature is decided among the melting temperature of the polymer and the degradation temperature of natural fibers. If the mold temperature is lower than a certain value, the fibers will fail to be properly wetted by the viscous resin. A higher temperature beyond the optimum level can degrade the reinforcement [107].

Figure 1-21 shows the decomposition temperature of most of the natural fibers, which is approximately 200°C. Some polymers like Nylon 6.6, Polyvinylchloride and Polycarbonate require molding temperature higher than 200°C, which is higher than the degradation temperature of most of the natural fibers, but meanwhile the polymers like LDPE (low density polyethylene), Polypropylene, Polylactic acid and HDPE (high density polyethylene) have better compatibility with natural fibers, and their molding temperature can be set under the fiber degradation temperature. The molding temperature, for natural fibers should not be less than 192°C for better composite quality with a minimum safe temperature of 160°C [99].
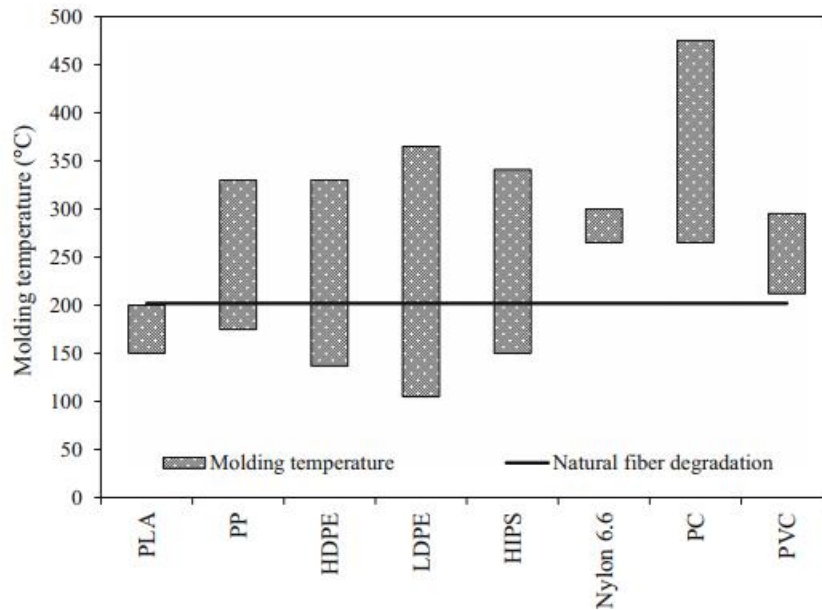
Figure 1-21. The molding temperature range for different thermoplastic polymers used for natural yarns composites. The degradation temperature of most of the natural yarns is 200°C [108]

Rokbi el al., [109] investigated the mechanical properties of jute and recycled polypropylene composites with varying temperatures in the range of 190, 210, 230, 250 °C using similar pressure of 20 bars. They made four specimens A1, A2, A3 and A4 for these four temperatures ranges (Figure 1-22). They found that the tensile modulus of the jute/PP composite increases with increase of temperature up to 230°C. This is possibly due to the reason that higher temperature value reduces the matrix viscosity and thus making the flow easier through the dense fibrous structure. After 230°C degradation of jute fibers occurs resulting in to reduced modulus at 250°C.
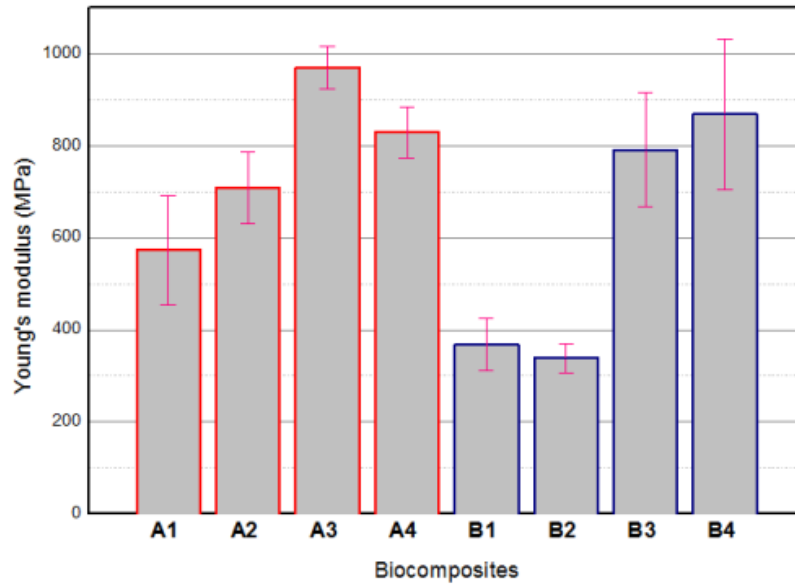
Figure 1-22. The effect of molding temperature on tensile modulus of jute/polypropylene composites with temperature range of 190 (A1), 210(A2), 230 (A3), 250°C (A4) and a at constant 20 bar pressure [109]

The breaking strength of the composite is shown in Figure 1-23. Interestingly the temperature effect on breaking stress is adverse to that of modulus. As the temperature increases from190 to 250°C the breaking strength decreases. This can be justified by the reason that with increase of temperature the cellulosic structure of the jute fibers in likely to deteriorate. As the temperature increases beyond 200°C the structure is affected as verified by the TGA curve (Figure 1-12), which intern makes the material brittle due to 'baking effect' on fibers.
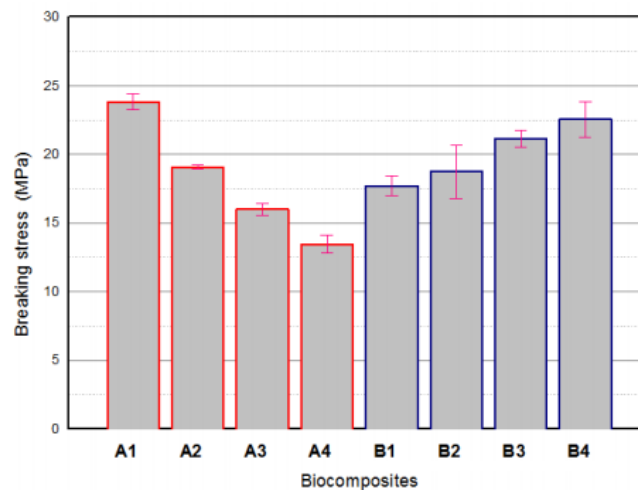
Figure 1-23. The effect of molding temperature on breaking strength of jute/polypropylene composites with temperature range of 190 (A1), 210(A2), 230 (A3), 250 °C (A4) and at a constant 20 bar pressure [109]

The effect of molding temperature on elongation at break was also studied by Rokbi el al., [109]. Figure 1-24 explains this effect. As the temperature increases, the elongation at break decreases. From 190 (A1) to 250°C (A4) there is a marginal decrease in elongation at break (almost 3 times).
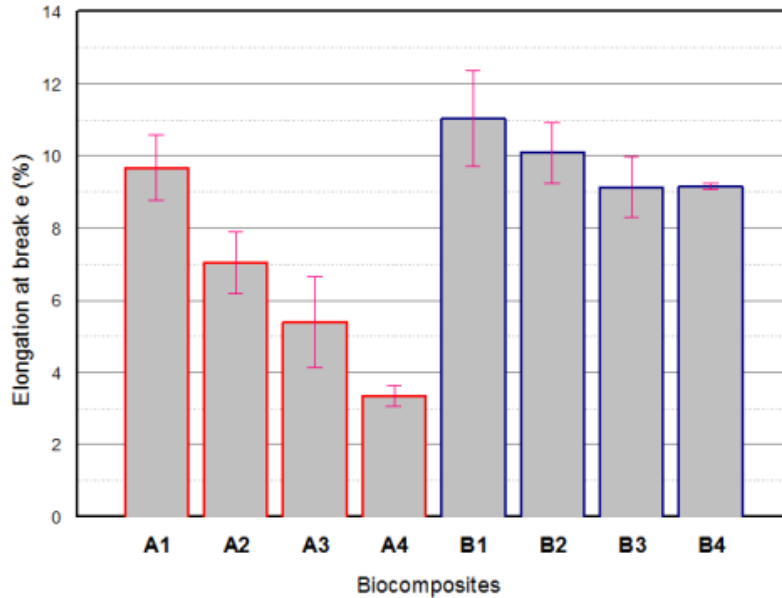
Figure 1-24. The effect of molding temperature on elongation at break of jute/polypropylene composites with temperature range of 190 (A1), 210(A2), 230 (A3), 250 °C (A4) and at a constant 20 bar pressure [109]

The influence such 'baking-effect' on jute fibers by increasing the molding temperature has also been reported by Anin et al., [110]. They mentioned increase in tensile modulus and decrease in tensile strength from 185 to 235°C. The increase in modulus has been attributed to better wetting out of the fibers by lower viscosity at higher temperatures and decrease in tensile strength was associated to the deterioration of jute fibers, which is verified by the change of jute fiber's color with increased temperature (Figure 1-25). With increase of temperature jute fiber color gets darker and darker.

Figure 1-25. The effect of molding temperature on jute/PLA composite with temperature range of 185, 195, 205, 215, 225, 235 °C and at a constant 20 bar pressure [110]

1.8.2.2   Effect of molding pressure on the fabrication of composites

Application of pressure is compulsory during the compression molding, which reduces defects such as porosity and air-bubbling and helps increasing fiber packing. Pressure also helps to flow the matrix into the reinforcement [111].

Rokbi el al., [109] also investigated the mechanical properties of jute and recycled polypropylene composites with varying pressures in the range of 10, 20, 30 and 40 bars using similar temperature of 200°C for all composite specimens. Four specimens were fabricated B1, B2, B3, and B4 respectively for four pressure ranges. Figure 1-22 explains the effect of varying pressure on the tensile modulus of jute/PP composite. The initial increase in pressure seems to have no significant effect on tensile modulus till 20 bars pressure, as the pressure increases beyond 20 bars there is a rapid increase in the modulus which is mainly due to infiltration of the polypropylene resin in to the jute fabric up to 30-40 bars pressure. There is also a constant increase in the breaking strength of the composite from 10 to 40 bars (Figure 1-23). Figure 1-24 also explains the effect of pressure on elongation at break of the composite. As the pressure increases the elongation of the composite decreases, which is justified by better locking of the jute fibers/yarns inside the matrix at higher pressures reducing the fiber freedom towards 'pullout' behavior. As the pressure increases, the elongation at break decreases. There is a 10% decrease in elongation at break from 10 bars (B1) to 20 bars (B2) and from 20 bars to 30 bars (B3). However the elongation at break somewhat stabilizes at 9.1% at 30 bars as there seems no mentionable decrease in elongation

at break with further increase of pressure from 30 to 40 bars (B4). It is important to note that with increase in pressure, variation in elongation decreases.

There are few research papers discussing the effect of pressure variation on the mechanical properties of thermoplastic composites. Medina et al*.,* [112] investigated the process related to mechanical properties of thermoformed natural fiber composites considering the three major parameters; the molding pressure, temperature and mold pressing time. They also investigated about the maximum amount of pressure to be applied on natural fiber composites without reaching the threshold of fiber damage. They used hemp and kenaf fibers web along with Acrodur resin (an acrylic based green resin which works as thermoplastic under 130°C and thermoset above this temperature). They used preheated mold at 200°C and did eight experiments using molding pressure of 15, 20, 30, 60, 80, 100, 150 and 200 bars respectively with the pressure holding time being in the range of 40 to 60 seconds [112]. Graph between the mechanical properties and pressure is shown in Figure 1-26 below, it is clear that the tensile strength of the composite produced at 60 bars is at maximum, and the strength steadily decreases as the pressure exceeds 60 bars (MD and CD are the values in Machine Direction and Cross Direction, respectively). They found that the values of tensile and flexural modulus and strength are at maximum at 60 bars.
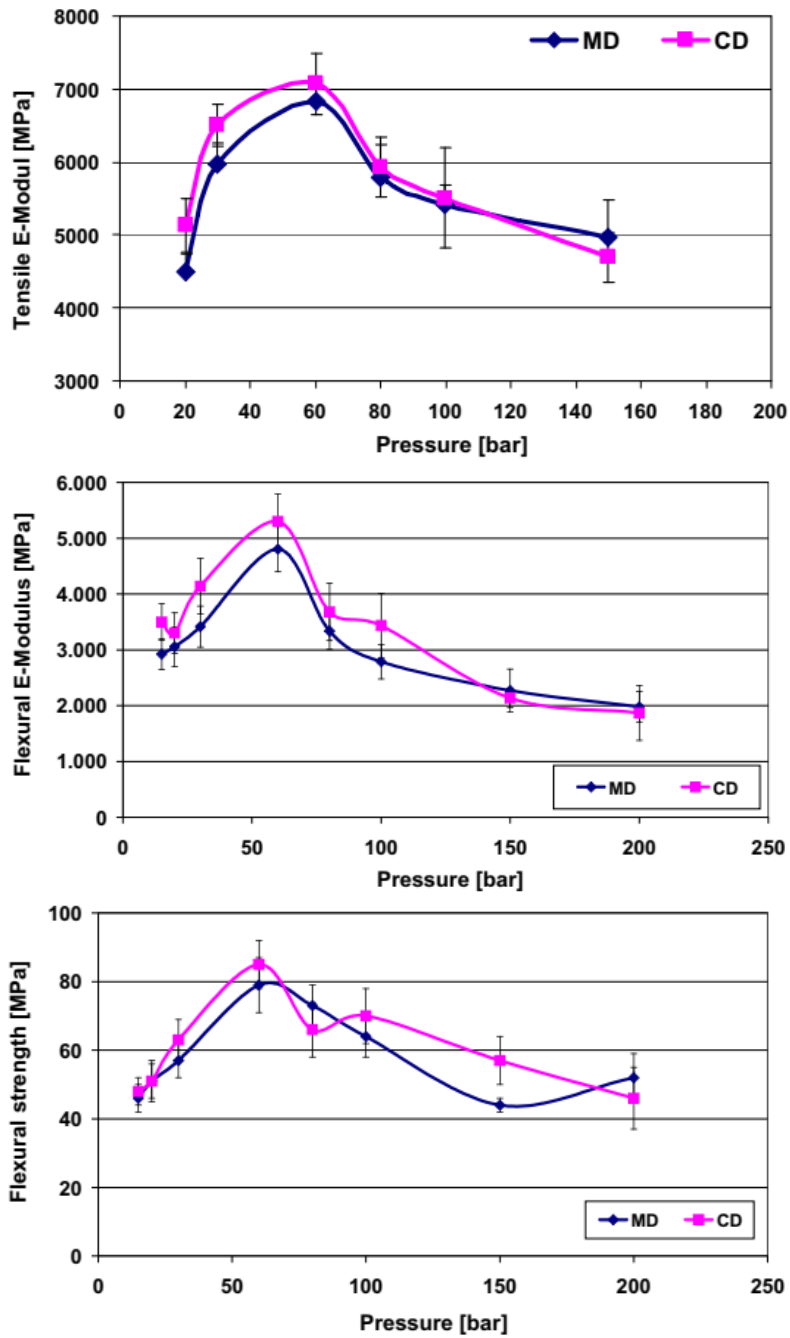
Figure 1-26. Mechanical properties of kenaf fibers vs. processing pressure, (a) tensile modulus, (b) flexural modulus, (c) flexural strength. The maximum values are at about 60bars. MD and CD are machine and cross directions. [112]

Figure 1-27 explains the effect of increased pressure on kenaf fibers. At 60 bars pressure the lumen walls of Kenaf fibers look stable which is verified by the higher mechanical properties of the composite at 60 bars (a). As the pressure is increased to 80 bars the fiber lumen collapses (b).
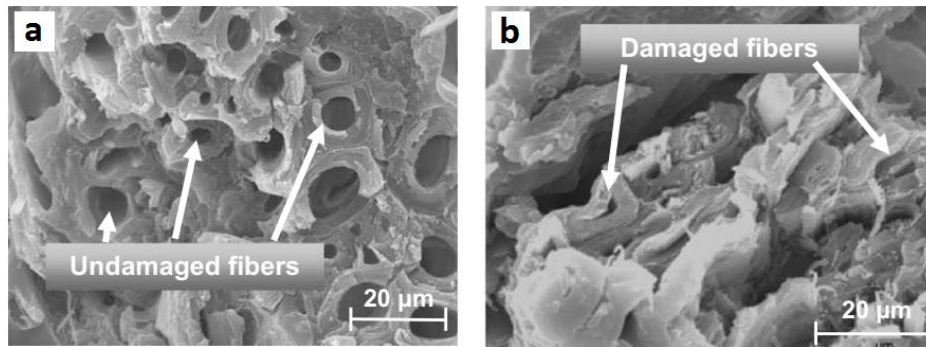
Figure 1-27. Microscopic examination of kenaf fibers (a) undamaged fibers with healthy lumen at 60 bars (b) damaged fibers with collapsed lumen at 80 bars [112]

As far as the molding pressure is concerned a range of 15 to 200 bars has been used by the author, but with a fact that different composites were separately prepared by thermoforming techniques at different pressure ranges of 15, 20, 30, 60, 80, 100, 150 and 200 bars, i.e., eight samples were prepared at eight different pressures), for every specimen a small pressing time of 45 to 60 seconds was employed. The method of gradual loading was however not employed.

Xie et al*.,* [113] investigated the effect of various molding parameters on the mechanical properties of carbon thermoset composites. They used a ready-made prepreg consistent of T300 12K Toray woven carbon fabric with 2/2 twill weave with a thermoset resin content of 40% (matrix name has not been mentioned). The parameters, under the investigation were molding temperature, molding pressure, molding pressure holding time, rate of cooling and mold opening temperature. Molding temperature was used in the range of 140 to 170 °C, molding pressure in the range of 400 to 550 bars, molding pressure holding time 10 to 25 minutes. They found the maximum values of mechanical properties at a molding pressure of 500 bars, molding temperature of 150°C and 20 minutes of pressure holding time. Maximum mechanical properties at a pressure of 500 bars had been justified with greater cause of resin flow along with better impregnation. Maximum mechanical properties at 150°C were justified by the reason that the resin does not flow and do not wet out the fibers below 150°C and above this temperature the resin is likely to degrade. Maximum mechanical properties at 20 min pressure holding time were justified with the reason that below 20 min, the time is inadequate to properly wet out the fibers and above this time there is not mentionable change/increase in the composite performance just resulting into wastage of time (some degradation of resin may occur).

As far as the molding pressure is concerned a range of 400 to 550 bars had been used but with a fact that different composites were separately prepared by thermoforming techniques at different pressures (400, 450, 500, 550 bars), for every value instant pressure loading technique was used, the gradual loading method was however not employed.

Lebaupin et al., [114] investigated the mechanical properties of a thermoplastic composite made using unidirectional flax fiber and polyamide-11 thermoplastic matrix on the bases of instant and gradual loading techniques during thermoforming. The authors used three different pressure values (25, 40 and 65bars) at a constant temperature (210°C). They produced two different composite specimens using:

1) Instant loading technique and
2) Gradual loading technique

In instant loading method, the composite was subjected to an instant load of 65 bars, and for gradual loading the same type of composite was subjected to a molding load of 25 bars for 2 min, then a load of 40 bars for 2 min and last a load of 65 bars (till the end of process for mold opening). Both composites were made under a constant temperature of 210°C. They found the tensile strength of gradual specimen to be 174 MPa and on the other hand the tensile strength of instant specimen was 92 MPa, which means the strength of gradual specimen is about 89% more than instant loaded specimen. However there is not much variation in tensile modulus. The values of tensile moduli for instant and gradual loaded specimens are 35GPa and 35.8GPa, which is only 2.3% higher for the gradual specimen. The main reason behind this is much higher failure strain value of gradual specimen at 0.65% as compared to instant specimen (0.34%), which is a 91% increase.

The SEM study of instant and gradual specimens is also very interesting, as shown in the Figure 1-28 below.
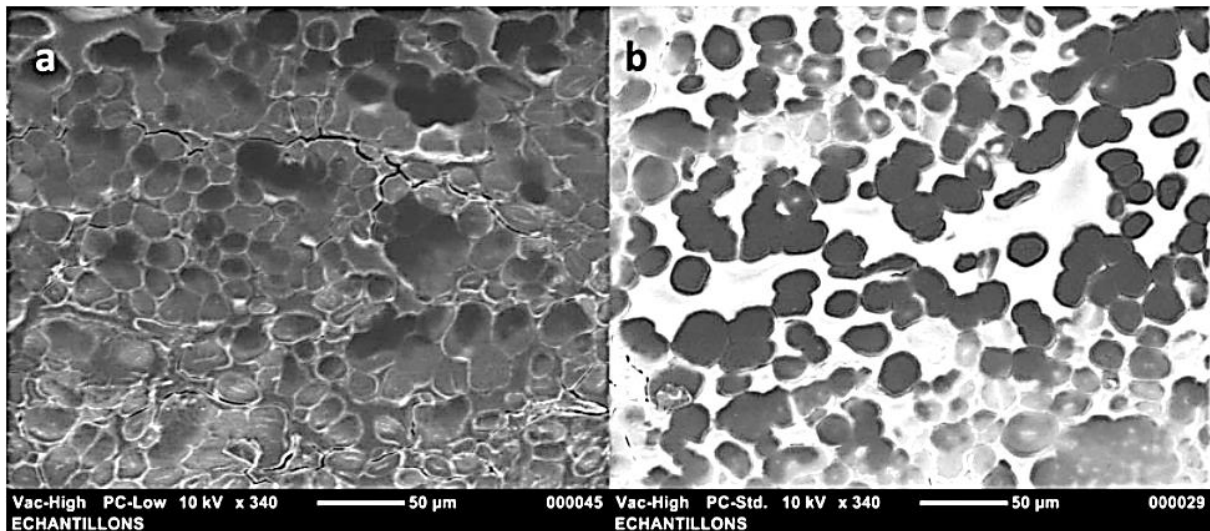
Figure 1-28. A SEM comparison of composites under instant (a) and gradual (b) pressures

[114]

Grouping of fibers is a clear difference between (a) instant and (b) gradual loading specimens. This may be due to the reason that instant loading, while the resin is still in non-molten form, tends to bring the individual fiber together (which are already well parallel in UD form) in bundles Figure 1-28(a). While Figure 1-28(b) shows that in gradually loaded composite most flax fibers are well surrounded by the matrix. This is mainly due to the increase of impregnation pressure in gradual steps.

It is quite visible in SEM images that the flax fibers in instant loaded specimen are grouped in the forms of bundles (more grouping of fibers causes darker color), while in gradual loaded specimens the fibers are somewhat more scattered, and their surroundings are more occupied by the impregnated resin (characterized by light color resin).

The amount of molding pressure on the natural fiber composites mainly depends upon their end-use. If damping and acoustic properties are more import then the composites is subjected to lower molding pressure. For such end-use the molding pressure is kept as high as 15 bars so that the hollow lumen inside the fiber is not damaged which is necessary for heat and sound isolation properties of the composites. However higher molding pressure values are preferred when the mechanical properties of the composites are of more importance, as high as 60 bars, such as use in brief case manufacturing [115]. For higher performance fibers the molding pressure can go much higher without damaging the non-hollow fibers. a thermoforming pressure in the range of 500 bars has been reported by Xie et al., for the manufacturing of carbon/thermoset composites with maximum mechanical properties [113].

1.8.2.3   Effect of molding time on the fabrication of composites

Molding time for thermoforming mainly depends upon the type of resin used. For the thermoforming of thermoset composites, a higher time range is required mainly dependent on the resin curing time. As the curing of thermoplastic resins is mainly dependent on the temperature, hence they used much lesser in-mold time as compared to thermoset composites. Thermoforming time for thermoplastic composites can be reduced with faster cooling rate of the mold. The processing time is a critical factor for compression molding as it determines the viscosity, level of impregnation, curing of polymers and final properties of the fabricated composites [106]. Michaud et al., [116] investigated glass-matt polypropylene thermoplastic composites. They studied the impregnation behavior of polypropylene resin on the glass matt with respect to different impregnation times (60, 900, 3600 seconds) and found with increase of impregnation time the void formation decreases as shows in the Figure 1-29. For a small time-span of 60 seconds the void content is in the range of 15 to 25%, but as the time increases the void content decreases to around 2 to 3 %. The void content was calculated indirectly from the values of fiber volume fraction of the composite by density method (see 2.9).

Distance from mold wall (mm)
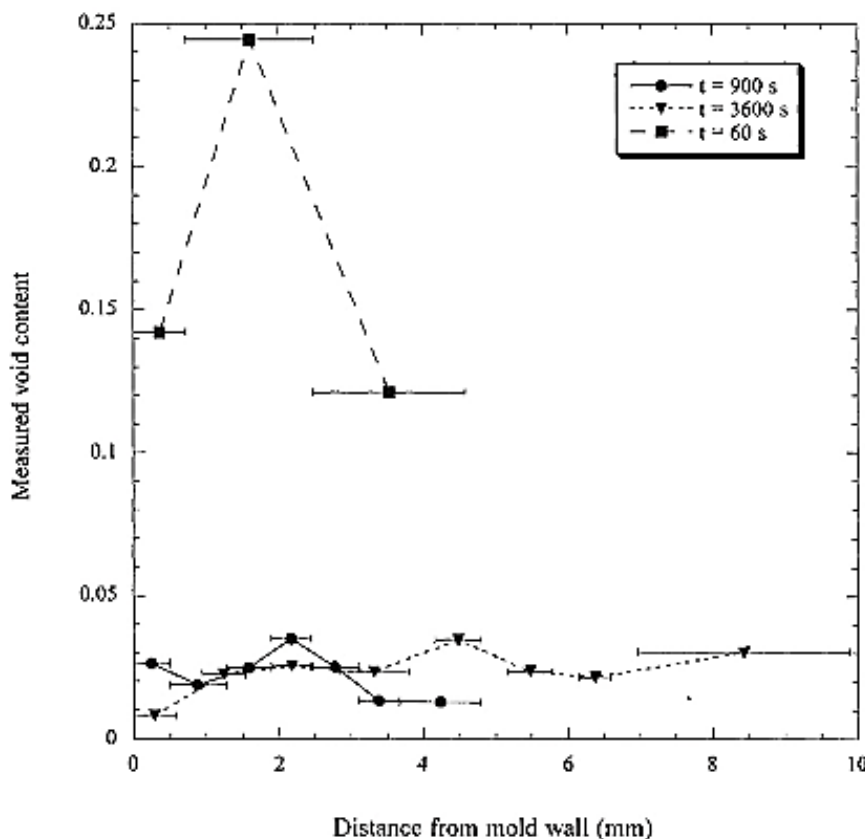
Figure 1-29. Experimental void content distribution for various impregnation times for glass-matt polypropylene thermoplastic composites (60, 900, 3600 seconds)[116]

1.8.3 Comparison of Thermoforming and Injection molding process for composite manufacturing

Thermoforming or Compression molding offers several advantages as compared to injection molding process, such as low cost and with minimum material waste, whereas injection molding involves flow channels, sprues and bleed points. Compression molded products have superior mechanical properties than injection molded parts, resulting in higher tensile modulus and higher specific density. Compression molded products have lesser voids as compared to injection molded products, thus making it stronger than injection molding parts. Zampaloni et al*., [91] have concluded that the optimum manufacturing method for the fabrication of natural fiber reinforced polymer composites is compression molding, but necessarily included with careful setting of parameters in order to melt down the matrix for ultimate penetration to the fiber bundles, resulting into better properties and performance of natural fiber composites. One of the major advantages of thermoforming is that, different textiles reinforcements can be placed in the mold at desired angles. One can use woven, knitted, braided structures, but on the other hand injection molding can only use the non-woven web technique as the fibers are injected into to 'empty' mold along with the molten resin. Larger textile structures like woven, knitted, braided are not possible to be injected along with the resin passing through different hurdles like flow channels, sprues and gates. Even if these structures are placed into the mold, prior to injection, there would be extreme resistance to the flow of chopped fibers through these textile skeletons, and thermoplastic resin would simply fail to reach the 'tail-end' of the mold.

Compression molding for composites is a double side molding process. It is achieved by placing a raw material (mixture of fibers and matrix) in a mold subjected to heat and pressure applications.

While the condition is entirely different for injection molding, in which the thermoplastic resin is instantaneously mixed with the fibers just before the injection, the mixture is forced to the mold through the injection screw, with limited fiber lengths as the longer strand of fibers are likely to whirl/stuck inside the dimensionally limited extrusion channels. This process may have several disadvantages. The introduction of fibers resists the flow of molten thermoplastic resin, increasing the viscosity. The fiber volume fraction (FVF) would also

suffer, which is inversely proportional to the flow through extruder. If we want to increase FVF, more fibers are to be introduced and consequently more resistance to flow. Hence compression molding process will give more FVF as compared to injection molding, as there is no resin/fibers mixture flow is involved. In compression molding, the fibers are already simultaneously present along with the thermoplastic resin inside the mold. The only thing the compression molding needs to do is to "squeeze out" the additional resin from the fibers vicinity. In this "squeezing out" process there are minimum chances of fibers to flow out due to entanglement with other fiber within the fabric, thus increasing the FVF to a greater extent as compared to injection molding. In injection molding process both the fibers and the thermoplastic matrix are subjected to flow, while in thermoforming only the matrix flows leaving behind the fibers with increased FVF. As already discussed, injection molding involves flow-channels, sprues, gates and bleed points. These 'paths' might be ok for the resin but not for the fibers.

In injection molding process the fiber length decreases subsequently as the material passes though the extruder, due to fiber breakage, especially the brittle fibers like carbon and glass. It was reported by Robert et al., [117] where they used PBT and PP resins with glass fibers. Average short fiber lengths found in the composite were 0.026, 0.023, and 0.028 in., with 0.125, 0.188, and 0.25in., input lengths.

Vlastimil Kunc et al., [118] studied the effect of injection molding on damaging the fibers of carbon and glass. They also reported significant fiber length attrition. They also noted that, composite samples with carbon fibers suffer lesser fiber length attrition as compared to glass fibers composites molded under the same conditions. It was also interesting to note that the fast mold filling process has resulted into greater fiber length attrition. The main area of damage was at the passage of fibers through the screw of injection molding.

D. J. Lee et al., [119] compared the mechanical properties of carbon/PEEK (polyether ether ketone) composites prepared separately by compression and injection molding techniques. Fiber breakage during injection molding has been observed. It results due to fiber contact with mechanical surfaces, fiber-fiber interaction and fiber-polymer interaction. As the fiber content increases the fiber to fiber and fiber to mechanical parts interaction increases resulting into the decrease of fiber length. However, in compression molding fiber breakage is much reduced resulting into the utilization of much longer fiber length, hence a significant increase in the mechanical properties can be achieved by increasing the initial fiber length as

compared to the composite made by using the injection molding system. For injection molded specimens, 10, 20, 30 and 40 % of carbon (by weight) was used with the PEEK resin, and carbon fiber length being in the range of 2.5 mm (minimum) to 12.7 mm (maximum). For compression molded samples, carbon/PEEK prepregs were used with controlled fiber orientation (not possible in injection molding) having fiber content of 30 and 40 % weight by adding the PEEK powder in between the layers and compressing to 5 bars at 310° C. Table 1-10 shows that the tensile properties of compression molded composite are dominant in all fiber ranges (30% weight to 40%). For short fibers (2.5mm range) the tensile strength of compression molded part is 61% and 77% higher (30% and 40% weight content) than injection molded part. For long fibers (12.7mm range) the tensile strength of compression molded part is 81% and 95% higher (30% and 40% weight content) than injection molded part. It is clear that difference of values is more for long fiber composite than short fibers composite, which is an indication that long fibers are more likely to damage in injection molding process as compared to short fibers during their passage through different channels, spruces and gates.

Table 1-10. Comparison of compression molded vs injection molded composites[119]

Molding technique		Short fiber 30% wt	Short fiber 40% wt	Long fiber 30 % wt	Long fiber 40 % wt
Injection molding	Tensile strength [MPa]	223.8 ± 15.3	236.4± 16.4	232.7 ± 20.1	240.7 ± 21.0
	Flexure strength [MPa]	301.4	314.6	316.4	327.3
	Modulus [GPa]	23.9	29.5	25	30.1
Compression molding	Tensile strength [MPa]	360.5 ± 23.3	419.1 ± 24.6	420.2 ± 25.3	468.3 ± 26.1
	Flexure strength [MPa]	-	-	-	-
	Modulus [GPa]	27.8	32.7	29.6	34.5

1.8.4 Comingling technique

Jute fiber reinforced composites can be made with the thermoplastic matrix using conventional non-commingling [120] or commingling [75,85,121] techniques.

The non-commingling is the commonly used technique for the fabrication of thermoplastic composites. However the high viscosity of thermoplastic matrix cause fabrication problem [122–126]. Another problem specially when using the natural fiber is low fiber volume fraction and poor wettability [127].

To cater these problems the use of commingled thermoplastic composites is continuously increasing as they behave like a ready-made dry prepreg as reported by Friedrich et al., [128]. It is also being lesser prone to void formation due to the existence of more bleed channels as compared to conventional thermoplastic composites resulting into better wetting out of the fibers. Due to these reasons the commingled composites have better mechanical properties as compared to non-commingled composites [85].

The properties of composites mainly depend on the adhesion and interface between the matrix and fiber reinforcement. Hence, proper impregnation is necessary to achieve composite material for optimum properties.

The viscosities of most of the thermoplastic matrices are quite high, which hinders the proper wetting of fiber reinforcement. The flow distance during impregnation is needed to be reduced in order to overcome this problem. Partially impregnated intermediate material stage such as commingled yarns or fiber bundles impregnated with powder, offer a better route for rapid manufacturing process of thermoplastic composites due to the reduced flow distance.

Commingling is the most cost-effective way of intermingling fiber reinforcement and matrix [129]. Commingling can be carried out at fiber, yarn or fabric level [75]. Thermoplastic commingled composites can also be formed through the rapid pultrusion process[130]. The typical example is pultruding long fiber pallets for injection molding [100]. Commingled yarns are manufactured by mixing the reinforcement fibers with the thermoplastic matrix fibers during the spinning process or simply by twisting reinforcing and matrix yarns in doubling process. Commingled fabrics are made by interlacing the reinforcement and matrix yarns. Production of thermoplastic composites by commingled technique is one of the most promising and faster routes for thermoplastic composite fabrication as commingled yarns have better reinforcement-matrix distribution in the non-molten state before processing. The solid matrix is more evenly distributed around the reinforcement fibers. Division of the polymer matrix can be carried out using fiber or powder form (Figure 1-30).
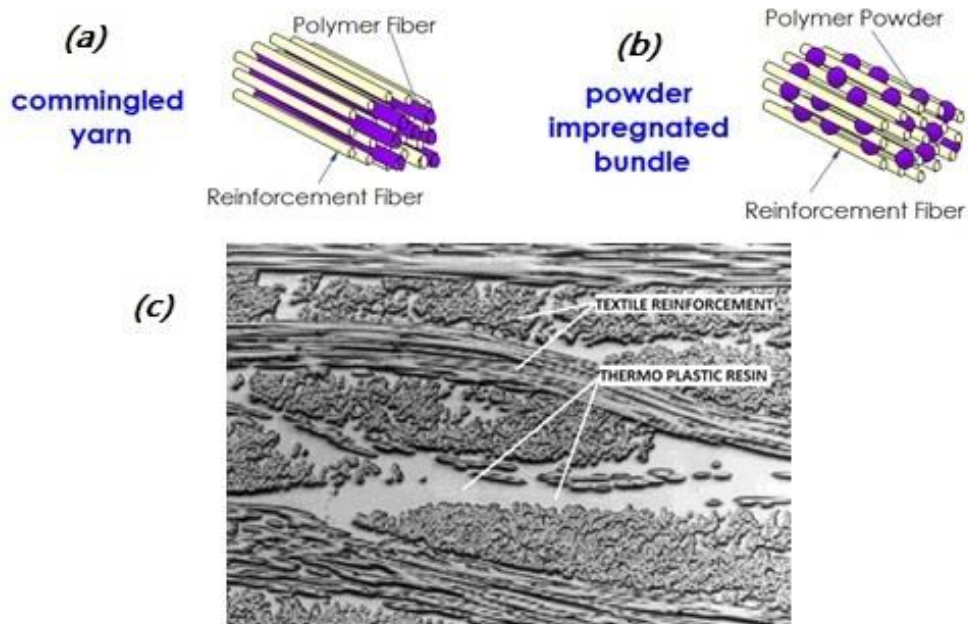
Figure 1-30. (a) Commingled yarn technique, (b) powder impregnated bundle and (c) microscopic view of textile reinforced commingled composite [131]

Commingling is a simple process with high production capacity. The product is cheaper (for cheaper resin used). Complex shapes can be made. This technique is also being employed in 3D-printer technology, in which mostly textile fibers with thermoplastic monofilaments are used. Commingled woven prepregs can be used in thermoforming with two-sided hot mold. A two-sided hot press mold would give higher FVF, as excessive resin would squeeze out. An expensive two-sided mold is required with the heating arrangement. Single-sided mold can also be used with vacuum bagging. However, due to the use of thermoplastic resins, it cannot be employed for high-temperature applications.

The commingling is done at various levels from fiber level to yarn to fabric level. The details of different type of commingling techniques are given below;

In order to make the commingled composites, different commingling techniques are employed, as shown in Figure 1-31 [132]. The first one (a) uses the technique of mixing the reinforcement fibers with the thermoplastic fibers at blow room stage during spinning process, which is the best mixing of reinforcement and matrix at fiber stage. Both reinforcement and matrix materials are in short-fiber form and twist weightage is quite similar for both. The second one (b) is the wrapping of core yarn reinforcement with outer thermoplastic fibers layer during spinning, called as core-spun commingled yarn in which the

core yarn (the reinforcement) is wound around with the thermoplastic fibers (both reinforcement and matrix materials are in short-fiber form). The third one (c) also uses the wrapping technique in which the core yarn (the reinforcement) is wrapped with the thermoplastic filament; the process is carried out at doubling stage of yarn in which the core reinforcement remains almost straight and most of the twist is taken by the outer wrapped filament. Both materials are in the form of yarns and the resultant yarn is called co-wrapped commingled yarn. The fourth one (d) also uses the wrapping technique in which the core yarn and the thermoplastic filament are twisted around each other, the process is carried out at doubling/twisting stage of yarn, in which both yarns attain same amount of twist per unit length. Both materials are in the form of yarns and the resultant yarn is called co-twisted commingled yarn. The co-twisted commingling technique has been employed in our current research work.
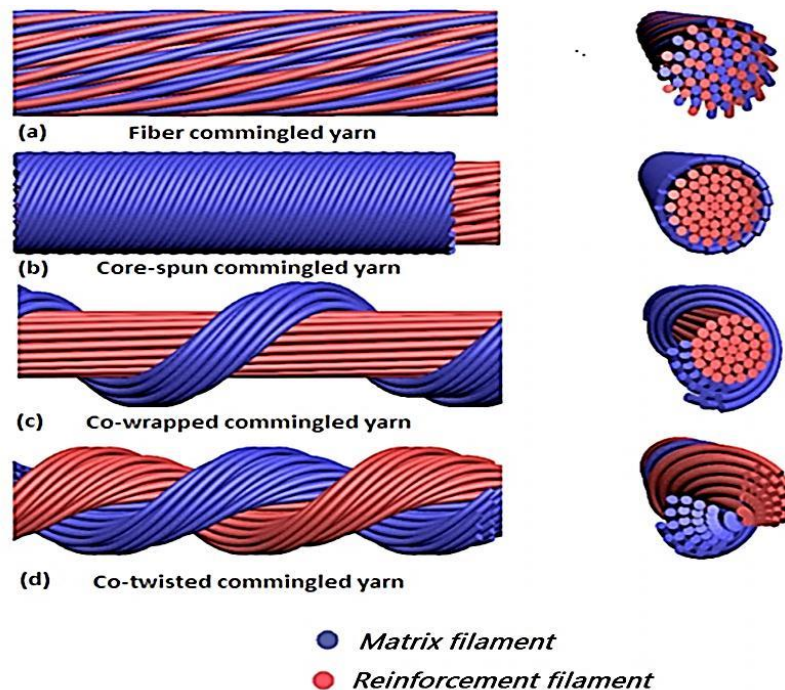
Figure 1-31. Hybrid yarn structures (a) fiber commingled (b) core-spun commingled (c) co-wrapped commingled (d) co-twisted commingled [85]

Commingling at nonwoven stage has been reported by Ameer et al., [121]. They inter-mingled the non-woven web of jute and polypropylene fibers. This is also a fiber stage commingling without the need of spinning process. The intermingled jute/PP web was subjected to thermoforming as shown in the Figure 1-32

Figure 1-32 . Fiber to fiber stage jute/PP nonwoven commingled fabric [121]

In the study conducted by Awais et al., [133], knitted and woven fabric composites (Figure 1-33) were manufactured using non-commingling and comingling techniques with jute, hemp and flax fibers as reinforcements. They fabricated three types of composite laminated (Figure 1-33); woven composites (WC), woven commingled composites (WCC) and knitted commingled composites (KCC). Out of these three techniques only the woven composites (WC) were non-commingled, they were made by stacking alternate layers of woven jute fabrics and polypropylene thermoplastic sheets. Afterwards, the effect of such comingling techniques on the mechanical properties of cross-ply composites (Table 1-11) was studied.

Table 1-11. Specimen combinations for the development of fabric preforms [133]

Sample No.	Fabric architecture	Material	Fiber volume fraction (%)
1	Woven	Jute	35 ± 2
2	Woven	Hemp	35 ± 2
3	Woven	Flax	35 ± 2
4	Woven commingled	Jute	35 ± 2
5	Woven commingled	Hemp	35 ± 2
6	Woven commingled	Flax	35 ± 2
7	Knitted commingled	Jute	35 ± 2
8	Knitted commingled	Hemp	35 ± 2
9	Knitted commingled	Flax	35 ± 2
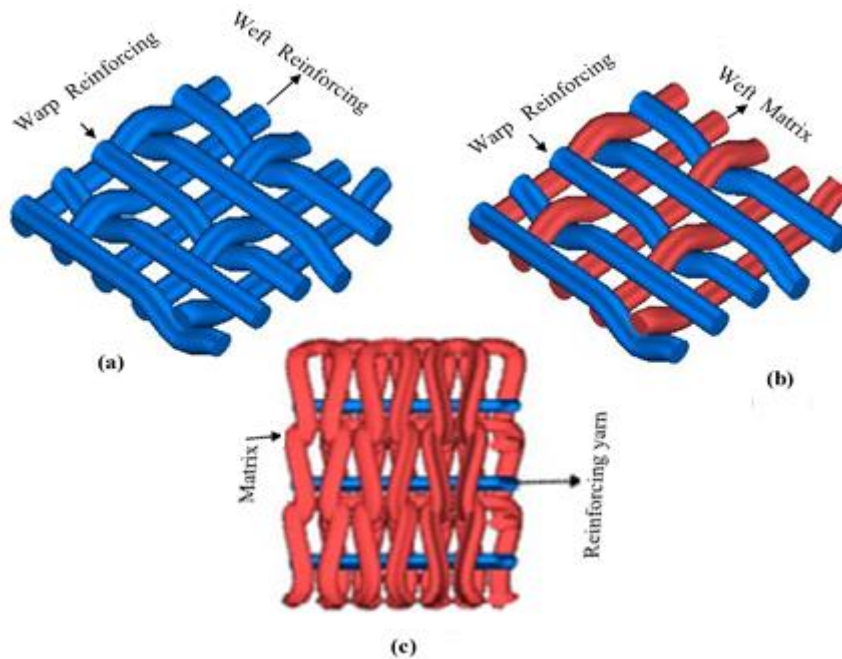
Figure 1-33. Graphical representation of fabric preforms (a) woven non-commingled, (b) woven commingled, and (c) knitted commingled [133]

The composites were subjected to short beam strength test. Flax composites (WC) have shown the highest value of short beam strength (10.6 MPa) than the hemp (6.35 MPa) and jute (4.93 MPa) composites (Figure 1-34). Flax composites (WC) have around 40% to 53% higher short beam strength as compared to the hemp and jute laminates respectively. The short beam strength results are attributed to the inherent mechanical properties of the

reinforcement fibers as the flax fibers have better mechanical properties as compared to hemp and flax.
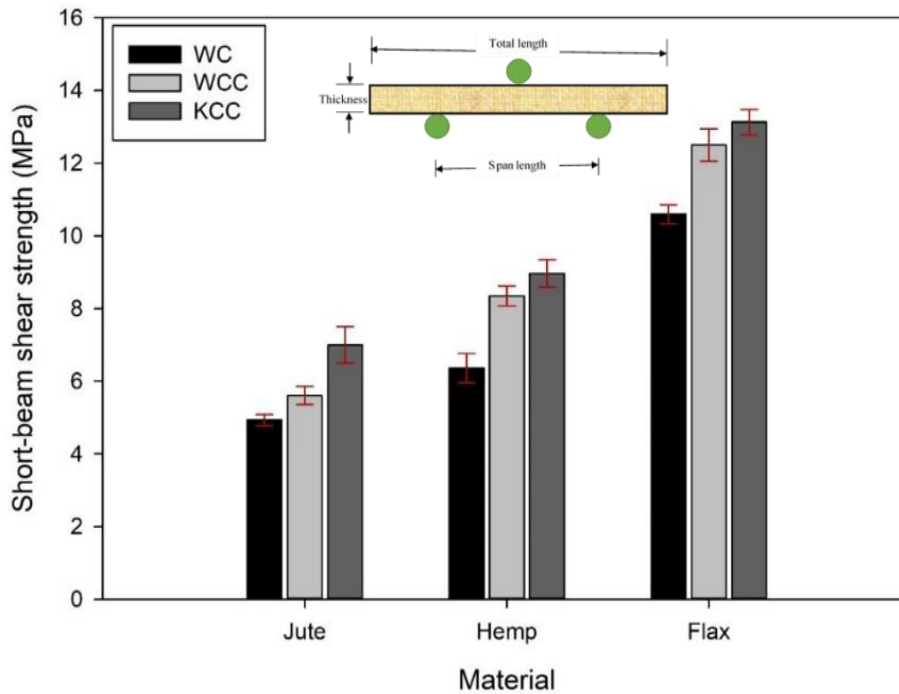
Figure 1-34. Short beam shear strength of the composite laminates [133]

A considerable difference was observed in the short beam strength of the composite laminates by with respect to fabric architecture. The short beam strength of knitted commingled composites (KCC) have shown higher values as compared to the woven composites (WC) and woven commingled composites (WCC). An increase of 20% to 29% in jute KCC, 7% to 29% in hemp KCC and 5% to 19% in flax KCC was observed as compared to their WCC and WC composites laminates. Figure 1-35 shows the load-displacement curves of short beam strength test.
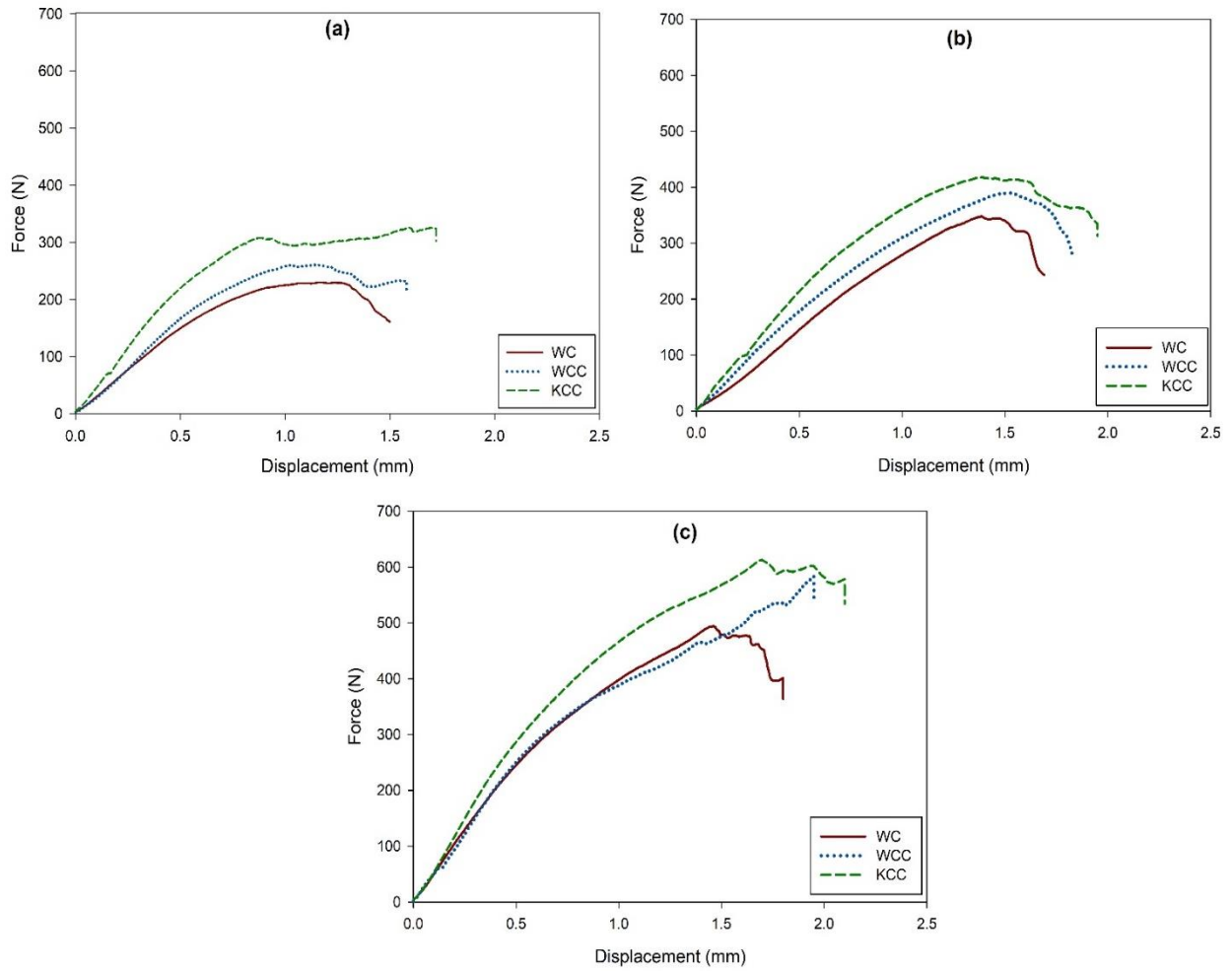
Figure 1-35. Load-displacement curves of (a) jute, (b) hemp and (c) flax laminates by the SBS test [133]
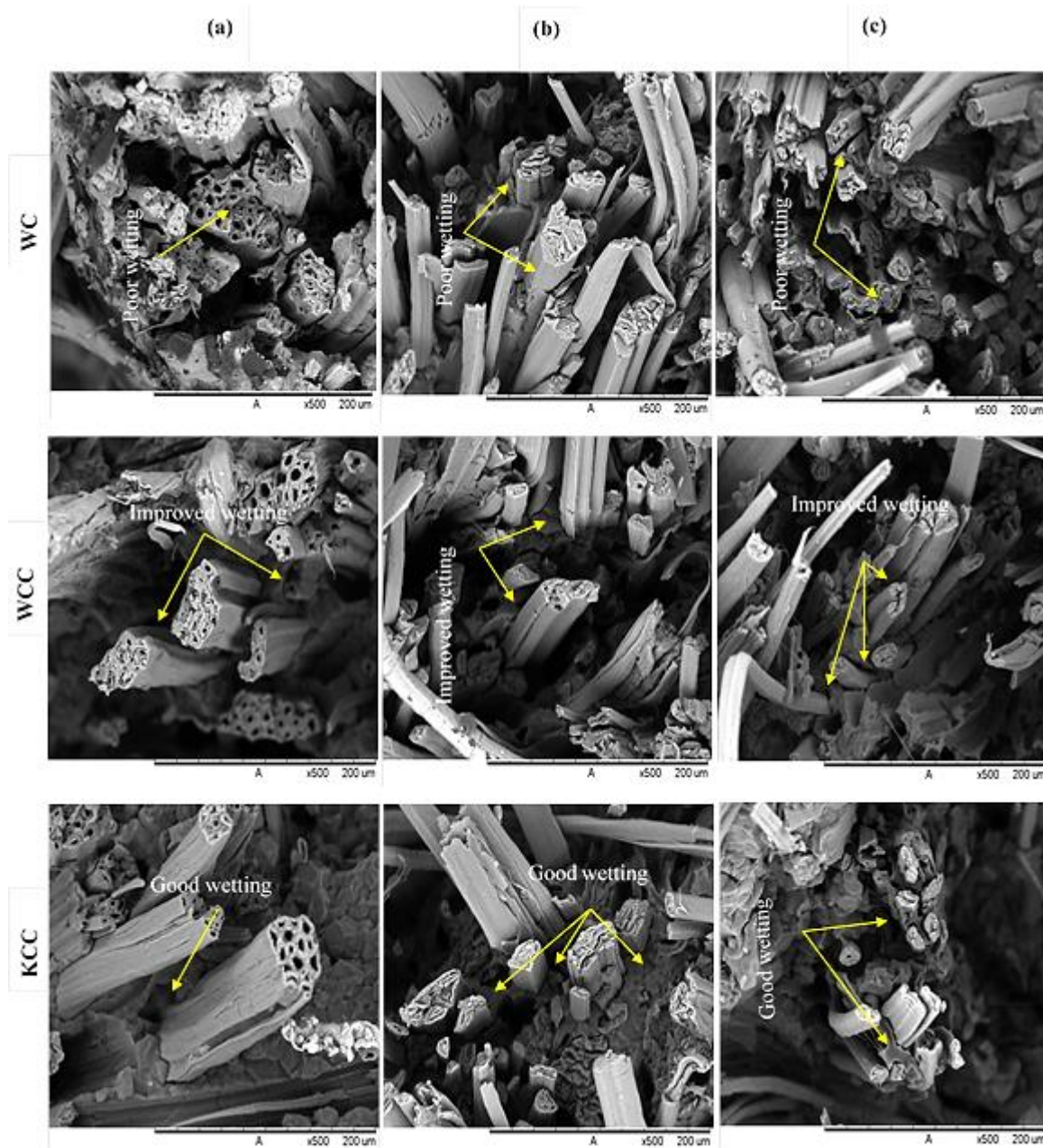
Figure 1-36. SEM analysis of impregnation behavior of (a) jute, (b) hemp and (c) flax laminates [133]

In the short beam strength load-displacement curves, first the load gradually increases to the peak value, and then with the initiation of the crack the first load-drop occurs. The KCC laminates shows higher peak load as compared to WCC and WC laminates. Beyond the peak load value, the KCC curve sustains and did not drop abruptly due to flexible reinforcement structure on the other hand, a the load curve drops more rapidly in WC laminates (Figure 1-35). This is mainly due to the better fibers impregnation in knitted commingled composites (Figure 1-36, which improves fiber-matrix interface. The CAI (compression after impact) test

was performed on the drop weight impacted composite specimens in order to measure the CAI strength values (Figure 1-37).
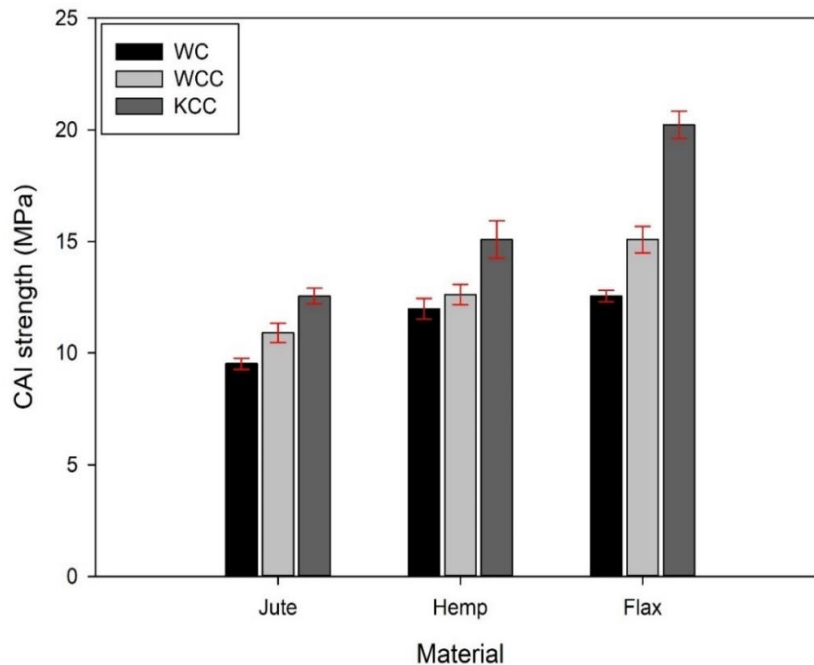
Figure 1-37.The CAI strength of the laminates [133]

The CAI strength of knitted commingled laminates was found maximum. Flax KCC laminates have exhibited 25.3% to 37.9% higher CAI strength, hemp KCC laminates have nearly 16% to 20.5% higher CAI strength and Jute KCC laminates have exhibited almost 13% to 24% higher CAI strength as compared to WCC and WC laminates, respectively.

The higher CAI strength in KCC laminates is due higher yarn orientation in knitted composites as these yarns were placed as straighter inlay-yarns with minimum crimp (Figure 1-38). Adversely, on the other hand, in the WCC laminates, the yarns were interlacing due to change in weave pattern resulting into lower orientation after melting-out of matrix yarns the waviness still remains in the WCC at the interlacement leftover points. The woven non-commingled composite behaves the same, as the reinforcement yarns are present both in warp weft directions, so after melting of the matrix yarns, higher amount of crimp sustains resulting in to lower CAI strength values of the WC laminates as compared to the WCC and KCC laminates [75,133].
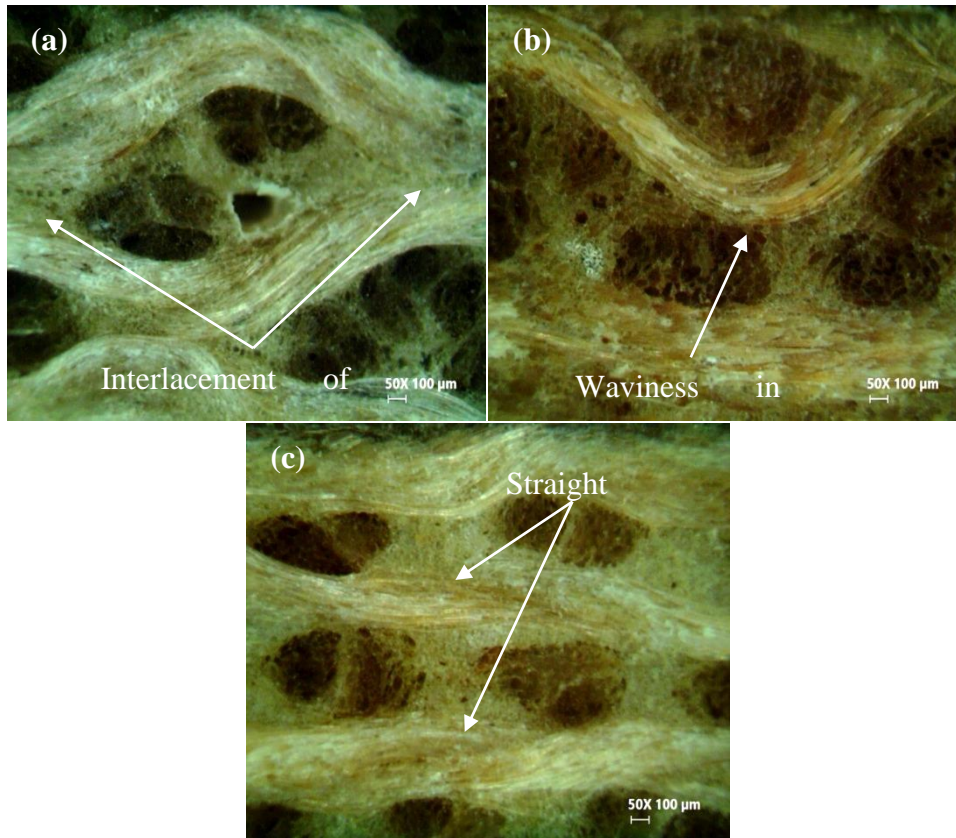
Figure 1-38. Optical microscopic images of (a) woven, (b) woven commingled and (c) knitted commingled laminates [133]

1.9   Summary

Natural fibers, in general, have a rough surface, which hinders in close packing of the fibers in a composite to have high FVF. The packing condition even becomes worse in spun fibers having hairiness as compared to filaments yarns. This area of research is likely to be addressed.

I.   There are several techniques reported in literature for surface treatments of natural fiber-based yarns and/or fabrics with an objective to improve fiber-matrix adhesion, however, no literature is found on burning of extruding fibers using the yarn singeing process.

As per the best knowledge of the author, there is no study available regarding the singeing of jute fibers in order to increase its tensile strength and weavability without the use of conventional sizing (coating) process upon the yarn.

II.   As per the best knowledge of the author 3D commingled weaving technique has not been used for natural fiber composites to date. The major issue is the poor melting-out of thermoplastic material in the thick inner layers, which do not directly contact the hot-plates/heating system. This is a major problem to be addressed, especially for thick 3D structures.

III.   Few works existed on the development of natural fiber-based prepregs and associated composites. The use of prepreg, especially the dry commingled prepregs, may result in the development of more homogenous and high-quality natural fiber composites with rapid fabrication.

IV.   As per the best knowledge of the author, there is no detailed study available regarding the manufacturing of thermoplastic composites through the application of gradual loading technique during thermoforming process.

Chapter 2. Materials, fabrication methods and Testing

This chapter discusses the details of materials, reinforcement manufacturing techniques, composite fabrication methods and testing methods used in this thesis. The jute yarn was used to make all type of reinforcement and was singed at flame to remove protruding fibers prior to weaving. After singeing the reinforcement was made either with the jute commingled or non-commingled yarns. The commingled yarn was prepared by twisting jute-PP yarn at simplex frame. The 1D (unidirectional), 2D and 3D reinforcements were prepared. The composites were made at compression hot press using instant and gradual loading techniques to check the effect of both the techniques. The tensile, flexural, short beam strength and Charpy impact tests were conducted as per standards to compare the mechanical properties of difference composites, later the tested samples were checked microscopely.

This chapter discusses the details of materials, reinforcement manufacturing techniques, composite fabrication methods and testing methods used in this thesis. The jute yarn used to make all type of reinforcement and singed at flame to remove protruding fibers before reinforcement weaving. After singeing the reinforcement was made either with the jute commingled or non-commingled yarn. The commingled yarn was prepared by twisting jute/polypropylene yarn at simplex frame. The 1D (unidirectional), 2D and 3D reinforcements were prepared. The composites were made at compression hot press using instant and gradual loading techniques to check the effect of both the techniques. The tensile, flexural, short beam strength and Charpy impact tests were conducted as per standards to compare the mechanical properties of difference composites, later, the tested samples were checked microscopely.

2.1 Jute fibers

In the current study, the yarns and fabrics made from jute fiber were used as reinforcement to make thermoplastic composites. These fibers were of origin of Bangladesh. The jute fibers used in current study are shown in microscopic image in *Figure* 2-1. The diameter of fibers was found mainly in the range 10-100 micrometer. These fibers were twisted to make yarn as reported in detail in the later sections.
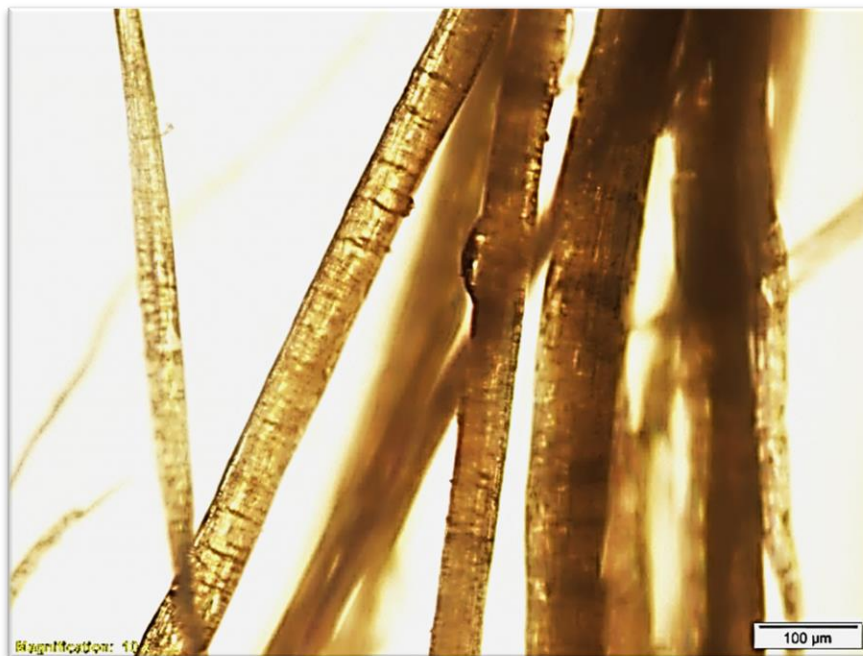
Figure 2-1. A microscopic image of jute fibers used in this study

FTIR analysis was carried out to observe non-cellulosic contents (e.g., hemicelluloses and lignin). *Figure* 2-2 shows the FTIR curve of untreated jute fibers. The C=O bonds in carboxylic acid shows the peak at ~1730 cm^{-1} which is due to stretch vibration ester components of cellulose and hemicellulose [134] and also due to the carbonyl group of lignin [135,136]. The peak at ~1240 cm^{-1} is due to C–O–C asymmetric stretching of the acetyl group of lignin [67].
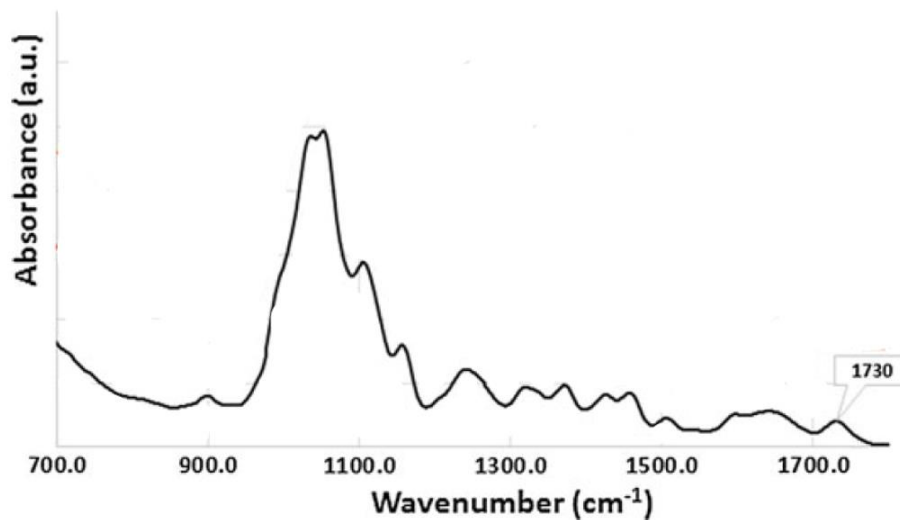
Figure 2-2. FTIR spectra of untreated jute fibers [67]

2.2 Properties and fabrication of jute yarn

Jute yarn made of jute fiber was procured from Thal jute limited (a local jute yarn spinning industry). Jute yarn count system (a measure of yarn fineness) is a bit different from the cotton-count system which is measured in number of hanks per pound (1 hank equal 840 yards) and also differs from the tex-count system (number of grams per km). Fineness of jute yarn is measured in number of pounds per spyndle (1 spyndle equals 14400 yards). A cotton count of 2.5 Ne means there are 2.5 hanks or 840 x 2.5 = 2100 yards in one pound weight of the yarn. In cotton system, as the count increases the yarn becomes finer and lighter. Thus a 2.5 Ne yarn is finer than 2.3 Ne (as used in our research work). A 236-tex count means; one-kilometer yarn length weighs 236 grams. In tex system, as the count increases the yarn becomes coarser and heavier. We used a 5-spyndle jute yarn for our research work, which means our jute yarn has 5 pounds weight for a length of 14400 yards. A comparison of cotton, tex and jute count system is given in Table 2-1[137].

Table 2-1. Cotton, Tex and Jute yarn count system [137]

No	Jute yarn types	Cotton count (Ne) hanks/lb	Tex count (g/km)	Jute count (lbs/spy)[b]
1	Fine jute yarn	9.8-5.3	60-103	1.75-3.0
2	CBC[a] yarn	4.9-2.9	120-205	3.5-6.0
3	Hessian warp	2.5-1.9	240-310	7-9
4	Hessian weft	2.5-1.44	240-410	7-12
5	Sacking warp	2.15-1.69	275-350	8-10
6	Sacking weft	0.84-0.42	700-1400	20-40
7	Carpet yarns	1.23-0.72	480-820	14-24
8	Jute blended yarns	11.8-2.15	50-275	1.5-1.8

[a]Carpet back cloth yarn, [b]Pounds (lbs) per spindle (=14400 yards)

The flow process of jute yarn manufacturing involves various steps. In first step the selection of Jute for batch is made. In this step the defects in the jute yarns are removed and then the yarn bales are sorted out on the bases of end use whether the coarser or the finer yarns are to be made. On the bases of yarn fineness jute is divided into three major types A (fair), B (good) and C (fine). Second is the piecing up process in which the jute strands are cut and packed tightly and then they are hammered to make fibers loose and soft so as to be processed further. Skilled workers keep the defective jute aside for use in low grade products. Third step is the softening process which includes lubrication of jute fibers with mineral oil so as to make fibers soft and pliable. In this process the fiber strands are also passed through fluted rollers in an oil emulsion bath for soaking. This process makes the fibers soft enough to be process on carding machine. In the fourth batching process the oil emulsion-soaked jute is placed under a closed cover for 48-72 hours, this makes the fibers further softer for the carding process. Next is the carding process in which the meshy web of jute fibers is made into a parallel fiber strand. Breaker carding removes the dust and impurities from the jute mesh, inner carding makes the fibers more parallel in sliver form and then finisher carding makes the sliver more uniform in terms of weight per unit length for spinning uniform yarn. The process of drawing-in involves mixing of four to six slivers of jute to further reduce its irregularity in terms of weight per unit length with more evenness in yarn orientation along the sliver length. The drawing-in stages may vary from two to three stages depending upon

the end product quality. The roving frame makes fine roving from thick carding slivers with slight amount of twist. Roving process is essentially required to making better quality jute yarns. The ring frame finally spins the roving into the end product with desired number of twists per unit length for required strength and end use. The yarns from the ring frame are then wound into larger packages of desired length on winding frames. The end product is then ready for weaving. Next step is the preparation of weaver's beam. The beam is fitted to the weaving machine, the fabric is woven and cut to desired length, folded and sewed for desired product like sacks, bags or baskets, and the end product is then packed in bails for sale.

Figure 2-3 [138] explains the jute yarn manufacturing process in pictures. (a) Shows the selection and (b) shows the grading of jute strands. (c, d) lubricating and pilling of jute batches. (e, f) shows the carding of jute from back and front of the machine. (g, h) Show the drawing-in process from back and front of the machine. (i, j) Show the spinning of jute yarn on smaller spinning bobbins with back and front views of ring frame and (k) shows the winding of jute on larger packages.

Figure 2-3. (a) Jute yarn selection, (b) grading of jute strands

Figure 2-3. (c, d) Lubricating and pilling of jute batches
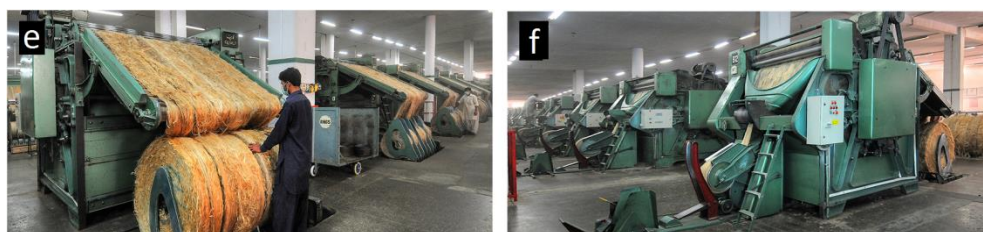
Figure 2-3. Jute carding, machine back(e) and front (f)

Figure 2-3. Drawing-in of jute fibers, machine back (g) and front (h)
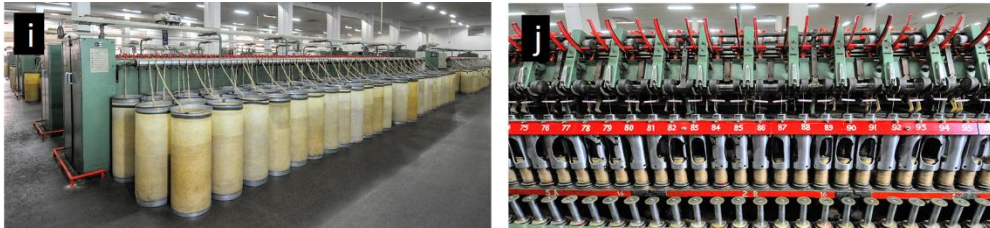
Figure 2-3. Spinning of jute yarn, ring frame back (i) and front (j)

Figure 2-3. (k) Winding of jute yarn [138]

2.3   Jute yarn singeing

In order to make 2D and 3D woven preforms, the jute yarn has to come across the stage of weaving. During the weaving process a textile yarn, especially the warp yarn is habitual of bearing various hurdles like tensile stresses, friction of yarns with the machine parts and abrasion among the yarns during shedding. In order to overcome these hurdles, the textile yarns are to undergo a preparatory process. Jute yarn, like cotton, has a larger amount of hairiness which needs size coating prior to weaving process (Table 2-2). The sizing process upon the yarn is followed by the desizing process. It is very unlikely to remove the sizing material completely. During the composite fabrication such size coating works as an obstacle hindering to have a good interface between the fiber and the matrix.

We employed a new technique for jute fiber, in order to make it more weave-able without using the hectic sizing/desizing process. The technique was to burn out the protruding fiber on the outer surface of jute yarn through singeing (Figure 2-4). Jute yarn was passed through gas burner at a yarn-linear speed of 80 m/min and flame length of 500mm; this resulted into

the burning of protruding fibers without damaging the yarn inside. The singeing technique is normally employed for sewing threads for a good quality surface finish [83]. Currently research related to singeing of jute yarn is not available. However, there are some papers mentioning singeing technique for cotton yarn. Zhigang Xia et al., [84] have reported removal of cotton yarn hairiness to 80% by the singeing process. But their main emphasize was to enhance yarn quality with lesser hairiness and better evenness, the effect of reduction of yarn hairiness on the improved weave-ability was not targeted. Singeing of jute yarn is shows in *Figure 2-4*. The jute yarn from larger size spinning package (4kg) was passed through the guide eye then through the gas burner tube with a jute yarn effective length of half meter passing through the flame, then through different guides and yarn tensioners and then finally wound on the package for further processing for weaving/commingling.
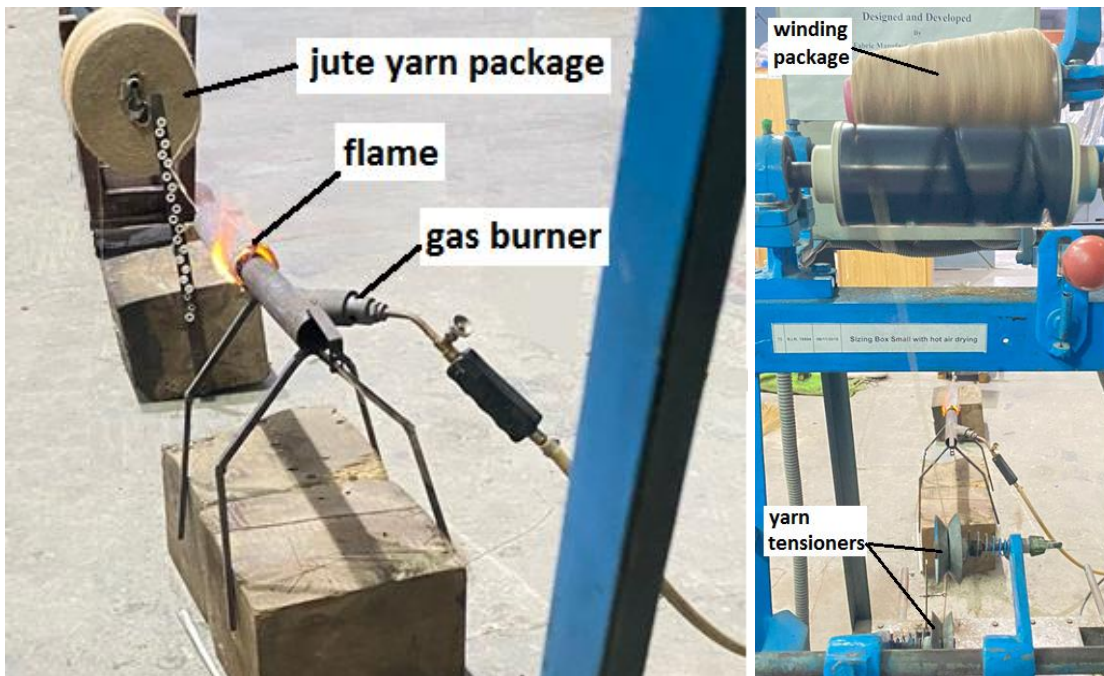
Figure 2-4. The singeing process of jute yarn

Figure 2-5 explains a clear difference of hairiness between singed and unsinged yarns, which can also be confirmed by Table 2-5 with 52% reduction in hairiness.
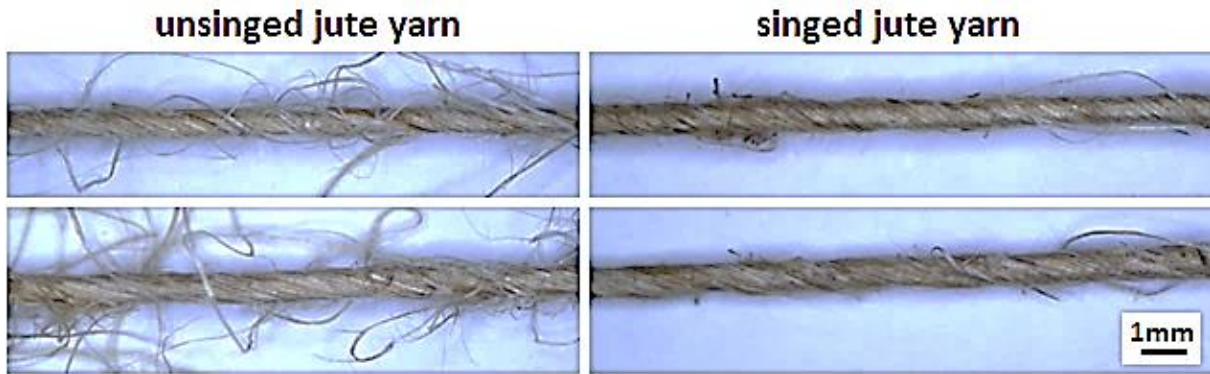
Figure 2-5. The difference of hairiness between unsinged and singed jute yarns

While on the other hand, Figure 2-6 shows even a better comparison of hairiness between the two yarn packages wound by unsinged and singed jute yarns. There is a great difference in their appearance; the unsinged yarn package shows a hairy and meshy appearance. Fabric made by using hairy unsinged jute yarn in warp and weft directions was woven with great difficulty, with lots of warp breakages. The weaving machine had to run pick by pick as there were lots of abrasion among the warp threads during shedding, resulting in to shed sticking providing no path for weft insertion. The warp shed was needed to be opened manually a number of times, hence the option of weaving with unsinged warp yarns was simply not employed.

Figure 2-6. Optical images of unsinged and singed jute yarns

Both singed and unsinged jute yarns were subjected to single yarn tensile test and it was strange to note that the strength of singed jute yarn was higher than the unsinged jute yarn.

The unsinged jute yarn count was 2.3 Ne as compared to singed yarn count at 2.5 Ne, but still, the breaking strength of singed yarn was 9.33% higher than the unsinged yarn. This is possibly due to the presence of lignin leftover in jute yarn. Jute yarn has a higher lignin content (13.3%) [139] as compared to other cellulosic non-bast fibers like cotton (0.4-1%)[140]. During the singeing process, as the yarn is passed through the flame, the leftover lignin around the fibers locally melts and as it moves away from the flame; again cools down and re-joins the jute fibers, which results in to sticking of the fibers in jute yarn, thus increasing its tensile strength. While, on the other hand, as reported by Zhigang Xia et al., [84], there was no increase in the tensile strength of singed cotton yarn and in fact the strength of cotton yarns was decreased by 1.4% after the singeing process. In cotton yarn no increase in the strength can be attributed to very low amount of lignin as compared to bast jute fiber.

Table 2-2 gives a comparison of the mechanical properties of unsinged and unsinged jute yarn. The tensile strength of singed jute yarn is 9.3% higher than the unsinged yarn, besides the fact that the singed yarn is 8% finer. Hence in fact a finer 236.2 tex yarn is 9.3% stronger than a coarser 256.7 tex yarn. The single yarn tensile tests were performed according to ASTM D2256 standard. The amount of Uster hairiness is some 52% lower for the singed jute yarn with lower value of coefficient of variation (CV%) than the unsinged. Uster hairiness is abbreviated as 'H'. The amount of hairiness 'H' is the amount of light transmitted by the protruding fibers of the natural yarn and detected by a light sensor as shown in Figure 2-7. It is a measure of the total length of protruding fibers divided by the length of the sensor (sensor length being 10mm). As hairiness is a length to length ratio hence has no units. Main body of the yarn does not transmit light and remains black.[141]
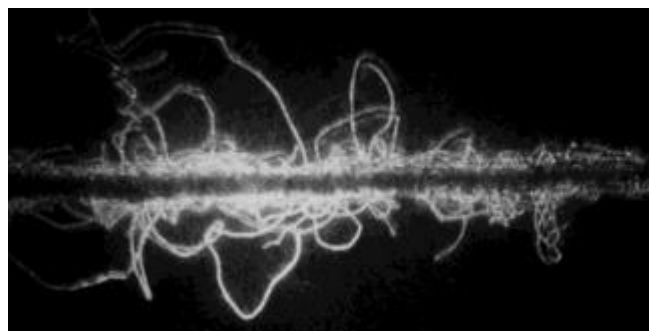
Figure 2-7. Method for measuring hairiness 'H' by the Uster-hairiness tester as a measure of amount of light transmitted by the protruding fibers and detected by a light sensor[141]

The increase in tensile strength due to singeing process upon the jute yarn is a 'remarkable discovery' of this research work.

Table 2-2. Testing results of single jute and cotton yarns (singed and unsinged)

	Yarn linear density	Breaking force (cN)	Elongation at Break (%)	CV Strength (%)	Uster Hairiness (H)[a]	CV Hairiness (%)	Comparisons
Unsinged Jute Yarn	2.30 Ne (256.73 tex)	1843±36.86	1.47	27.99	14.36	5.81	
Singed Jute Yarn	2.50 Ne (236.2 tex)	2015±39.29	1.63	22.83	6.94	2.83	9.3% stronger than unsinged / 52% less hairiness
Unsinged cotton yarn	40 Ne	305.9[b]	NA	NA			1.4 % weaker than unsinged
Singed cotton yarn	40 Ne	301.7[b]	NA	NA			

(H)[a]: a measure of natural yarn hairiness as per Uster standards, [b] Zhigang Xia et al., [84]

2.4 Polypropylene yarn and web

The Polypropylene (PP), a thermoplastic polymer, was used as matrix material. In order to make jute polypropylene non-commingled composite a felt-cloth sheet of polypropylene with an areal density of 133 g/m^2 was procured from the local market, as shown in Figure 2-8.
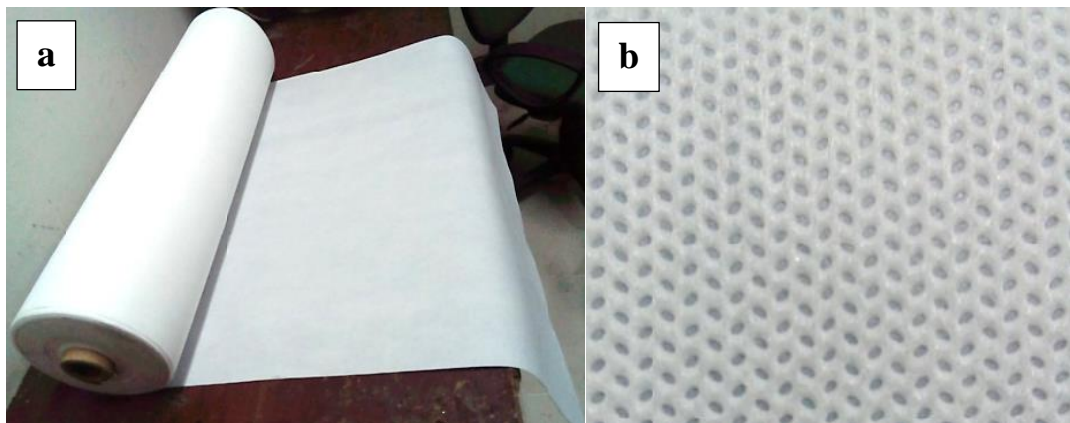
Figure 2-8. Polypropylene (a) felted sheet, (b) close-up view of PP sheet showing thermoforming spots with regular intervals to keep the non-woven fibers intact

For commingling purpose, polypropylene multifilament yarn was purchased from the local market, the specifications of which are given in the Table 2-3.

Table 2-3. Properties of the polypropylene filament yarn used for commingled composites

	Units	Polypropylene yarn
Yarn fineness	tex[a]	533.33[b]
	g/m	0.53
Density	g/cm^3	0.9
Single yarn strength	N	34.55±0.55
Elongation	%	35.62

[a] Linear density of yarn as grams/km, [b] yarn supplier data

Both the polypropylene yarns and polypropylene non-woven web were separately subjected to thermoforming at a temperature of 180°C and a pressure of 0.5bars, resulting into two different pure polypropylene thermoformed sheets. Both of these sheets were then subjected to the tensile tests in accordance with the ASTM D3039 standard; their results are shown in the Table 2-4.

Table 2-4: Tested mechanical properties of thermoformed sheet made from polypropylene yarn and non-woven web

Parameter	Units	PP yarn sheet	PP web sheet
Tensile strength	MPa	18.4±1.0	22.14±1.6
Young's modulus	MPa	518±8	585±27
Strain at break	%	4.2±1.0	3.42±0.4

2.5   Yarn Comingling Technique (YCT)

In the yarn commingling process four polypropylene filament yarns were co-twisted with one singed jute yarn. The yarn co-twisting was performed on the Simplex frame (in spinning) with a twist range of 1.5±0.5 twists per inch (TPI). For technical applications the optimum value of twist multiplier for yarns is 1.1, which equalizes to maximum amount of 2.4 twist per inch for 1100-tex Kevlar yarn as reported by DuPont [142].

Figure 2-9 represents the commingled yarn made from co-twisting of 1-jute and 4-polypropylene filament yarns using Z-twist on simplex frame in spinning, (a) shows the commingled yarn schematic, (b) shows the zoomed-in picture of polypropylene filament yarn

(c) shows the zoomed-in picture of jute yarn and (d) shows the actual photograph of commingled yarn with brownish jute and whitish polypropylene yarn. A one-to-one comparison of jute and jute/PP commingled yarn is given with scale. Diameter of jute yarn is around 0.7mm while the diameter of jute/PP commingled yarn is 1.8 to 2.0mm.
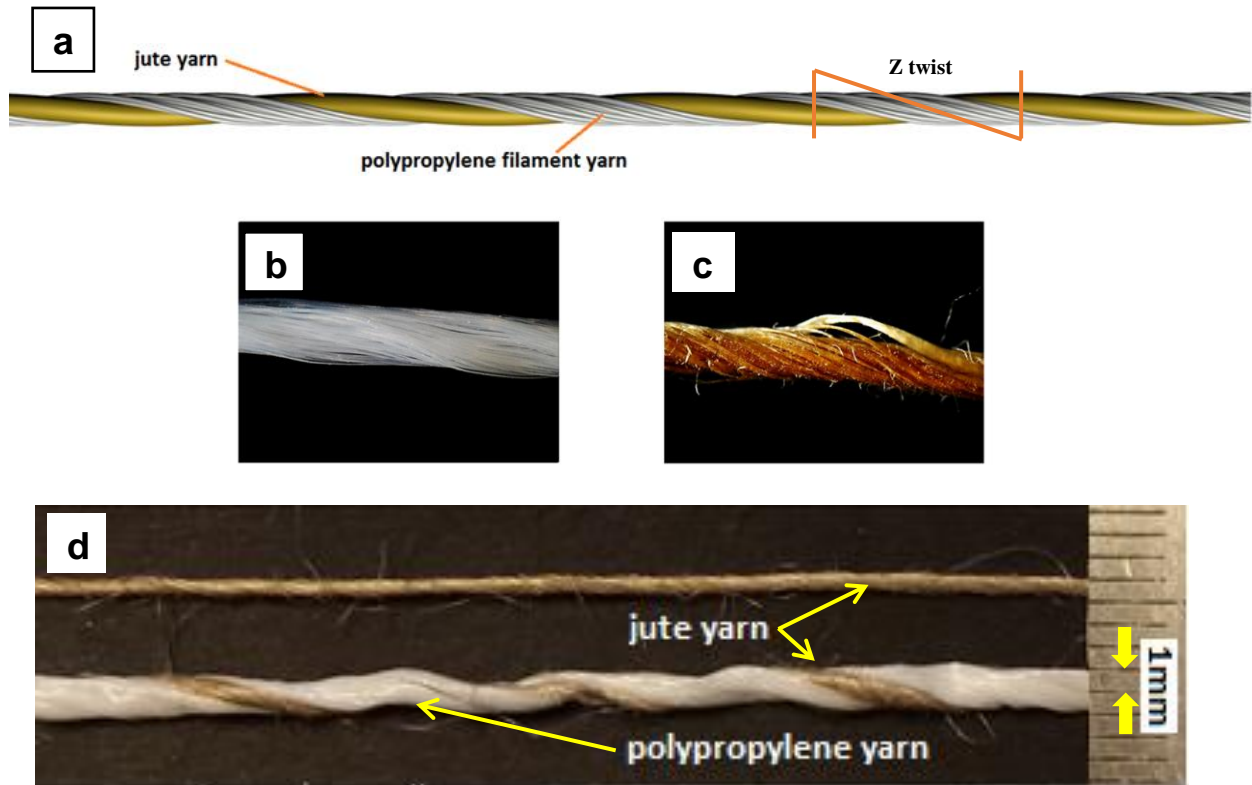
Figure 2-9. Commingled yarn made from co-twisting of 1-jute and 4-polypropylene yarns (a) commingled yarn schematic (b) Polypropylene yarn (c) Z-twisted jute yarn (d) one to one comparison of Z-twisted jute and Z-twisted jute/PP commingled yarn with scale

Figure 2-10 illustrates photographically the doubling process of commingled yarn on the simplex frame of spinning. (a) Shows the machine back where the jute and polypropylene packages were placed for doubling in a ratio of 1-jute:4-PP. (b) shows the frontal part of the simplex frame with the jute yarn being co-twisted to the polypropylene yarns. A zoomed-in view is also given. (c) Shows the lower front of the simplex frame where the doubled yarn is being wound on the simplex bobbin. (d) Shows the suspended array of simplex bobbins wound on the machine. (e) Shows the zoomed-in view of the doubled yarn on the simplex bobbin. (f) Shows the winding of the yarn on the larger cone package for the ease of further processing.
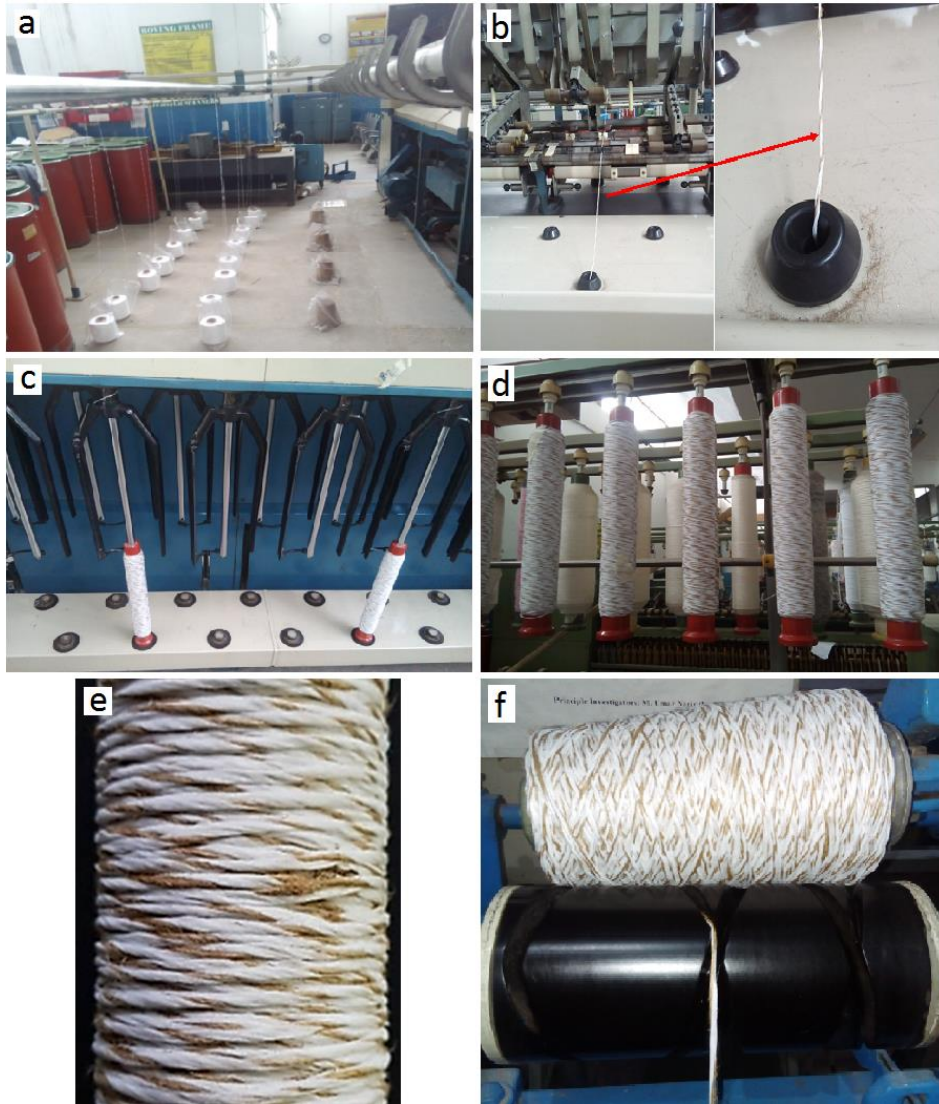
Figure 2-10. (a) Jute and PP packages placed at back of simplex machine for doubling in a ratio of 1:4, (b) frontal part of the simplex frame, jute yarn is being co-twisted with PP yarns, (c) doubled yarn being wound on the simplex bobbin, (d) array of simplex bobbins with commingled yarns. (e) zoomed-in view of doubled yarn on the simplex bobbin, (f) winding of the yarn on larger cone package

Table 2-5 details the parameters of jute yarn used for the weaving of commingled reinforcement and a comparison of the mechanical properties of singed and un-singed jute yarn. Singed jute yarn is some 8.7% finer than the unsinged yarn but with 9.3% higher strength and having 10.8% higher elongation. All yarn tests were performed according to ASTM D2256 standard.

Table 2-5. Properties of the jute yarn used for weaving of reinforcement

Parameters	Singed yarn	CV%	Un-singed yarn	CV%
Yarn linear density	2.5 Ne[a] (236.2 tex[b])		2.3 Ne (256.73 tex)	
Breaking force (CN[c])	2015 ± 39.29	22.83	1843 ± 36.86	27.99
Elongation %	1.63	22.37	1.47	22.01

[a]Ne: yarn linear density in English system (hanks/pound, 1 hank= 840 yards), [b]tex: yarn linear density in tex system (as grams/km), [c] CN: centi-newton

2.6 Fabric manufacturing techniques, unidirectional (UD), two dimensional (2D) and three dimensional (3D)

2.6.1 UD fabric manufacturing

Unidirectional preforms were made by simply wrapping the yarns, either commingled or non-commingled, in a parallel sheet form on a specially developed wrapping machine. A small mechanical system was designed, as shown in Figure 2-11 below, to wrap unidirectional parallel sheet of jute fibers stacks in 0° and 90°. A lead screw mechanism was used to wrap equi-distant jute yarns on a flat frame. The pitch of lead screw was responsible for laying 20 threads per inch in a parallel sheet form. The machine was operated manually. There were two inner layers of 0° followed by two outer layers of 90°, hence a total of 4 layers. Thus, unidirectional sheets were stacked at 90°/0°/0°/90° to form a composite.

As there were 20 threads per inch per layer in both directions, there were a total of 40 threads per inch in 0° direction and 40 threads per inch in 90° direction. The main reason of choosing four layers is simply to select an evenly biased combination both in longitudinal and transverse direction, so that both directional may have equal impact on mechanical properties. An uneven layer stacking e.g., 3 layers (90°/0°/90°) or 5 layers (0°/90°/0°/90°/0°) would have resulted into to the dominance of mechanical properties either in one direction.
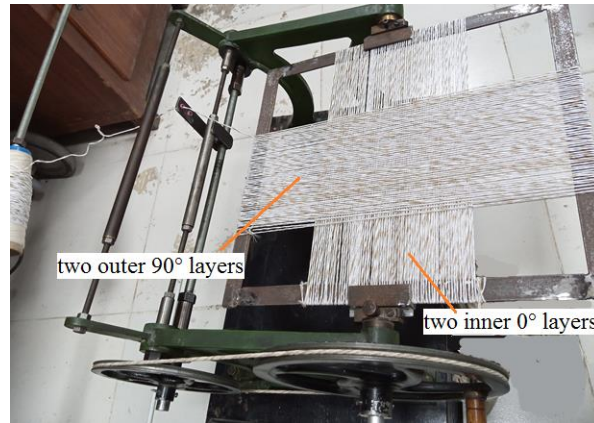
Figure 2-11. Mechanism for wrapping jute/polypropylene commingled and non-commingled performs (the image is showing wrapping of commingled UD)

Table 2-6 presents the parameters of unidirectional preform to be made from both non-commingled and commingled jute yarns. The areal density of non-commingled specimen was 247.3 g/m^2 and that of commingled was 989.3 g/m^2.

Table 2-6. Properties of unidirectional preform used for fabrication of non-commingled / commingled composites

Type of UD	Non-commingled	Commingled
Stacking sequence / angle	4 layers at 90°/0°/0°/90°	4 layers at 90°/0°/0°/90°
Threads / inch (0°)	20	20
Threads / inch (90°)	20	20
UD GSM / 4-layers	247.3 g/m^2 (only jute yarn)	989.3 g/m^2 (commingled yarn)
Average dry thickness	7mm (including PP sheets)	6mm

2.6.2 2D woven fabric manufacturing

In this study, for weaving 2D fabric, the jute yarn with a linear density of 2.3 Ne (256.7 tex) was used. The jute yarn was subjected to singeing process, prior to the weaving, in order to reduce the hairiness. The singed yarns were then used for the weaving of all non-commingled and commingled woven fabrics (Figure 2-12).

Figure 2-12. Weaving of Jute fabric

After the completion of singeing and commingling process, these jute yarns were then subjected to weaving preparatory process including, yarn rewinding in order to have required number of ends in the fabrics, preparation of weaver's beam and preparation of yarn packages for weft insertion.

The weaving of 5-end satin fabric (each with non-commingled-jute and commingled-jute/PP yarns) was then carried out on a conventional weaving machine (Figure 2-12). The reason for choosing the 5-end satin weave is to have longer floats of warp and weft threads across the fabric, resulting into higher yarn orientation in the direction of fabric thus having higher mechanical properties as compared to smaller float weaves like plain weave, which has lesser yarn orientation in the fabric direction with reduced mechanical properties (Figure 2-13) [143].
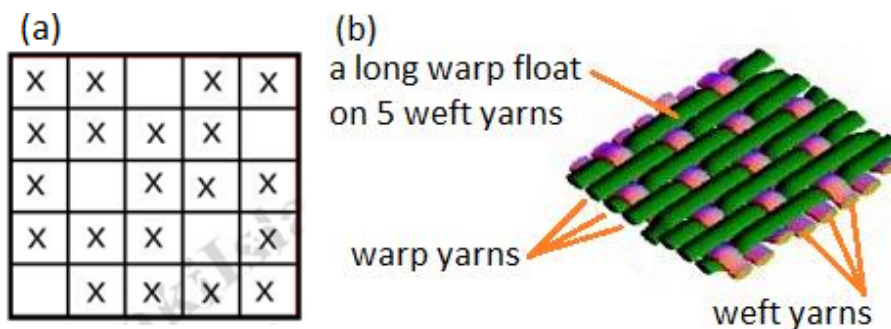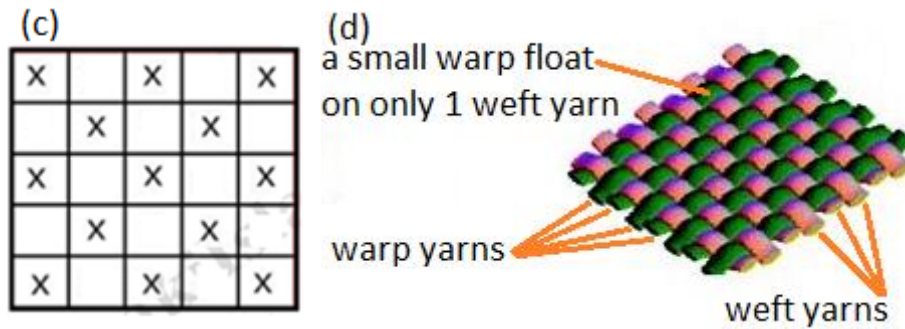
Figure 2-13. Comparison of short and long float weaves, (a) a design of long float 5-end satin weave, (b) fabric schematic of 5-end satin weave, (c) a design of small float plain weave, (d) fabric schematic of plain weave

Figure 2-14 illustrates the face side of 2D commingled and non-commingled woven fabrics made on conventional weaving machine with one-to-one same scale comparison.
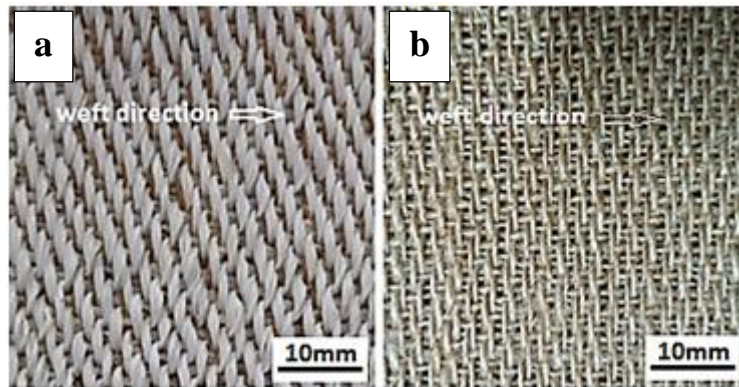
Figure 2-14. 2D woven fabrics (a) commingled (b) non-commingled

Table 2-7 illustrates the specifications of weaving machine and the specifications of non-commingled and commingled woven fabrics. Same singed jute yarn was used in both warp and weft directions (2.5Ne, 236.2 Tex) for non-commingled and commingled weaving.

The measured areal density of 2D non-commingled fabric was 442 grams per square meter and that of 2D commingled fabric was 1157 grams per square meter. The higher areal density of commingled fabric was due to the use of jute/polypropylene commingled yarn (one jute yarn was co-twisted with four polypropylene filament yarns). However, the density of pure jute in the commingled fabric was 388 grams per square meter and 769 grams per square meter for PP (388+769=1157 g/m^2).

Table 2-7. Woven fabric / weaving-machine specifications (for non-commingled and commingled)

Type of 2D fabric	Non-commingled	Commingled
Jute yarn count (singed)	2.5 Ne[a] (236.2 tex[b])	2.5 Ne (236.2 tex) jute / 2133 tex PP
Fabric weight	442 g/m^2 (only jute)	1157 g/m^2 (388 g/m^2 jute + 769 g/m^2 PP)
Fabric weave	5-end satin	5-end satin
Fabric width	24 inches	24 inches
Type of shedding	Dobby	Dobby
No., of heald frames	05	05

[a]Ne: yarn linear density in English system (hanks/pound, 1 hank= 840 yards),

[b]tex: yarn linear density in direct system (as grams/km),

GSM (g/m^2) is areal density in grams per square meter

2.6.3   3D commingled fabric manufacturing

With respect to weaving process the 3D fabrics can be divided into two types, the 2D woven 3D fabrics and 3D woven 3D fabrics. 2D woven 3D fabrics, with limited thickness, can be woven on conventional 2D weaving machines with little modifications. 3D woven 3D fabrics are woven on specially modified weaving machines with higher thicknesses.

In our current research work we wove 3D orthogonal fabric on a conventional 2D rapier weaving machine with certain modifications. Three set of yarns are used in the 3D orthogonal fabric, the x-yarns, y-yarns, and z-yarns considered in weft direction, warp direction and in vertical through the thickness direction, respectively.

Figure 2-15 represents a schematic of a 5 layer 3D orthogonal jute/polypropylene commingled fabric (5 layers of weft). (a) Represents schematic warp cross-section showing two types of warp yarns, the stuffer y-warp yarns and the z-warp yarns. The repeat size of stuffer yarns is being completed on 24 ends (warp yarns), while the repeat size of z-yarns is completed on 6 ends (warp yarns), including 2 commingled and 4 pure polypropylene yarns (b) Represents the actual 3D woven fabric, in which the proportional ratio of z commingled and z pure polypropylene (1:2) is clearly visible (pure polypropylene yarns can be characterized by white filaments). (c) Represents schematic weft cross-section of 5 (weft) layers 3D orthogonal fabric with 4 layers of stuffer warp and z-yarns holding the outermost weft layers in position. The repeat size being completed on ten picks. (d) Represents the schematic prospective view of 3D orthogonal structure.
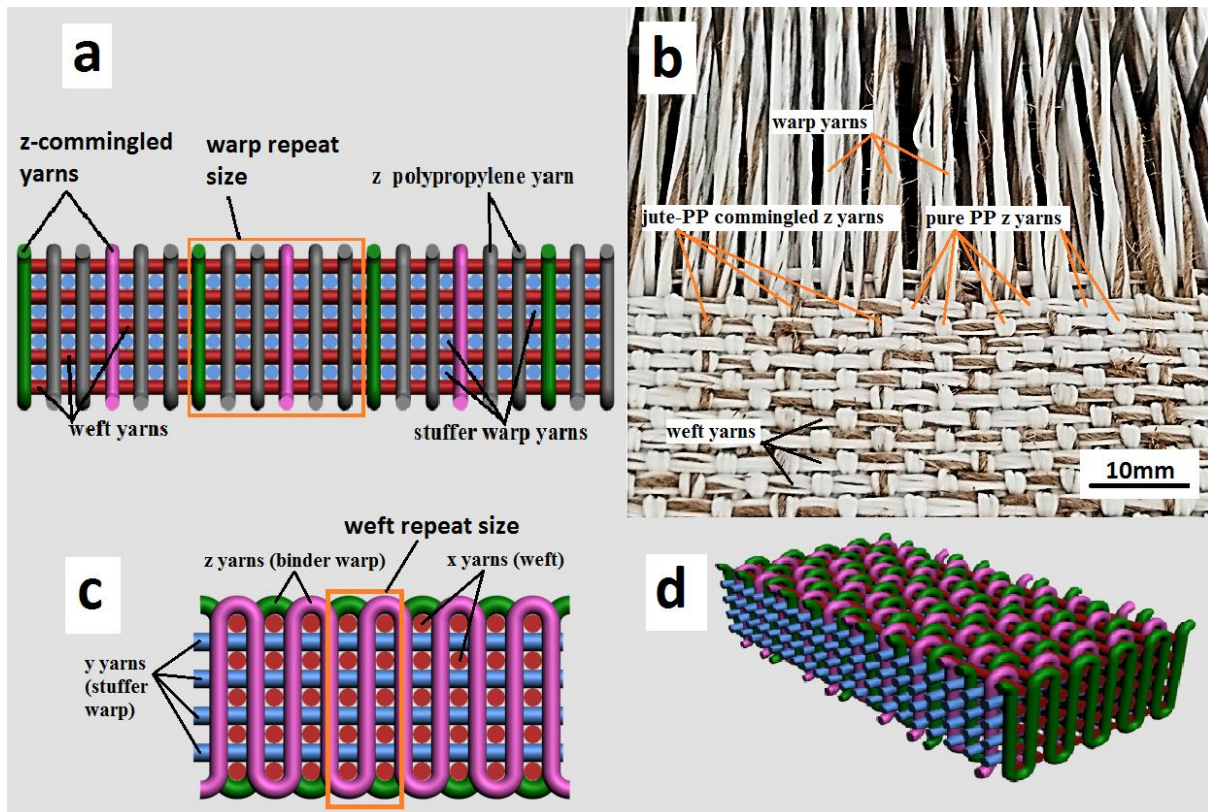
Figure 2-15. Schematic representation of 5 layer 3D orthogonal commingled fabric (a) warp cross-section showing z jute yarns, PP jute yarn, warp repeat size, (b) actual on loom 3D woven fabric, (c) weft cross-section showing 5 layers weft, 4 layers warp, weft repeat size (d) 3D view

Both y and z yarns are used in warp direction, coming from the creel. In 3D orthogonal fabric y yarn are considered as stuffer and z-yarns are considered as binder. Both x and y yarns have almost zero amount of crimp (waviness), while the calculated crimp of z-binder yarn was at the highest level (2.5 times of the y-stuffer yarn). Due to this huge difference of crimp between y and z yarns, weaving from a single beam is not possible. Weaving directly from the yarn creel is a better option which minimizes the tensions variations in a much better way.

2.6.3.1   Advantages of weaving directly from the creel

There are several advantages of weaving a 3D fabric from the creel, one major advantage is to minimize/compensate the tension variations among the warp threads, in conventional 2D weaving where the warp threads are coming from the weaver's beam, there is always a risk of tension variations among the warp threads due to the difference of crimp among the warp threads, especially while weaving the fabrics with unequal warp floats like Bedford cords, in

which plain and twill weaves run parallel to each other. In such a case the warp yarns with higher amount of crimp becomes tighter in the fabric (e.g., plain weave) and the warp yarns with lower crimp becomes loose (e.g., 3/1, 4/1 twill weaves). The use of creel eliminates this type of problem, where the warp yarns work on an 'on-demand-supply' method. In a negative creel system, the drive/linear-speed of the warp yarns is governed by the dragging force of cloth take-up (this mechanism is called a negative let-off mechanism, while in a positive let-off mechanism the spindles upon which the warp packages are mounted are to be rotated by some power motor drive). In such negative let-off system, if a warp yarn has higher amount of crimp (like the z-yarns) then it will have a higher dragging pull (per unit length of the woven fabric) by the cloth take roller, as compared to the stuffer yarn having almost zero amount of crimp.

Figure 2-16 explains the layout of weaving machine upon which 3D orthogonal commingled fabric has been woven. The creel capacity of weaving machine is 800 ends. The commingled yarns were wound upon the spools and a side-end with-drawl technique was used to unwind the yarns from the packages. The spools were mounted on metallic spindles and rotated under spring tension. Average tension on warp yarns was kept at 1 newton (100gf, grams force). For technical yarns side-end with-drawl is preferred to over-end with-drawl, in order to prevent the introduction of twist, which is imparted to the yarn during the over-end with-drawl (one turn is introduced to the yarn per one coil unwinding). As already discussed, a twist range up to 2 tpi (twists per inch) was used during the commingling process of jute/polypropylene, hence additional amount of twist must be avoided (for a z twisted yarn, an over-end with-drawl in clockwise direction would add one twist per one yarn coil unwinding from the package and vice versa for anticlockwise with-drawl). Besides this, in an over-end with-drawl, additional tensioning mechanism is required which will have a direct contact/friction with the yarn, which in turn again affects the mechanical properties. Moreover, in an over-end with-drawl, the unwinding coils also suffer friction with the inner layers of yarns on the package. An over-end with-drawl, by default, imparts almost negligible tension to the yarn especially when the with-drawl is at very creeping speed (e.g., weaving directly from the warp creel), however high speed over-end with-drawl causes ballooning tension (e.g., ballooning tension on weft in airjet weaving) upon the with-drawled yarn. In a side-end with-drawl the package rotation is a must that means the friction is between the spool and the spindle, thus this friction can be used to impart tension on the with-drawled yarn, in order to increase the yarn tension the amount of friction is to be increased by increasing this frictional force (through increased spring pressure etc.). However there in a drawback of this side-end

with-drawl, with decrease in diameter of the unwound package the yarn tension will increase, more decrease in diameter will cause more increase in yarn tension. This variation in tension can be minimized by using an initial larger diameter spool core. If a predetermined length of yarn is unwound from a larger core diameter, there will be less change/decrease in package diameter from the start till the end of with-drawl as compared to a core with very small diameter. In our case we used a larger 3.5 inches initial core diameter with a commingled yarn length of 130 meter especially for the z-yarns which have much higher consumption during weaving (a calculated 2.5 times higher). Winding of 130 meters resulted only in to an increase of ½ inch in diameter from start to end, consequently during the with-drawl of 130 meters the diameter is only decreased by half an inch which do not increment the warp tension to a greater amount. Different sections of weaving machines have been explained in Figure 2-16. The warp yarns (stuffer and z-yarns) from the packages (a) on the creel (b) were passed through the low friction ceramic guides (c). In order to minimize the friction, quite a few numbers of guides/contact-points were used per warp thread. For each warp thread, right from the creel to the fell of cloth, there were a total of four friction points, first ceramic guide eye at the creel (a), second ceramic guide eye behind the heald frames (d) at about 2 meters distance, third the unavoidable heald wire eye (e) and forth the unavoidable reed (f), then comes the 3D fabric weaving region. A complete perspective view of 3D weaving machine is shown in (g), while the dobby shedding system along with the design pattern is shown in (h). Average distance of each warp thread, from creel to the fell of cloth, was 3.5+ meters (technically called effective warp length). Average elongation of warp yarns was 5%, that means a yarn length of 3.5 meters can be stretched to 3.5 x 5% = 175mm or 7 inches. This additional stretch length of 7 inches helps to compensate during the shedding process, hence additional "easing motion" was not required. This additional length helps to increase the back-shed length, which greatly reduces the warp tension during shedding. Practically no slackness was observed in the warp threads during shed crossing (a point of minimum warp tension), thanks to the 3.5m of effective length of warp threads with an additional compensation of 7 inches to eliminate the need of additional easing motion (a system used on weaving machine in order to compensate against the reduced warp tension during shed crossing/closure and conversely to compensate increased warp tension during shed opening for weft insertion).
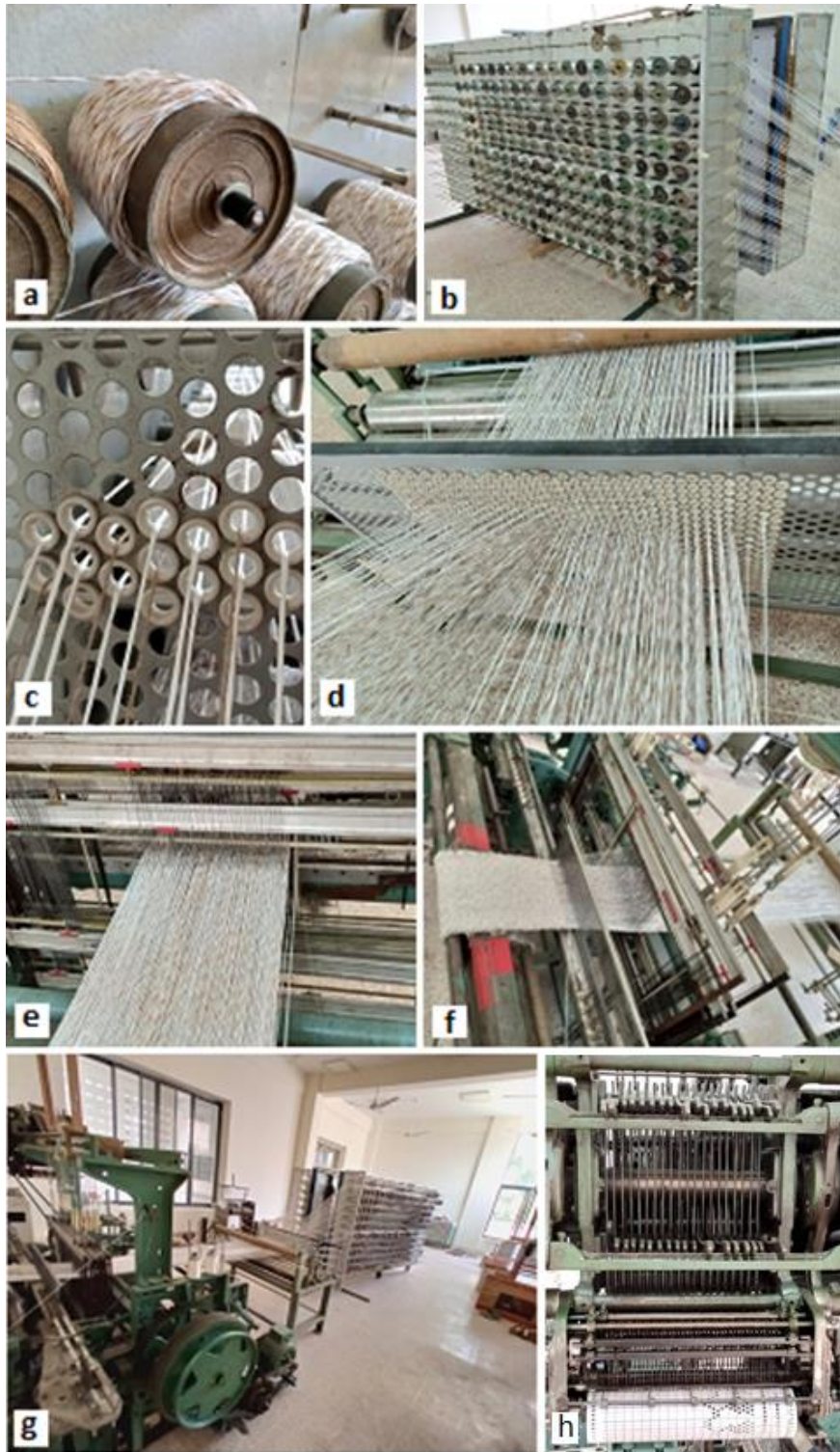
Figure 2-16. Layout of rapier weaving machine to weave 3D orthogonal fabric, (a) creel portion, (b) warp yarns packages at creel, (c) ceramic guide at creel,1ˢᵗ warp guide, (d) 2ⁿᵈ warp guide behind weaving machine, (e) yarn passage through heald frames, (f) machine front view with 3D woven fabric, (g) weaving machine, (h) the dobby shedding mechanism along with design pattern

The technique to be used for 3D orthogonal weaving is different from that for conventional 2D weaving. It is explained step by step as under:

2.6.3.2 The "shedding without shedding technique" for weaving 3D orthogonal fabrics

The phenomenon of shedding to weave 3D orthogonal fabrics is somewhat different form the shedding of conventional 2D weaving. Firstly, in conventional 2D weaving, every warp thread is involved in shedding process resulting into interlacement of warp with the weft, causing crimp in both threads, but in 3D orthogonal weaving certain warp threads need not to cross each other, these are called stuffer warp threads. Figure 2-15 shows schematic cross-sectional view of a 5-layer 3D orthogonal fabric, in which there are four layers of stuffer (y) yarns as a, b, c and d. there are two binder (z) yarns B1 and B2 and five layers of weft (x). Figure 2-18 explains the "shedding without shedding technique" for weaving 3D orthogonal fabrics. The heald frames of the two z-yarns B1 and B2 interchange their positions after every five picks. For the 1st pick (a) only B1 is up and all other heald frames are down. For the second pick (b) the heald frames of stuffer yarns 'a' and B1 are up and all others down. For the 3rd pick (c) the heald frames of stuffer yarns 'a' and 'b' and B1 are raised and all remaining are down. For the 4th pick (d) the heald frames are up for a, b, c and B1 and remaining down. For the 5th pick (e) the heald frames for a, b, c, d and B1 are up and all others are down. Now for the 6th pick (f), heald frames for a, b, c, and d remains up B1 moves down and B2 moves up and so on... It is interesting to note that the heald frames for a, b, c and d need not to cross each other, as clear from the cross-sectional view (Figure 2-15) that they are well apart from each other. During the shedding process a special shedding technique can be employed so that the warp threads coming from a, b, c and d heald frames do not come across each other, hence any sort of abrasion among these groups of stuffer warp threads would be out of question. This special weaving technique is called as "shedding without shedding technique", in which the stuffer warp threads a, b, c and d take part in the shedding process, means they do move in between top bottom shed lines as required but do not enter in each other's vicinity at any stage. This is carried out by staggering the heald frames in height. In this technique the heald frame are so adjusted that even in a complete shed closure position the warp shed forms multiple lines one above the other (in the same order as 'a' shed line is above 'b' shed line, 'b' shed line is above 'c' shed line and 'c' shed line is above 'd' shed line).

2.6.3.3   Weaving machine settings for keeping the weft threads in vertical columns

In a 3D orthogonal fabric, ideally, the layers stacking of weft threads are such that they are exactly one above the other in vertical columns. In order to arrange these threads in right angle columns certain machine settings are required.

The 3D orthogonal fabric was woven on a rapier weaving machine, in which the fabric take-up system (the fabric dragging forward system) was equipped with an intermittent ratchet and pawl mechanism. Conventionally this mechanical pawl system is bound to rotate the ratchet wheel on every pick (weft yarn). As the weaving machine was equipped with dobby shedding system, so this shedding system was used to disable the rotation of the take-up roller on every 5th pick by the used to special harness arrangement which attaches the take-up driving pawl to the lifting jack of dobby. By the use of this arrangement the weft threads were beaten-up one above the other forming a vertical column of five picks. Figure 2-17 explains how the commingled picks are arranged in vertical columns in the actual 3D woven fabric.
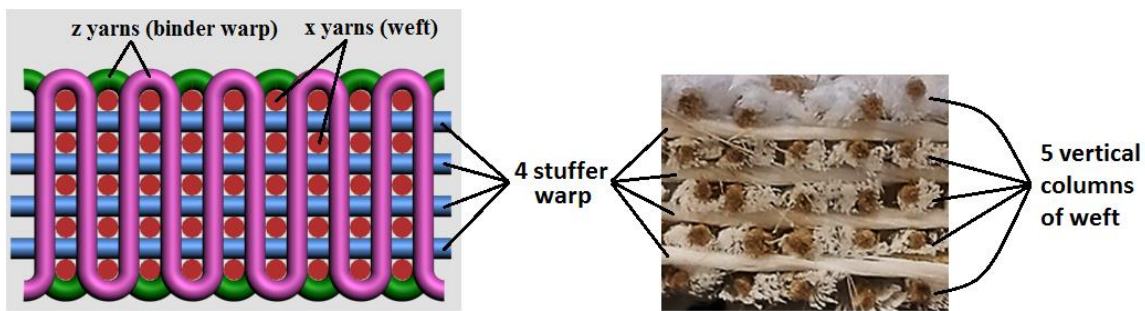
Figure 2-17. Schematic weft crossectional view with actual 3D woven fabric
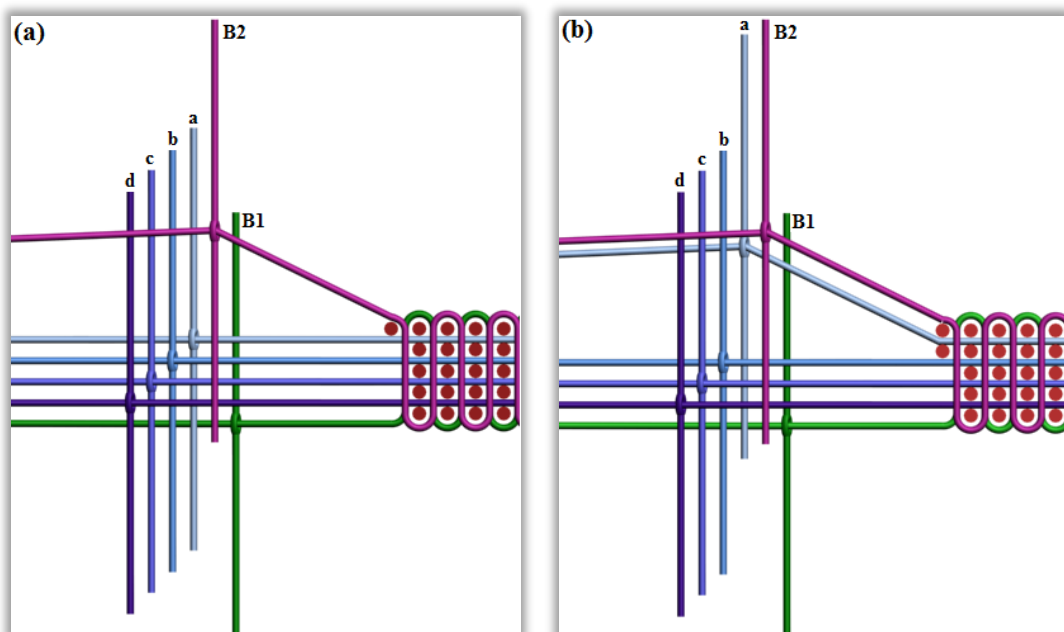
Figure 2-18. Use of 'shedding without shedding technique' by the use of shed staggering in height and arrangement of picking order in 3D orthogonal weaving, (a) binder B2 raised B1 down, all stuffers a, b, c, d down and 1st pick inserted, (b) B2 raised B1 down,, stuffer a raised, b, c, d down and 2nd pick inserted
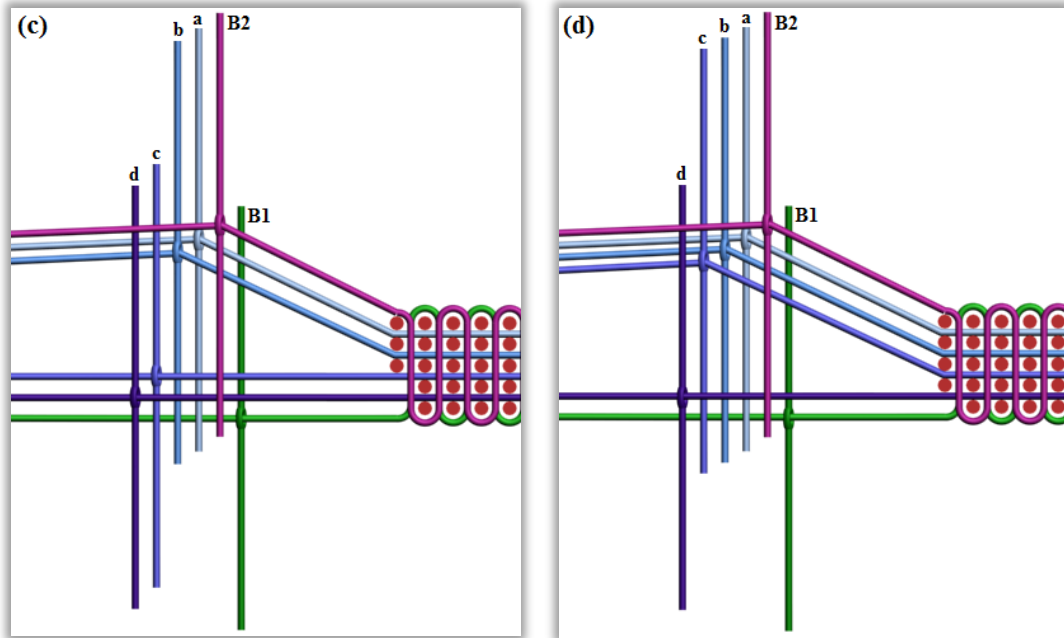
Figure 2-18. (c) B2 raised B1 down,, stuffer a, b raised c, d down, 3rd pick, (d) B2 raised B1 down,, stuffer a, b, c raised d down and 4th pick inserted
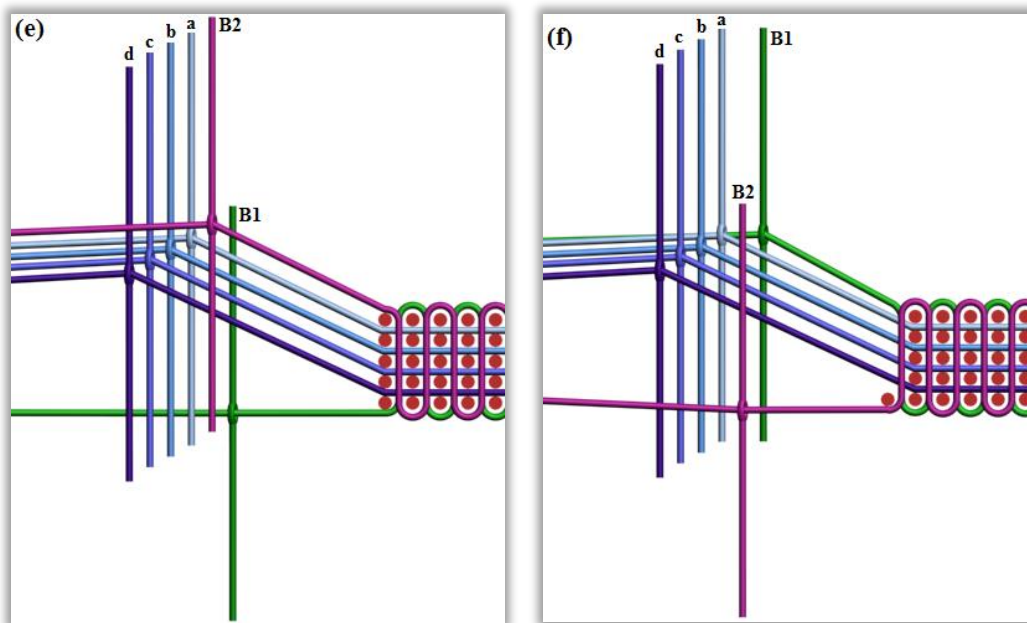
Figure 2-18. (e) B2 raised B1 down,, stuffer a, b, c, d raised, 5th pick, (f) B2 down, B1 raised, stuffer a, b, c, d raised, 6th pick,
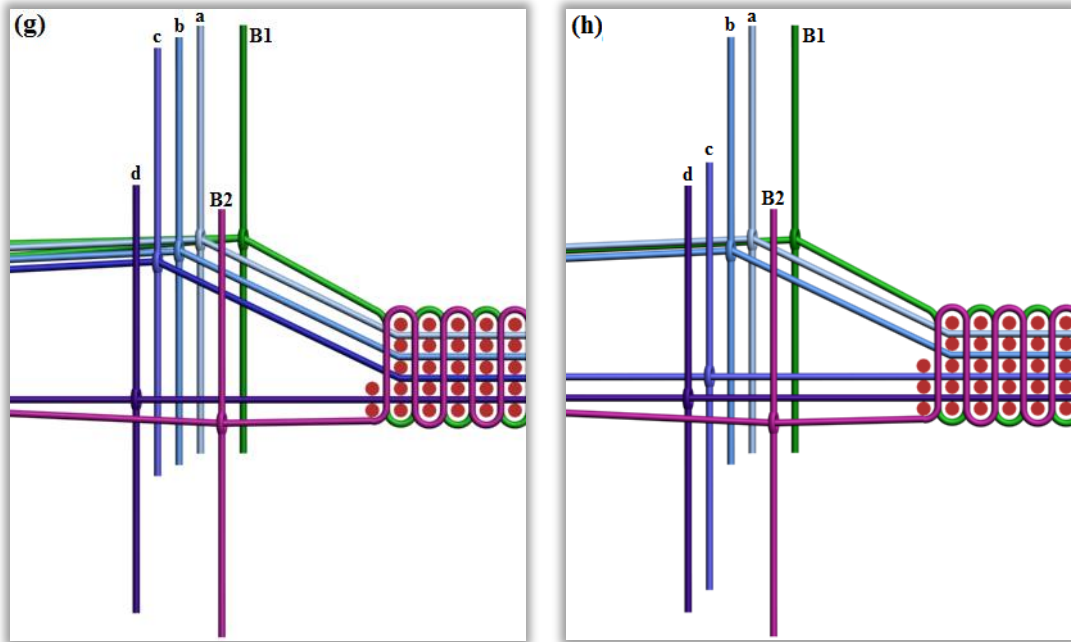
Figure 2-18. (g) B2 down, B1 raised, stuffer a, b, c raised, d down, 7th pick, (h) B2 down, B1 raised, stuffer a, b raised c, d down and 8th pick inserted
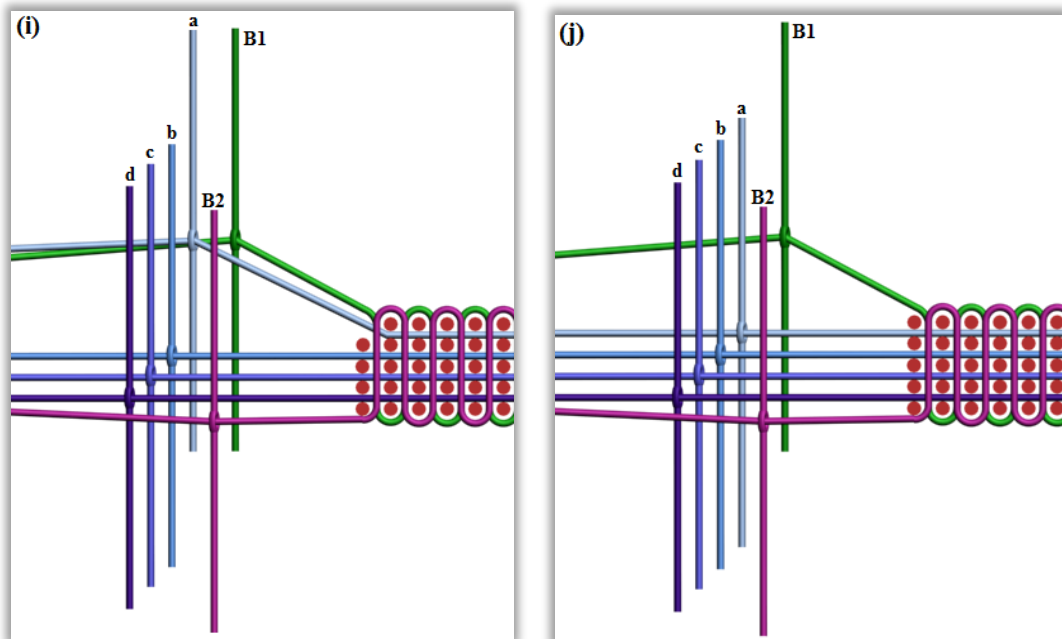
Figure 2-18.(i) B2 down, B1 raised, stuffer a raised, b, c, d down, 9th pick, (j) B2 down, B1 raised, stuffer a, b, c, d down and 10th pick inserted

2.6.3.4   Modification in picking order for weaving 3D orthogonal fabric

Figure 2-19 explains two different possible arrangements of picking orders to be used for weaving 3D orthogonal fabric, (a) explains the normal conventional picking order with weft

cross-sectional view, while (b) explains the corresponding lifting plan of heald frames. (c) Explains a modified picking order with weft cross-sectional view. (d) Explains the corresponding lifting plan of heald frames. Apparently there seems no difference between the designs of the two 3D orthogonal weaves. Both designs can weave same type of fabric. But with respect to the ease of weaving, lesser loads on the weaving machine, lesser busyness of the heald frames and lesser stresses on the warp threads and for the sake of better fabric quality, the modified picking order (d) is a better choice. Both weaving designs are same, starting from pick number 1 to pick number 5. There are a total of six heald frames; hence the shedding movement of one frame is 16.7% of all frames. Considering Figure *2-19* (d), for 1st pick all the heald frames of stuffer yarns are down, the heald frame of binder yarns B1 is up and the heald frame of the binder yarn B2 is down. Only one frame is up. For the 2nd pick the heald frames 'a' and B1 are up and all remaining frames are down. There is only one change from 1st to the 2nd pick (16.7% change). For the 3rd pick there is only one change (16.7% change) i.e., only heald frame 'b' raises up. For the 4th pick there is again only one heald frame 'c' raises up (16.7% change), and for the 5th pick again only one frame 'd' raises up (16.7% change). Up to this stage both designs behave similarly. The major difference between the two weave designs starts from the 6th pick. From 5th to 6th pick an abrupt change takes place in the design of conventional weave (b), as for the 5th pick the heald frames a, b, c, d and B1 are up and B2 is down, but on the next (6th) pick, there is a reversal. All raised heald frames of the 5th pick (a, b, c, d, B1) moves down and B2 raises up that means all frames are busy which is a 100% change. On the other hand there is minimum movement in case of modified (sequential) shedding (d) in which from 5th to 6th pick only two heald frames move, i.e., B1 moves down and B2 moves up which means a 16.7 x 2 = 33% change (67% less than the conventional). Consequently, after ever 5th pick there is a 100% change in conventional weave design (b), but on the other hand the maximum change is only 33% for the sequential way of picking. Except from 5th to 6th and from 10th to 1st pick, both weave designs behave similarly with only 16.7% change. The sudden abrupt change in case of conventional picking (b) is associated with maximum movement of the heald frames, causing much more abrasion among the warp threads during shedding as compared to sequential picking (d). This also makes a sudden load on the shedding system which is likely to cause more wear and tear of the mechanical parts. In sequential picking (c) it is interesting to note that after the completion of 5 picks at the lower most, the 6th pick also starts from the lower side instead of starting from the top side with only a change of binder yarns B1 and B2 (which is an unavoidable in both designs). Thus sequential arrangement of

picking imparts minimum disturbance to the warp threads during shedding, minimizing the abrasion among the warp threads with least chances of pill formation, minimizing the chances of shed sticking; which in turn may lead to warp breakage and hindrance in weft insertion.
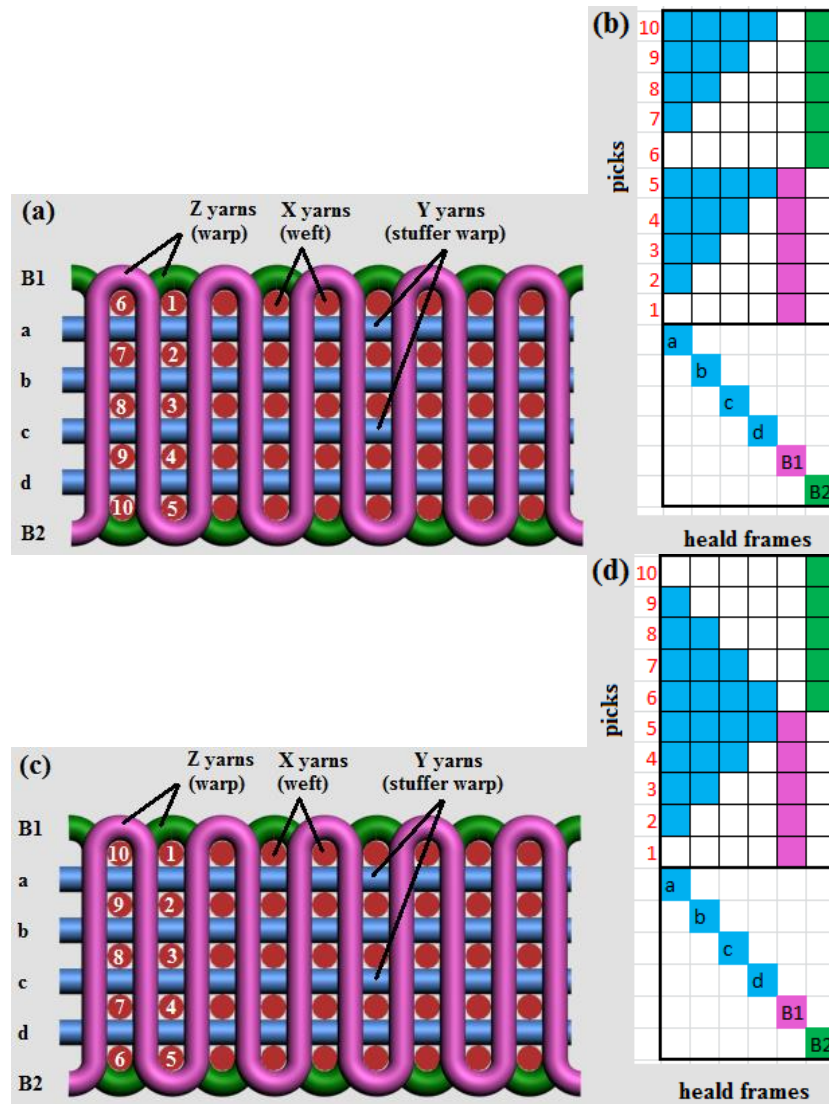
Figure 2-19. Picking order in 3D orthogonal weaving, (a) conventional picking order, (b) weave design of conventional picking order, (c) modified picking order for gradual change in lifting order, (d) weave design of modified picking order with minimum busyness of heald frames

Table 2-8 represents the details of 3D orthogonal preform woven using commingled jute/polypropylene yarns. 3D orthogonal fabrics are biased by default. This means an unequal number of layers in warp and weft direction. If there are 'n' layers in warp direction then there would always be 'n+1' layers in weft direction. This is an unavoidable for 3D orthogonal fabrics because one layer of weft above the warp threads and one layer below the warp

threads are essentially required in order to hold those stuffer warp threads. And finally, z-yarns in the warp direction are used to hold these upper and lower most picks. In order to weave a square fabric (means 50% weight in warp direction and 50% in weft direction) a careful calculation was required (due to unequal number of layers in warp and weft) to predict the yarn densities (threads per unit length) so that the weight distribution is kept equal for both in warp and weft directions. Moreover, z-yarns were also involved in the calculation as they are coming in the warp direction, so their weight percentage is shared with the stuffer warp yarns. The z-warp yarns were further divided into two types with respect to material, the jute/polypropylene commingled z-yarns and pure polypropylene z-yarns. The ratio of commingled to polypropylene in z-yarns was kept at 1:2, means for everyone commingled z-yarn there were two pure polypropylene z-yarns (Figure 2-15). The main purpose for keeping this ratio was to reduce the weight proportion of jute z-yarns in total weight of jute material in warp direction (as pure polypropylene z-yarns, working as a matrix, vanish after thermoforming). With 1-commingled: 2-polypropylene ratio, the weight proportion of z-jute was 29% as compared to the weight of stuffer jute at 71%. if, instead, all commingled z-yarns would have been used, then the weight proportion of z-jute would have become 45%, with 55% of stuffer warp in total weight of warp yarns (z-yarns + stuffer yarns), thus reducing the weight proportion of stuffer warp to a greater extent with respect to weft yarns, which was not required because the main purpose was to minimize the weight difference between stuffer warp and weft yarns. Increase of weight proportion in z-yarns directly affects/reduces the weight proportion of stuffer yarns, it do not affect the weight proportion of weft (z-yarns are coming from the creel, in warp direction), especially when the weft yarns, in a 3D orthogonal fabric, have a default advantage of one additional layer (5 layers) over stuffer warp yarns (4 layers).

Table 2-8. Parameters of 3D orthogonal woven preform

Parameters	Calculated	Actual	% difference with calculated values
Weft threads/inch (per layer/all layers)	9.4/47	9.88/49.4	5.1% higher
Stuffer warp threads/inch (per layer/all layers)	8.3/33.2	7.4/29.7	10% lower
Z warp threads/inch [a]	2.76	2.42	12% lower

Stuffer warp weight (%) (w.r.t., total warp weight)	70.6 [b]	71.1[b]	0.7% higher
Z warp weight (%) (w.r.t., total warp weight)	29.4 [b]	28.9[b]	1.7% lower
Weight proportion in weft	50%	54.16 %	8.32% higher
Weight proportion in warp	50%	45.84 %	8.32% lower
Areal weight (GSM)[c]	1163	1140	2% lower

[a] *Z warp are common for all layers,* [b] *as a percentage of total weight of warp,* [c]*GSM (g/m²)*

2.7 Composite manufacturing techniques, unidirectional (UD), two dimensional (2D) and three dimensional (3D)

2.7.1 UD composite manufacturing

Figure 2-20 represents the schematic of non-commingled jute/polypropylene layers stacking sequence. A total of four layers of unidirectional jute yarns were laid with a polypropylene (PP) sheet layer in-between every two layers of jute, hence there were a total of five layers of polypropylene. Figure 2-20(a) represents the stacking sequence of the order of PP/90°Jute/PP/0°Jute/PP/0°Jute/PP/90°Jute/PP, while (b) represents the unidirectional non-commingled yarn layup on wrapping frame, the wrapping process was carried out manually, (c) is showing the zoomed view of unidirectional non-commingled jute/polypropylene composite and (d) shows the actual specimen ready for testing. Excessive molten/frozen polypropylene resin, being squeezed out of the hot thermoforming plates, is visible and non-commingled yarns beyond the range of thermoforming plates are also visible.
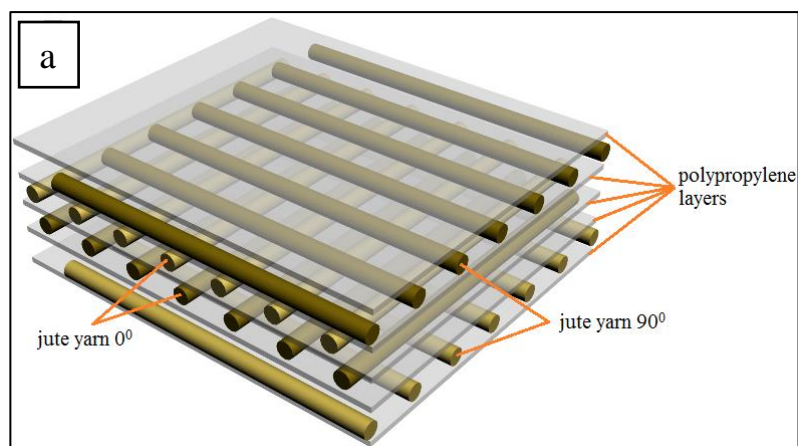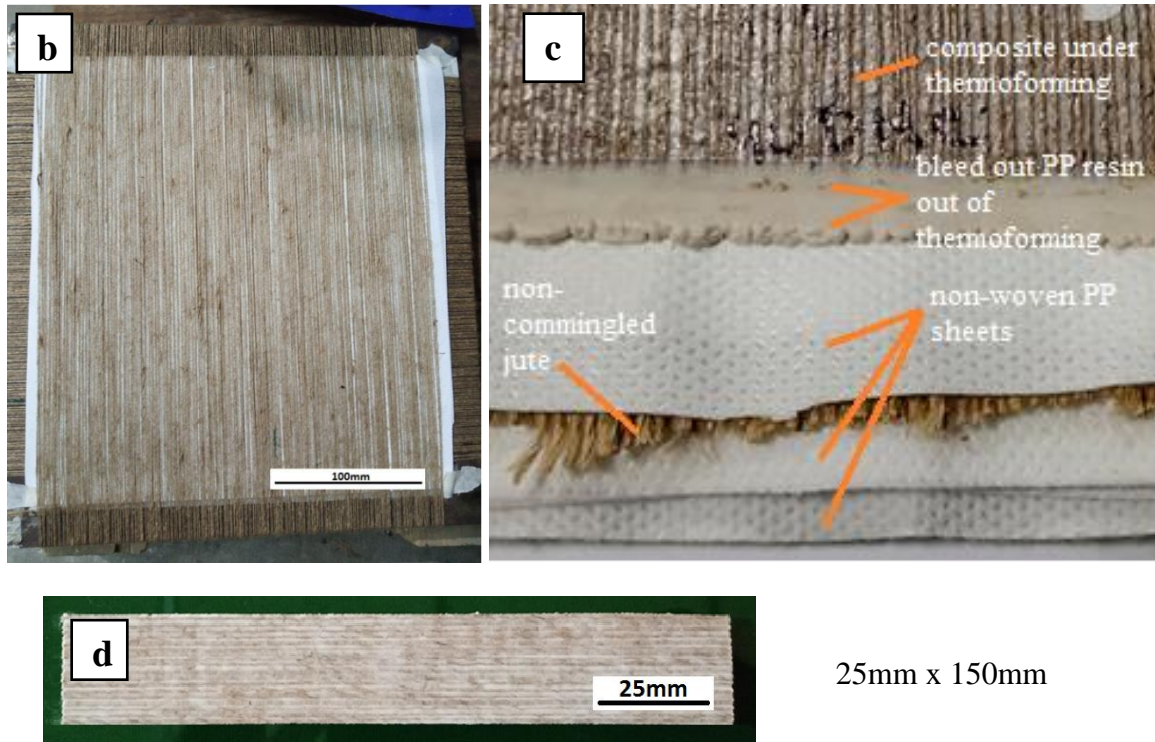
Figure 2-20. (a) The schematic of the layout sequence of stacking 4 layers of UD jute/PP non-commingled yarns, (b) UD non-commingled yarn layup on wrapping frame, (c) UD non-commingled composite zoomed view, molten PP resin and non-commingled yarns are visible, (d) actual specimen ready for testing

Figure 2-21 represents the schematic layout sequence of stacking four layers of unidirectional jute/polypropylene commingled yarns, (a) represents the stacking sequence in the order of 90°/0°/0°/90°, while (b) represents the unidirectional commingled yarn layup on wrapping frame, the wrapping process was carried out manually, (c) is showing the zoomed view of unidirectional commingled jute/polypropylene composite. Excessive molten/frozen polypropylene resin, being squeezed out of the hot thermoforming plates is visible and commingled yarns beyond the range of thermoforming plates are also visible.
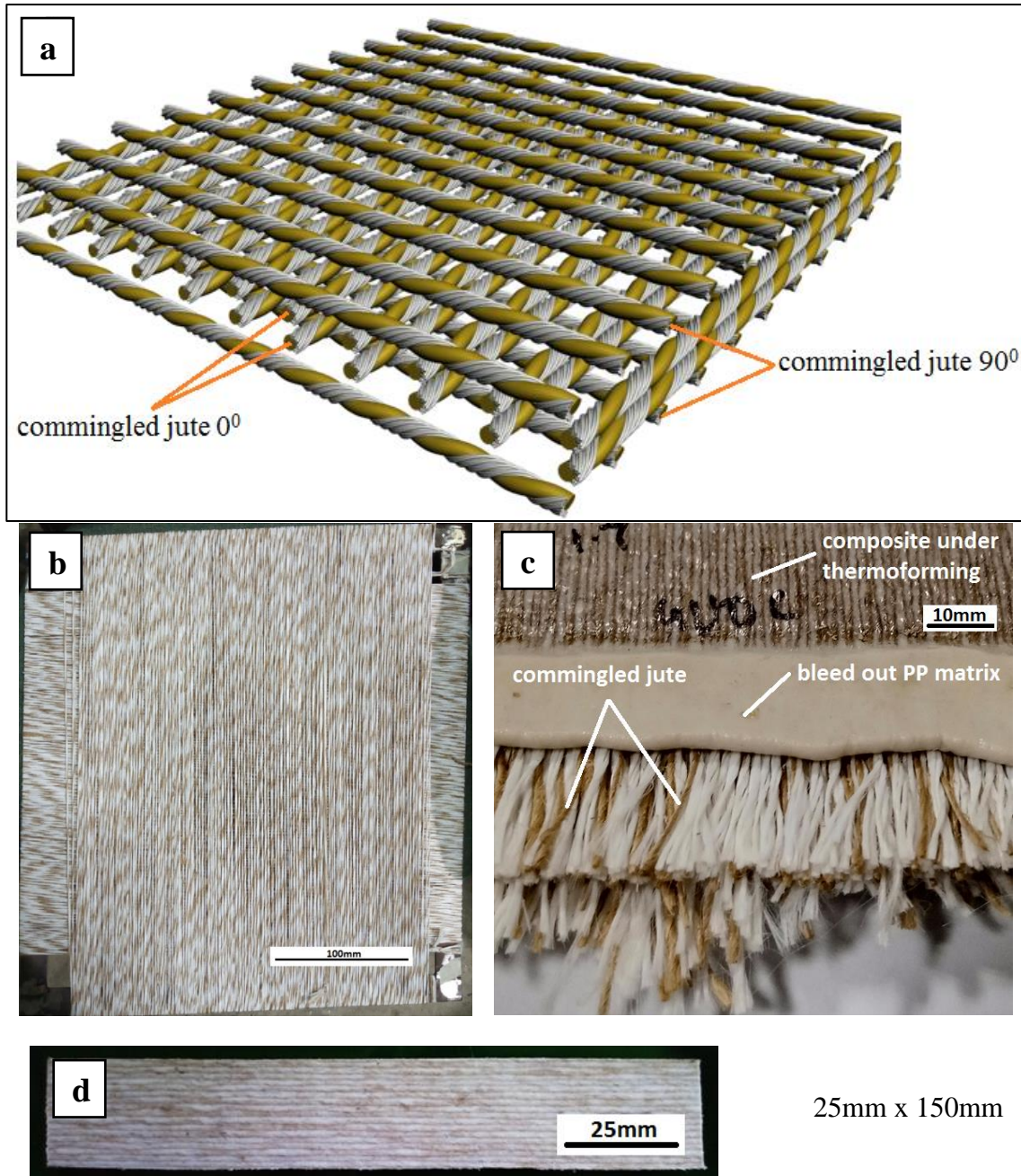
Figure 2-21. (a) The schematic layout sequence of stacking 4 layers of unidirectional jute/PP commingled yarns, (b) the unidirectional commingled yarn layup on wrapping frame (c) the zoomed view of unidirectional commingled jute/PP composite, molten PP resin and commingled yarns are visible

Table 2-9 explains the details of jute/polypropylene thermoplastic UD composites made through non-commingled and commingled yarns. Both composites were subjected to a pressure of 10 bars through gradual loading technique (as explained in chapter 5) up to a temperature of 200°C. Pressure holding time was 100min and mold opening temperature being 100°C.

The dry thickness of non-commingled stacking, before thermoforming, is 7mm and that of commingled is 6mm, however after thermoforming, a thickness of 7mm was compressed to 1.66mm for non-commingled composite (76% thickness reduction) and 6mm commingled was compressed to 1.76 mm (71% thickness reduction). Under the same load of 10 bars the commingled composite is 6% thicker than the non-commingled composite. Due to this lesser thickness of non-commingled composite its fiber volume fraction is 7.8% higher than commingled composite (0.48 vs 0.44).

Table 2-9. Details of the non-commingled and commingled thermoplastic composites made through gradual loading technique

Type of thermoplastic composite	4UDNC[a]	4UDC[b]	Remarks
Average dry thickness (mm)	7 (4 layers of jute yarn + 10 layers PP sheet)	6 (4 layers of commingled jute yarn)	Dry non-commingled fabric 17% thicker
Average thickness of the composite (mm)	1.66	1.76	Commingled 6% thicker
Thermoforming pressure (bars)	10	10	
Thermoforming temperature (°C)	200	200	
Calculated fiber volume fraction (FVF)[c]	0.48	0.44	Non-commingled 7.8% higher FVF

[a]4: layers, UD: unidirectional Jute, NC: non-commingled,

[b]4: layers, UD: unidirectional Jute, C: commingled,

[c](FVF) value calculated by weight/mass fraction formula (see part 2.9).

2.7.2   2D composite manufacturing

The conventional thermoformed 2D composites were fabricated by stacking the alternate layers of 2D jute non-commingled woven fabric and thermoplastic polypropylene sheets in a sequential order. One the other hand the stacking of commingled fabric layers was carried out in a cross-ply sequence without using pure thermoplastic non-woven layers in between. The layer stacking was in the order of 0° and 90°, similar for commingled and non-commingled specimens. The stacking of 0° layer (warp direction) was started at the middle. Nomenclature of 2D woven non-commingled and commingled specimens has been explained in Table 2-10, where the numerical digits (3, 4 and 5) explain the number of layers to be stacked, J represents the jute yarn, P represents the polypropylene filament yarn and C represents the commingled notation. For the comparison of a total of six types of 2D composites were to be

fabricated. Three specimens types for non-commingled composites with three, four and five layers were fabricated and similarly three specimens types for commingled composites with three, four and five layers were fabricated for one to one comparison, i.e., three layer non-commingled composite was to be compared to three layer commingled composite, four layer non-commingled composite was to be compared to four layer commingled composite and five layer non-commingled composite was to be compared to five layer commingled composite.

Table 2-10. Nomenclature of the prepared composite samples

Number	Sample type	Sample descriptions
1	3JP[a]	3-layer jute/PP Non-commingled
2	4JP	4-layer jute/PP Non-commingled
3	5JP	5-layer jute/PP Non-commingled
4	3JPC	3-layer jute/PP Commingled
5	4JPC	4-layer jute/PP Commingled
6	5JPC	5-layer jute/PP Commingled

[a]3, 4, 5: number of stacked layers, J: jute yarn, P: polypropylene filament yarn,
C: commingled

The stacked dry samples were then placed in hot thermoforming press. The pressure values during thermoforming were 1.4bars, 4.3bars and 7.1 bars respectively for 3, 4 and 5 layered composites. The composites were then heated for 25 minutes at a temperature of 180°C. After 25 min the heater was switched off and the composite was subjected to cooling. It took around 30 minutes to cool down to 60°C, the press was then opened after releasing the hydraulic pressure and the samples were removed. A metallic spacer was used around the periphery of hot plates in order to prevent the over pressing of composites. This technique was used to retain the composite thickness in 4±0.3 mm range. Woven Teflon sheet were used between the plates and the composite specimen in order to prevent the sticking of thermoplastic matrix with hot plates. Figure 2-22 (a) shows the thermoforming machine, (b) shows the schematic of thermoforming, (c) shows the fabricated composite specimen of jute/PP and (d) shows the actual specimen ready for testing. Same thermoforming technique was employed for both non-commingled and commingled specimens.
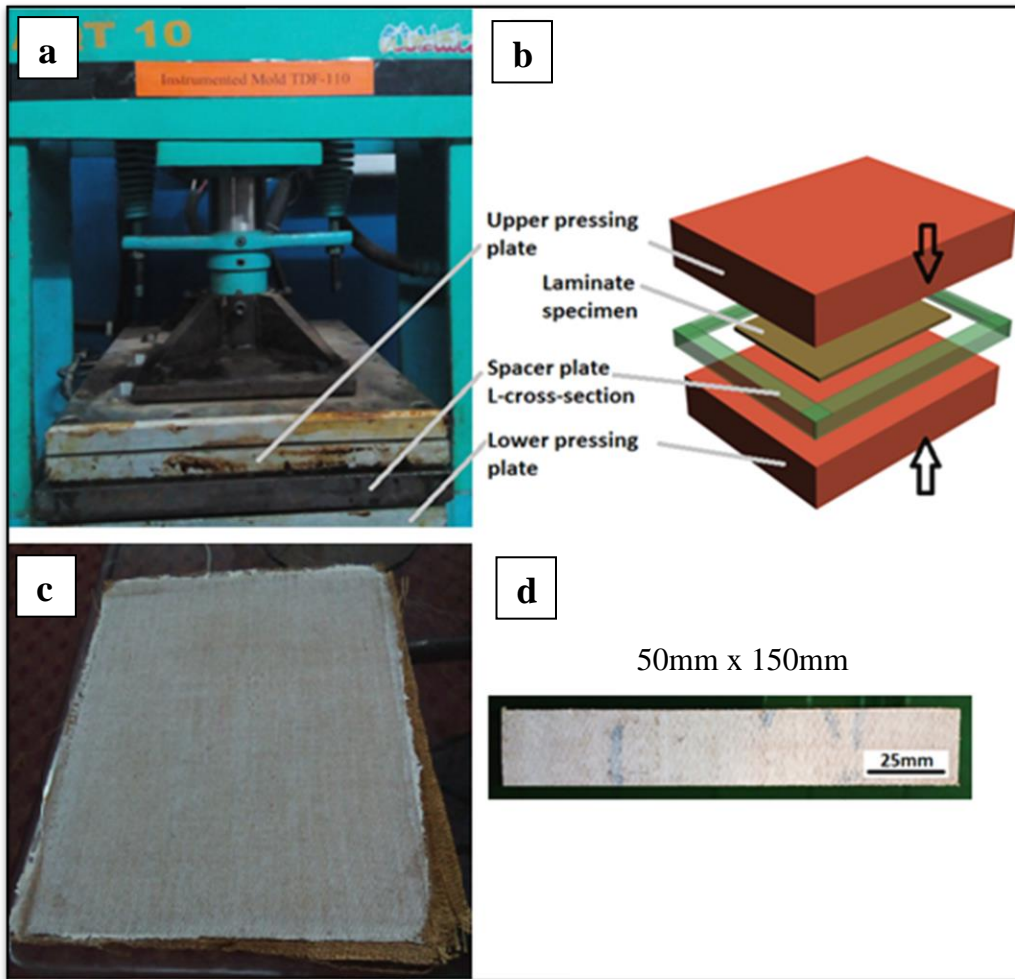
Figure 2-22. (a) Compression molding machine used for thermoforming of composite samples, (b) schematic of compression molding, (c) fabricated composite specimen (non-commingled of jute/PP, (d) actual specimen ready for testing

Table 2-11 explains the specifications of 2D non-commingled and commingled composite specimens. The fiber volume fraction (FVF) values for 3, 4 and 5 layers non-commingled composites were 0.26, 0.35 and 0.41 respectively while the values for 3, 4 and 5 layers commingled composites were 0.19, 0.21 and 0.24. The main reason these lower values were simply the combined thickness of co-twisted (1-jute + 4-polypropylene = 2368 tex) commingled yarn, which was much higher than a single non-commingled jute yarn (236 tex). Thus, a larger combined diameter of commingled yarn was the main bottle neck against achieving higher warp and weft yarn count (threads/inch) during weaving. Diameter of jute yarn was around 0.7mm while the diameter of jute/polypropylene commingled yarn was 1.8 to 2.0mm (Figure 2-9). This lower thread count both in warp and weft resulted into resultant lower fiber volume fraction values for the commingled composite. However, in order to

86

compare the mechanical properties of non-commingled and commingled composites the tested values were normalized against the average fiber volume fraction values of both composites.

Table 2-11. Details of thermoplastic composites made through non-commingled and commingled techniques

Type of thermoplastic composite	Non-commingled	Commingled Experimental (normalized)
Fiber Volume Fraction (FVF)[a]		
3 layers	0.26	0.19 (0.26)
4 layers	0.35	0.21 (0.35)
5 layers	0.41	0.24 (0.41)
Average thickness of composite (mm)		
3 layers	3.5	3.6
4 layers	4.1	3.9
5 layers	4.3	4.2

[a](FVF) value calculated by weight/mass fraction formula (see part 2.9)

2.7.3   3D commingled composite manufacturing

3D woven composites have additional yarn reinforcement in out of plane direction which results in to increased mechanical properties compared to 2D woven composites. The delamination resistance of 2D woven composites is on the lower side due the absence of yarns in 3rd dimension [144,145]. 3Ds are much stronger structures, especially against out of plane forces, as compared to 2D laminates. Boussu [146] reported that 3D fabrics are more suitable for ballistic applications due to higher delamination resistance as compared to laminated composites. Vaidya et al., [147] have also confirmed that 3D composite structures possess higher impact resistance.

In order to make our 3D orthogonal commingled composites, the gradual loading technique was employed (explained in chapter 5). The thermoforming technique used for the manufacturing of 3D commingled composite was the same as used for the unidirectional and 2D composite laminates. Figure 2-23 (a) shows the actual 3D commingled composite specimen fabricated on thermoforming machine, while (b) shows the zoomed-in view of specimen during thermoforming with bleeding out of extra polypropylene matrix. During

thermoforming the 3D specimen was subjected to a pressure of 10 bars through gradual loading technique 200°C temperature and 100 min holding time. Molding opening temperature was 100°C.

50mm x 150mm
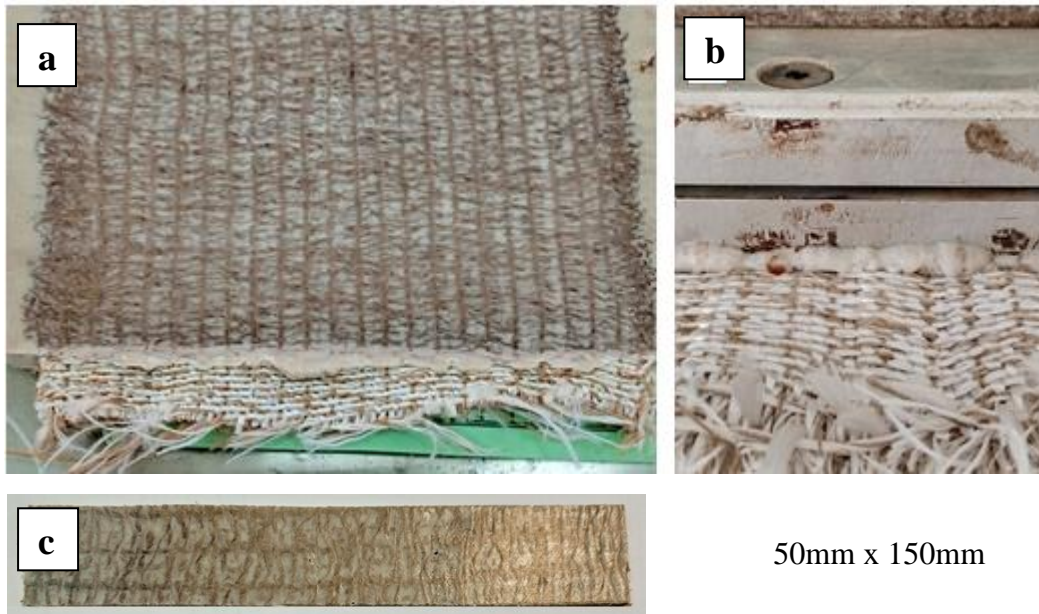
Figure 2-23. (a) The 3D woven commingled jute/PP composite sample after fabrication, (b) zoomed-in view during fabrication, (c) tensile sample ready for testing

The dry thickness of 3D commingled preform was 7mm. However, after thermoforming, a thickness of 7mm was compressed to 3.54 mm (50% thickness reduction) under a load of 10 bars. As already discussed, this reduction in thickness mainly affects the z-yarns, which no longer remains straighter in vertical direction and follows some zigzag paths [148]. Figure 2-24 illustrates this explanation, where (a) represents the non-composite 3D orthogonal dry preform with a measured thickness of 7 mm, (b) shows the average composite thickness of 3.54 mm, (c) shows the actual profile of z-yarn after 50% compression from fabric to composite stage, (d) shows the warp cross-section with binder z-warp, all four layers of stuffer y-warp and all five layers of weft x-yarns.
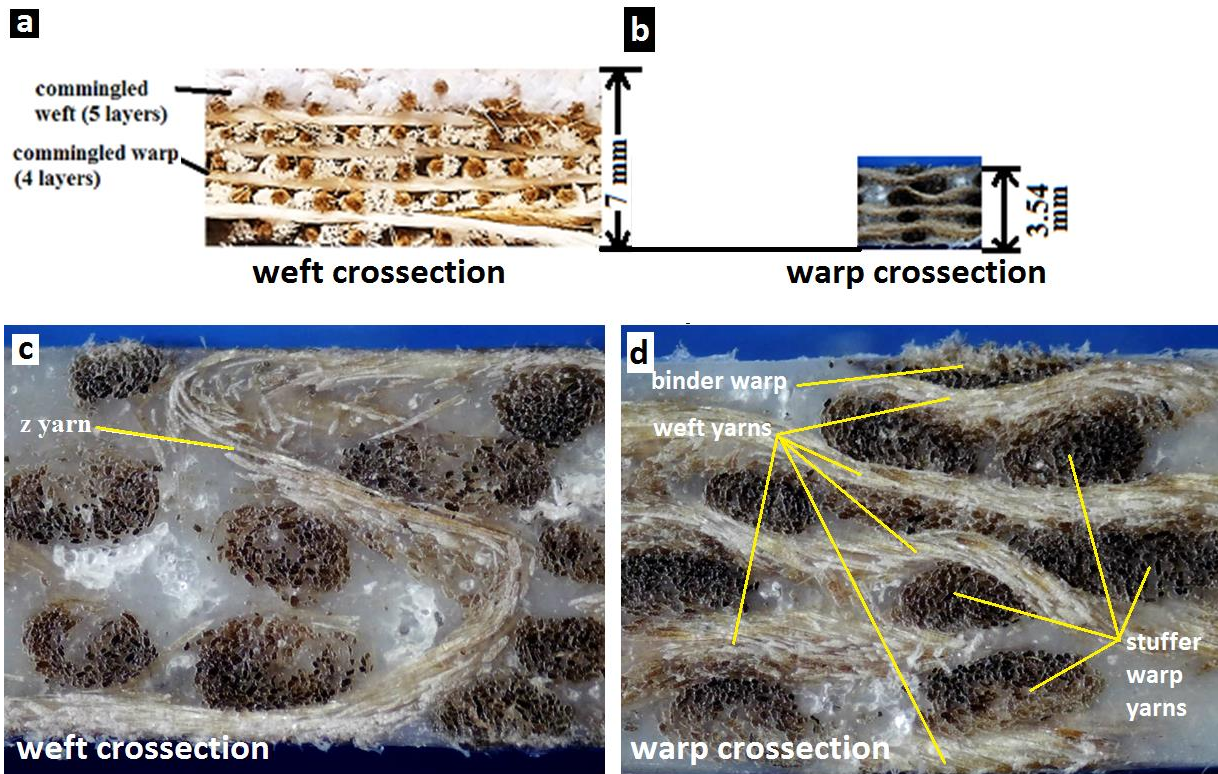
Figure 2-24. (a) The non-composite 3D orthogonal dry preform with thickness 7mm, (b) average composite thickness 3.54 mm, (c) actual profile of z-yarn in the composite, (d) warp cross-section with binder warp(z), all four layers of stuffer warp (y), all five layers of weft yarns (x)

In 3D orthogonal composite the measured weight fraction of pure jute fiber was 0.35 and proportion of pure polypropylene thermoplastic matrix was 0.65. The value of fiber volume fraction (FVF) was calculated using the mass density equation (see part 2.9). The calculated value of fiber volume fraction, using this formula, was 0.23 for 3D orthogonal commingled composites. Table 2-12 shows the details of 3D orthogonal commingled thermoplastic composites made through gradual loading technique.

Table 2-12. Details of 3D orthogonal commingled thermoplastic composite made through gradual loading technique

Type of thermoplastic composite	3DJPC5[a]
Weight fraction of pure jute fiber w.r.t., weight of composite	0.35
Average dry thickness	7 mm (5 layers of commingled weft + 4 layers commingled warp)
Average thickness of the composite	3.54 mm

Thermoforming pressure	10 bars
Thermoforming temperature	200°C
Calculated fiber volume fraction (FVF)[b]	0.25

[a]3DJPC5: three-dimensional orthogonal jute/PP commingled composite with 5 weft layers, [b](FVF): values calculated by weight/mass fraction formula (see part 2.9).

2.8   Mechanical testing of composites

There was a total of four types of tested performed for all commingled and non-commingled unidirectional, 2D and 3D composite specimens including tensile, 3-point bending, short beam strength and Charpy impact tests. The prepared composite specimens were cut according to different templates in accordance with the ASTM standards. The composite specimens were cut on a band saw cutting machine. Figure 2-25 shows the template used for cutting composite specimens for testing.
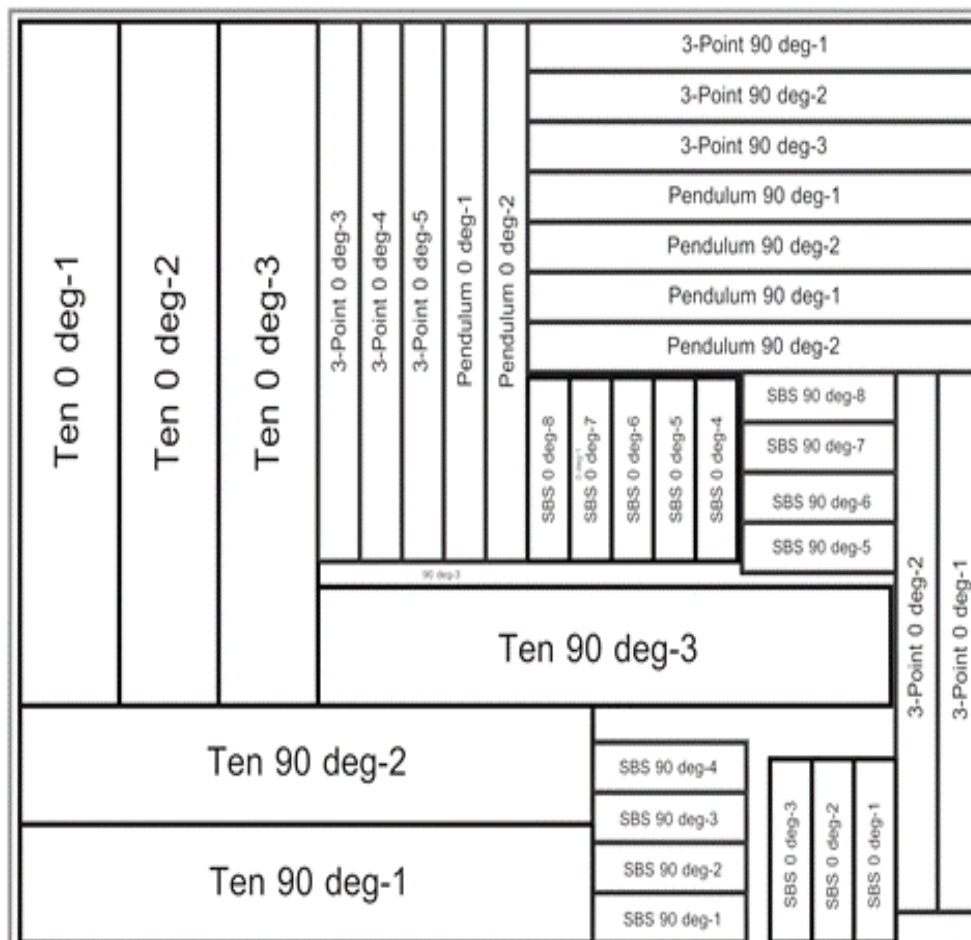
Figure 2-25. Template used for cutting jute/PP composites

2.8.1 Tensile test of composite samples

Tensile properties of single jute yarn were measured on Universal single yarn testing machine (Lloyd Ametek, Model LRX plus) using ASTM D 2256 -2015 standard with gauge length of 250mm. A crosshead speed of 25mm/min was used according to given ASTM standard. Machine image along with the jute yarn is shown in Figure 2-26.

Figure 2-26. Single yarn testing machine (Lloyd Ametek)

The tensile strength of fabricated composite specimens was tested on Universal testing machine, Zwick Roell (Z100 All-round, Zwick). The test was performed using ASTM D3039 standard with a crosshead speed of 2mm/min. The samples were cut to 25mm x 150mm dimensions with a gauge length of 100mm. In order to accurately measure the specimen's extension value an extensometer was also used as shown in the Figure 2-27. Span length for extensometer was adjusted at 50mm, which was 25mm away from the jaws.
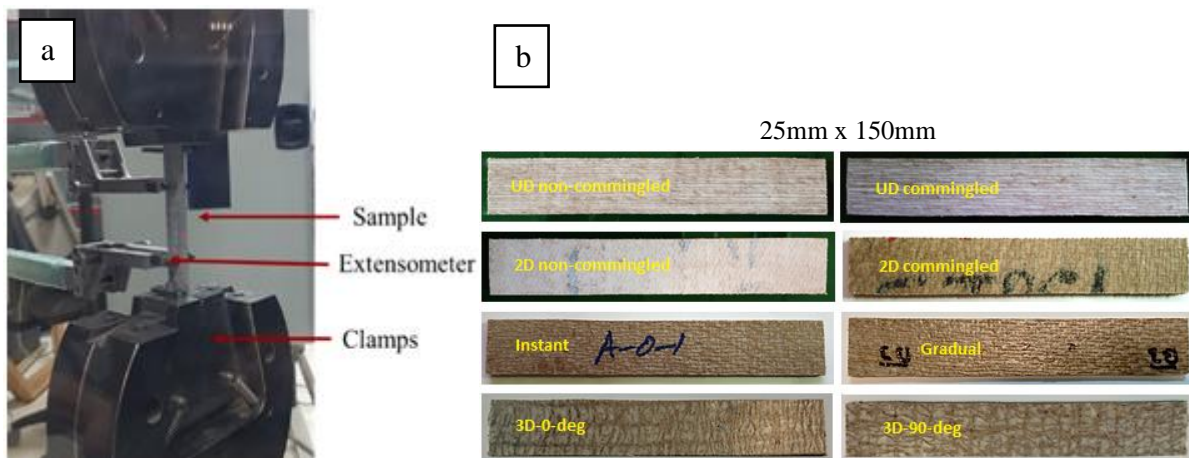
Figure 2-27. (a) Universal tensile testing machine (UTM Z100), (b) specimens ready for tensile test, (25mm x 150mm)

2.8.2 Flexural test of composite samples

The flexural test of fabricated composite specimens was perfirned on Universal testing machine, Zwick Roell (Z100 All-round, Zwick. The flexural test was performed using ASTM D7264 standard at a crosshead speed of 1mm/min. The samples were cut to 10mm x 120mm dimensions with a span length (L) equal to 32 x d, in accordance with given ASTM standard, where 'd' is the thickness of specimen to be tested. The testing machine along with fixtures and sample to be tested is shown in Figure 2-28.
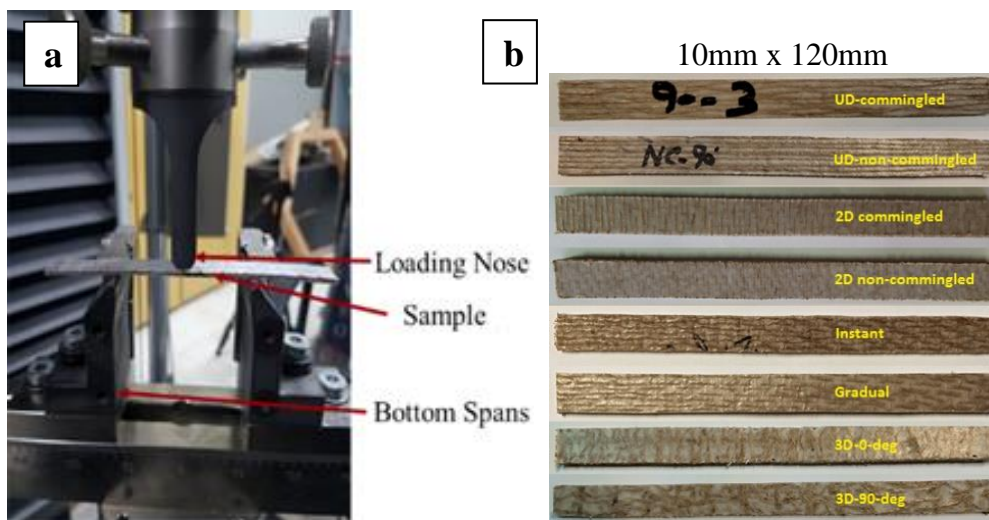
Figure 2-28. (a) Zwick Roell Universal testing machine (Z100 All-round, Zwick) for 3-point bending test, (b) specimen for 3-point bending test (10mm x 120mm)

2.8.3 The Short Beam Strength (SBS) test

The short beam strength was performed as per ASTM D2344 standard using Zwick Roell Universal testing machine, (Z100 All-round, Zwick) with SBS fixture. The samples were cut to 10mm x 40mm dimensions with a span length equal to 4 x h, in accordance with given ASTM standard, where 'h' is the thickness of specimen. The testing machine along with fixtures and sample to be tested is shown in Figure 2-29. The shear load is applied on the specimen until the following condition reach [149].

    a) A load drop-off of 30 %
    b) Two-piece specimen failure
    c) The head travel exceeds the specimen nominal thickness.
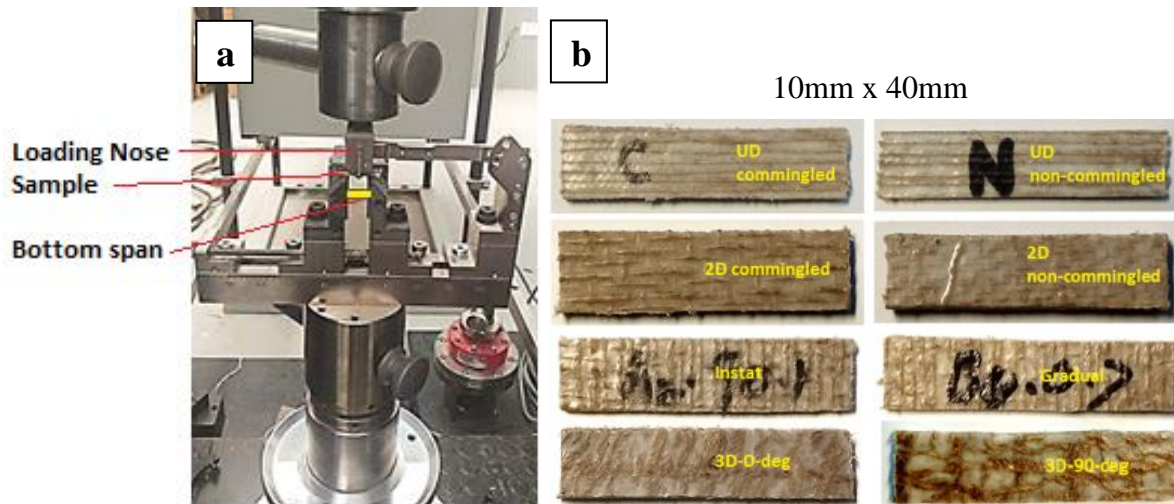
Figure 2-29. (a) Zwick Roell Universal testing machine (Z100 All-round, Zwick) for SBS test, (b) specimen for SBS test, (10mm x 40mm)

2.8.4 Charpy impact test

In order to measure the impact strength and energy absorbed of composite specimens Charpy impact test was conducted. The testing was performed as per ISO-179-2 on Zwick/Roell HIT 5.5 (with 5 Joule hammer capacity). The samples were cut to 10mm x 120mm dimensions with a span length of 60mm. The testing machine along with the tested sample is shown in **Error! Reference source not found.**.
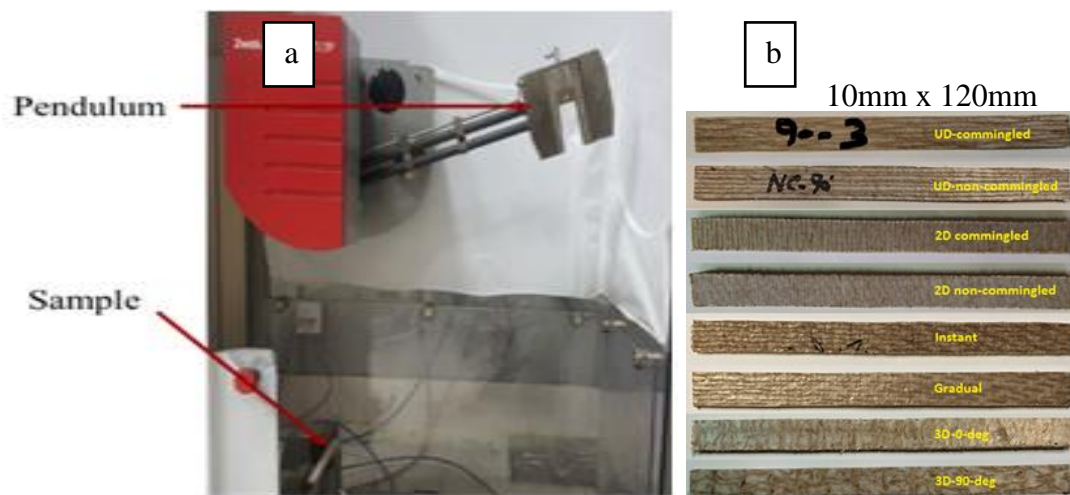
Figure 2-30. The Zwick/Roell HIT 5.5 Charpy impact test, (b) specimen for Charpy test, (10mm x 120mm)

2.9   Measurement of fiber volume fraction of the composite samples

In the current study, for all non-commingled and commingled UD, 2D and 3D composites, the values of the fiber volume fraction (FVF) were measured using the following mass/density formula;

$$FVF = \frac{Mf/\rho f}{\frac{Mf}{\rho f} + \frac{Mm}{\rho m}}$$

Equation 2-1

Where;

Mf   =   mass of fibers (jute),

ρf =   density of the fibers (jute density: 1.5g/cm^3),

Mm   =   mass of the matrix (polypropylene),

ρm =   density of the matrix (polypropylene: 0.9 g/cm^3).

Chapter 3. Mechanical performance of UD commingled and non-commingled composites

This chapter entails the mechanical properties of 4-layered UD commingled and non-commingled composites made using gradual loading. The tensile, flexural, short beam strength and Charpy impact test were conducted to compare the properties of both types of composites. The results show that the tensile strength of commingled composites was higher as compared to non-commingled composites. Similar results were observed for flexural, SBS and Charpy impact. The overall failure strain is also higher for commingled composites due to higher amount of yarn waviness present in the composite which positively resulted into marginally higher impact properties. The commingling technique improved overall mechanical properties of the composite with better distribution of fiber matrix.

This chapter entails the mechanical properties of 4-layered UD commingled and non-commingled composites made using gradual loading technique (discussed in detail in chapter 5). The tensile, flexural, short beam strength and Charpy impact test were conducted to compare the properties of both types of composites. Six tests were performed each for UD commingled and non-commingled composites specimens; six tested were performed for commingled and six were performed for non-commingled specimen. The results show that the tensile strength of commingled composites was higher as compared to non-commingled composites. Similar results were observed for flexural, SBS and Charpy impact. The overall failure strain is also higher for commingled composites due to higher amount of yarn waviness present in the composite which positively resulted into marginally higher impact properties. The commingling technique improved overall mechanical properties of the composite with better distribution of fiber matrix.

3.1.1 Tensile properties of UD commingled and non-commingled composites

In this part, we are presenting results on tensile properties of UD commingled and non-commingled composites.

The tensile behavior of UD composites has been explained in Figure 3-1, which displays a stress-strain curve of jute polypropylene UD commingled composite. The curve looks like typical stress-strain curve of natural fiber reinforced thermoplastic composites with an initial linear region leading to a nonlinear region and abrupt fracture. The linear region relates to strain hardening, the nonlinear region starts with the matrix cracking and once the matrix cracking starts the fiber-matrix interface gets weakened and reinforcement starts exposing, then finally the composite fails completely due to fiber failure.
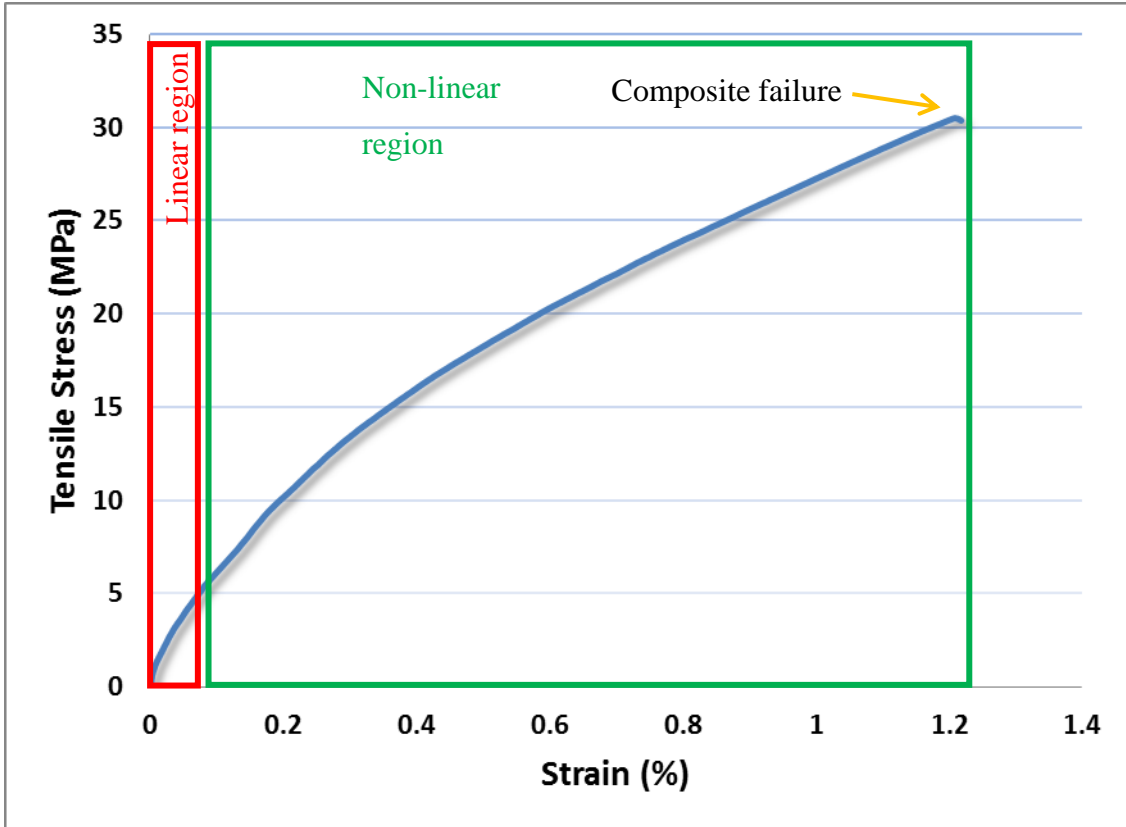
Figure 3-1. A typical stress-strain curve of unidirectional commingled composite

Figure 3-2 shows the tensile stress-strain curves of composites made through non-commingled and commingled techniques.

Figure 3-2. The tensile strength of unidirectional non-commingled and commingled composite specimens, (a) three dispersion curves of 4-layers unidirectional non-commingled composite (4UDNC), (b) three dispersion curves of 4-layers unidirectional commingled composite (4UDC)

Figure 3-2(a) shows the three dispersion curves of 4-layers unidirectional non-commingled composite (4UDNC) and (b) shows the three dispersion curves of 4-layers unidirectional commingled composite (4UDC). Figure 3-3 shows the comparison curves of 4UDNC and

97

4UDC. The curves show higher tensile strength and strain for commingled specimen as compared to non-commingled specimen. The tensile strength is around 12.8% higher in commingled composites. The reason for higher tensile strength for commingled specimen is due to better interface between the fibers and the polypropylene matrix. On the other hand, the strain at break is higher for the commingled specimen (1.2 vs 0.90), which is 33.3% higher as compared to non-commingled specimen. This is mainly due to the reason; in commingled composite the yarns are not laying straight as compared to the yarn layup in non-commingled composite. As early mentioned in part 2.4 (Materials and methods), the commingled yarns for making the unidirectional specimen were prepared by doubling on Simplex machine of yarn spinning process, using up to two twists per inch. This twist makes the individual jute yarn to follow a zigzag path in the commingled yarn, in which the polypropylene yarns are co-twisted with jute. The Figure 3-4 explains the zigzag pattern of jute yarns in the commingled composite, which in turn increases its waviness and hence increasing the elongation in the composite. As the tensile stress is applied on the commingled composite, the jute yarn tends to straighten before they are subjected to the ultimate tensile force to break the composite. This yarn straightening before failure is responsible for more strain in commingled composite. On the other hand, the jute yarns suffer lesser amount of strain before failure in non-commingled composite specimen, due to the reason that unlike commingled yarns these are not co-twisted, instead they are laid straight on the winding frame and the polypropylene thermoplastic sheets are laid in-between the layers of parallel unidirectional layers of jute yarns. These straighter jute yarns have more orientation in the direction of tensile force, and they get their elongation limit earlier, hence having lower strain than the commingled composite.
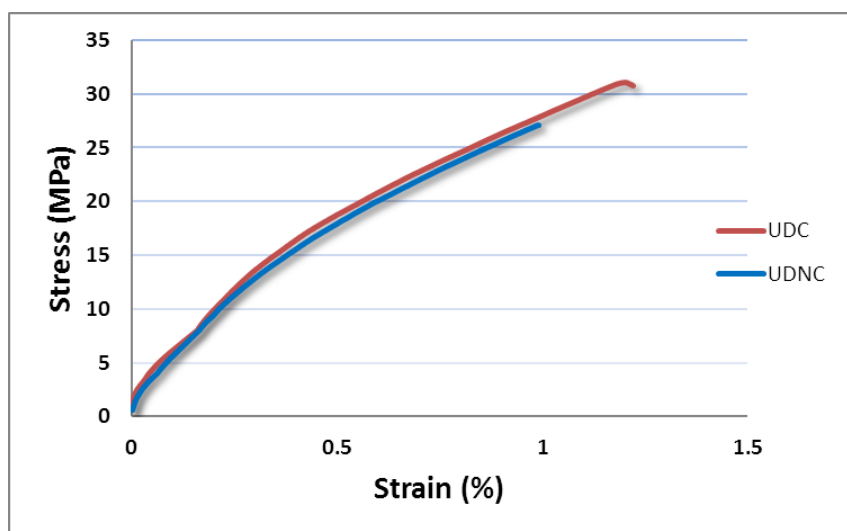
Figure 3-3. Tensile strengths of unidirectional non-commingled (4UDNC) and commingled (4UDC) composite specimens

Table 3-1 illustrates the tensile properties of non-commingled and commingled UD specimens. The value of tensile modulus, strength and strain has been compared. The variations from the mean values are also shown. Tensile modulus of non-commingled is some 23% higher mainly due to higher strain value in the commingled composite, which is mainly due to higher amount of jute yarn waviness (Figure 3-4).

Table 3-1. Tensile properties of non-commingled and commingled UD composites

Type of Composite	Tensile Modulus (GPa)	Tensile Stress (MPa)	Strain at Break (%)
Non-commingled	4.5±0.4	27.4±3.1	0.9±0.12
Commingled	3.65±0.2	30.9±0.51	1.2±0.03
Difference %	23	12.8	33.3

The optical microscope comparison of commingled and non-commingled specimens for tensile test shows interesting difference (Figure 3-5). (a) Shows the non-commingled composite specimen before tensile test, (b) shows the commingled specimen before test. The interface line, between the two parts of broken specimens, looks quite different for both specimens. In non-commingled specimen (c) the breakage line is quite linear showing a much brittle failure against the tensile force as compared to the zigzag breakage line for commingled specimen (d) which speaks of a non-brittle breakage due to the presence of more elastic behavior of commingled specimen for more jute yarn waviness. The difference of waviness among the jute yarns in the commingled composite may result into breakage of yarn one after the other (non-simultaneous yarn breakages, less wavy yarn with low strain value is likely to break earlier) resulting into zigzag fracture line. However in general, the non-simultaneous breakage of jute yarn in the commingled composite must have a negative impact on the tensile strength of the composite specimen but still the tensile strength of the commingled is 12.8% higher which speaks of a better fiber matrix interface in the commingled composite.
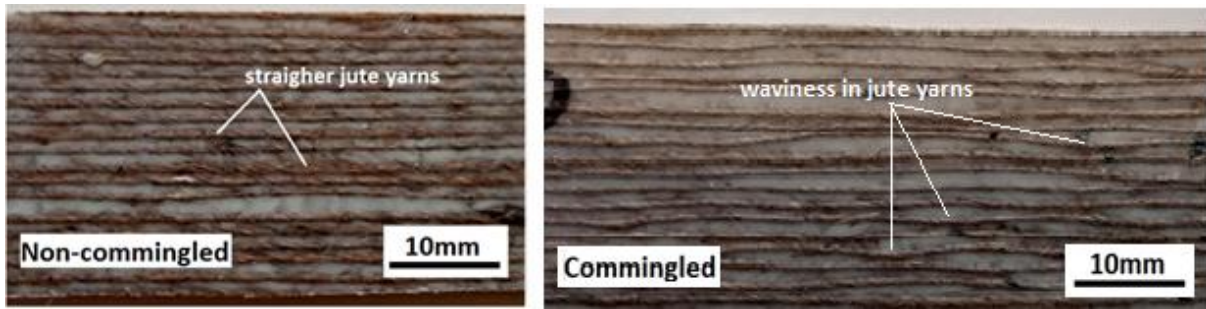
Figure 3-4. The placement of yarn in the non-commingled and commingled composites
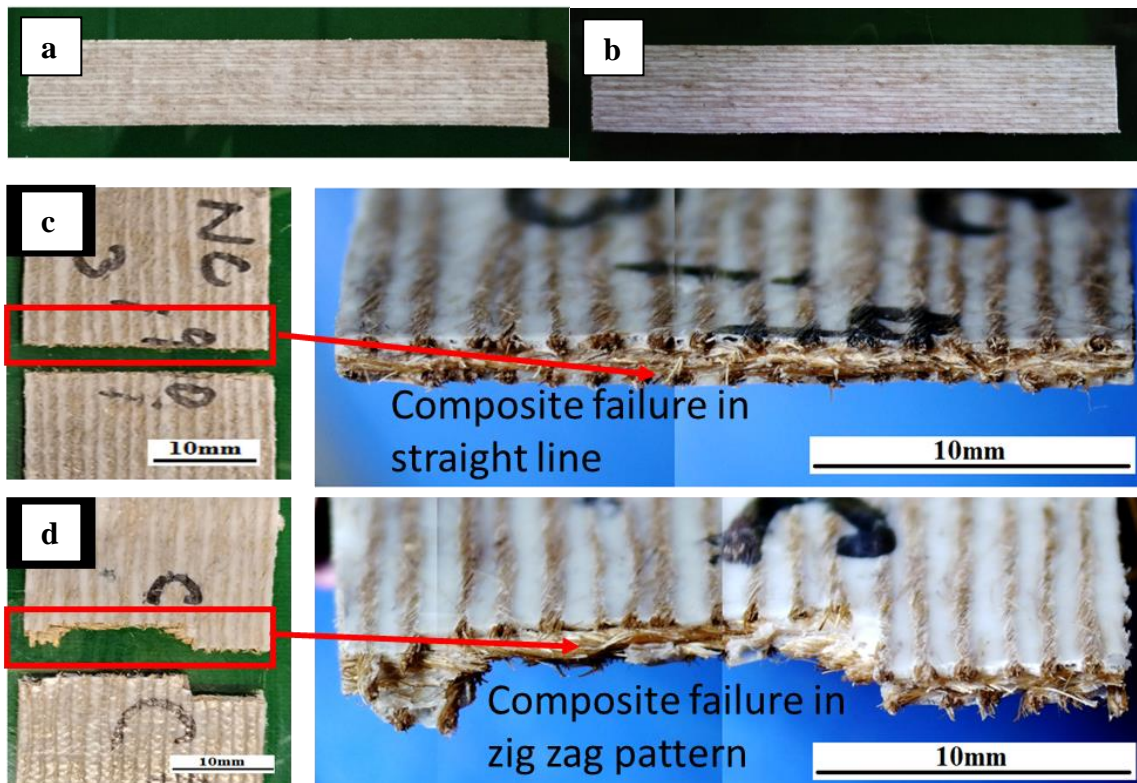
Figure 3-5. Microscopic image of tested specimens of non-commingled and commingled composites, (a) non-commingled specimen before test, (b) commingled specimen before test,(c) non-commingled specimen after test with zoomed view, (d) commingled specimen after test with zoomed view showing a non-brittle composite failure in zigzag pattern

3.1.2 Flexural Properties of UD commingled and non-commingled composites

In this section flexural properties of 2D commingled and non-commingled composites are discussed in detail.

The behavior of UD composites against the flexural load has been explained in Figure 3-6, which displays a typical flexural stress-strain curve of a UD commingled composite with an

initial linear region followed by the non-linear region. Then there is peak load followed by matrix cracking, ending into gradual fiber failure.
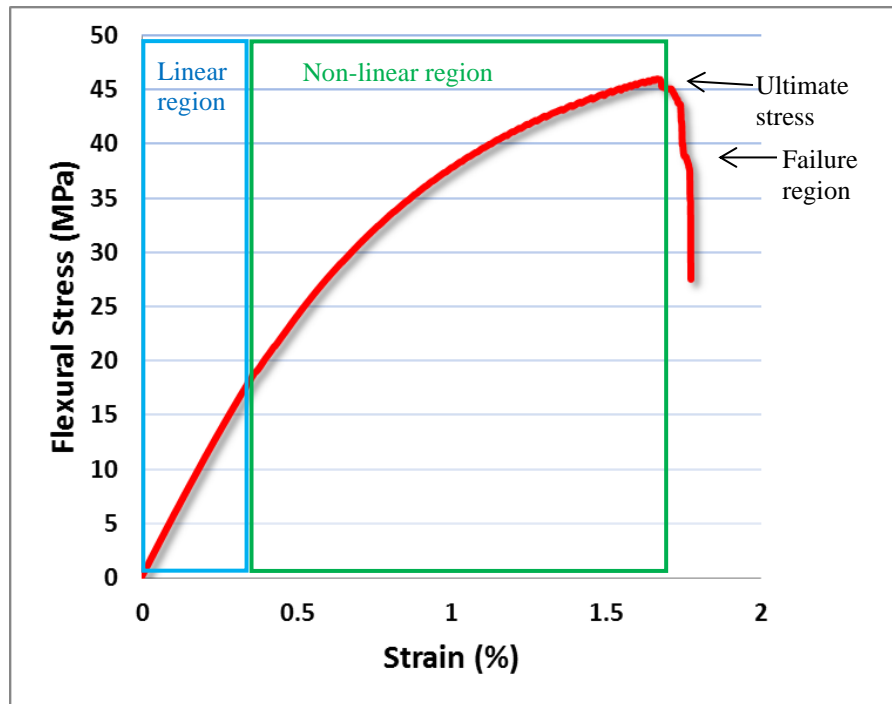
Figure 3-6. Typical flexural stress-strain curve of unidirectional commingled composite showing the linear region followed by the non-linear region and fiber failure

Figure 3-7 illustrates the flexural strengths of non-commingled and commingled composite specimens. (a) Shows the three dispersion curves of 4-layers unidirectional non-commingled composite (4UDNC) and (b) shows the three dispersion curves of 4-layers unidirectional commingled composite (4UDC). (c) Shows the comparison curves of 4UDNC and 4UDC. Flexural properties of both non-commingled and commingled composites are quite comparable to each other. The flexural strength of 4UDNC is 44.4MPa and that of 4UDC is 46MPa. The flexural strength of 4UDC is only 3.6% higher than 4UDNC. One the other hand the strain of commingled 4UDC is 80% higher than the 4UDNC (1.8% vs 1.0%). This is, as previously discussed, due to higher amount of waviness present in the commingled specimen as shown in Figure 3-4.

Figure 3-7. Flexural strengths of unidirectional non-commingled and commingled composites, (a) three dispersion curves of 4-layers unidirectional non-commingled composite (4UDNC), (b) three dispersion curves of 4-layers unidirectional commingled composite (4UDC),
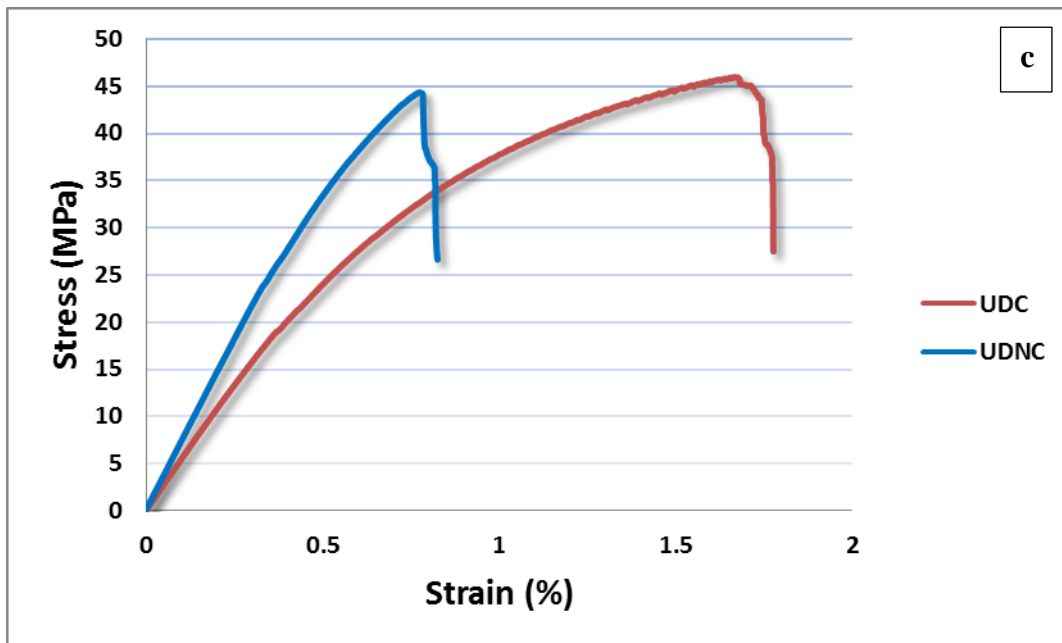
Figure 3-7.(c) A comparison of average curves of flexural strengths of unidirectional non-commingled and commingled composites.

Figure 3-8 shows the non-commingled and commingled specimens against flexural test. (a1, b1) shows the non-commingled and commingled specimens before test, (a2, b2) shows side view of these specimens after flexural test, (a3, b3) shows the zoomed in side view of these specimens with clear crack propagation in non-commingled specimen, (a4, b4) shows the tensile side (opposite side of depression probe) of the specimens and (a5, b5) shows the tensile side in a zoomed view. A more brittle behaviour of non-commingled specimen under the bending force has been observed as compared to the commingled specimen, explained by

the formation of more prominent crack in non-commingled specimen. On the other hand the commingled specimen shows a very small amount of crack. This is mainly due to the reason of more crimp in commingled specimen as compared to the non-commingled composite in which the jute yarns are comparatively straighter. Both specimens did not completely break for the test being performed up to 30% of maximum load.
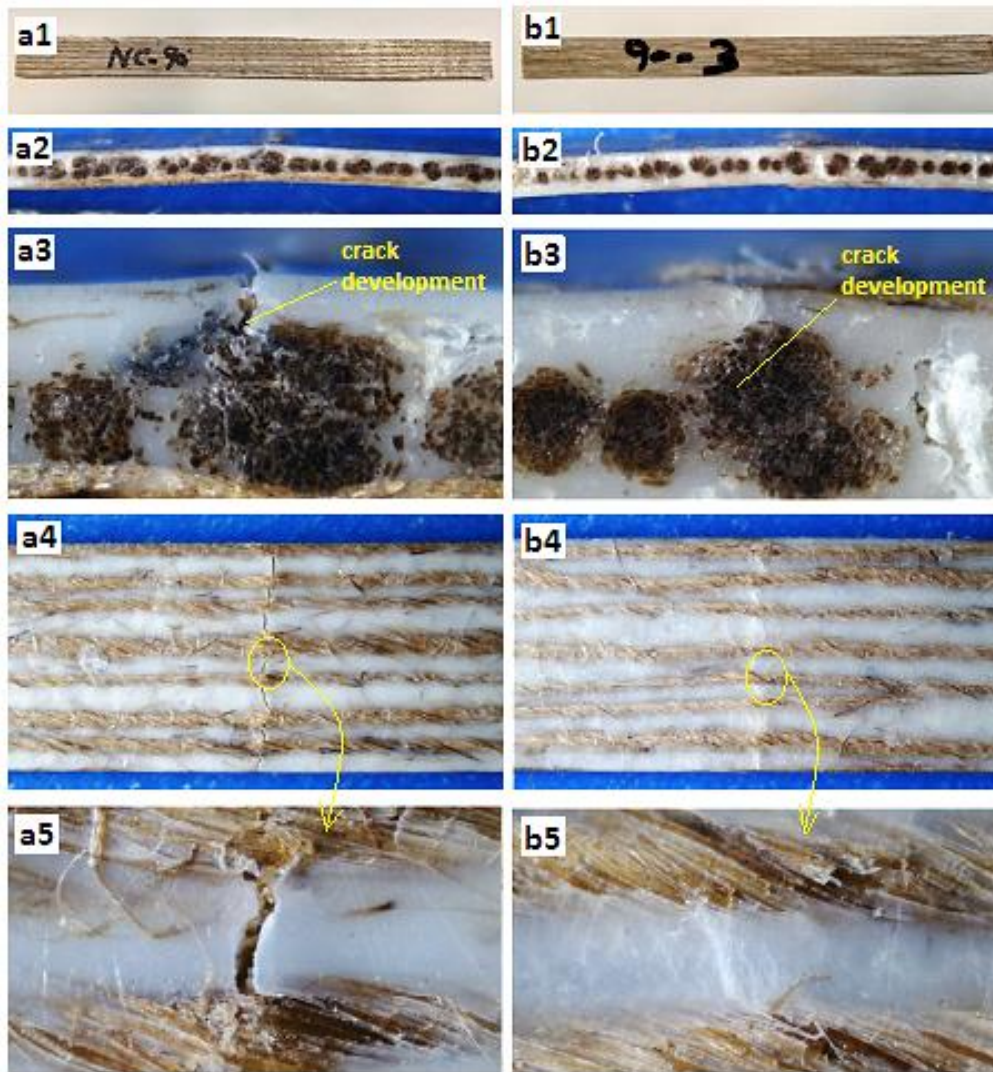
Figure 3-8. Tested samples of non-broken 3-point bending, (a1, b1) non-commingled and commingled specimens before test, (a2, b2) side view of tested specimens, (a3, b3) side zoomed in view of tested specimens with crack propagation, (a4, b4) tension sides of the specimens (a5, b5) tension side with zoomed view

Table 3-2 illustrates the flexural properties of non-commingled and commingled specimens. The value of flexural modulus, strength and strain has been compared. The variations from the mean values are also shown. Flexural modulus of non-commingled is 21.2% higher than the commingled UD composite mainly due to higher strain value in the commingled

composite (80% higher), which is mainly due to higher amount of jute yarn waviness (Figure 3-4).

Table 3-2. Flexural properties of non-commingled and commingled UD composites

Type of Composite	Flexural Modulus (GPa)	Flexural Strength (MPa)	Strain (%)
Non-commingled	6.3±0.17	44.4±1.2	1.0±0.14%
Commingled	5.2±0.11	46±3.6	1.8±0.1%
Difference %	21.2	3.6	80

3.1.3 Short beam strength of UD commingled and non-commingled composites

This section details the flexural properties of 2D commingled and non-commingled composites. A typical curve of short beam strength of UD composites has been explained in Figure 3-9, which displays a typical short beam strength-displacement curve of a UD commingled composite. During the early stage of loading a linear trend is observed followed by the non-linear region, then there is peak load F^{SBS} followed by significant decrease in load which is associated to multi stage matrix cracking, ending into fiber failure, known by the development crack initiation on the tensile side of the specimen (Figure 3-11).
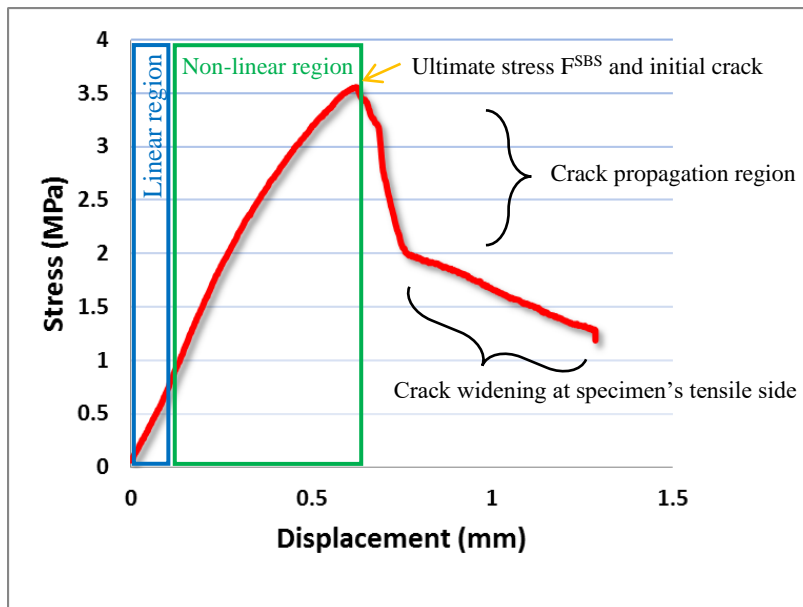
Figure 3-9. Typical short beam strength-displacement curve of unidirectional commingled composite showing the linear region followed by the non-linear region, matrix cracking and fiber failure

Figure 3-10 shows the short beam strengths of non-commingled and commingled tested specimens. (a) Shows the three dispersion curves of 4-layers unidirectional non-commingled composite (4UDNC) and (b) shows the three dispersion curves of 4-layers unidirectional commingled composite (4UDC). (c) Shows the SBS curves of 4UDNC and 4UDC. The short beam strength of commingled specimen is 3.62MPa and that of non-commingled being 3.28MPa, that means the shear strength of commingled composite specimen is 10.4% higher than the non-commingled specimen. This is due to a better interface between the jute fibers and polypropylene matrix in the commingled composite (4UDC) as compared to non-commingled composite (4UDNC).

On the otherhand the displacement of commingled specimen is also on the higher side, with a 25% increased value than the non-commingled speciemen (1.29mm vs 1.03mm). this is due to the presence of crimp in the commingled yarns as discussed earlier (see Figure 3-4).
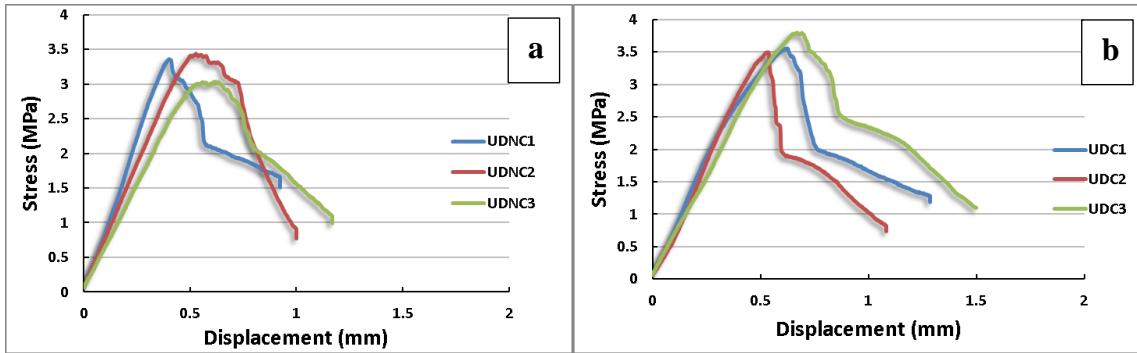
Figure 3-10. Short beam strengths of unidirectional non-commingled and commingled composites, (a) dispersion curves of 4-layers unidirectional non-commingled composite (4UDNC), (b) dispersion curves of 4-layers unidirectional commingled composite (4UDC)
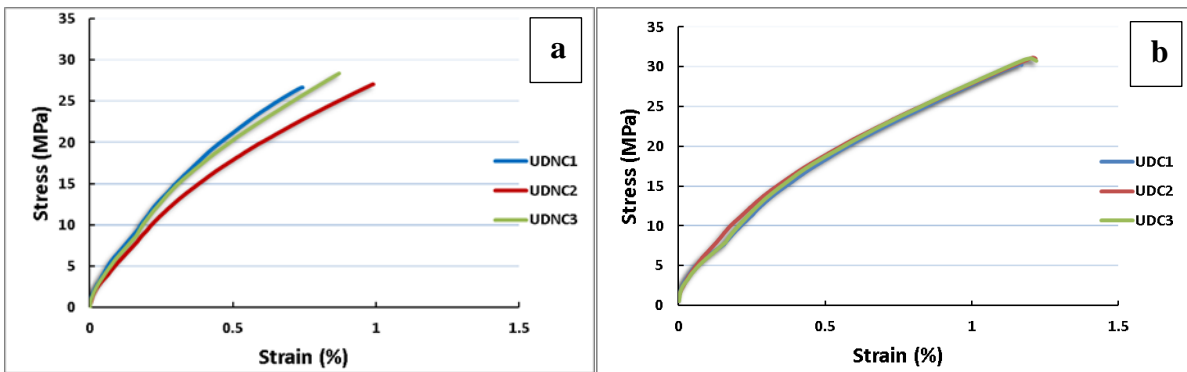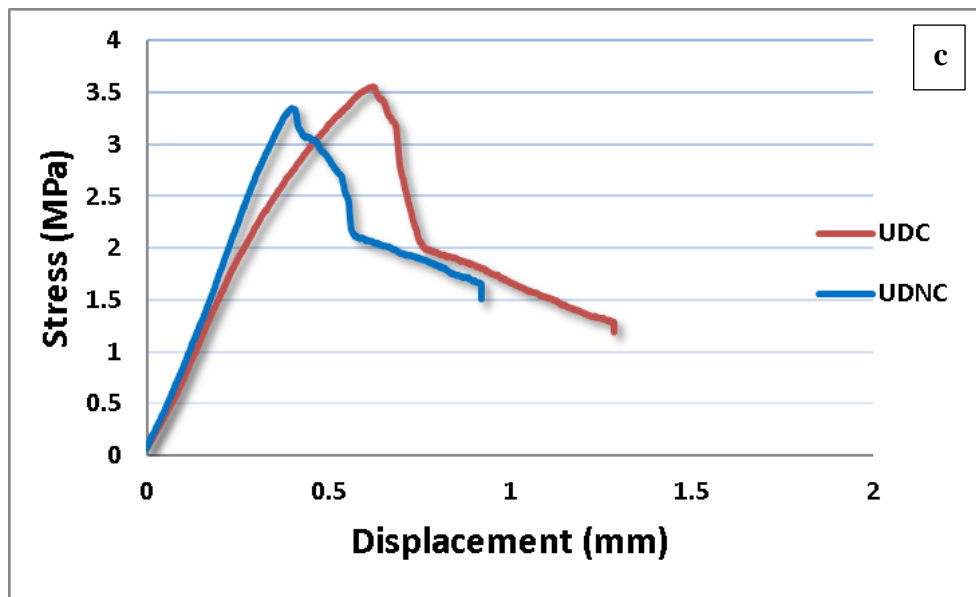

Figure 3-10. (c) Comparison of short beam strength of unidirectional non-commingled and commingled composites, curves of 4UDNC and 4UDC

In case of SBS test both the non-commingled and commingled composite specimens do not show any prominent sign of interlayer delamination. The basic reason behind the non-existence of delamination is the lack of integrity in individual unidirectional layers. Unlike the woven/knitted/stitched UDs, the existing is a true non-woven UD, in which there is lesser amount of integrity within one layer, due to the non-existence of lateral binding yarns. In case of a woven warp unidirectional the weft is always available to hold the warps in an integrated form. The same is true for knitted and stitched unidirectionals where an interconnected network of intermingled yarns is always available to hold the main unidirectional yarns in an integrated form. When a shear force is applied to an interlaced type of unidirectional, the shear force tends to cause slippage in-between the layers at the weakest points. These weakest

points exist in-between the laminate layers at matrix dominant regions where there is no reinforcement (unlike 3D structures in which vertical binder yarns are present). Clearly this is the region in-between the two adjacent layers, as much stronger forces are present within the interlaced unidirectional layers, so the weaker regions in-between the layers suffer delamination. In case of true-non-woven unidirectionals, with the application of shear force, the rupture within a yarn sheet layer is likely to take place earlier than the phenomenon of delamination may start to occur between the two adjacent unidirectional yarn sheets. The force of rupture within a layer dominates the force of delamination in-between the matrix rich regions of two adjacent layers. In other words delamination, with in layers, starts earlier than the phenomenon of delamination in-between the region of two adjacent layers.

Figure 3-11 shows a microscopic comparison between the non-commingled and commingled SBS tested specimens. (a1, b1) shows the non-commingled and commingled specimens before test, (a2, b2) shows side view of these specimens after short beam strength test, (a3, b3) shows the zoomed in side view of these specimens with clear crack propagation, (a4, b4) shows the tensile side (opposite side of depression probe) of the specimens and (a5, b5) shows the tensile side in a zoomed view with crack propagation and damaged yarns. As mentioned earlier, it is clear from the image (Figure 3-4), that the jute yarns are following a crimpier path in a commingled composite due to which they are suffering higher amount of displacement. As the yarns are laying straighter in a non-commingled composite so they exhibits lower amount of strain and breaks earlier at a lower amount of displacement, the same reflects from the side view of SBS tested specimens where the commingled composite specimen is deflected to higher amount of angle (b2) than the non-commingled up to a load drop-off of 30 %.
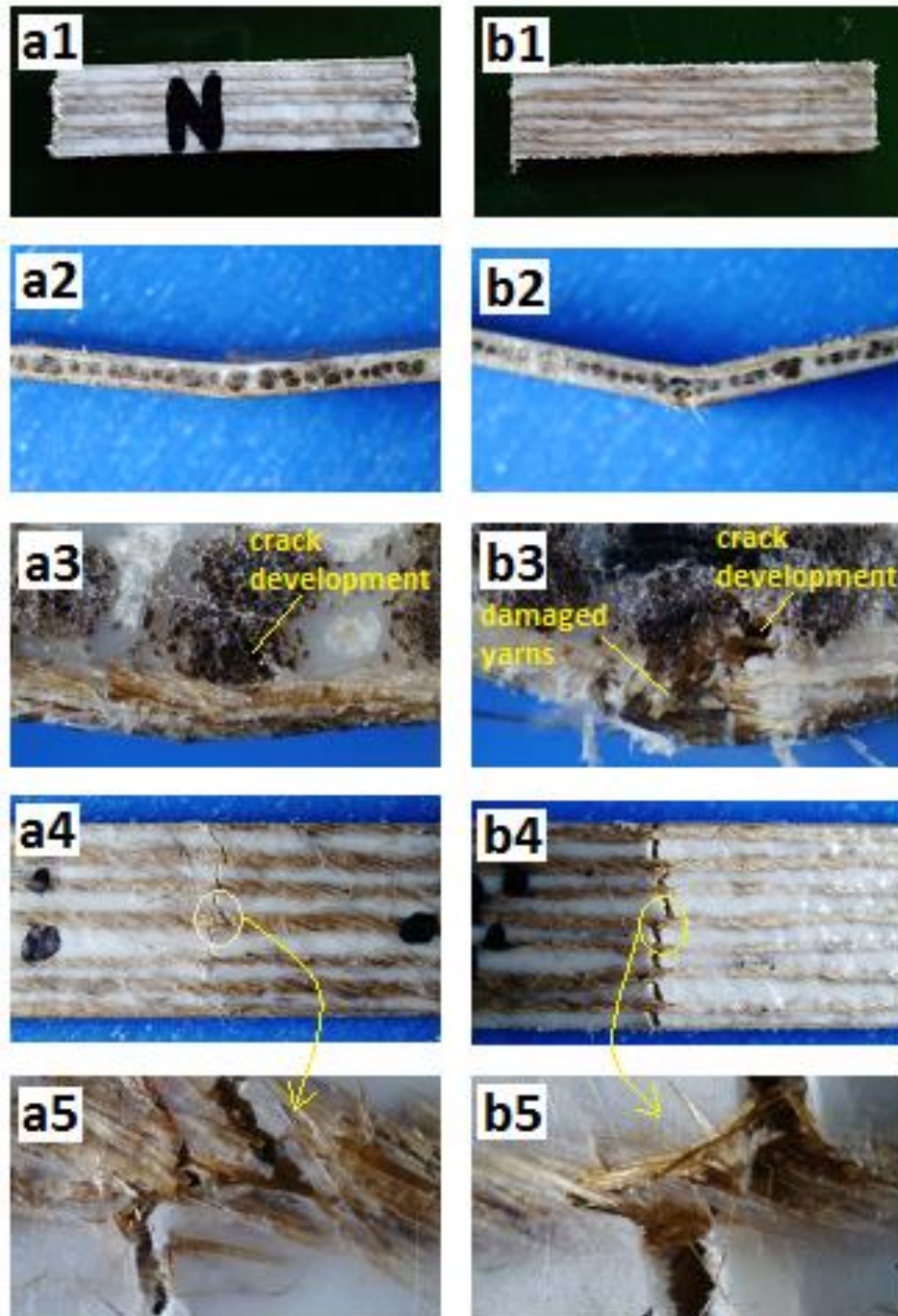
Figure 3-11. A Comparison of unidirectional non-commingled and commingled specimens against short beam strength test, (a1, b1) non-commingled and commingled specimens before test, (a2, b2) side view of tested specimens, (a3, b3) side zoomed in view of tested specimens with crack propagation, (a4, b4) tension sides of the specimens (a5, b5) tension side with zoomed in view

Table 3-3 illustrates the short beam mechanical properties of non-commingled and commingled specimens. The value of strength and strain has been compared. The variations

from the mean values are also shown. Short beam strength of non-commingled is barely 10.4% higher than the non-commingled UD composite. The strain of commingled UD is marginally higher than the non-commingled composite at 25%, which is mainly due to higher amount of jute yarn waviness as discussed earlier (Figure 3-4).

Table 3-3. Short beam properties of non-commingled and commingled UD composites

Type of Composite	Short beam Strength (MPa)	Displacement (mm)
Non-commingled	3.28±0.24	1.03±0.14%
Commingled	3.62±0.52	1.29±0.47%
Difference %	10.4	25

3.1.4 Charpy impact Properties of UD commingled and non-commingled composites

The typical work-displacement curve of Charpy impact test is shown in Figure 3-12. The initial part of the curve gives information of material initial resistance to deformation and stiffness. This zone is referred as crack initiation zone. The last part of curve tells about the behavior in the crack propagation zone/failure zone. The propagation of curve in this zone gives information whether the material failed suddenly or gradually.
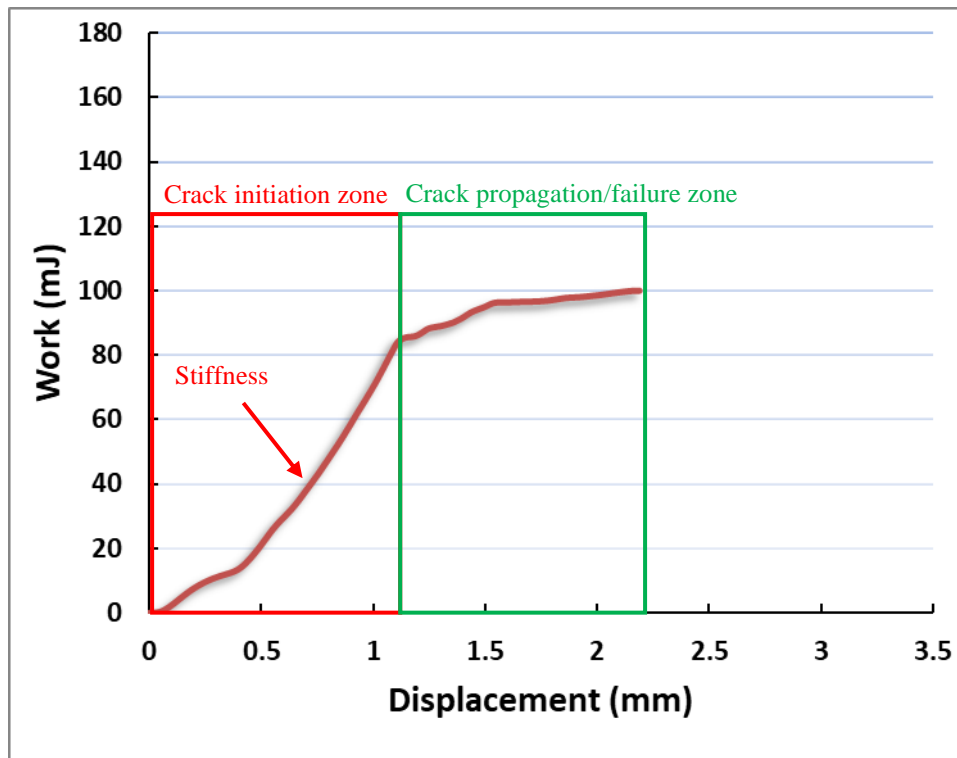
Figure 3-12. Typical Work-displacement curve of unidirectional non-commingled composite

Figure 3-13 illustrates the Charpy impact energies of the non-commingled and commingled composite specimens. (a) Shows the three dispersion curves of 4-layers unidirectional non-commingled composite (4UDNC). (b) Shows the three dispersion curves of 4-layers unidirectional commingled composite (4UDC). (c) Shows the comparison curves of 4UDNC and 4UDC. The impact energy of the non-commingled and commingled specimens is at the order of 94.13mJ and 146.8mJ, so the calculated impact energy of commingled specimen is an unsurpassed 56% higher than the non-commingled specimen. This is a big difference, showing the dominance of commingled specimen over non-commingled specimen and mainly it is due to two reasons. First is the better jute yarn interface with the polypropylene matrix in the commingled composite. Second reason is the higher amount of waviness of jute yarn present in the commingled composite. Due to this higher mount of waviness the commingled composite lasts longer against the impact force as compared to the non-commingled composite. In non-commingled specimen the weaker interface between the matrix and jute yarns results into lower impact properties. The same reflects from the comparison of impact strength of the two specimens. The impact strength of non-commingled and commingled specimens is at the order of 5.38kJ/m^2 and 8.19kJ/m^2, which means that the calculated impact strength of commingled specimen is 52% higher, which again shows a

dominance of commingled composite over the non-commingled composite, caused by a much better fiber matrix interface in commingled specimen as compared to non-commingled specimen. The same is verified by the microscopic images as described in Figure 3-14.
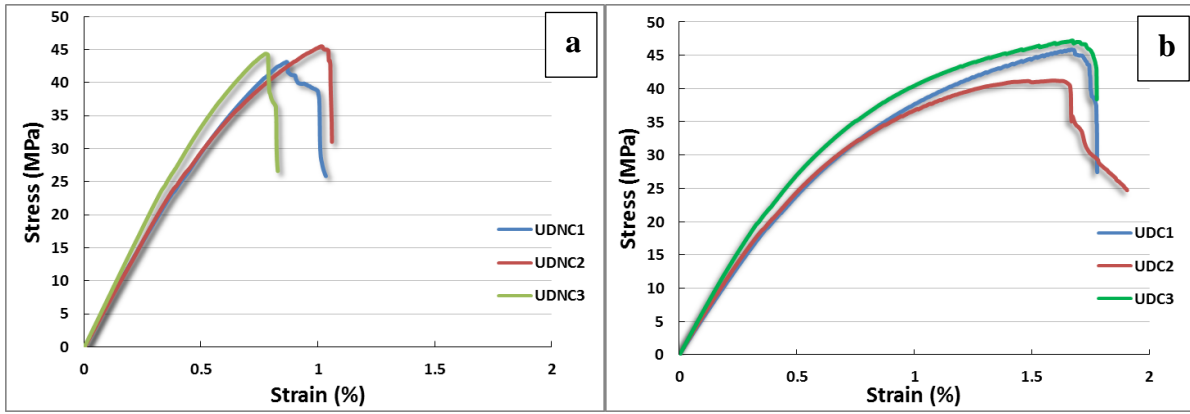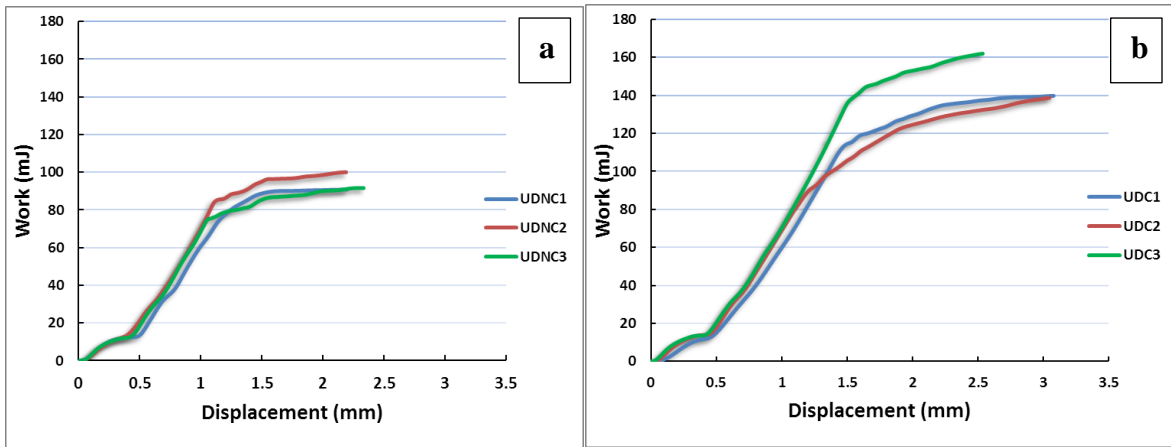

Figure 3-13. Work-displacement curves of unidirectional non-commingled and commingled composites, (a) dispersion curves of 4-layers unidirectional non-commingled composite (4UDNC), (b) dispersion curves of 4-layers unidirectional commingled composite (4UDC)
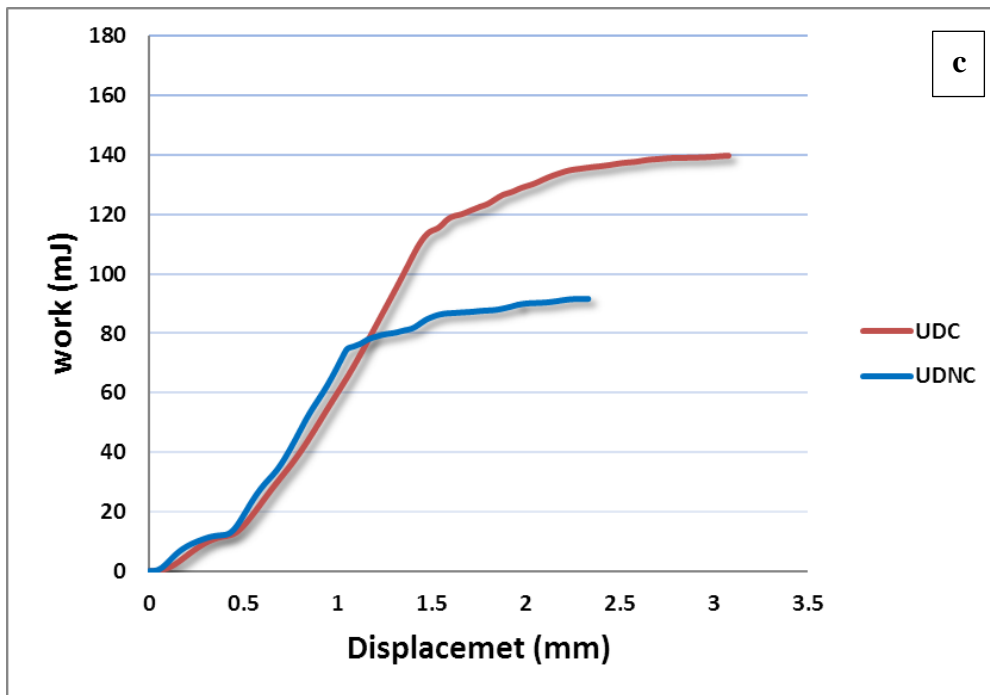

Figure 3-13. (c) Work-displacement curves of unidirectional non-commingled (4UDNC) and commingled (4UDC) composites

The microscopic comparison of commingled and non-commingled specimens for Charpy impact test shows some interesting differences (Figure *3-14*). The interface line, between the two parts of broken specimens, looks quite different for both specimens. In non-commingled

111

specimen (a, b) the breakage line is quite smoother; on the other hand, the breakage line looks zigzag for commingled specimen (c, d). It seems that the breakage phenomenon goes deep into the body of commingled specimen which speaks of a better adhesion between the jute fibers and the polypropylene matrix. On the other hand, the smoother breakage line between the two interfaces of non-commingled specimen speaks of a matrix dominant breakage, instead of showing a composite breakage behavior.
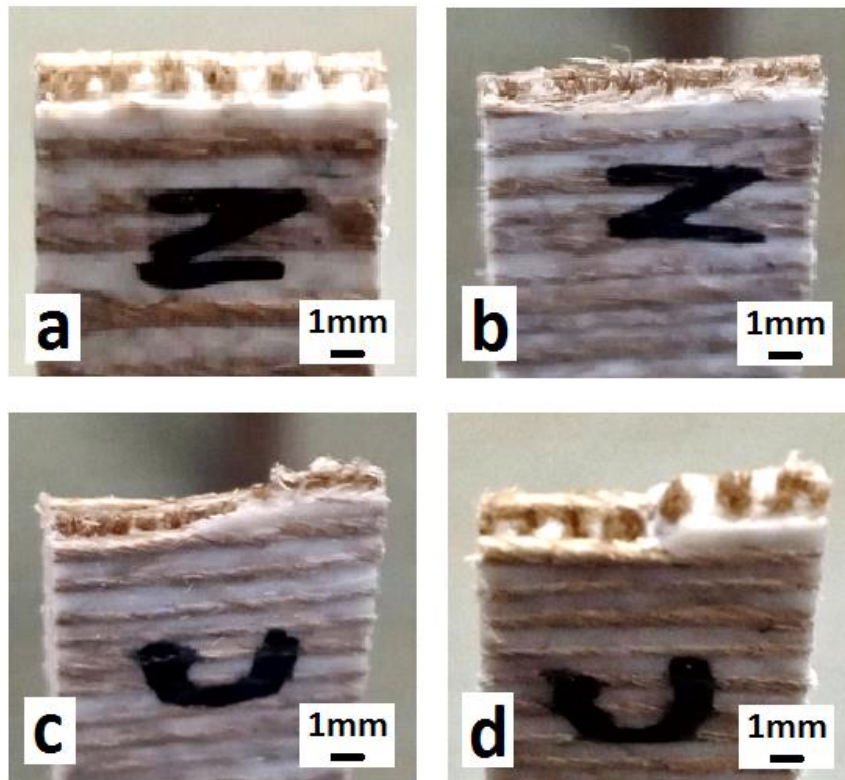
Figure 3-14. A comparison of Charpy impact tested samples of jute/PP composites, (a) completely broken non-commingled specimen, (b) non-commingled counterpart, (c) completely broken commingled specimen, (d) commingled counterpart

Table 3-4 illustrates the impact properties of non-commingled and commingled specimens. The value of impact energy and strength has been compared. The variations from the mean values are also shown. Impact energy on commingled composite is a marginal 56% and Impact strength is also a marginal 52% higher than the non-commingled UD composite. This is mainly due to better energy absorption characteristics of commingled composites. The strain of commingled UD is marginally higher than the non-commingled composite at 29.5%, which is mainly due to higher amount of jute yarn waviness as discussed earlier (Figure 3-4). The higher strain results into more energy absorption during the impact.

Table 3-4. Impact properties of non-commingled and commingled UD composites

Type of Composite	Impact Energy (mJ)	Impact Strength (KJ/m²))	Displacement (mm)
Non-commingled	94.13	5.38±0.93	2.24±0.1
Commingled	146.84±15.1	8.19± 0.82	2.9±0.35
Difference %	56	52	29.5

Figure 3-15 shows the typical force displacement curves of Charpy impact test for unidirectional non-commingled and commingled composites. the Fmax value for the unidirectional commingled specimen is some 17% higher than the non-commingled composite specimen (123N vs 144N). Initial impact force of commingled specimen is around 12% higher than the non-commingled composite (65N vs 73N), followed by quite matching curves of both composites till the Fmax value of non-commingled composite. After Fmax the non-commingled curve falls steeply showing more brittle fracture due to straighter lower crimp jute yarns in the non-commingled composite specimen, while on the other hand the commingled curve follows an inclined slope showing a bit more toughened energy-absorbing fracture than the non-commingled counterpart due to higher amount of crimp in jute yarns in the commingled composite. The displacement value at Fmax is also higher for commingled composite due to the presence of higher amount of jute yarn waviness (Figure 3-4). Displacement value for commingled specimen at Fmax is about 1.5mm as compared to 1.0mm of non-commingled composite (50% higher).
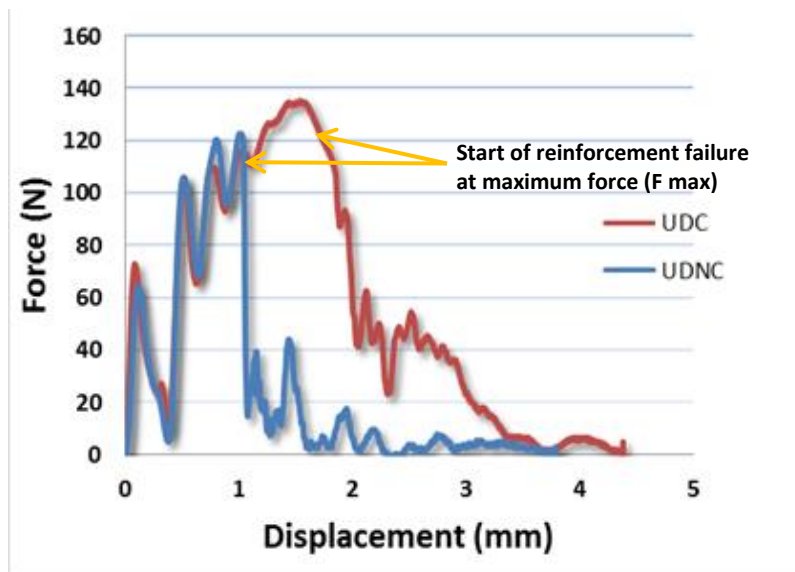
Figure 3-15. Force-displacement curves of 4 layer unidirectional commingled (4UDC) and non-commingled (4UDNC) composites obtained from instrumented Charpy impact tester

3.1.5   Summary

In this chapter the properties of UD commingled, and non-commingled composite made with the jute yarn and PP matrix were investigated in detail. The tensile, flexural, short beam strength and Charpy impact test were done. The tensile test results show that the commingled composite has higher tensile strength due to better impregnation of jute yarn within the matrix. The non-commingled composite had high stiffness and low strain due to straighter jute yarns. The flexural results showed the similar trends with the higher flexural strength for commingled composites as compared to non-commingled composites. The flexural strain of non-commingled composite was however lower as compared to commingled composite due to straighter jute yarn placement in the composite after fabrication. The short beam strength of commingled composite was also higher as compared to non-commingled composites. The Charpy impact strength of commingled composites was marginally higher due to better distribution of matrix and reinforcement as well as higher strain which causes more energy absorption during the impact. The overall results showed that the UD commingled composite has better mechanical properties and can be employed for thermoplastic composites fabrication.

Chapter 4. Effect of commingling on the mechanical properties of Jute/Polypropylene Composites

The present chapter includes the comparison of mechanical properties of jute/polypropylene composite samples fabricated using the conventional thermoforming technique with those fabricated using the commingled yarn technique. The yarn commingling simplifies/shorten the composite fabrication process. The cross-section of samples shows that the commingling technique improves the overall distribution and impregnation of reinforcement. Mechanical properties, i.e. tensile, flexural and instrumented Charpy impact properties, were tested using standard testing methods for both types of composites. The commingled composites showed better tensile, flexural, SBS and Charpy impact properties.

As early mentioned in chapter 2 above, three different layers combinations were used to make three different thicknesses of composites, 3, 4 and 5 layers, both in commingled and non-commingled categories. Based on these composites, following comparisons were made;

3 layer jute/polypropylene non-commingled composite (3JP) was compared with 3 layers commingled composite (3JPC), 4 layer jute/polypropylene non-commingled composite (4JP) was compared with 4 layers commingled composite (4JPC), 5 layer jute/polypropylene non-commingled composite (5JP) was compared with 5 layers commingled composite (5JPC). Six tests were performed each for 2D commingled and non-commingled composites specimens; six tested were performed for commingled and six were performed for non-commingled specimen. Comparisons of these tested specimens are described as under;

4.1   Tensile properties of non-commingled and commingled 2D composites

In this part, we are presenting results on tensile properties of 2D commingled and non-commingled composites.

A typical tensile behavior of 2D composites has been explained in Figure 4-1, which displays a stress-strain curve of jute polypropylene commingled composite. The curve looks like typical stress-strain curve of natural fiber reinforced thermoplastic composites with an initial linear region leading to no-linear deformation and abrupt fracture. The linear region relates to strain hardening, the nonlinear region starts with the matrix cracking and once the matrix cracking starts the fiber-matrix interface gets weakened and reinforcement starts exposing, then at the final failure point the composite fails completely due to fiber failure.
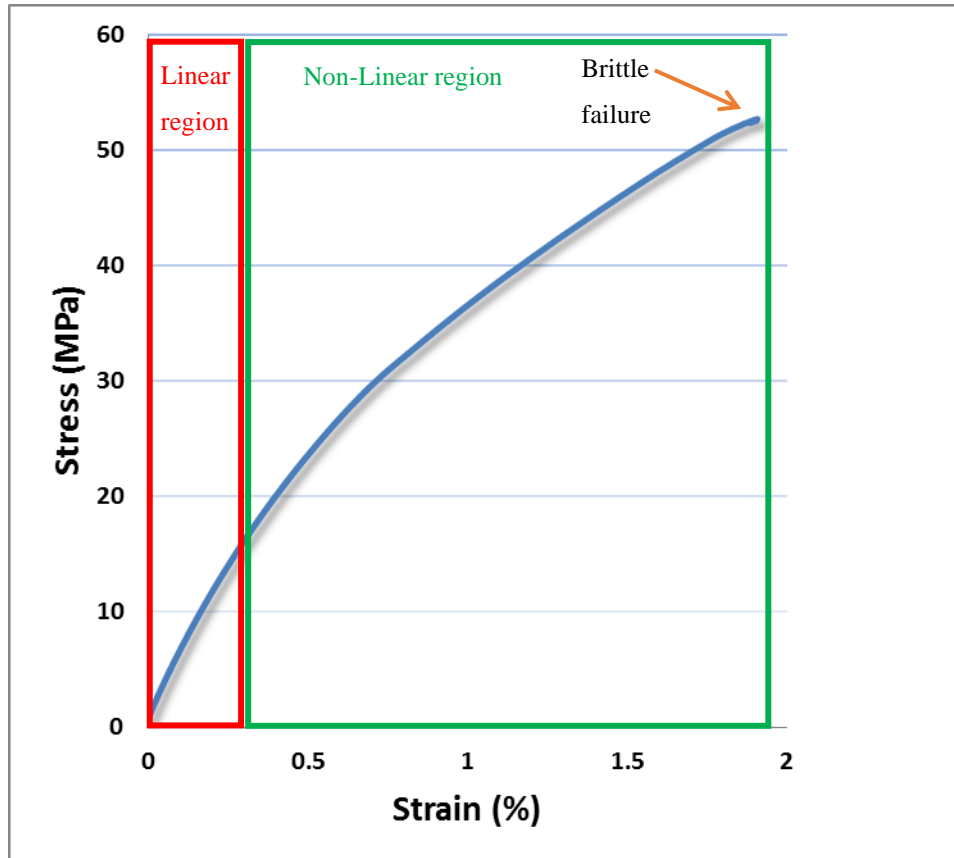
Figure 4-1. Typical stress-strain curve of 5-layer jute/PP commingled composite showing the linear region followed by the non-linear region and brittle failure

4.1.1 Effect of the number of layers on the tensile properties of non-commingled and commingled 2D composites

Figure 4-2 (a) shows the effect of the number of layers on tensile properties of 2D non-commingled and commingled composites. The values of ultimate tensile strengths of 3JP, 4JP, and 5JP are 30.3MPa, 34MPa and 35MPa, respectively. From 3JP to 4JP there is an increase of 12.2% but this increase is only 3% from 4JP to 5JP. The increase in ultimate tensile strength with an increase in the number of plies is not linear and not very significant. The tensile strength of 4JP and 5JP were almost same, the reason of this behavior is that even the numbers of plies were increased in 5JP, but the inter-ply adhesion causes the overall decrease in the tensile strength. As the composite was made by conventional thermoforming technique, so the properties heavily depend on the fiber-matrix interface and inter-ply adhesion. With increasing the number of plies, the effect of poor inter-ply adhesion becomes more prominent.

Figure 4-2 (b) shows the tensile strength of 2D 3, 4 and 5 layered commingled specimens. The values of ultimate tensile strengths of 3JPC, 4JPC, and 5JPC are 34.2MPa, 43.6MPa and 52.7MPa, respectively. The increase in tensile strength from 3JPC to 4JPC is 27.5% and 21% from 4JP to 5JP. The increase in ultimate tensile strength with the number of layers is significantly higher. As compared to non-commingled composites, the properties are more pronounced, and the effect of numbers of plies is also very significant. The inter-ply adhesion also improved due to commingling, as a strong partially self-reinforced polypropylene network formed in which jute yarns were evenly distributed.
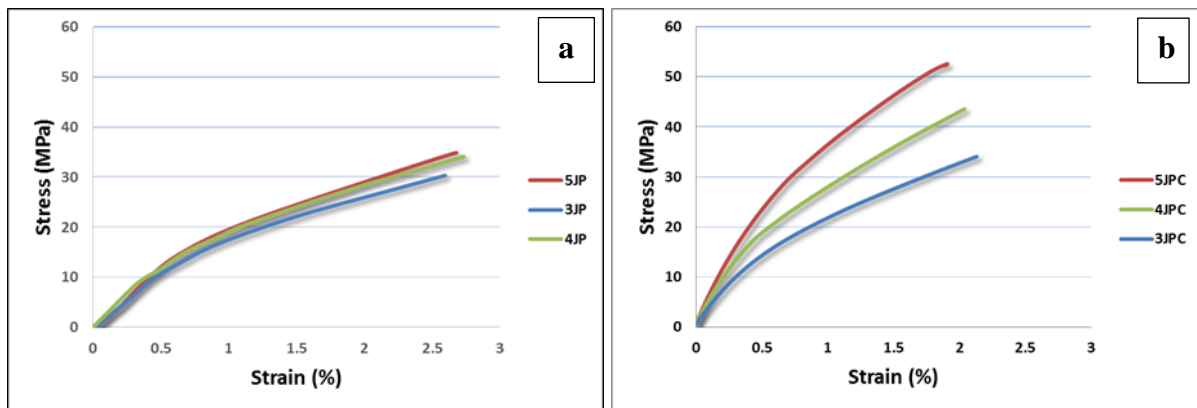
Figure 4-2. The effect of number of layers on tensile strength of non-commingled and commingled 2D composites, (a) comparison between 3, 4 and 5 layers of non-commingled composites, (b) comparison between 3, 4 and 5 layers of commingled composites

4.1.2 Comparison of commingled and non-commingled 2D composites for tensile properties

Figure 4-3 explains the tensile strengths of 3-layered non-commingled and commingled composites specimens. (a) shows the three dispersion curves for 3-layered jute/PP non-commingled (3JP) composite, (b) shows the three dispersion curves for 3-layered jute/PP commingled (3JPC) composite and (c) shows a comparison between the 3-layered non-commingled (3JP) and commingled (3JPC) composite specimens. The values of ultimate tensile strengths of 3JP and 3JPC are 30.3MPa and 34.2MPa respectively, which shows that the commingled composite is 13% stronger than the non-commingled composite specimen.
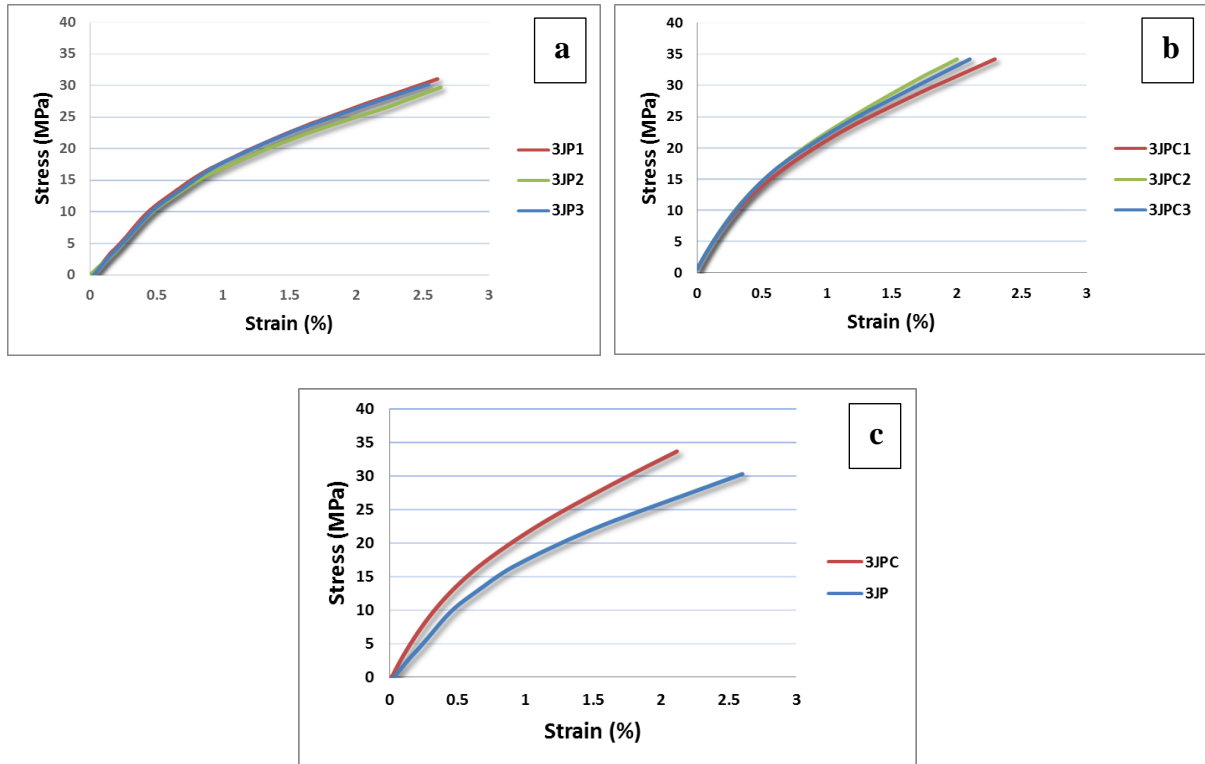
Figure 4-3. The Stress-Strain curves of 3-layered non-commingled and commingled 2D composite specimens, (a) three dispersion curves for 3JP, (b) three dispersion curves for 3JPC, (c) a comparison between the 3JP and 3JPC composites

Figure 4-4 explains the tensile strength of 4-layered non-commingled (4JP) and commingled (4JPC) composites specimens. (a) shows the three dispersion curves for 4-layered jute/PP non-commingled (4JP) composite, (b) shows the three dispersion curves for 4-layered jute/PP commingled (4JPC) composite and (c) shows a comparison between the 4-layered non-commingled and commingled composite specimens. The values of ultimate tensile strengths of 4JP and 4JPC are 34MPa and 43.6MPa respectively, which shows that the commingled composite is 28.2 % stronger than the non-commingled composite specimen.
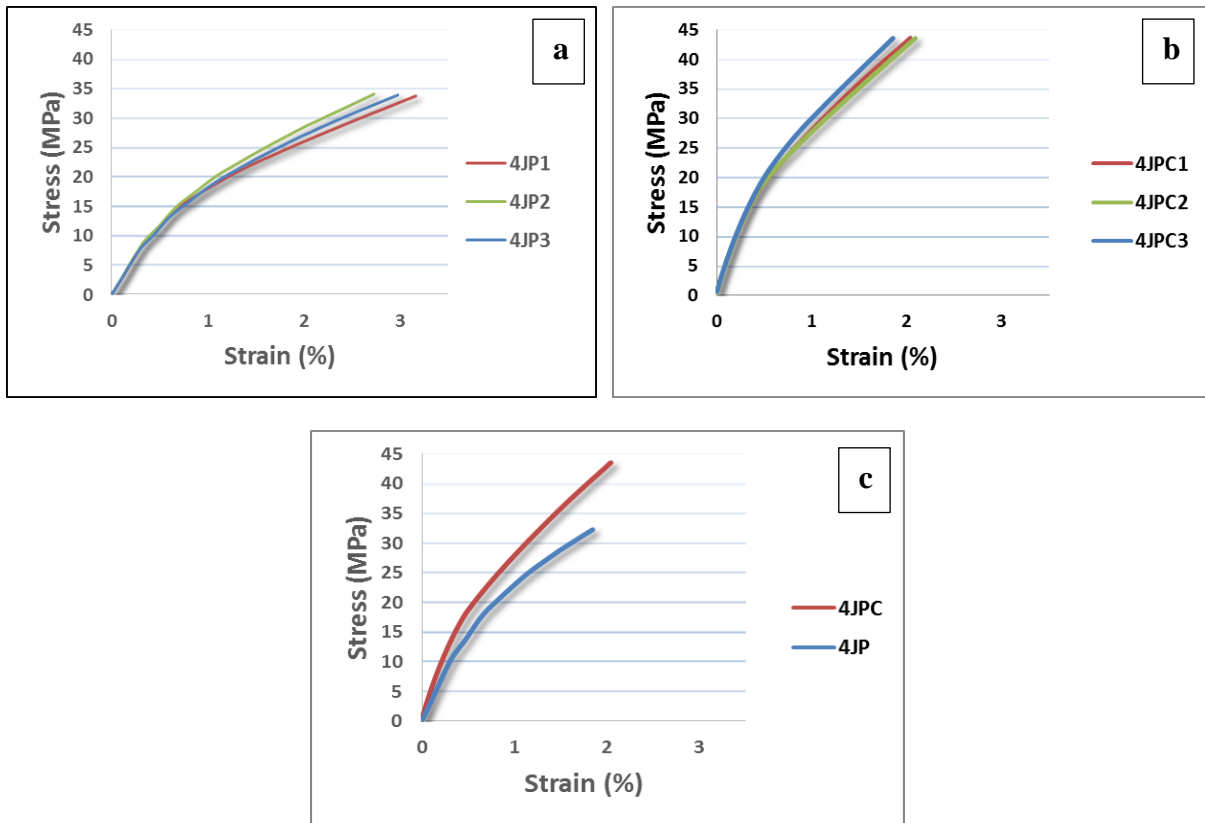
Figure 4-4. The Stress-Strain curves of 4-layered non-commingled and commingled 2D composite specimens, (a) three dispersion curves for 4JP, (b) three dispersion curves for 4JPC, (c) a comparison between the 4JP and 4JPC composites

Figure 4-5 explains the stress-strain curves of 5-layered non-commingled (5JP) and commingled (5JPC) composites specimens. (a) shows the three dispersion curves for 5-layered jute/PP non-commingled (5JP) composite, (b) shows the three dispersion curves for 5-layered jute/PP commingled (5JPC) composite and (c) shows a comparison between the 5-layered non-commingled and commingled composite specimens. The values of ultimate tensile strengths of 5JP and 5JPC are 35.5MPa and 52.7MPa respectively, which shows that the commingled composite is 48.5 % stronger than the non-commingled composite specimen.
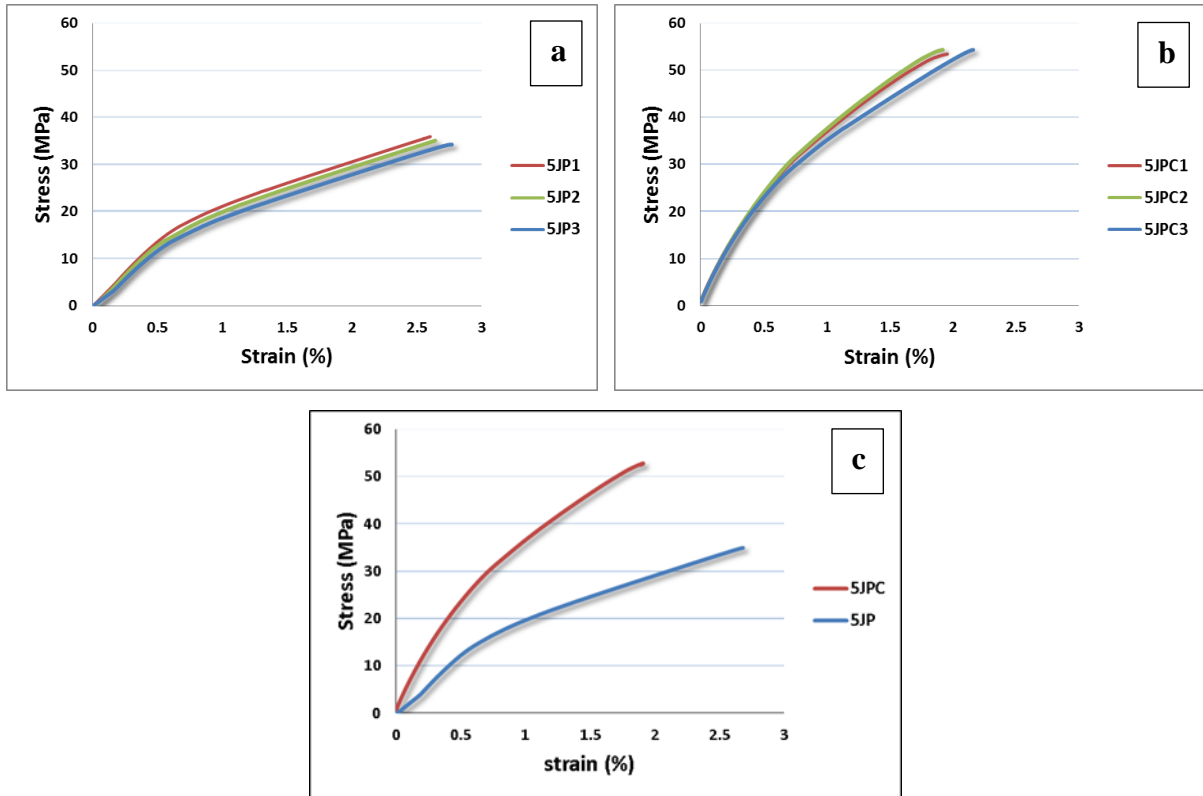
Figure 4-5. The Stress-Strain curves of 5 layered non-commingled and commingled 2D composite specimens, (a) three dispersion curves for 5JP, (b) three dispersion curves for 5JPC, (c) a comparison between the 5JP and 5JPC composites

Table 4-1 shows the tensile strength and strain percent of the non-commingled and commingled composites. The 3JPC specimen is showing an increase of 12.9% in the tensile strength as compared to 3JP (34.2MPa vs 30.3MPa), which indicates a better-commingled composite as compared to non-commingled composite.

The strain behavior of 3JPC is also on the better side, indicating a more robust commingled composite with the higher trend of tensile modulus. On the other hand, the tensile strength of 4JPC at 43.6MPa is also higher than 4JP at 34MPa, which is approximately an increase of 28.2%. The strength of 5JPC is also on the higher side (52.7 vs 35.5 MPa for 5JP), which is 48.5%. The results show that the tensile strength of commingled composites is dominant on non-commingled composites, which indicates a better wetting of the jute fiber with commingled thermoplastic resin as compared to non-commingled). This may be due to the reason the distance between the fibers and the resin for non-commingled is more (defined by the distance between the alternate stacks of layers of jute and thermoplastic resin one above the other) than the commingled composite in which co-twisted polypropylene and jute yarn are laying side by side in each and every layer. This is a clear indication that matrix

distribution and adhesion is better in commingled composites as compared to the non-commingled ones, which us further verified by the microscopic analysis (Figure 4-6)

Table 4-1. Tensile strengths of non-commingled and commingled 2D composites

	Non-commingled composites (JP)		Commingled composites (JPC)		Difference between commingled and non-commingled composites (%)	
	Tensile strength (MPa)	Strain at break (%)	Tensile strength (MPa)	Strain at break (%)	Tensile strength (MPa)	Strain at break (%)
3 layer	30.3±1.21	2.45±0.052	34.2±1.15	1.94±0.092	12.9	26.3
4 layer	34±1.01	2.94+0.069	43.6±1.97	1.92±0.065	28.2	53.1
5 layer	35.5±1.67	3.32±0.035	52.7±2.35	2.25±0.05	48.5	47.6

Figure 4-6 shows the fractured samples of commingled and non-commingled composites after tensile test. As can be seen that the commingled composite have even yarn and matrix distribution. That even distribution formed a partial self-reinforced jute/PP network that resulted in better tensile properties. This partial self-reinforced jute/PP network can be characterized by lighter color of the commingled composite in the crossectional view, which is mainly due to white colored PP matrix around the jute yarns. More over the surface color of the commingled composite looks darker which is an evidence of lesser PP matrix on the surface. Hence in the commingled composite there is lesser surface coating and more matrix penetration. The fracture path also showing that the fracture was difficult which caused a zig-zag crack path. Both matrix and yarn offered even resistance to tensile force. The non-commingled composite however had least distribution of matrix and reinforcement, which caused a slight straighter fracture path. There can be seen more fiber pullout in the non-commingled composite that is showing effect of un-even matrix distribution. The uneven and poor matrix distribution in the non-commingled composite can be characterized by the darker color in the crossectional view of the composite, while the surface color of the non-commingled composite looks more whitish caused by more surface coating of the non-commingled composite. Hence in the non-commingled composite there is more surface coating and lesser matrix penetration as compared to commingled composite.

The same can be verified by the SEM analysis (Figure 4-7) showing improved wetting of fibers in the commingled composite and more fiber pullout trend in the non-commingled

composite. The better mechanical properties of commingled composites are mainly due to improved wetting of jute yarn, which led to improved interfacial adhesion of fiber and matrix. The yarns are well placed in the matrix which led to improved interfacial adhesion.
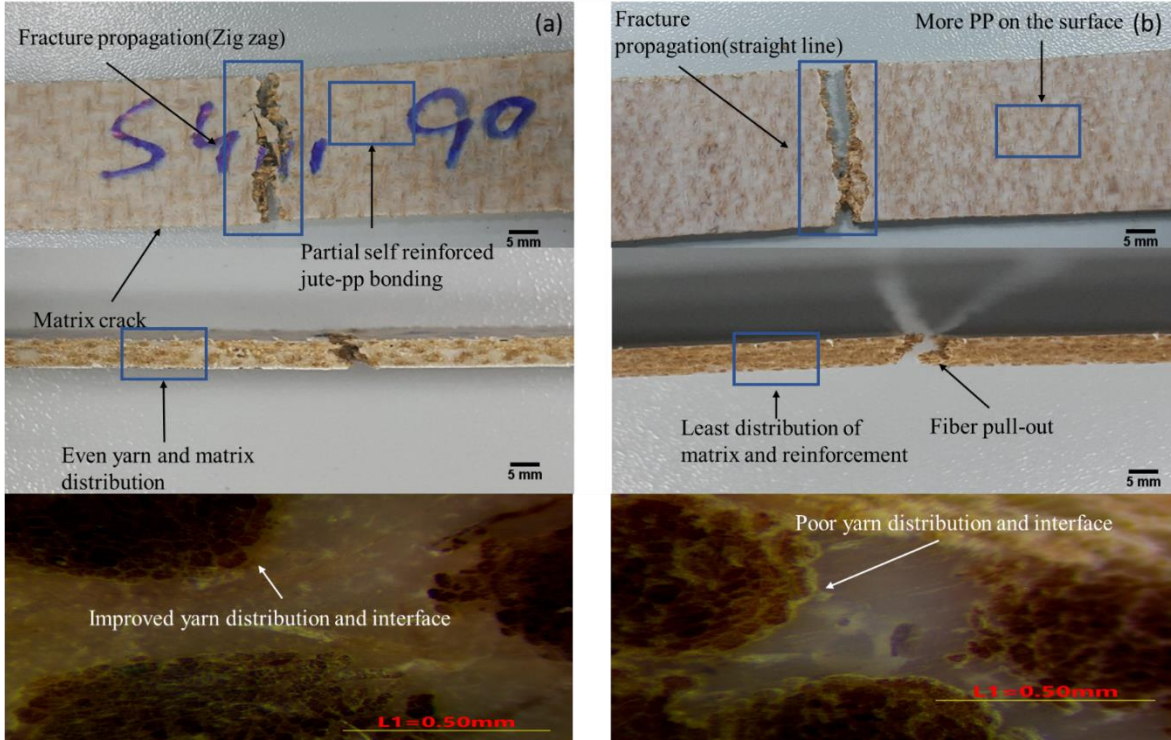
Figure 4-6. Fracture sample after tensile test (a) commingled (b) non-commingled
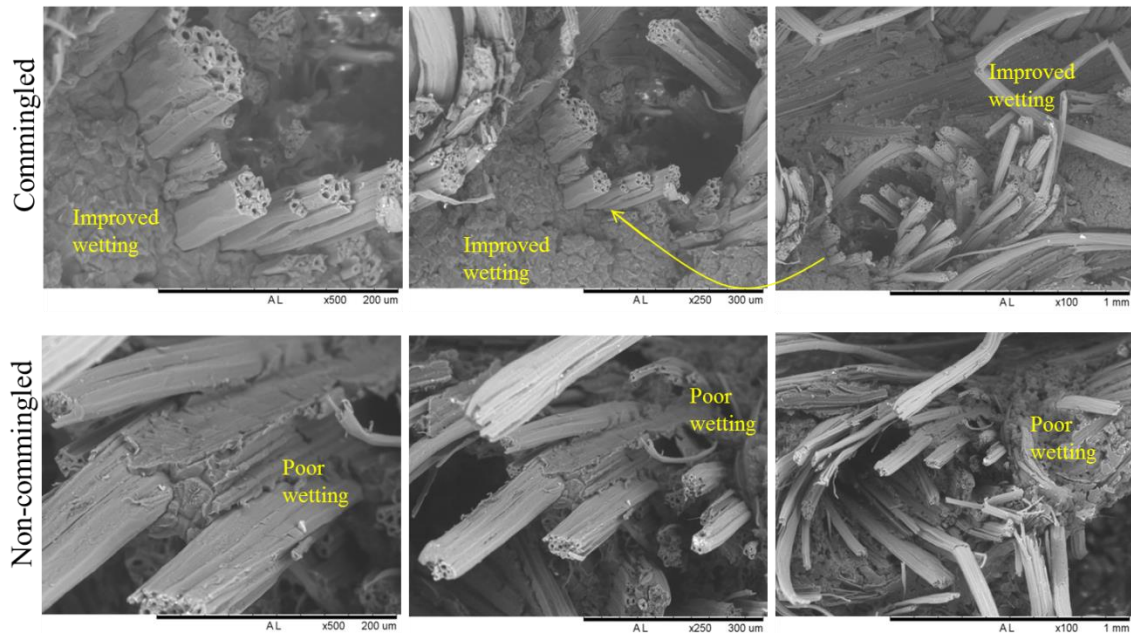
Figure 4-7. SEM analysis of impregnation behavior of commingled and non-composites

4.2 Flexural properties of non-commingled and commingled 2D composites

In this section flexural properties of 2D non-commingled and commingled composites are discussed in detail.

The behavior of 2D composites against the flexural load has been explained in Figure 4-8, which displays a typical flexural stress-strain curve of jute/polypropylene non-commingled composite with an initial linear region followed by the non-linear zone. Then there is peak load followed by matrix cracking, ending into gradual fiber failure.
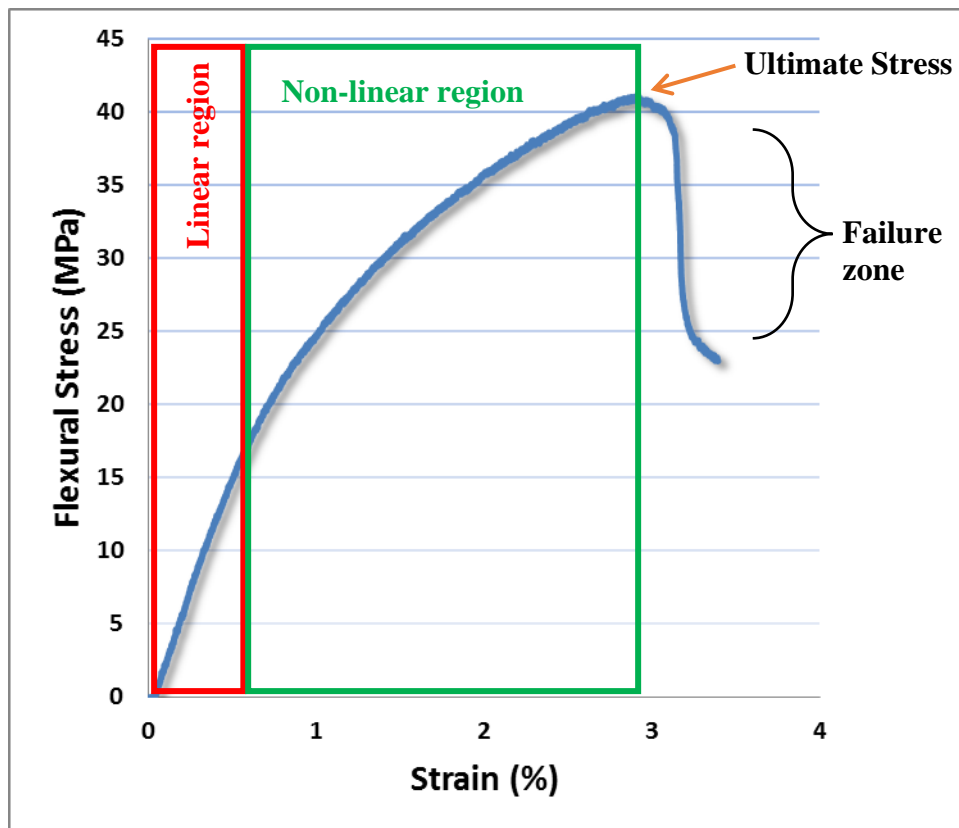
Figure 4-8. Typical flexural stress-strain curve of jute/PP non-commingled composite showing the linear region followed by the non-linear region and fiber failure

4.2.1 Effect of the number of layers on flexural strength of non-commingled 2D composites

Figure 4-9 illustrates the stress-strain curves of the flexural test for all 2D non-commingled (made using conventional Thermoforming technique) 3, 4, and 5 layered thermoplastic composite specimens. There is an increase of flexural strength with the increasing number of

layers from 3 to 5 layers. However, this increasing trend is not very linear. The values of flexural strengths of 3JP, 4JP and 5JP are found equal to 28.1MPa, 38.2MPa and 42.1MPa, respectively. From 28.1MPa to 38.2 MPa there is an increase of 35% for 3JP to 4JP, while from 4JP to 5JP the increase is relatively on the lower side with 10.2%. The main factor that contributes to this behavior, when the number of layers increases from 3 to 4, there is an increase of reinforcement material by 33.3%, but from 4 to 5 layers the increase is only 25%, and consequently, the phenomenon of strength works accordingly with a higher trend from 3 to 4 layer (28.1 to 38.2MPa) and lower trend from 4 to 5 layers (38.2 to 42.1MPa).
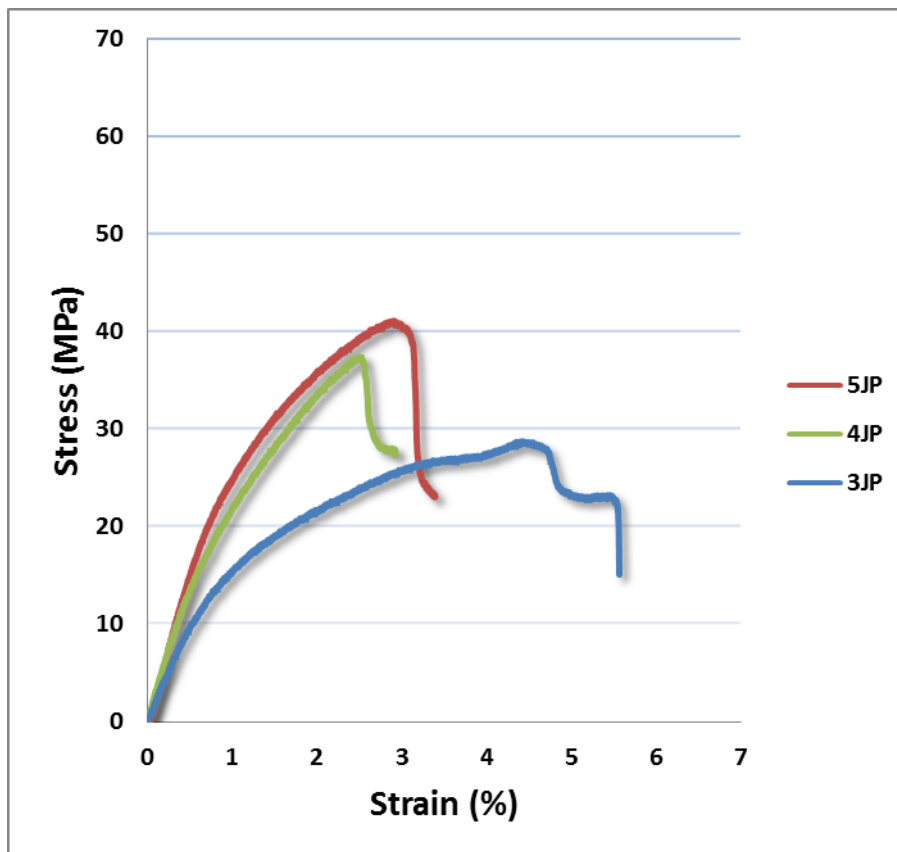
Figure 4-9. flexural stress-strain curves for all non-commingled 2D composites

4.2.2 Effect of the number of layers on flexural strength of commingled 2D composites

The trend of increase in the flexural stress for 2D-commingled 3 layer, 4 layer and 5 layer specimens (Figure 4-10) is quite similar to that of 2D non-commingled specimens, i.e., there is an increase of strength from 3 to 4 to 5 layers. However, this increasing trend is also not linear. The values of flexural strengths of 3JPC, 4JPC, and 5JPC were found equal to 51MPa, 61.1MPa and 66MPa, respectively.
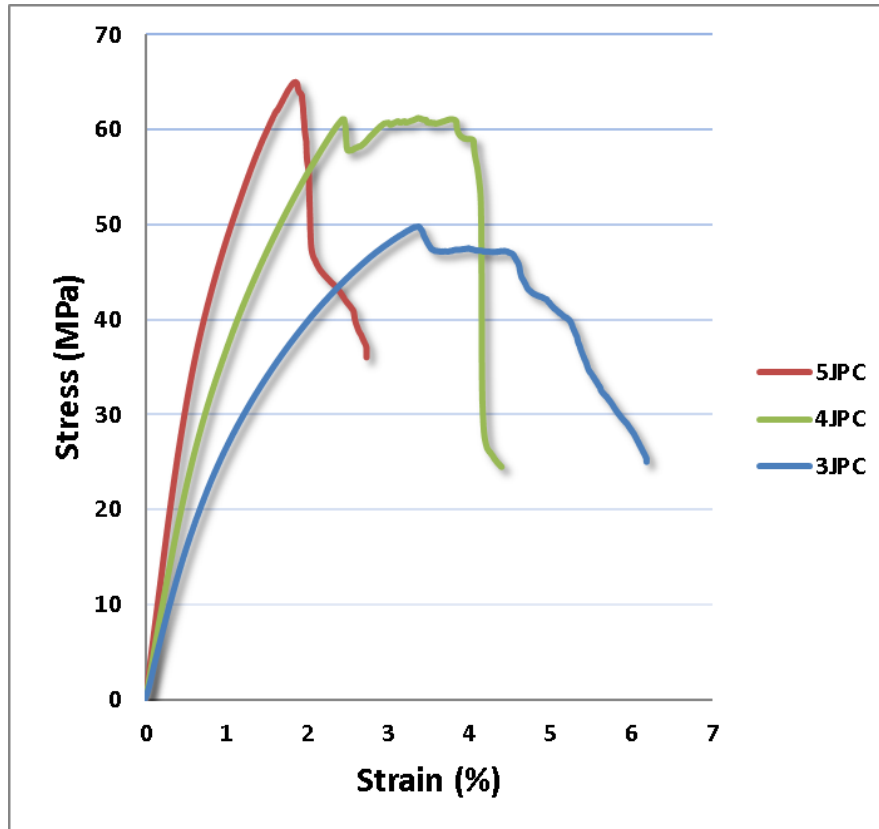
Figure 4-10. Flexural stress-strain curves for all commingled 2D composites

4.2.3   Comparison of commingled and non-commingled 2D composites for flexural properties

Figure 4-11 shows the flexural stress-strain curves of 3-layer 2D-non-commingled and 3-layer 2D-commingled composites. The flexural strength of 3JPC at 51MPa is also higher than 3JP at 28.1MPa, which is a marginal 81.5% higher in the flexural strength (Table 4-2), which indicates a better commingled composite as compared to non-commingled composite. In the commingled composites a better fiber composite interface, even yarn distribution within the matrix, partially self-reinforced polypropylene network formation and better inter-ply adhesion are achieved due to commingling.

Figure 4-12 shows the flexural stress-strain curve of 4-layer 2D non-commingled and 4-layer 2D commingled composite. The flexural strength of 4JPC at 61.1MPa is also higher than 4JP at 38.2MPa, which is approximately 60% higher (Table 4-2). Figure 4-13 shows the flexural stress-strain curve of 5-layer 2D-non-commingled and 5-layer 2D-commingled composites. The flexural strength of 5JPC is also on the higher side (66MPa vs 42.1 MPa), which is 57% higher. The results show that the flexural strength of commingled composites is dominant on

126

non-commingled composite, which indicates a better wetting out of the jute fiber with commingled thermoplastic resin as compared to non-commingled.
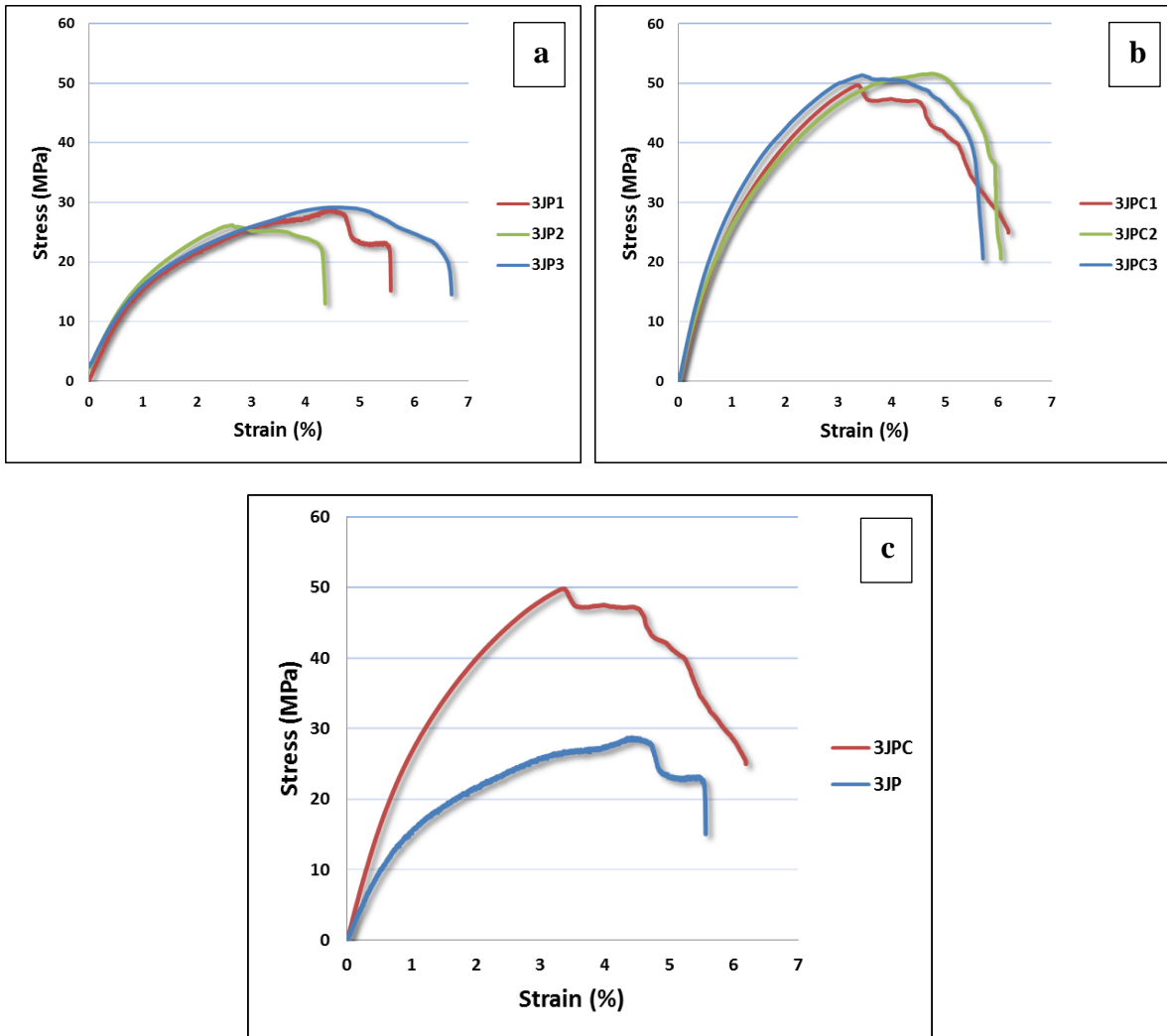
Figure 4-11. Flexural strength of 3-layered non-commingled (3JP) and commingled (3JPC) 2D composites (a) three dispersion curves for 3JP (b), three dispersion curves for 3JPC, (c) comparison of average curves of 3JP and 3JPC
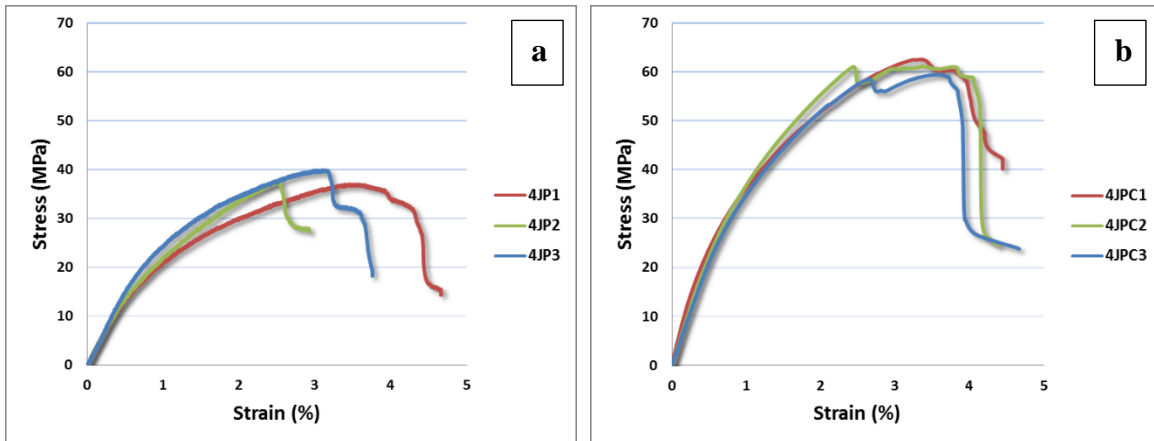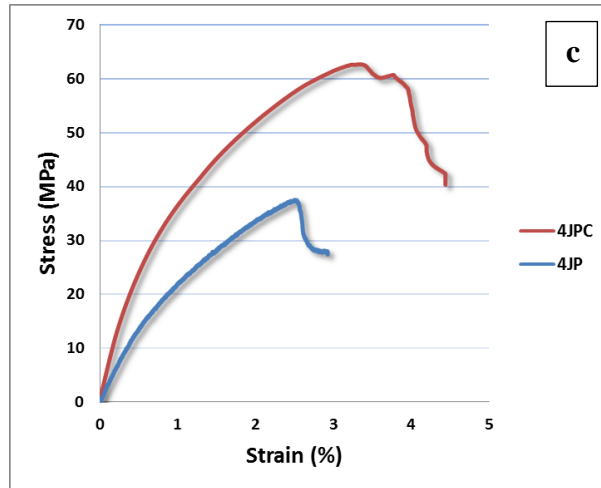
Figure 4-12. Flexural strength of 4-layered non-commingled (4JP) and commingled (4JPC) 2D composites (a) three dispersion curves for 4JP (b), three dispersion curves for 4JPC, (c) comparison of average curves of 4JP and 4JPC
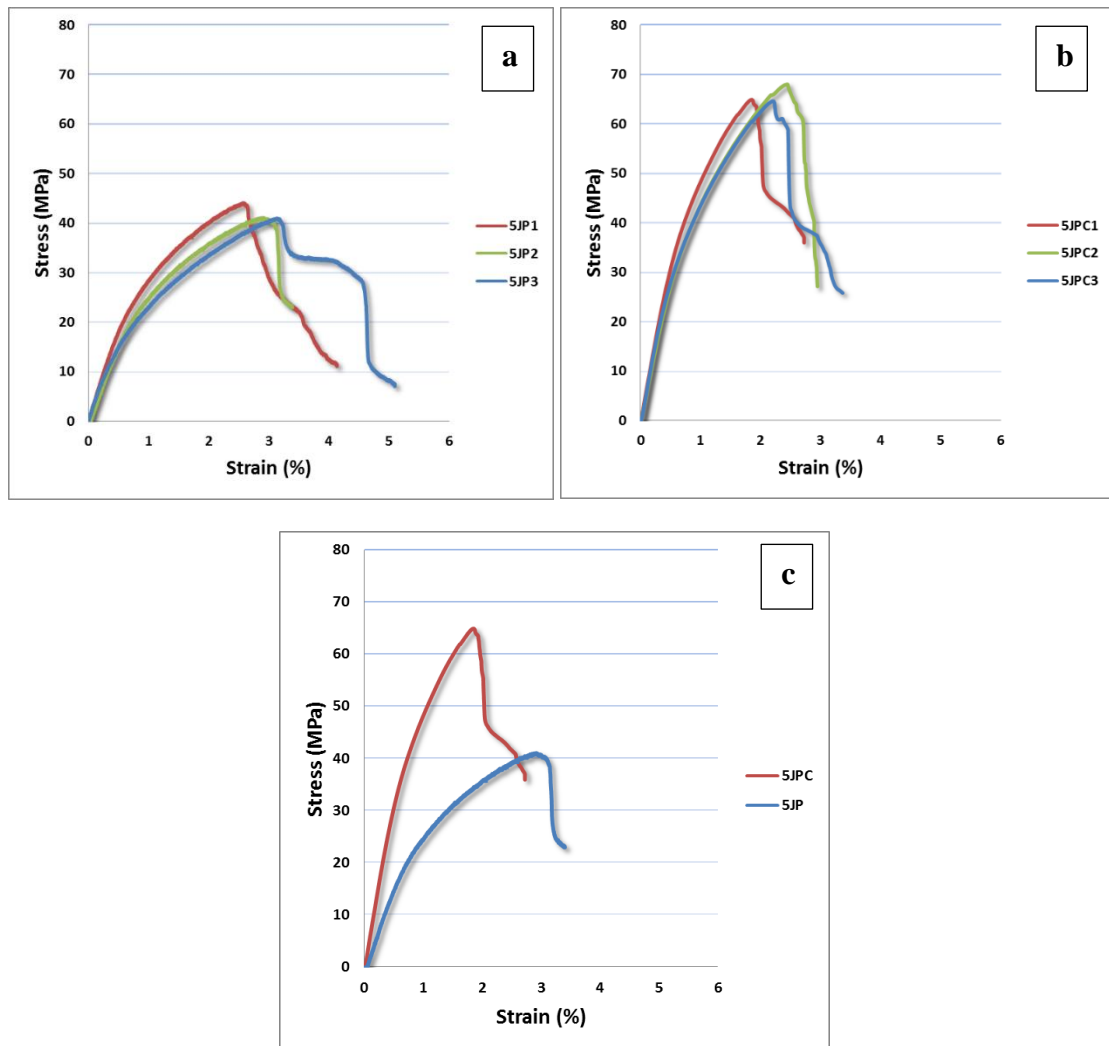
Figure 4-13. Flexural strength of 5-layered non-commingled (5JP) and commingled (5JPC) 2D composites (a) three dispersion curves for 5JP (b), three dispersion curves for 5JPC, (c) comparison of average curves of 5JP and 5JPC

Table 4-2 gives a comprehensive comparison of the flexural properties of 3, 4 and 5 layered non-commingled and commingled composites along with the variation from the mean value.

Table 4-2. Flexural properties of 3, 4 and 5 layered non-commingled and commingled 2D composites

	Non-commingled composites (3JP)		Commingled composites (3JPC)		Difference between commingled and non-commingled composites (%)	
	Flexural strength (MPa)	Strain (%)	Flexural strength (MPa)	Strain (%)	Flexural strength (MPa)	Strain (%)
3 layer	28.1±1.9	5.54±1.19	51±1.17	5.98±0.28	81.5	7.2
4 layer	38.2±1.73	3.8±0.88	61.1±1.6	4.5±0.16	60	18.4
5 layer	42.1±2.0	4.2±0.89	66±2.2	3.0±0.35	57	40

4.3 Short beam strength of non-commingled and commingled 2D composites

In this section SBS properties of 2D non-commingled and commingled composites are discussed in detail.

4.3.1 Effect of the number of layers on short beam strength of non-commingled and commingled 2D composites

Figure 4-14 illustrates the short beam strength (SBS) curves of all 2D non-commingled and commingled 3, 4 and 5 layered thermoplastic composites. There is an increase of short beam strength with the increasing number of layers from 3 to 5 layers. However, this increasing trend is not very linear. The values of SBS strengths of 3JP, 4JP and 5JP are found equal to 331MPa, 393MPa and 397.5MPa, respectively. From 331MPa to 393 MPa there is an increase of 19% for 3JP to 4JP, while from 4JP to 5JP the increase is relatively on the lower side with barely 1.1%. The main factor that contributes to this behavior, when the number of layers increases from 3 to 4, there is an increase of reinforcement material by 33.3%, but from 4 to 5 layers the increase is only 25%, and consequently, the phenomenon of shear strength works accordingly with a higher trend from 3 to 4 layer (331 to 393MPa) and lower trend from 4 to 5 layers (393 to 397.5MPa). The same comes true from the results of 3JPC, 4JPC and 5JPC for which the SBS strength values are 483.6MPa, 627.5MPa and 718MPa, respectively. From 483.6MPa to 627.5MPa there is an increase of 30% for 3JPC to 4JPC, while from 4JPC to 5JPC the increase is relatively on the lower side with barely 14.4%. The

average overall short beam strength of 3, 4 and 5-layered commingled composites is 62% higher than non-commingled composites.
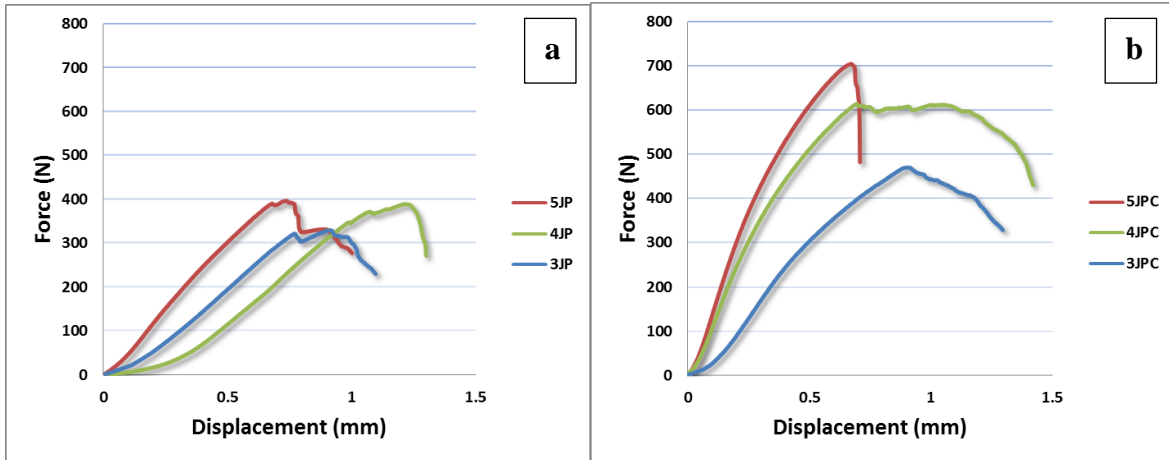
Figure 4-14. Short beam strength curves of all 3, 4 and 5-layered 2D composites, (a) non-commingled (3, 4, 5JP) composites (b) commingled (3, 4, 5JPC) composites

4.3.2 Comparison of commingled and non-commingled 2D composites for short beam strength

Figure 4-15 explains SBS curves of 3-layered non-commingled and commingled composites, (a) shows multiple curves of 3-layered non-commingled (3JP) composites, (b) shows multiple curves of 3-layered commingled (3JPC) composite and (c) shows a comparison of 3-layered non-commingled and commingled composites. The SBS strength of 3-layered commingled composite is 46% higher than the non-commingled composite.
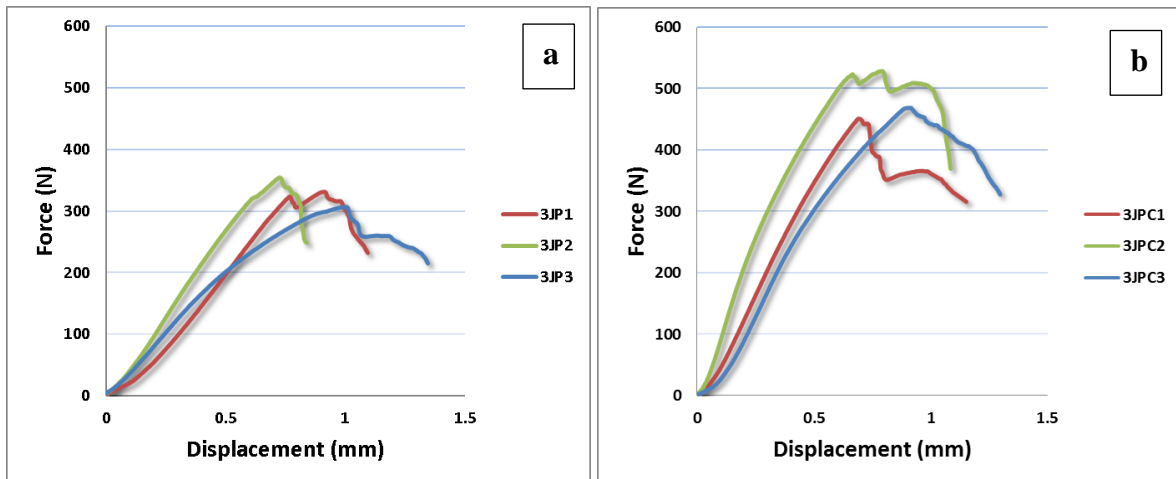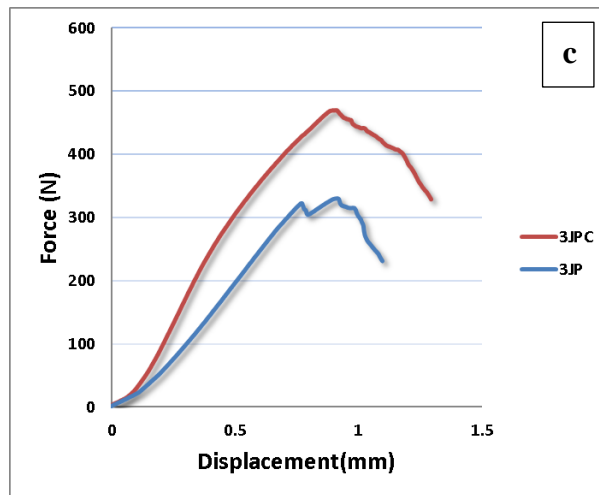
Figure 4-15. SBS curves of 3-layered non-commingled and commingled 2D composites, (a) three dispersion curves of 3-layered non-commingled (3JP) composites, (b) three dispersion curves of 3-layered commingled (3JPC) composite, (c) a comparison of 3JP and 3JPC, 3JPC 46% stronger

Figure 4-16 explains the SBS curves of 4-layered non-commingled and commingled composites, (a) shows multiple curves of 4-layered non-commingled (4JP) composites, (b) shows multiple curves of 4-layered commingled (4JPC) composite while (c) shows a comparison of 4-layered non-commingled and commingled composites. The SBS strength of 4-layered commingled composite is 60% higher than the non-commingled composite.
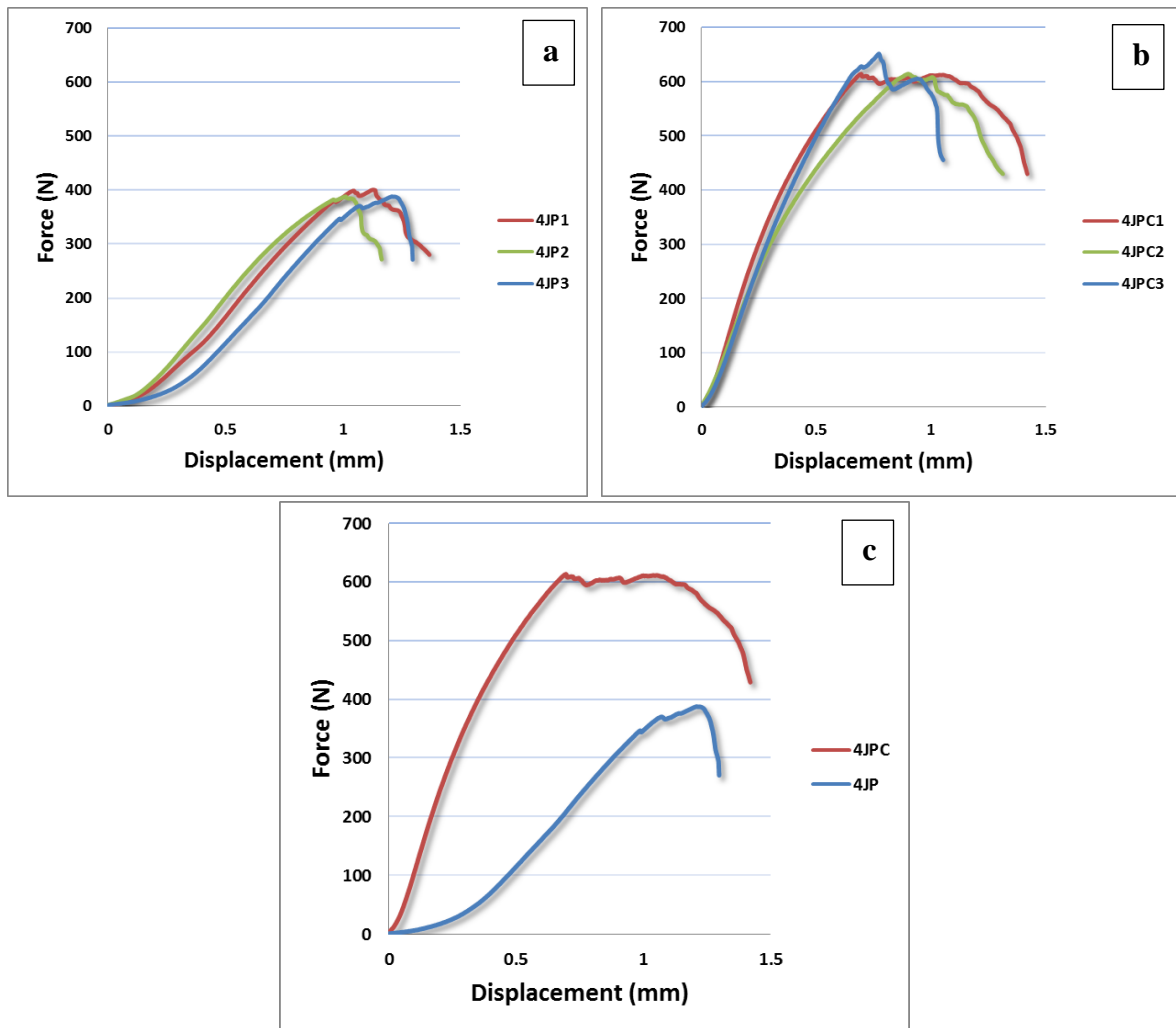
Figure 4-16. SBS curves of 4-layered non-commingled and commingled 2D composites, (a) three dispersion curves of 4-layered non-commingled (4JP) composites, (b) three dispersion curves of 4-layered commingled (4JPC) composite, (c) a comparison of 4JP and 4JPC, 4JPC 60% stronger

Figure 4-17 explains SBS curves of 5-layered non-commingled and commingled composites, (a) shows multiple curves of 5-layered non-commingled (5JP) composites, (b) shows multiple curves of 5-layered commingled (5JPC) composite while (c) shows a comparison of 5-layered non-commingled and commingled composites. The SBS strength of 5-layered commingled composite is 81% higher than the non-commingled composite.
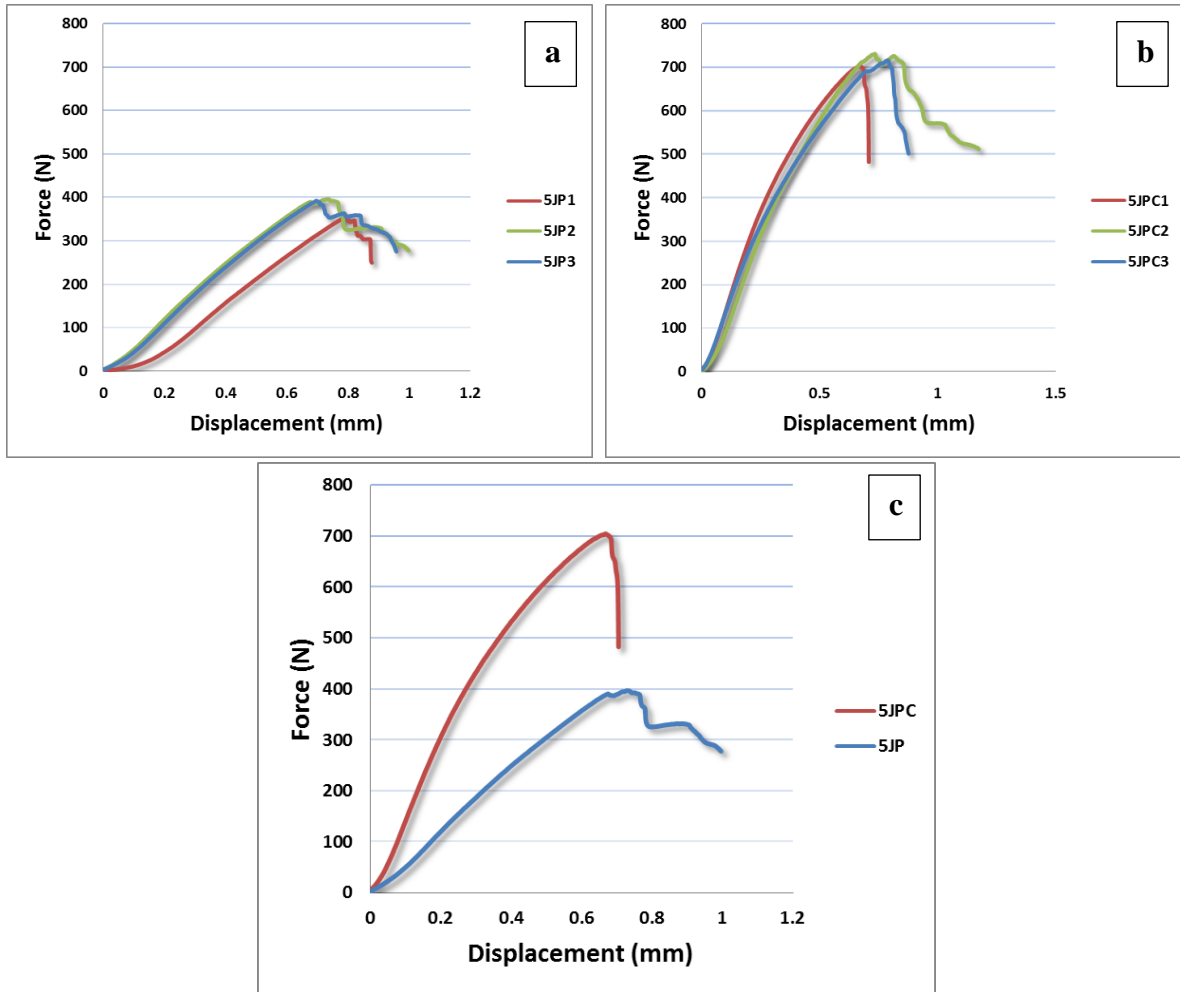
Figure 4-17. SBS curves of 5-layered non-commingled and commingled 2D composites, (a) three dispersion curves of 5-layered non-commingled (5JP) composites, (b) three dispersion curves of 5-layered commingled (5JPC) composite, (c) a comparison of 5JP and 5JPC, 5JPC 81% stronger

Table 4-3 gives a comprehensive view of SBS properties of 3, 4 and 5 layer non-commingled and commingled composites along with the variation from the mean value.

Table 4-3. Short beam strengths (SBS) of 3, 4 and 5 layered non-commingled and commingled 2D composites

	Non-commingled composites (3JP)		Commingled composites (3JPC)		Difference between commingled and non-commingled composites (%)	
	Short beam strength	Displacement	Short beam strength	Displacement	Short beam strength	Displacement

	(MPa)	(mm)	(MPa)	(mm)	(MPa)	(mm)
3 layer	331±24	1.1±0.25	483.6±46	1.18±0.11	46.1	7.3
4 layer	393±8.1	1.28±0.11	627.5±25.1	1.26±0.21	59.6	1.6
5 layer	397.5±40	1.06±0.1	718±14.3	0.92±0.25	80.6	15.2

4.4 Charpy impact properties of non-commingled and commingled 2D composites

This section details the Charpy impact properties of 2D non-commingled and commingled composites. The instrumented Charpy impact tester recorded displacement, impact energy and impact strength response of 3, 4 and 5 layered samples when subjected to impact force.

Typical force-displacement curves of non-commingled and commingled composites are given in Figure 4-18. From the curve, it can be clearly seen that the commingled composites have shown excellent impact performance as compared to non-commingled composites. When comparing the displacement at maximum force (Fmax), the commingled composites suffer lesser displacement at maximum force (Fmax). The commingled composites have shown overall high toughness with stable breakage as compared to non-commingled composites. The reason of better impact properties of commingled composites as compared to non-composites is that they have better fiber-matrix interface and the composite is partially self-reinforced composites due to commingling of jute yarn with PP yarn. It can be noted that there is relatively a sharp peak in commingled composite corresponding to the beginning of fracture. This demonstrates the fracture of a robust composite at a single point due to good adhesion of fiber and matrix in the composite.

The force-displacement curve of commingled sample shows a much higher peak (92% higher than non-commingled (424MPa vs 221MPa). This corresponds to a much better interface between the fibers and thermoplastic matrix in commingled composite as compared to non-commingled composite.
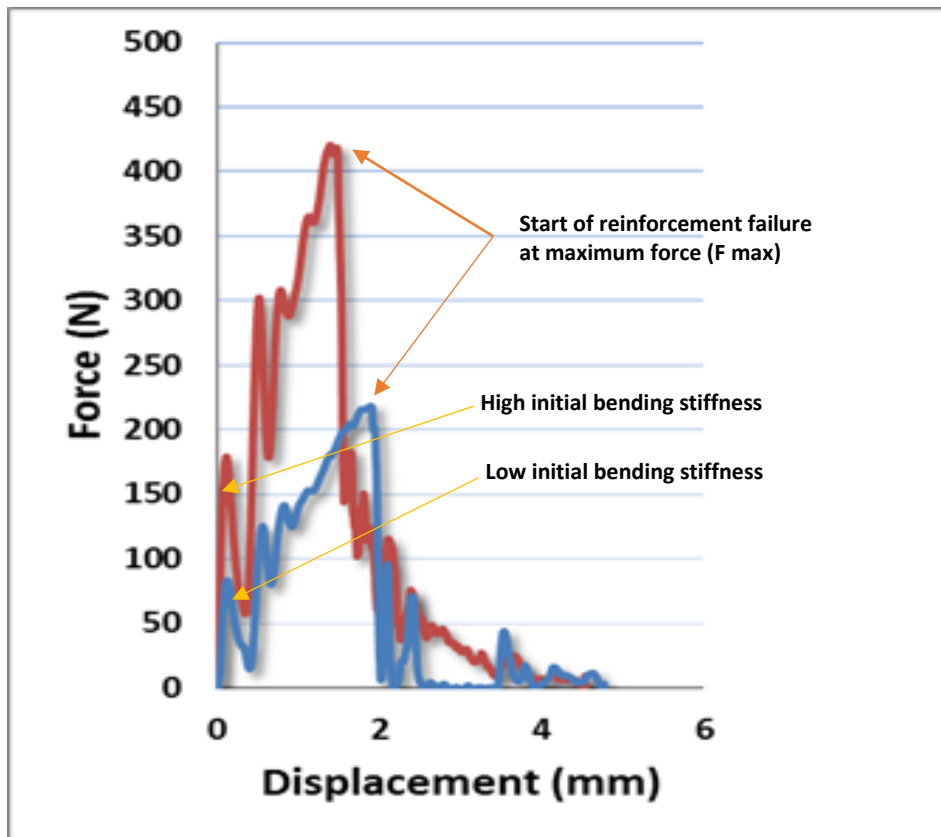
Figure 4-18. Force-displacement curves obtained from instrumented Charpy impact tester for 5 layered commingled and non-commingled 2D composites

4.4.1 Effect of the number of layers on the impact properties of non-commingled and commingled 2D composites

The Charpy force-displacement curves of 3, 4 and 5 layered commingled and non-commingled composites are given in Figure 4-19 to Figure 4-21.

Figure 4-19 explains the force-displacement curves of 3-layered non-commingled and commingled composites, (a) shows multiple curves of 3-layered non-commingled (3JP) composites, (b) shows multiple curves of 3-layered commingled (3JPC) composite and (c) shows a comparison of 3-layered non-commingled and commingled composites. Fma*x* for commingled composites is 69% higher than the non-commingled composites.

Figure 4-20 explains the force-displacement curves of 4-layered non-commingled and commingled composites, (a) shows multiple curves of 4-layered non-commingled (4JP) composites, (b) shows multiple curves of 4-layered commingled (4JPC) composite while (c) shows a comparison of 4-layered non-commingled and commingled composites. Fmax for commingled composites is 75% higher than the non-commingled composites.

136

Figure 4-19 explains force-displacement curves of 5-layered non-commingled and commingled composites, (a) shows multiple curves of 5-layered non-commingled (5JP) composites, (b) shows multiple curves of 5-layered commingled (5JPC) composite while (c) shows a comparison of 5-layered non-commingled and commingled composites. Fmax for commingled composites is 91% higher than the non-commingled composites.

A significant difference between the Fmax values of commingled composites can be observed. The maximum displacement of commingled composite samples is higher as compared to non-commingled composites which show that the commingled composites stand/resists longer against the impact force as compared to non-commingled composites for their better fiber/matrix interface.
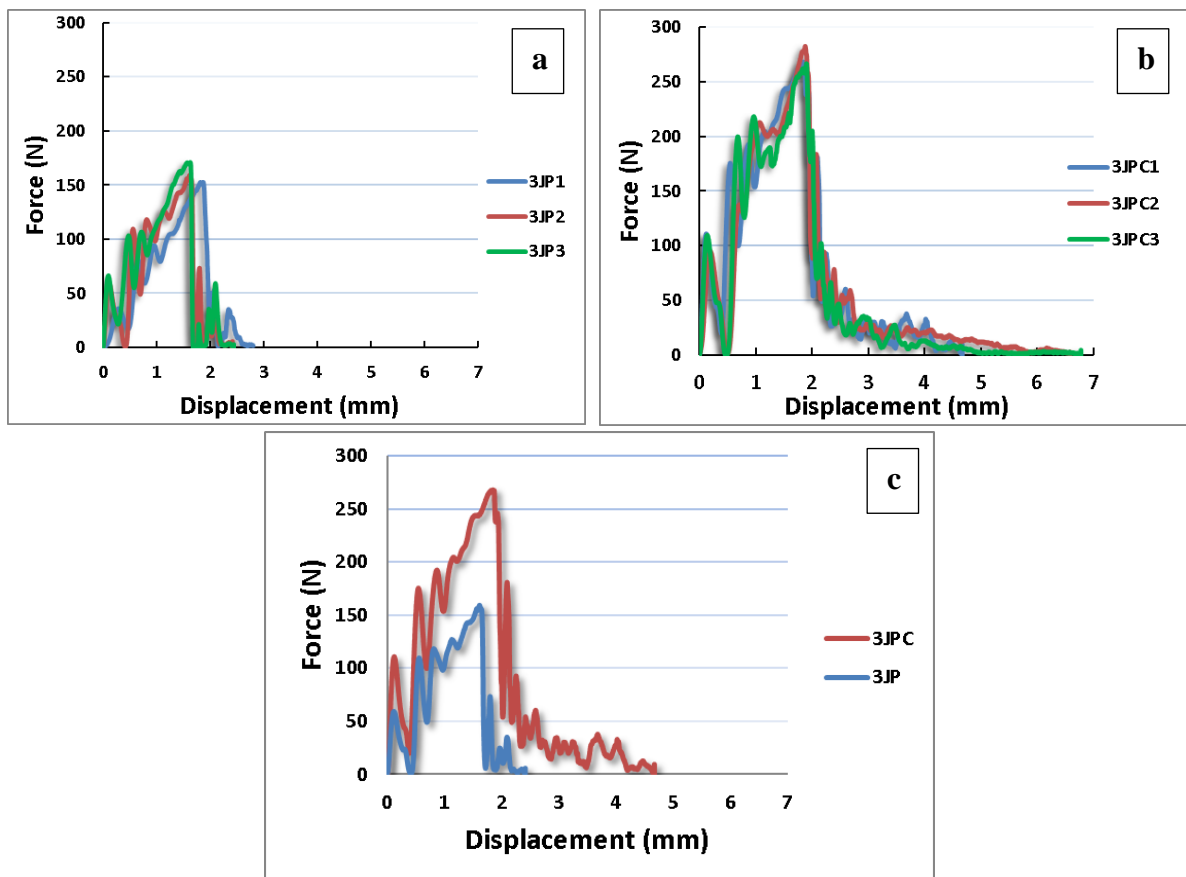
Figure 4-19. Force-displacement curves of 3-layered non-commingled and commingled 2D composites, (a) three dispersion curves of 3-layered non-commingled (3JP) composites, (b) three dispersion curves of 3-layered commingled (3JPC) composite, (c) a comparison of 3JP and 3JPC
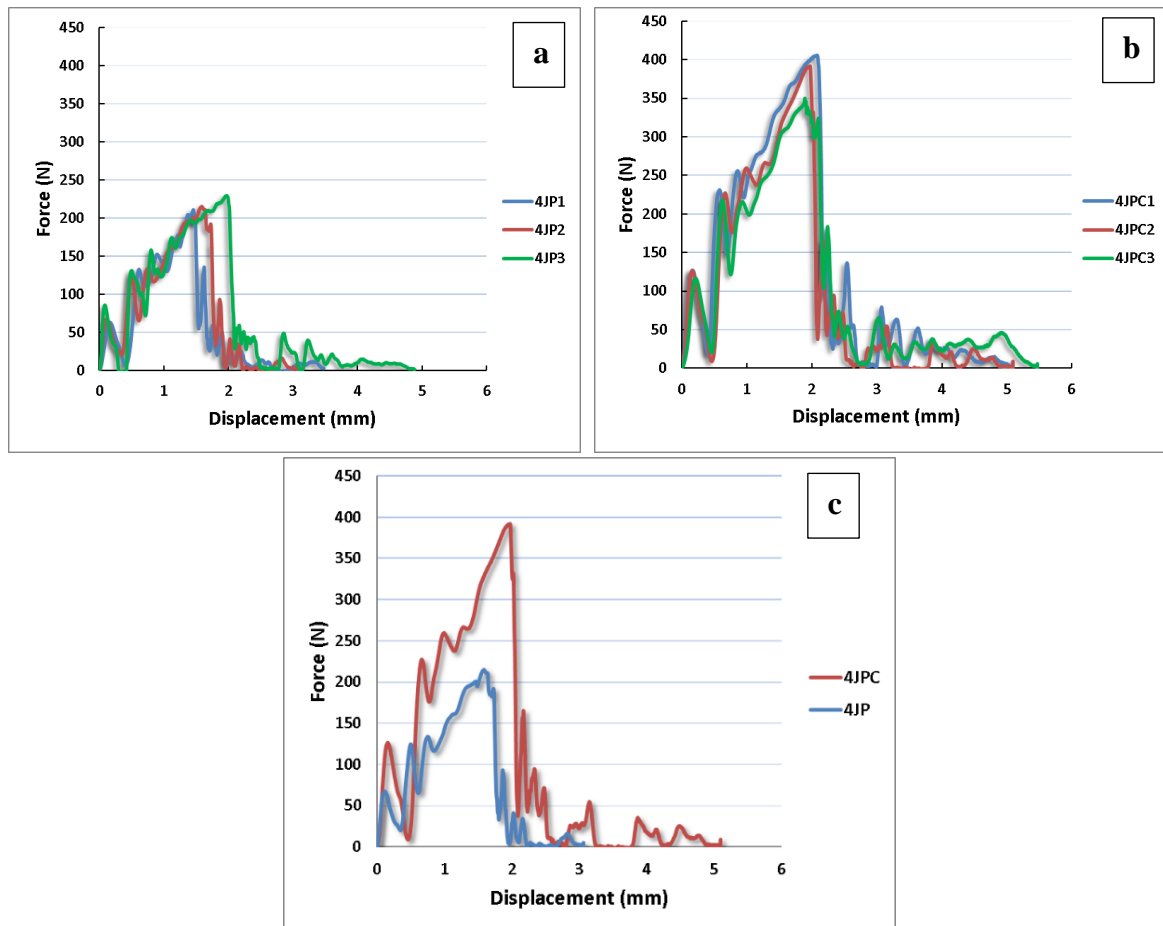
Figure 4-20. Force-displacement curves of 4-layered non-commingled and commingled 2D composites, (a) three dispersion curves of 4-layered non-commingled (4JP) composites, (b) three dispersion curves of 4-layered commingled (4JPC) composite, (c) a comparison of 4JP and 4JPC
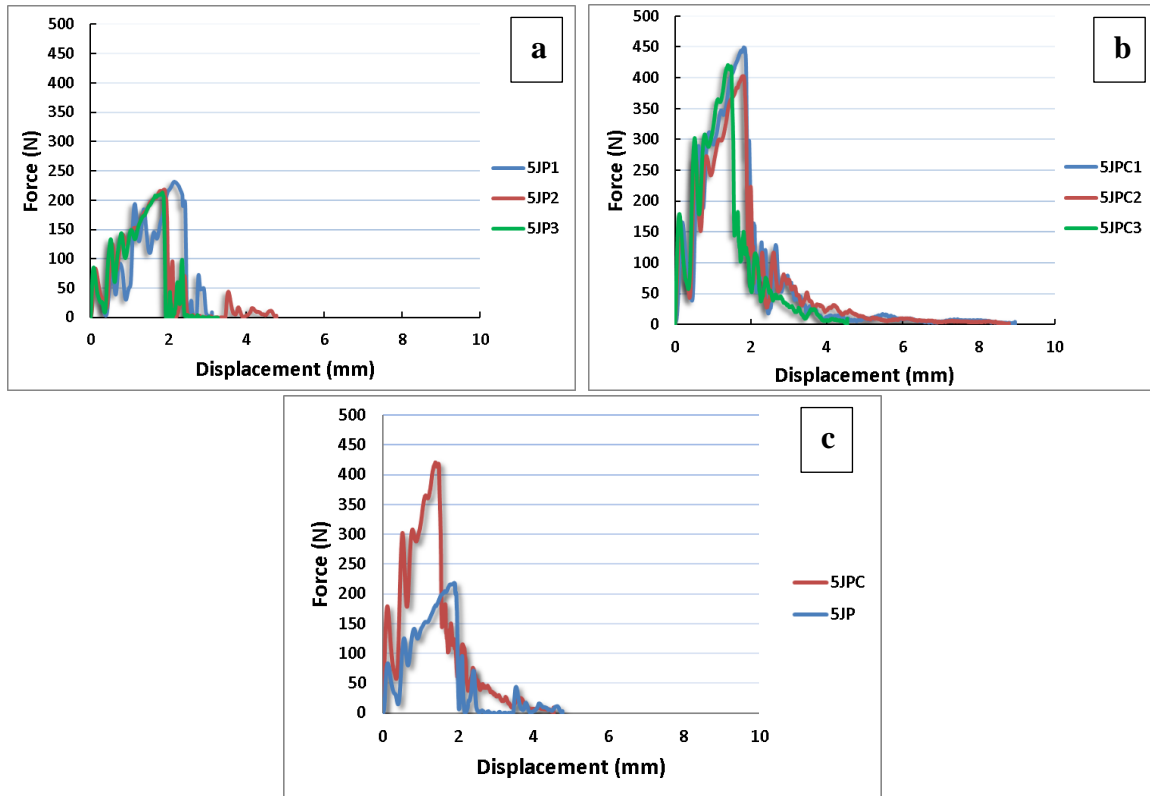
Figure 4-21. Force-displacement curves of 5-layered non-commingled and commingled 2D composites, (a) three dispersion curves of 5-layered non-commingled (5JP) composites, (b) three dispersion curves of 5-layered commingled (5JPC) composite, (c) a comparison of 5JP and 5JPC

The summary of results of 3, 4 and 5 layered composites is given in Table 4-4. A complete break was observed in all samples. It can be noted that impact energy (J) in both non-commingled and commingled samples increased with the increasing number of composite layers which is logical. However, the values of maximum impact force (N), impact strength (KJ/m²) and impact energy (J) of commingled samples are significantly higher than the values obtained for non-commingled samples. For example, impact energy values of 3, 4 and 5 layered commingled composites are 17, 22 and 15 % higher than non-commingled composites. This again validates the fact that fiber/matrix adhesion in commingled composites is better than non-commingled composites.

Table 4-4. Charpy impact properties of non-commingled and commingled 2D composites

	Max. Impact force (N)	Impact energy (J)	Impact strength (KJ/m²)	Break type
3JP	161±10	0.36	9.415±0.31	

3JPC	272±10	0.42	10.18±0.24	
Difference (%)	69	17	8	
4JP	218.4±11	0.41	9.65±0.19	
4JPC	382±32.6	0.5	11±0.26	Complete
Difference (%)	75	22	21	
5JP	221±10.6	0.48	10.45±0.21	
5JPC	424±25	0.55	11.52±0.34	
Difference (%)	91	15	10	

If we look at the damaged samples Figure 4-22, a brittle and non-tapered failure can be observed in non-commingled samples. On the other hand, the failure of commingled samples is tapered. This is typical fiber dominant behavior due to improved bonding of fibers and matrix. The fiber-matrix network formed in commingled composites is also partially self-reinforced as discussed earlier. Due to this partial self-reinforced structure, the crack propagation is difficult, resulting in breakage at higher force. The fiber-matrix interface in non-commingled composites is weak, therefore cause poor impact performance. The whitish lighter color of polypropylene on the surface of the non-commingled composites shows more coating, while on the other hand there is less coating and more penetration in the commingled composite.
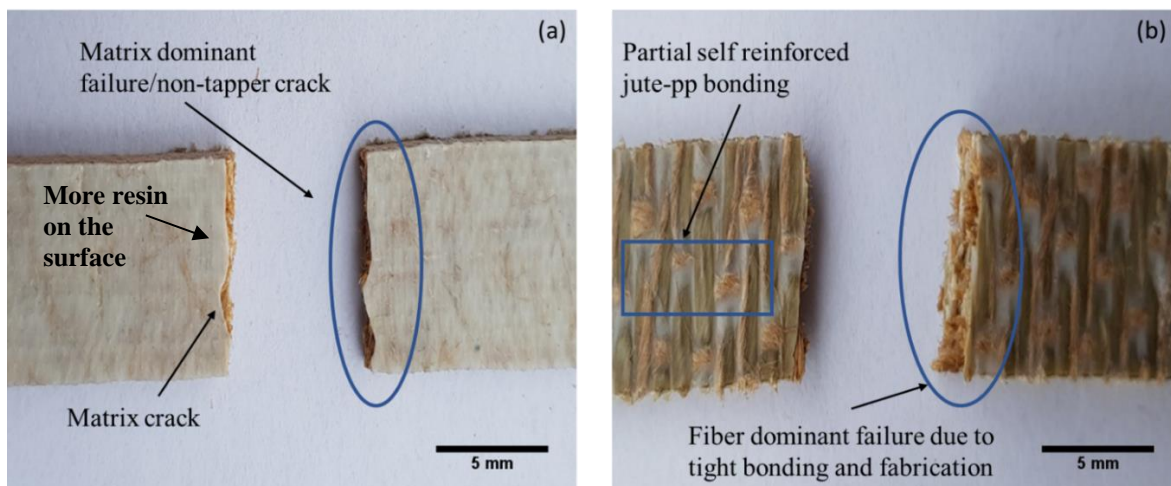
Figure 4-22. The damaged samples of (a) non-commingled and (b) commingled 2D composites after Charpy impact test showing damage mechanism

4.5   Summary

The commingled composites show their overall dominance to the non-commingled composites. The fabrication of composites using commingled yarns technique resulted in impregnation of reinforcement at fiber level, which leads to good adhesion of matrix with fibers. This good adhesion resulted in improved mechanical properties. The tensile strength improved up to 53%. The flexural strength of commingled composites found up to 81% higher than non-commingled composites. The impact energy of composites measured using instrumented Charpy impact tester, of commingled composites was found up to 22% higher than non-commingled composites. Furthermore, value of Fmax for commingled composites was found up to 91% higher than non-commingled composites. This shows the high quality and better fiber-matrix adhesion in commingled composites as compared to conventional non-commingled ones. The improvement in mechanical behavior was consistent for thin as well as thick composites. These results demonstrated that the fabrication of thermoplastic composites using the commingled technique is a quick and viable solution resulting in the development of high-quality composites with enhanced properties and lesser composite manufacturing time.

Chapter 5. Effect of gradual thermoforming pressure on the mechanical properties of Jute/Polypropylene commingled composites

This chapter concerns about the investigation of the effect of instant and gradual loading on the physical and mechanical properties of the commingled thermoplastic composites. The microstructure study was carried out up to fibril level in order to observe the physical effect of instant and gradual loading on the cellulosic structure of jute. The tensile, flexural, SBS and Charpy impact tests were conducted to check the mechanical properties of both composites. The microstructure of fibers of composites made using instant loading showed significant damage as compared to samples which were made with gradual loading. The fibers of composite made using gradual loading had very healthy fibers with smooth polygonal boundary. The tensile, flexural, SBS and Charpy impact results showed superior mechanical performance of gradual loaded samples.

During thermoforming the behavior of thermoplastic composites is entirely different from the thermoset composites. In thermoset composites the physical state of fiber reinforcement and matrix is quite different from each other; the fibers are in solid form, but the matrix is in liquid form. On the other hand, in thermoplastic composites both the fiber reinforcement and matrix are in solid form. When a thermoset composite is subjected to thermoforming, the liquid matrix tends to bleed out as soon as the composite is subjected to compression loading. On the other hand when the thermoforming pressure is applied on thermoplastic composites, the matrix will not tend to bleed out unless and until it is converted to molten form at its melting temperature; hence the stress distribution upon the fiber reinforcements in thermoplastic composites would be much higher than thermoset composites. At the application of pressure on thermoset composites the pressure helps to bleed out the matrix resin, on the other hand in thermoplastic composites the stress is both beard by the solid resin and the fiber reinforcement. As soon as the thermoforming pressure is applied the stress is simultaneously taken by the fibers and the non-molten matrix. The fiber bundles will tend to come closer and group together, allowing lesser space in between the fibers (which would have later on allowed the matrix to accommodate in these spaces at/beyond melting temperature) [114] . Once these fiber bundles come closer at the initial thermoforming pressure during a non-molten stage, there would be very little chances for these individual fibers inside the bundle to move away from each other at the later-on melting stage of the matrix.

In order to reduce those stresses during the thermoforming of thermoplastic composites, the gradual loading technique is to be applied which is the scope of this chapter. In such technique the thermoforming pressure is applied gently and gradually in small increments allowing the viscous thermoplastic matrix to take enough time to flow out through the fiber channels towards the composite outer periphery. In this way the flow behavior of thermoplastic matrix comes closer to that of thermoset resins, thus relaxing the reinforcement fibers.

5.1   Manufacturing of instant and gradual loaded composites

In order to prove the hypothesis, as mentioned in previous paragraph, an experiment was performed on jute polypropylene thermoplastic composites using commingled yarn technique. The specimens were prepared using two different pressing techniques. This is explained by a schematic in Figure 5-1. (a) Illustrates the composite under no pressure. As the instantaneous pressure is applied, it directly propagates between different layers of

143

thermoplastic composite one above the other. With the application of instantaneous pressure on dry non-melt composite, the thickness is reduced instantaneously as shown in *Figure 5-3* (b). The jute yarn is pressed along with the thermoplastic polypropylene yarns. This pressure sustains until the melting temperature of the thermoplastic matrix is achieved, the jute yarns get elliptical profiles. *Figure 5-1* (c) explains the composite under gradual loading in which the applied pressure is only 0.1 bar till the melting point is reached, and then the composite is gradually loaded in small steps (as explained below in Figure 5-2) and jute yarns due to gentle increase in thermoforming pressure gets near circular profiles. The specimen thickness under no load (x) is more than thickness under gradual loading (y) and gradual loading thickness is more than instant loading thickness (z).
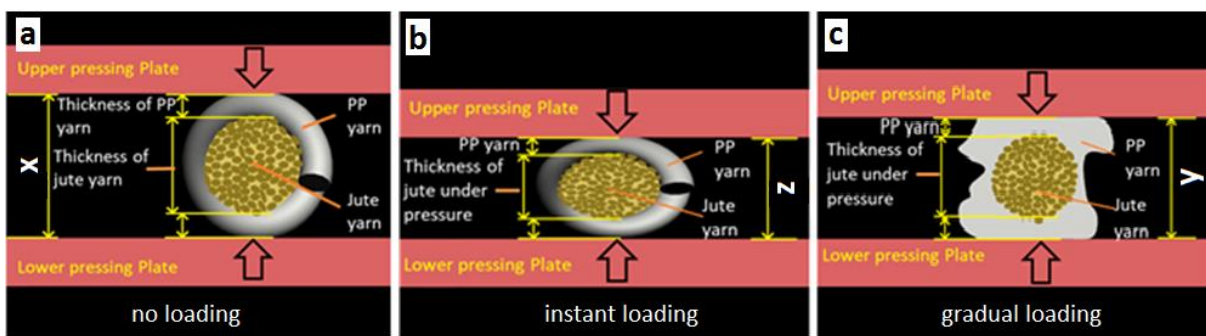
Figure 5-1. Schematic illustration of commingled yarn behavior during thermoforming (a) under no load, (b) under instantaneous loading before melting point till end of thermoforming, elliptical shaped jute yarns, (c) under gradual loading, circular shaped jute yarns

In order to make the composite using instant loading technique, the jute/polypropylene thermoplastic composite was subjected to a predetermined pressure of 15 bars as shown in Figure 5-2(a). The pressure was applied instantaneously at a temperature of 100°C, which is well under the melting point of polypropylene matrix. This resulted into severe and sudden pressure on commingled yarns (both jute and PP yarns). After about 20 min a temperature of 200°C was achieved which was further maintained for 30 min and then the composite was cooled down to 100°C in the next 75 min, at constant pressure of 15 bars.

On the other hand, the gradual loaded thermoplastic composite was made using parameters shown in the Figure 5-2(b). A pressure of 0.1 bars was applied initially, starting from 100°C up to the melting point of thermoplastic resin. At a temperature of 180°C the pressure gradient was started. A set temperature of 200°C was achieved only after 5 min of 180°C. The pressure was gradually increased from 0.1 bars to 15 bars in two major steps.

I.   Firstly, the pressure was increased from 0.1 → 1.0 bar with an increment of 0.1 bar, each 0.1 bar increment was maintained for 1 minute.

II.   Secondly, the pressure was increased from 1.0 → 15.0 bars with an increment of 0.5 bars, each 0.5 bar increment was maintained for 1 minutes.

It is important to note that from 0.1 to 15 bars pressure there were a total of 38 steps, so that the pressure increment was extremely gentle so as to have very low 'pressure surge' on the jute fibers during thermoforming allowing adequate time for the matrix to penetrate deep into the body of jute yarn which are well relaxed under gradual loading and also providing sufficient time for the excessive molten matrix to bleed out, with minimum of fiber damage and maximum composite performance during the testing phase.

After gaining a pressure of 15 bars a constant temperature of 200°C was maintained for the next 30 min. The sample was then cooled down to 100°C in the next 75 min without any change of pressure at 15 bars, so as to have similar temperature curve as of instant loading technique. The melting point of polypropylene according to literature is quite less than 180 °C [90], but there are the chances of local temperature variations within jute/polypropylene composite, jute and polypropylene are not very good conductor of heat [150], so being on the safer side an overall melting temperature of 180°C was assumed, as there are no embedded temperature sensors which can directly measure the live temperature with in the thick body of a bad-heat-conducting-composite (4 layers thickness is 9 mm).
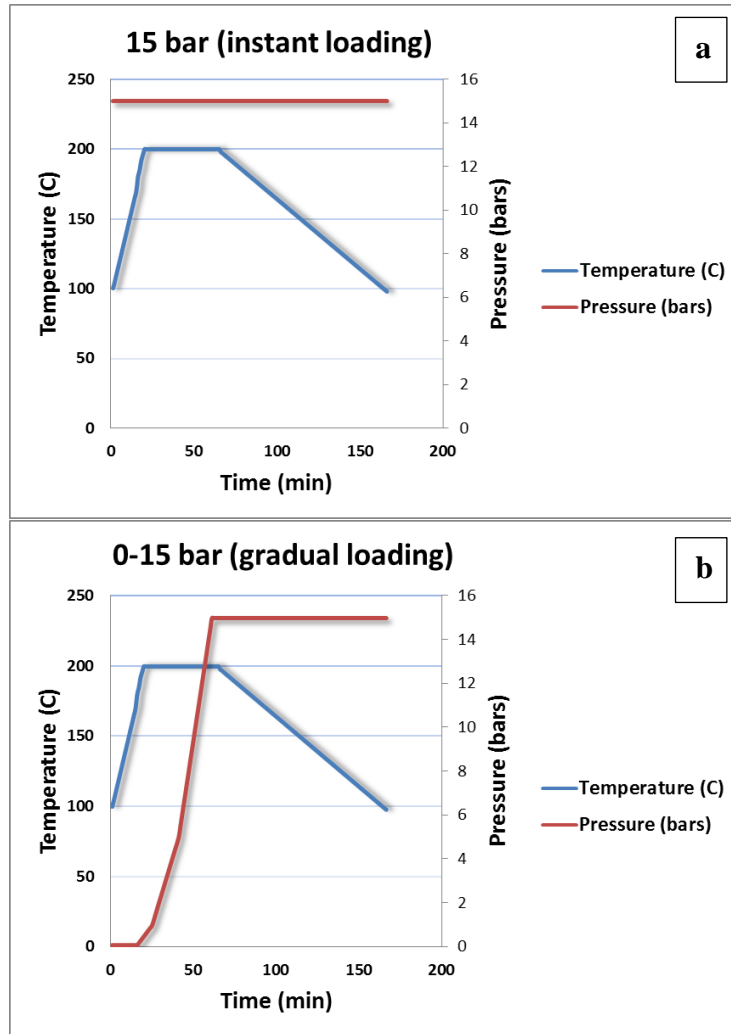
Figure 5-2. (a) Instant pressure 15 bars, (b) Gradual pressure $0 \rightarrow 15$ bars, similar temperature curve for both techniques with different loading techniques

Table 5-1 explains the detail of jute/polypropylene thermoplastic composite made through instant and gradual loading techniques. It is quite interesting to note that even under the same load of 15 bars; both instant and gradual loaded specimens have quite different properties, which are characterized by the resultant thickness of both specimens. The thermoplastic composite was made as a flat plate with dimensions (204 x 252 mm^2) in accordance with the size of cutting template. The composite specimens to be used for tensile, 3-point bending, short beam strength and Charpy impact tests were cut from this plate. Combined thickness of four layers of jute polypropylene commingled fabric was 9 mm. For instant loaded specimen, the thickness of 9 mm was compressed to just 2.41 mm under a constant load of 15 bars, but on the other hand for gradual loaded specimen the thickness of 9 mm was compressed to a 34% higher value at 3.23 mm. This huge difference of thicknesses is also reflected from the resultant fiber weight fraction of jute in both specimens, which is 0.62 for instant specimen

146

and 0.47 for gradual specimen. The same reflects from the fiber volume fraction which is 0.50 for instant specimen and 0.35 for gradual specimen (gradual specimen has almost 30% less fiber volume fraction as compared to Instant specimen. Both instant and gradual composites were made from the stacking of 4 layers of exactly the same type of commingled fabric with equal GSM. The higher fiber volume fraction of instant specimen was only due to collapsed lumen inside the jute fibrils causing a denser cellulosic material (characterized by reduced thickness of instant composite), which is verified by the forthcoming microscopic analysis and tested results (Figure 5-6). Besides higher fiber volume fraction, the mechanical properties of instant specimen are quite lower than that of gradual specimen; means a higher fiber volume fraction does not always guarantee higher mechanical properties.

Table 5-1. Details of thermoplastic composites made through instant and gradual loading techniques

Type of thermoplastic composite	Instant Loading	Gradual Loading
Fiber weight fraction[a] (W_f)	0.62	0.47 (24% less)
Average thickness (4 layers dry jute fabric)	2.25×4 = 9 mm	2.25×4 = 9 mm
Average thickness of the composite	2.41 mm	3.23 mm (34% thicker)
Fiber volume fraction[b] (V_f)	0.50	0.35 (30% less)

[a] ratio of weight of jute fibers to the weight of the composites, [b](FVF) value calculated by weight/mass fraction formula (see part 2.9)

Figure 5-3 shows a comparison of instant and gradual loaded specimens on real scale. Thickness of instant loaded specimen is 2.41 mm and gradual loaded specimen is 3.23 mm, with a difference of 0.82mm, indicating that the gradual loaded specimen is 34 % thicker than the instant specimen, which is a mentionable difference even under the same load of 15 bars.

During instant loading, the yarn bears the maximum load right from the beginning till the end, up to matrix curing resulting into elliptical shapes (*Figure 5-3* (a)), while on the other hand, in the gradual loaded specimen, the jute fibers, with in a yarn, are more relaxed. The yarns look bulkier and seem more inclined towards circular shapes (*Figure 5-3* (b)). It is also important to note that the yarns in instant specimen looks a bit of darker shade as compared to the gradual specimen, this is justified by the reason that in instant specimen the initial thermoforming pressure (far before the matrix melting point) brings the dark brown jute fiber bundles closer to each other and then they are lesser prone to return to their initial position even after the melting point is reached and do not retain original place once the matrix set.

Figure 5-3(c) shows a side-by-side view of instant and gradual specimens against mm scale for a better one-to-one comparison.
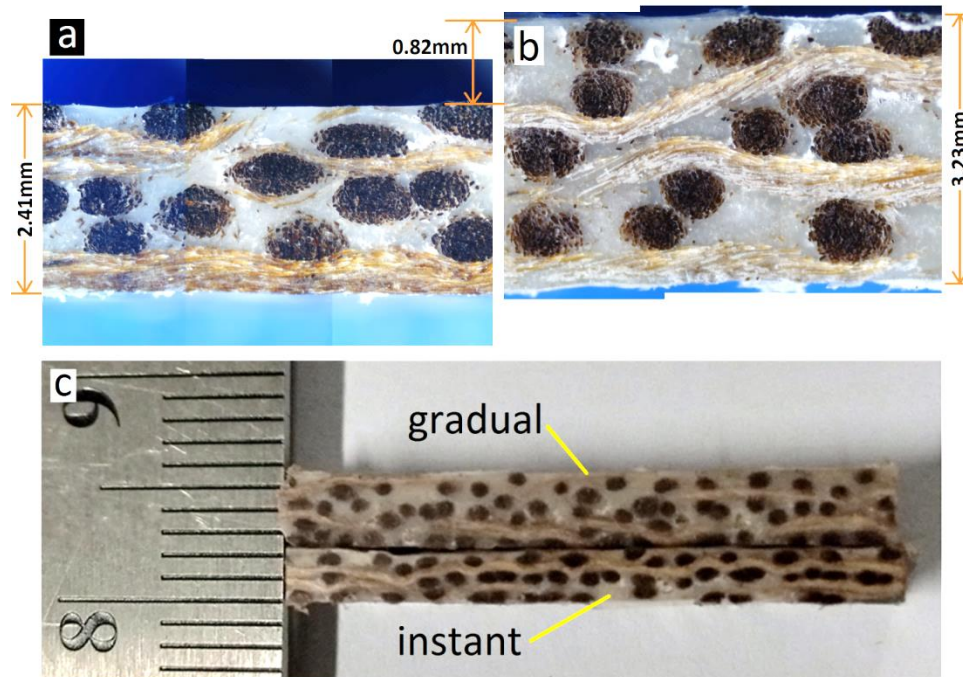
Figure 5-3. Crossectional views of (a) instant loaded specimen (thickness=2.41mm) and (b) gradual loaded specimen (thickness=3.23mm), (c) a side by side comparison of instant and gradual specimens against mm scale

5.2 Microstructure study

The microscopic analysis was carried out on Olympus BX 53 microscope equipped with DP80 camera having a resolution depth in the range of 40 to 1000 times as shown in the *Figure 5-4*. The samples were analyzed for 100, 400 and 1000x magnifications in order to deeply observer the difference of behavior of jute fibers under instant and gradual loading techniques. It is interesting to note that this is a refractive microscope that means in order to see the specimen the light must pass-through it. As thick jute/polypropylene composites are quite opaque in nature hence their inspection through a refractive microscope is not possible. In order to sort out this issue very thin plies of the composites were sliced (thickness less than 0.5mm), at this thickness the composite was more 'see through' as compared to higher thicknesses values. After cutting, these composite slices were then subjected to the process of manual sanding and polishing using sanding/polishing papers in the range of 400-2500 grit (44 to 7.8 microns, 100,000 Grit = 0.25 microns). For fine resolution images (400x and

1000x) a freelancing software 'ImageJ' [151] was used in order to superimpose multiple images into to one clear image.

Figure 5-4. Olympus BX 53 refractive microscope, resolutions range 40-1000 x

Figure 5-5 (a) is showing the picture of Besttom-T200 diamond cutting machine on which the fine slices of jute/polypropylene composite were cut. The machine is equipped with precision diamond disc which works in a cutting fluid (b). (c) Shows the < 0.5mm fine cut slice of instant specimen and (d) clearly shows the gradual specimen with wider width.
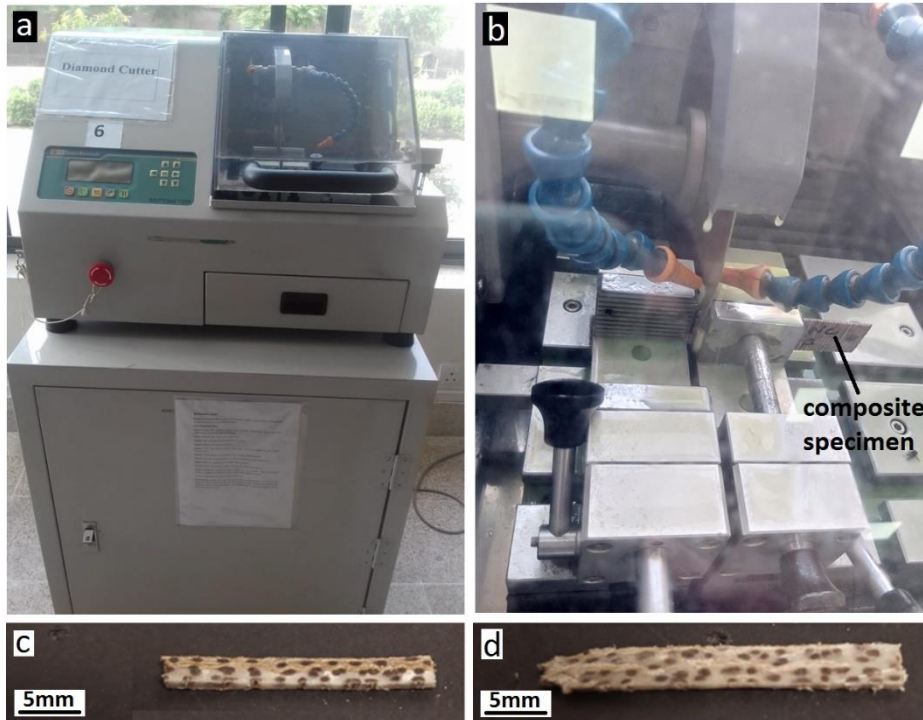
Figure 5-5. (a) Besttom T200 diamond cutting machine, (b)close-up view of composite specimen cutting, (c), (d) thin slices (<0.5mm thickness) of instant and gradual specimens respectively

Figure 5-6 shows a comparison between the microscopic images of instant and gradual loaded jute/polypropylene composites. The microstructure was studied using refractive microscope. (a) Shows the 400x image of fibers of composite made under instant loading, while the (b) shows the image made under gradual loading. The instant specimen shows a clear indication of damaged micro fibrils within the body of a jute fiber. Their inside lumen is mostly collapsed with clear indication of ruptured cellulosic wall, there is a clear indication that fibrils are badly compressed against each other so that most of their cellulosic walls are forming sharp edges instead of soft curvy periphery. While on the other hand the gradual loaded composite shows much healthier inside lumen with stronger/fatter cellulosic walls forming a smoother/curvy periphery. The jute fibers have a relative transparency as high as 60% so can be seen under refractive microscope [152], characterized by a glowing jute fiber in Figure 5-6(a). Further the individual jute fibers, composed of multiple fibrils, were observed at relatively higher magnification (1000x), as shown in Figure 5-6. In instant specimen (a) the fibril cell walls are so badly ruptured that it is even difficult to differentiate where one fibril cell ends and other begins, while on the other hand in gradual specimen (b) there are much healthier and distinct fibril cell walls and lumen.
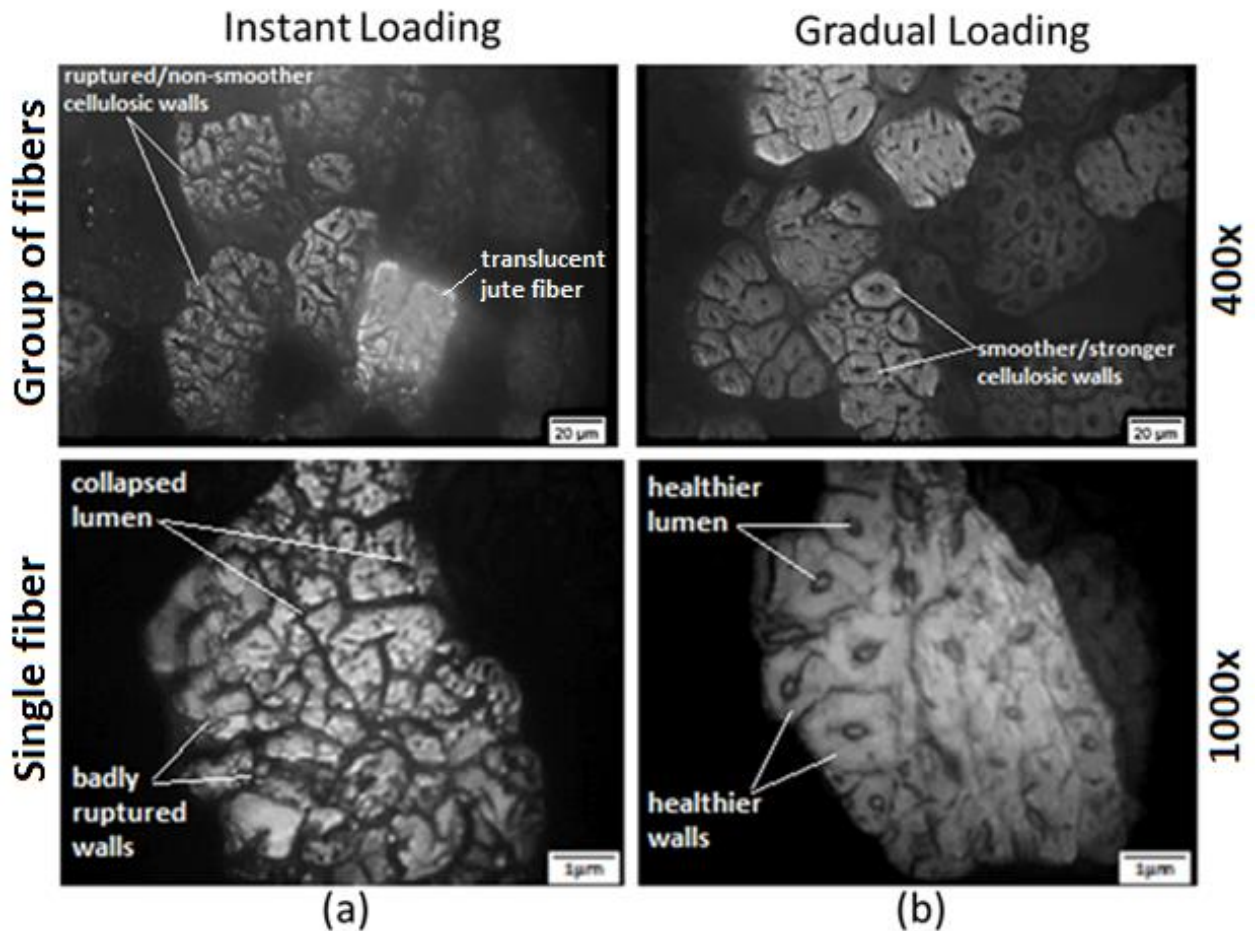
Figure 5-6. Comparison of microstructure of jute yarn composite made at (a) instant loading and (b) gradual loading

5.3 Mechanical Properties of instant and gradual loaded specimens

In this part, we are presenting the mechanical properties of 2D instant and gradual loaded commingled composites in detail. Instant and gradual loaded specimens were tested for tensile, flexural, short beam and impact properties. Six tests were performed each for instant and gradual loaded specimens; six tested were performed for instant and six for gradual loaded specimen. The mechanical properties of instant and gradual loaded specimens are described as below;

5.3.1 Tensile properties of instant and gradual loaded composites

Figure 5-7 shows the tensile stress-strain curves of composites made through instant and gradual loading techniques. (a) Shows three curves of instant specimen, (b) shows three curves of gradual specimen and (c) shows a comparison of average curves of instant and

gradual specimens. The curves clearly show higher tensile strength and strain for gradual loading as compared to instant loading. The tensile strength is around 27% higher in gradual loaded composites. The reason of better tensile properties achieved through gradual loading are that the reinforcement and matrix were more evenly distributed unlike the instant specimen in which fiber bundles tend to come closer and group together, allowing lesser space for the resin to flow in-between the fibers [114], the second reason, as seen in previous section that the gradual loaded fibers have healthier cellulose fibers which eventually leads to better tensile properties. On the other hand, the strain at break of gradual specimen is at the higher side as compared to instant loading. This is due to the reason that damaged cellulosic material behaves brittle and breaks earlier. Yet another reason for higher strain at break in gradual composite is higher matrix content as the fiber volume content of gradual specimen is 30% less than the instant specimen (0.35 vs 0.50, see Table 5-1). Lower fiber volume content means a higher matrix content, as the strain properties of pure polypropylene are higher than the jute fiber, hence the composite will be more inclined towards higher strain at break values in gradual specimen as compared to instant specimen.
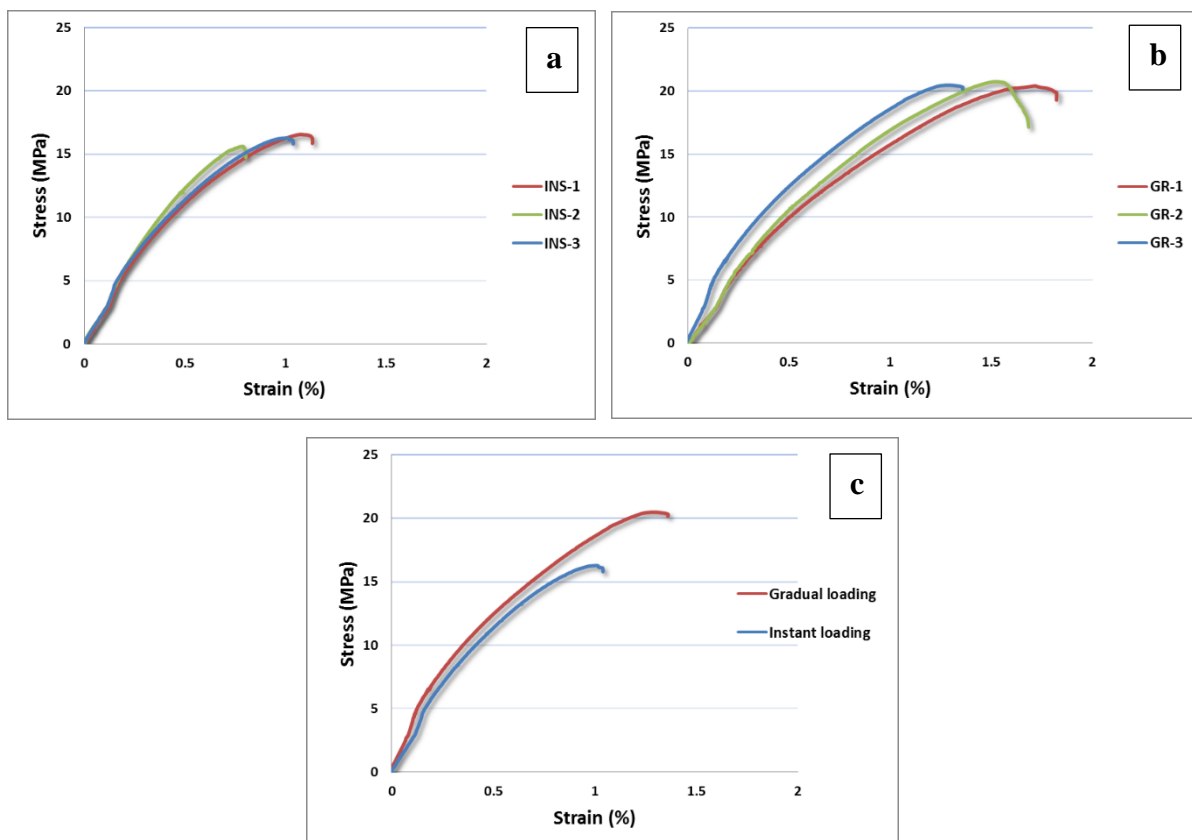
Figure 5-7. Stress-strain curves of instant and gradual loaded commingled composites, (a) three curves of instant specimen, (b) three curves of gradual specimen, (c) average curves of

instant and gradual specimens, the tensile strength of gradual specimen is 19 % more than the instant specimen

Table 5-2 illustrates the tensile properties of instant and gradual loaded specimens. The variation from the mean value is also shown. The tensile strength of gradual specimen is 27% higher but one the minus side its strain value is also 62% higher than instant specimen due to which both composite types have quite comparable modulus values. The tensile modulus of gradual loaded specimen is slightly higher than instant specimen, which is 9.6% (5.1 GPa vs 4.62 GPa). Modulus is a ratio of stress/strain. Hence as the strain value increases the value of tensile modulus decreases. Same can be verified by the research work of Lebaupin et al., [114] (see part 1.8.2.2 above) who compared the mechanical properties of instant and gradual loaded specimens. They found that gradual tensile modulus is only 2.3% higher than the instant specimen (35.8GPa vs 35GPa), due to 91% higher amount of failure strain in their gradual specimen.

Table 5-2. Tensile properties of instant loaded and gradual loaded composites

Properties	Tensile strength (MPa)	Tensile modulus (GPa)	Strain at failure (%)
Instant Loaded	16.17±0.52	4.62±0.12	1.0±0.19
Gradual Loaded	20.5±0.22	5.1±0.44	1.62±0.26
Difference %	27	9.6	62

Figure 5-8 shows a microscopic comparison of (a) instant and (b) gradual specimens for tensile test. The damaged and compressed jute fibers in instant specimen degrade its mechanical properties. Poor impregnation of jute fibers within the body of the yarn in instant loaded specimen results in fiber pullout (a-2, a-3). The crossectional profile of jute fibers for instant and gradual loading is also clearly different, with gradual loaded specimen showing smoother near to circular crossection (b-3) as compared to instant loaded specimen (a-3) where the yarns are more deformed.

153
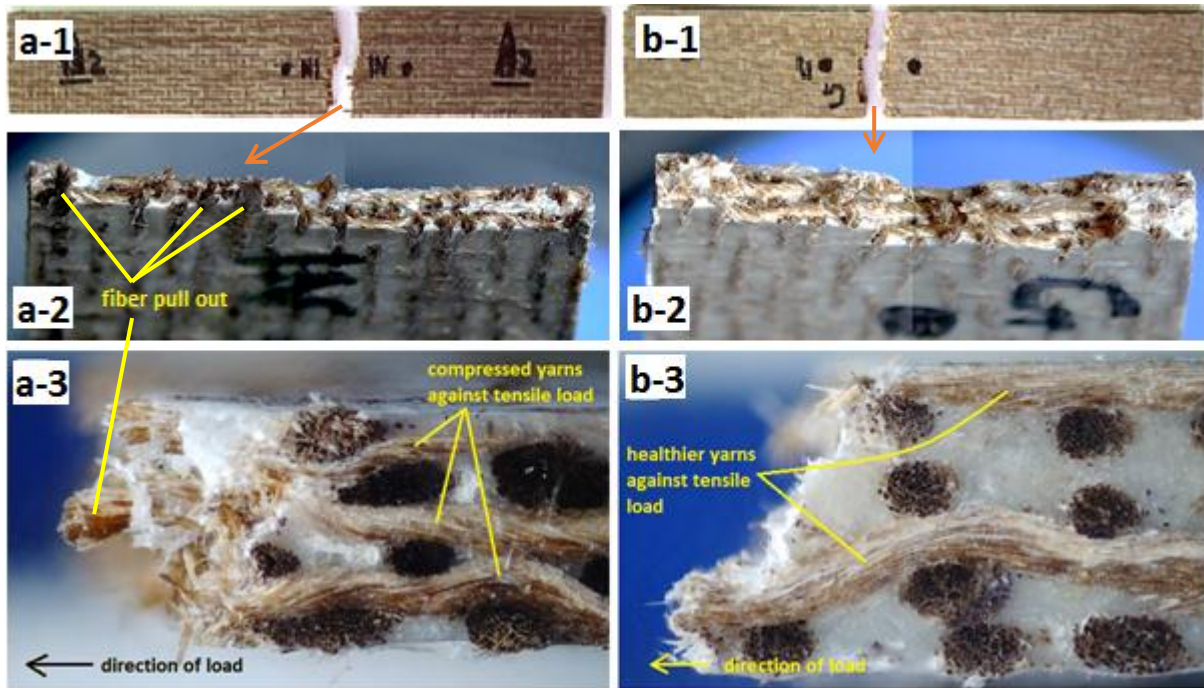
Figure 5-8. Tensile tested specimens of 4-layers jute/polypropylene commingled composites (a) instant loaded specimen with visible fiber pullout, (b) gradual loaded (no signs of fiber pullout)

5.3.2   Flexural properties of instant and gradual loaded composites

Figure 5-9 illustrates the flexural strengths of instant and gradual composite specimens. The flexural strength of the gradual loaded specimen is a marginal 64% higher than the instant specimen. This can be explained by the better yarn health in gradual specimen. In instant specimen the mechanical properties are deteriorated by the damaging of cellulosic material. On the other hand, the strain value is competitive for both gradual and instant specimens. Both specimens did not completely break (Figure 5-10).
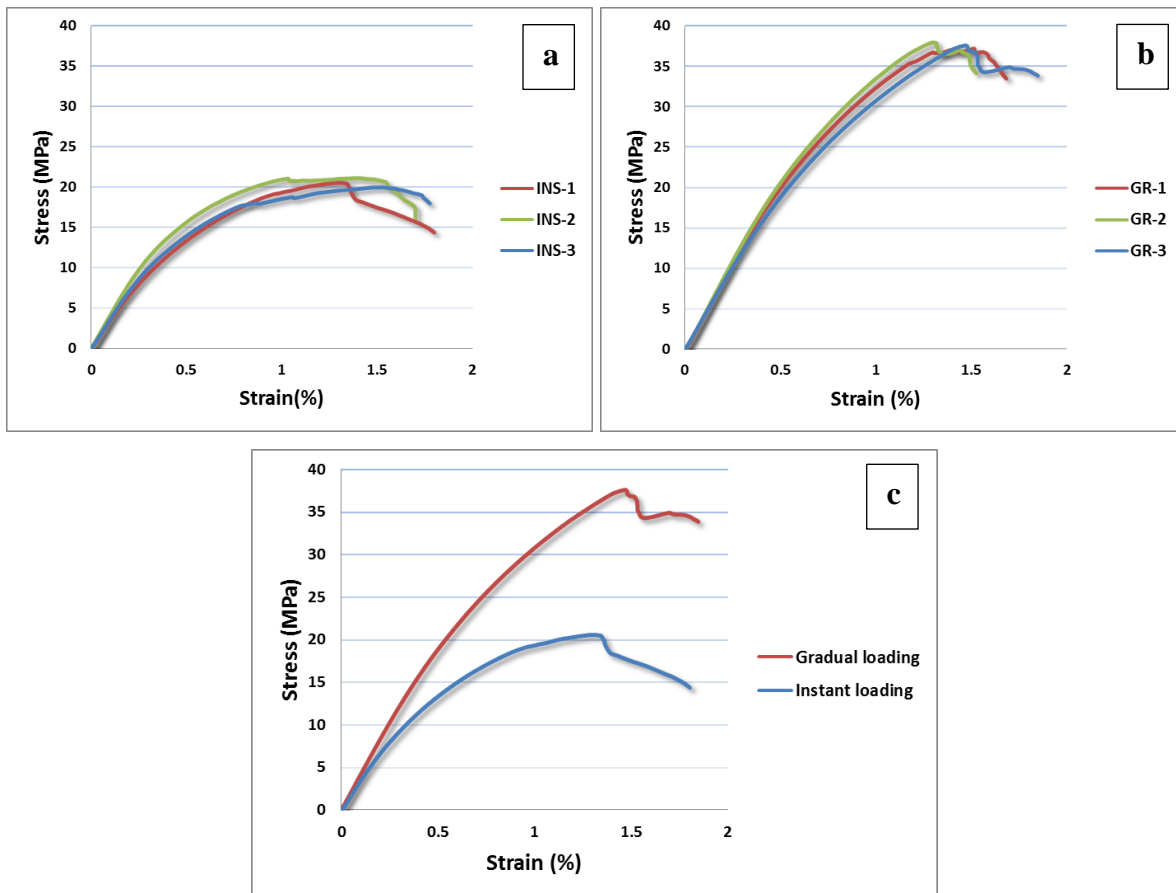
Figure 5-9. Flexural strengths of instant and gradual loaded commingled composites, (a) three curves of instant specimen, (b) three curves of gradual specimen, (c) average curves of instant and gradual specimens, the flexural strength of gradual specimen is 82 % more than the instant specimen.

Table 5-3 illustrates flexural properties of instant and gradual loaded specimens. The variation from the mean value is also shown. The tensile stress of gradual specimen is a marginal 82% higher. On the other hand, the strain percent is competitive for both gradual and instant specimens (1.68 vs 1.76). Strain of gradual specimen is slightly on the lower side at 4.5%.

Table 5-3. Flexural properties of instant and gradual loaded composites

Properties	Flexural strength (MPa)	flexural modulus (GPa)	Strain (%)
Instant Loaded	20.6±0.58	3.50±0.48	1.76±0.06
Gradual Loaded	37.6±0.39	3.98±0.36	1.68±0.16
Difference %	82.5	13.6	4.5

Figure 5-10 shows a microscopic comparison between gradual and instant specimens for flexural test. Images of both instant (a-1, a-2, a-3) and gradual (b-1, b-2, b-3) specimens do

155

not show any major differences. Both images show the damage and rupture of jute fibers almost of the same fashion. The main difference comes from the microscopic analysis (Figure 5-6), which shows damaged cellulosic fibril walls with collapsed lumen inside resulting into lower flexural properties of instant specimen as compared to gradual specimen.
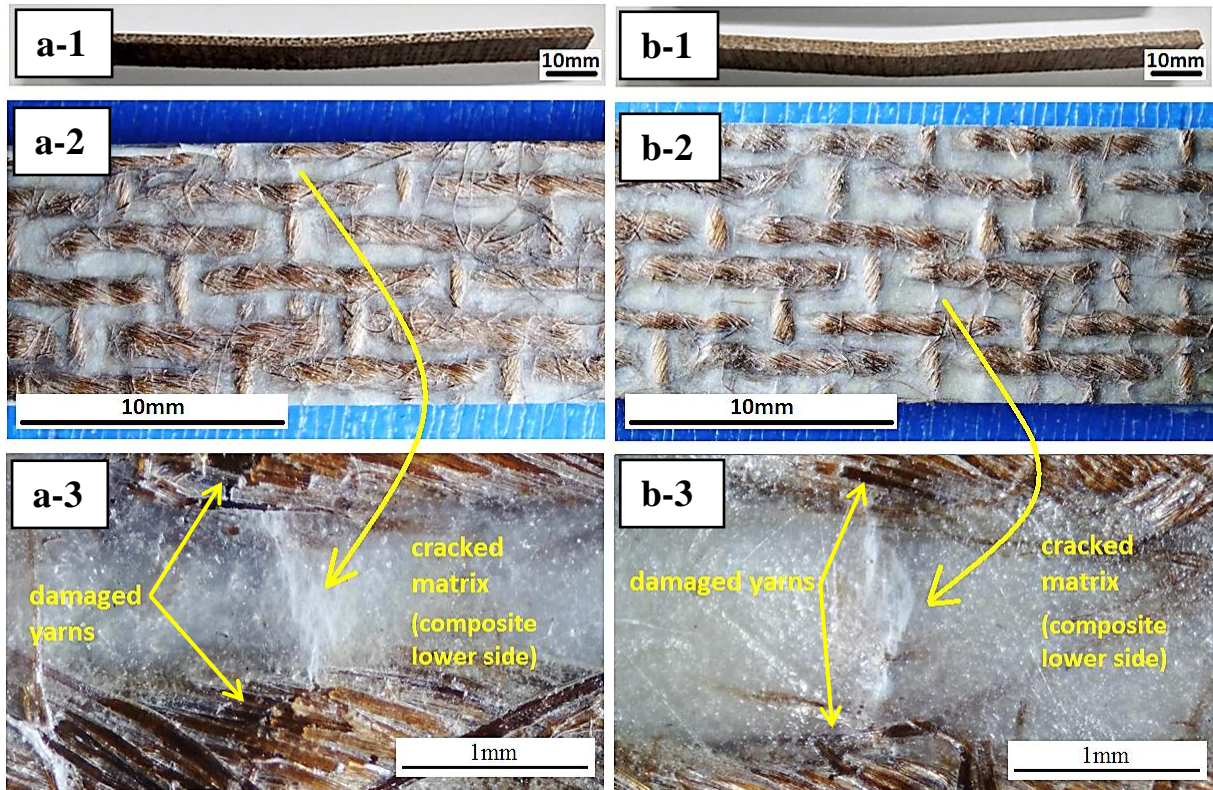
Figure 5-10. Tested samples of non-broken 3-point bending (a-1, a-2, a-3) instant and (b-1, b-2, b-3) gradual loaded tested specimens

5.3.3   Short beam strength of instant and gradual loaded composites

Figure 5-11 illustrates the shear beam strengths of instant and gradual composite specimens. The composites made through gradual loading showed overall high short beam strength and displacement. The instant loaded composite had low strength and after reaching the maximum stress the curve dropped sharply at around 0.25mm extension. While in case of gradual loaded composite the displacement is rather even and after initial drop at 0.4mm the composite deformed evenly. The short beam strength of the gradual loaded specimen is 34.5% higher than the instant specimen. This can be explained by the better yarn health in gradual specimen. In instant specimen the mechanical properties are deteriorated by the damaging of cellulosic material as explained in Figure 5-6.
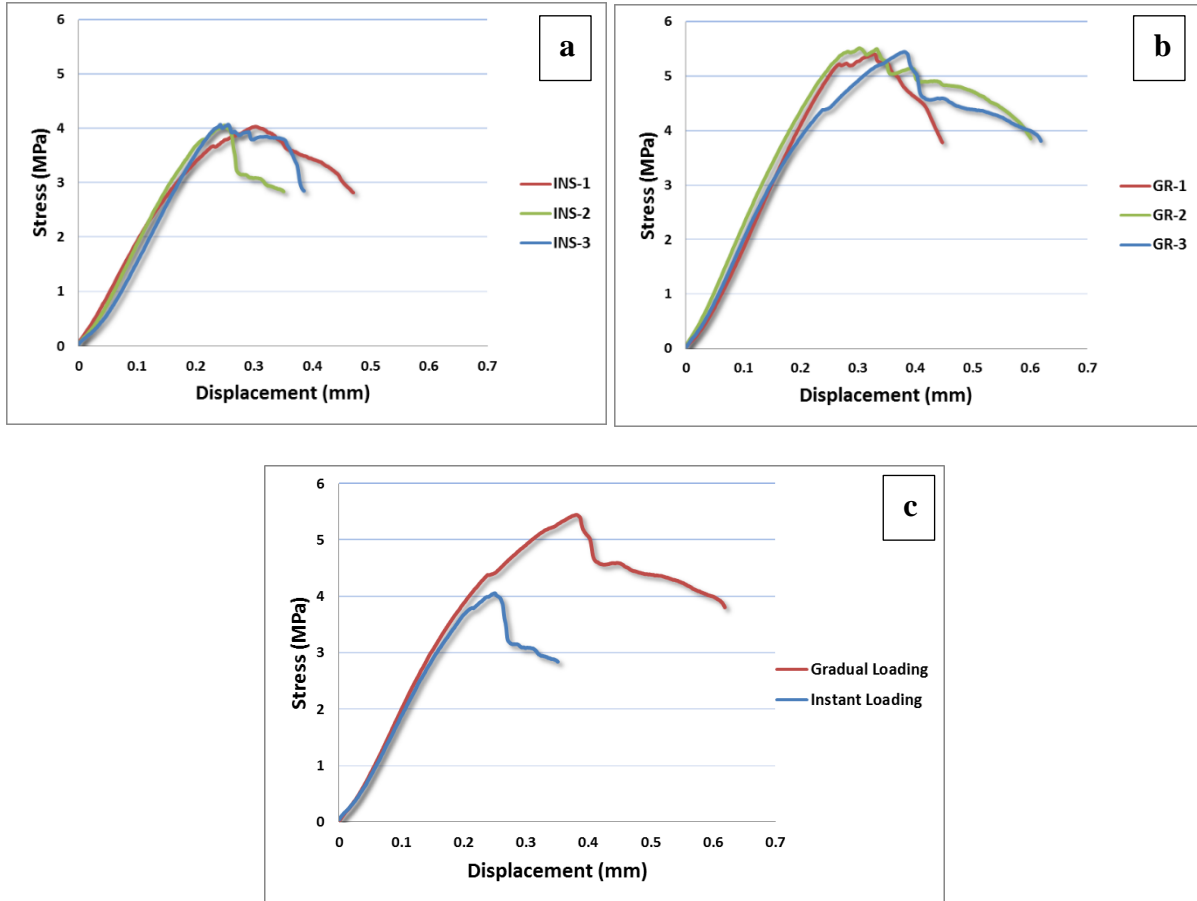
Figure 5-11. Short beam strength of instant and gradual loaded commingled composites, (a) three curves of instant specimen, (b) three curves of gradual specimen, (c) average curves of instant and gradual specimens, the short beam strength of gradual specimen is 34.5 % more than the instant specimen.

Table 5-4 illustrates the short beam mechanical properties of instant and gradual loaded specimens. The variation from the mean value is also shown. The displacement amount at peak-load for the gradual loaded specimen is 37.5% higher than the instant loaded specimen (0.55mm vs 0.40mm). This is again due to the reason that non-crushed and healthy fibrils impart better elongation in case of gradual specimen than the crushed and damaged fibrils in instant specimen which behave brittle.

Table 5-4. Short beam mechanical properties of instant and gradual loaded composites

Properties	Short beam strength (MPa)	Displacement (mm)
Instant Loaded	4.06±0.02	0.40±0.07
Gradual Loaded	5.46±0.06	0.55±0.1
Difference %	34.5	37.5

157

The microscopic comparison of gradual and instant specimens for short beam strength test is shown in the Figure 5-12. Images of both instant (a-1, a-2, a-3, a-4) and gradual (b-1, b-2, b-3, b-4) specimens do not show any major difference. Both images show the damage and rupture of jute fibers almost of the same fashion. The crack size in gradual specimen is wider as compared to instant specimen due to its higher thickness. The gradual specimen has 34% thicker than the instant specimen which would cause higher amount of stress on the tensile side (lower side opposite to depressing probe) resulting into wider crack. The main difference comes from the microscopic analysis (Figure 5-6), which shows damaged cellulosic fibril wall with collapsed lumen inside resulting into lower flexural properties of instant specimen as compared to gradual specimen.
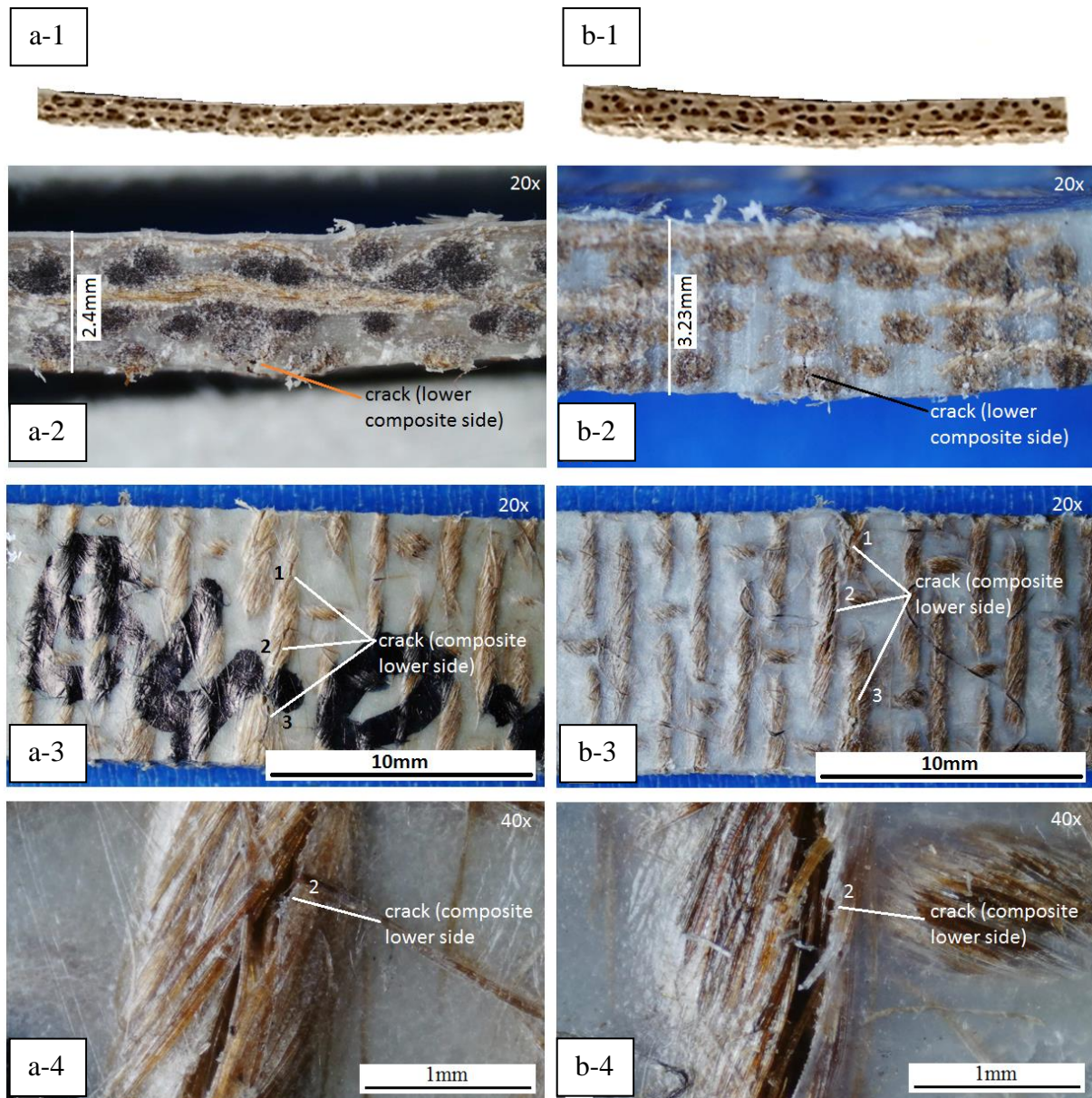
Figure 5-12. Short Beam Strength comparison of jute/PP composites (a-1, a-2, a-3. a-4) instant and (b-1, b-2, b-3, b-4) gradual loaded tested specimens

5.3.4 Charpy impact properties of instant and gradual loaded specimens

Figure 5-13 shows the typical force-displacement curves and impact strength comparisons of composite made through instant and gradual loading. The gradual loaded composite has a marginal 59% higher impact force than the instant loaded (215 N/mm vs 135N/mm). On the other hand, the impact strength of gradual loaded specimen is again a marginal 43% higher (8.036kJ/m^2 vs 5.6kJ/m^2). The reason for the better impact properties of gradual specimen is justified by healthier cellulosic fibrils as compared to instant specimen. In instant specimen the mechanical properties are badly deteriorated by damage of individual fibrils within the

159

fibers, consequently affecting the impact absorbing characteristics. The instant loaded sample has lower displacement while the gradual loaded sample has more displacement. The reason of earlier failure of instant loaded composite is that, as discussed earlier, it is already compacted (as a result of collapsed lumens inside the fibrils) so it will deform relatively earlier, and the curve drops sharply after peak load. In case of gradual loading the curve has multiple slopes in the failure zone, these peaks relate to resistance of reinforcement prior to complete failure. The crack propagation zone also shows the clear difference between gradual loaded and instant loaded composites, as the gradual loaded composites has higher crack propagation zone, which clearly shows the high resistance to displacement by gradual loaded composite.
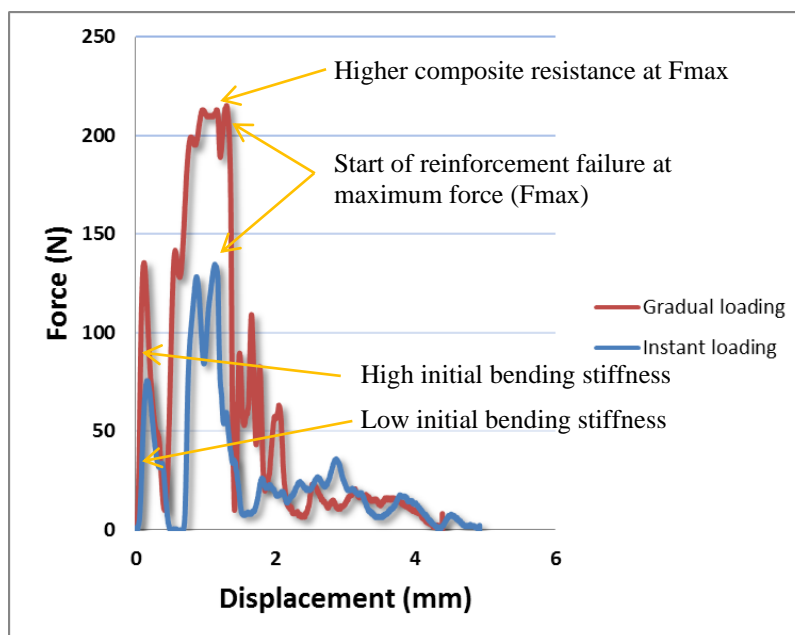
Figure 5-13. A comparison of Charpy impact results between instant and gradual loaded specimens (typical force-deflection curves)

Figure 5-14 describes the Charpy impact energies of instant and gradual composite specimens. The impact energy of the gradual and instant loaded specimens is 272mJ/mm and 141.3mJ/mm respectively, so the calculated impact energy of gradual specimen is an unsurpassed 93% higher than the instant specimen. This is quite a big difference, showing the dominance of gradual specimen over instant specimen and mainly, as discussed earlier, due to the better jute fiber health in gradual specimen as compared to instant specimen. In instant specimen the mechanical properties are badly deteriorated by the damaging of cellulosic walls around the lumen. The damaged fibers have lower energy absorption characteristics as compared to healthier jute fiber in case of gradual loading.
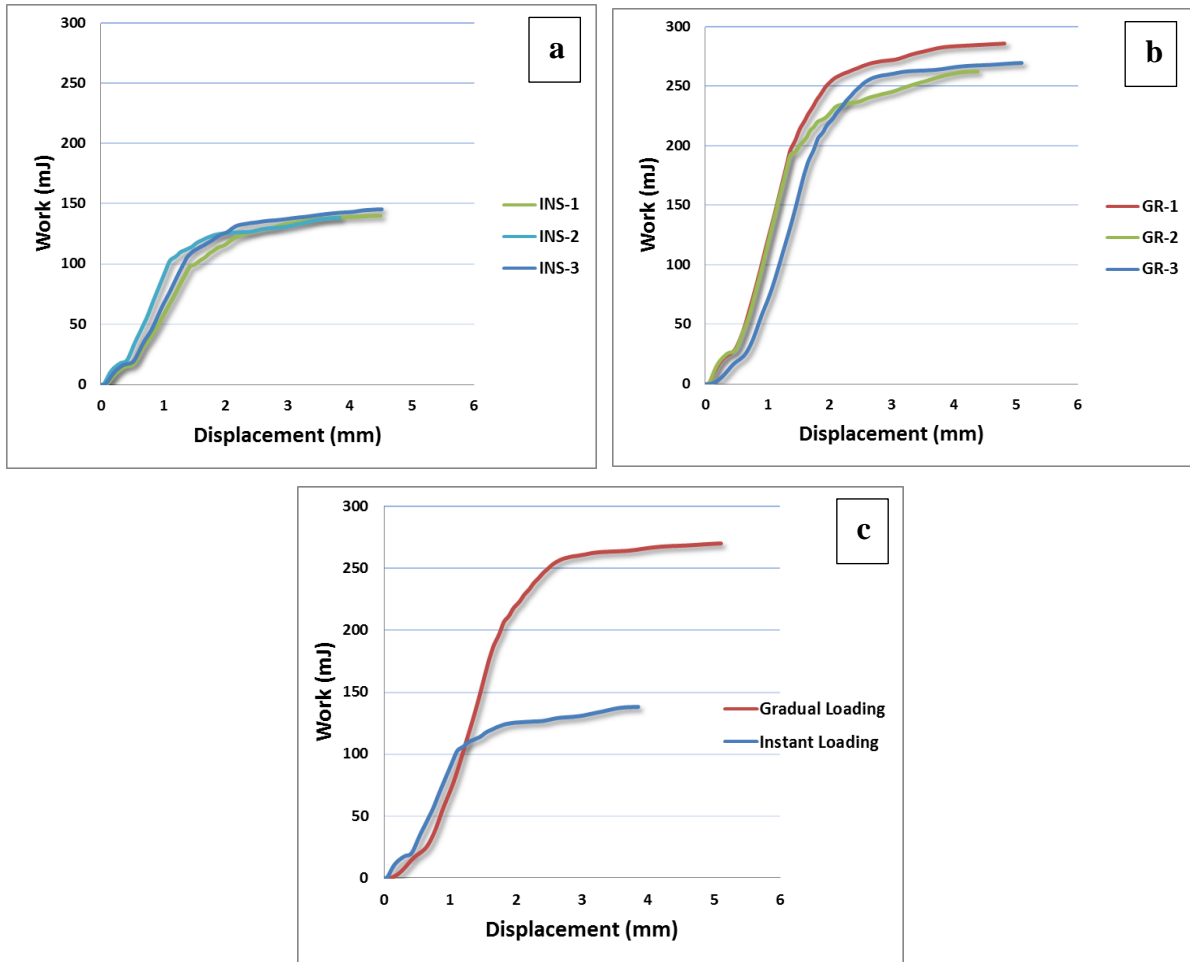
Figure 5-14. Work-displacement curves of instant and gradual loaded commingled composites, (a) three dispersion curves of instant specimen, (b) three dispersion curves of gradual specimen, (c) average curves of instant and gradual specimens

The microscopic images of gradual and instant specimens for Charpy impact test are shown in the Figure 5-15. A clear difference in the characteristics of instant and gradual loaded specimens can be seen. The jute fibers in the instant loaded specimen are in more compact and are in elliptical form (a-2), while in gradual loading the fibers are evenly placed in circular form (b-2) resulting into smoother shape as compared to instant loaded specimen. The darker shade of yarns in instant loaded specimen is explained by poor infiltration of polypropylene matrix deep inside the yarn body resulting into fiber pullout (a-1, a-2), while on the other hand the lighter shade of yarns in gradual loaded specimen is due to deeper penetration of lighter colored polypropylene matrix into to the fibers resulting into better fiber to fiber bonding inside the constituent yarns and thus imparting better mechanical properties to the composite as verified by the testing results.
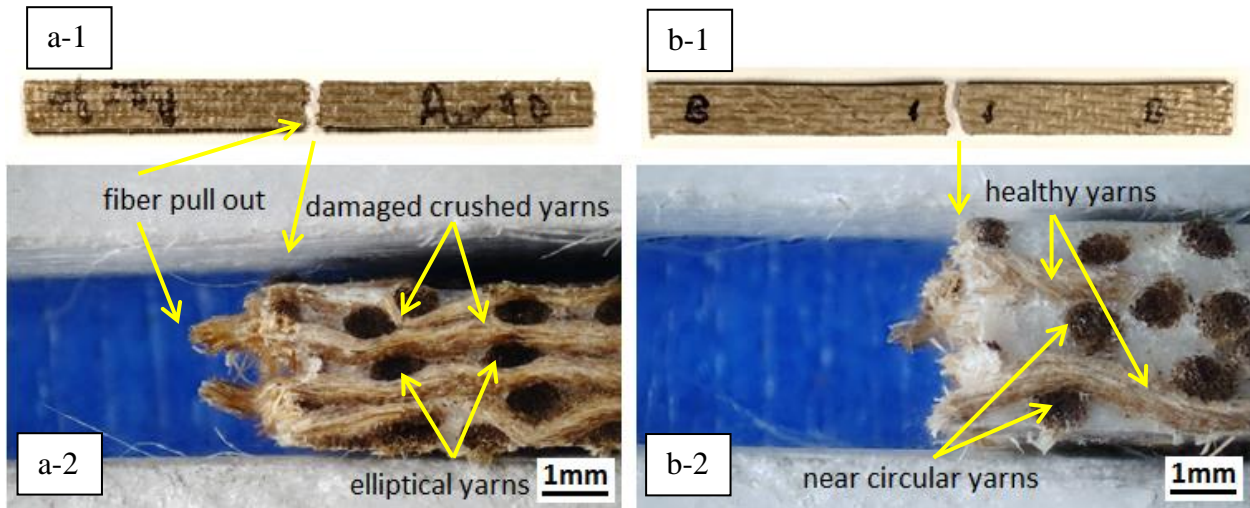
Figure 5-15. Charpy impact test sample of jute/PP composite made with (a-1, a-2) instant loading with visible fiber pullout, (b-1, b-2) gradual loading

Table 5-5 illustrates the impact energy, impact strength and displacement values of instant and gradual loaded specimen. The impact energy and strength values of gradual loaded specimen are 93% and 43.4% higher than instant specimen. Displacement against failure is also higher in gradual loaded specimen at 11.5%. This is mainly due to the reason that non-crushed and healthy fibrils impart better elongation in case of gradual specimen than the crushed and damaged fibrils in instant specimen which behave brittle.

Table 5-5. Charpy impact energy of instant and gradual loaded specimens

Sample	Impact force (N)	Impact energy (mJ)	Impact strength (kJ/m^2)	Displacement (mm)
Instant	135	141.3±7.2	5.6±0.74	4.27±0.44
Gradual	215	272±13.2	8.03±0.78	4.76±0.38
Difference %	60	93	43.4	11.5

5.4   Summary

In the present work 4-layer-jute/polypropylene-commingled composites was subjected to two different type of loading techniques, the instant loading and the gradual loading. In both cases the composites were subjected to a thermoforming pressure of 15 bars. It was observed that fibers remained round, without any damage, during gradual loading as compared to elliptical shape of instant loading. Initial high loading pressure in the instant specimen results into grouping together of the fibers within the jute yarns resulting into poor impregnation and

162

fiber pullout especially in tensile and Charpy impact tests where complete specimen breakage occurs. Furthermore, the global mechanical properties (tensile, flexural, short beam strength) and Charpy impact properties of composites produced with gradual loading technique are found significantly better than composites produced with instant loading technique. The reason being is least damage to the jute fibers with better impregnation. Comparing gradual to instant specimen is just like to compare two different types of cellulosic materials i.e., the jute in the instant loaded samples was damaged with weaker cellulose, on the contrary in the gradual loading the jute fibers are healthier with stronger cellulosic walls. It was also noticeable that a higher fiber volume fraction value does not always guarantee a composite with higher mechanical properties. Higher values of fiber volume fractions are related to instantaneous compression during thermoforming of the instantly loaded composite resulting into collapsed cellulosic walls around lumen. Instant thermoforming pressure is likely to damage the reinforcement fibers and eventually deteriorating the mechanical properties of the composite. In spite of the fact the commingled composite was made in both cases, the nature of loading pressure still affects the mechanical properties of the composite which is verified by the tested results.

Chapter 6. Development of jute 3D woven commingled composites and its mechanical characterization

In this chapter the mechanical properties of 3D woven commingled thermoplastic composites has been discussed. 3D woven natural fiber commingled composites were developed for the first time and composites samples were made with compression hot press using gradual loading technique. The samples were tested at 0° and 90° orientations. The tensile, flexural, short beam strength and Charpy impact tests were conducted to analyze the mechanical performance of 3D woven commingled composites. The results showed that the highest mechanical properties at 90° direction due to higher number of reinforcing yarns, whereas in 0° the fewer number of reinforcing yarn result into poor mechanical performance. The cross-section of samples shows that reinforcing yarn are placed in layers which through binding yarn with even fiber-matrix distribution.

This chapter deals with the mechanical properties of 3D commingled composites made using gradual loading technique. The tensile, flexural, short beam strength and Charpy impact test were conducted to compare the properties of 3D commingled composites in warp (0^0) and weft (90^0) directions. Ten tests were performed for 3D commingled composite specimens; five tested were performed for warp (0^0) and five for weft (90^0) specimens. The results showed that the tensile strength of weft (90^0) specimens were higher as compared to warp (0^0). Similar results were observed for flexural, SBS and Charpy impact.

6.1 Tensile properties of 3D commingled composites

In this section tensile properties of 3D commingled composites are discussed in detail. Figure 6-2 shows the tensile stress-strain curves of commingled composites made through 3D orthogonal weaving. The average tensile stress values of 3D orthogonal in warp ($0°$) and weft ($90°$) directions are 13MPa and 17.73MPa respectively. It is notable that the value of tensile strength is higher in weft direction as compared to warp direction which is 36.4% higher. It can be justified with the fact, as already discussed in part 2.6.3 above, that a 3D orthogonal preform is biased by default, i.e., if there are 'n' layers in warp direction then there would always be 'n+1' layers in weft direction. This is an unavoidable for 3D orthogonal fabrics because one layer of weft above the warp threads and one layer below the warp threads are essentially required in order to hold these warp threads. Hence in our study there are 5 weft layers and 4 warp layers (see

Figure *6-1*). Four layers in warp direction equal a stuffer warp density of 29.7 threads per inch and a weft density of 49.4 threads per inch, with the same jute yarn count in both directions (Table 2-8). Hence yarn density in weft direction is some 66% higher than in warp direction, which is verified by the result, as the tensile strength in weft direction is 35.4% higher than that in warp direction. However there are z-yarns present in the warp direction at a density of 2.42 threads per inch but they do not take part in warp tensile strength, mainly

due to the reasons that, during the tensile test, they are at perpendicular to the direction of applied force (due to much higher amount of crimp). For higher amount of crimp in z-warp yarns, under a tensile load the straighter stuffer warp yarns, being parallel to the direction of the applied force, would take the major tensile load and rupture much earlier than the out of plane z-yarns.

On the other hand, the strain at break in warp direction is on the lower side. These values are 2.23% and 2.33% respectively in warp and weft directions, which means the stiffness of 3D orthogonal composite is some 4.3% higher in warp direction. This is mainly due to higher amount of yarn tension in warp direction during weaving resulting into lower amount of crimp as shown in the

Figure *6-1* (a). The top layer on either side of the composite is composed of weft yarns and inner layers are of warp yarns (b).
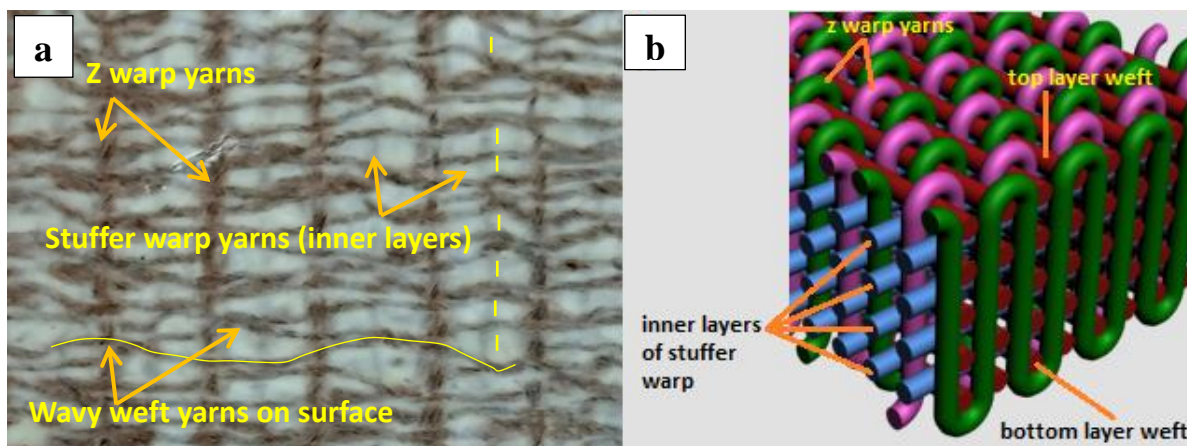
Figure 6-1. 3D orthogonal composite (a) Top view, weft yarns in the upper most layers are crimpier as compared to inner straighter layers of stuffer warp yarns, for which strain in weft is higher than in warp direction, z-yarns are binders, (b) Schematic of 3D orthogonal fabric showing 5 outer layers of red colored weft and 4 inner layers of stuffer blue colored warp

Figure 6-2. Stress-strain curves of 3D warp (0^0) and weft (90^0) composite specimens, (a) three curves for 3D warp (0^0), (b) three curves for 3D weft (90^0), (c) average curves of warp and weft specimens, tensile strength in weft direction is 35.4% higher than warp

Table 6-1 shows the tensile properties of 3D commingled composite in warp and weft directions. The tensile modulus and strength in weft direction is on the higher side as compared to warp direction mainly due to one additional layer (five weft layers verses four warp layers) in weft direction. However, the strain at break for warp is some 4.5% lower due to straighter stuffer yarns in warp direction (

Figure *6-1*).

Table 6-1. Tensile properties of 3D commingled composite in warp and weft directions

Sample	Tensile modulus (GPa)	Tensile strength (MPa)	Strain at break (%)
Warp (0°)	2.96±0.15	13±0.15	2.23±0.3
Weft (90°)	3.54±0.09	17.73±0.65	2.33±0.19
Difference %	19.6	36.4	4.5

The optical microscope analysis of 3D orthogonal commingled composite specimens against tensile test has been shown in Figure 6-3. The interface line, between the two parts of broken

167

specimens, looks zigzag for commingled specimen. It seems that the breakage phenomenon goes deep into the structure of this 3D commingled specimen which speaks of a better adhesion between the jute fibers and the polypropylene matrix indicating a fiber dominant breakage. The breakage line also looks quite crispy with minimum fiber pullout. Figure 6-3 (a) shows the tensile specimen before testing, (b) shown the specimen after testing, (c) shows the zoomed perspective view of one of the broken edges, (d) shows a zoomed top view of both of these counterparts laying side by side for a better comparison.
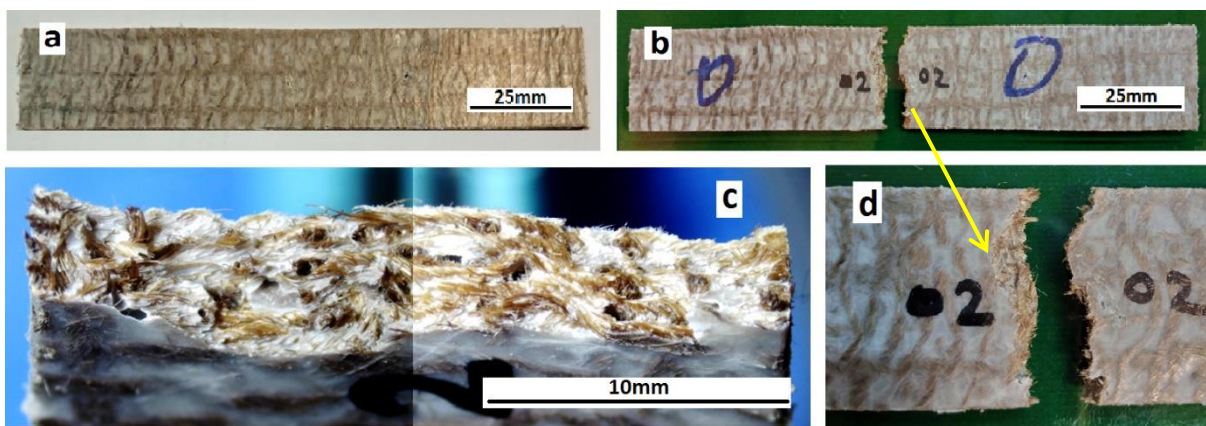
Figure 6-3. Microscopic image of 3D orthogonal tensile tested specimens in warp direction (a) tensile specimen before testing, (b) tensile specimen after testing, (c) zoomed perspective view broken edge, (d) zoomed top view of broken counterparts

6.2 Flexural properties of 3D commingled composites

In this section flexural properties of 3D commingled composites are discussed in detail.

Figure 6-4 illustrates the flexural strength of 3D commingled composite specimen. The flexural strengths of warp (0°) and weft (90°) directions have been compared. The average flexural strengths of 3D orthogonal in warp and weft directions are 18.73MPa and 36.62MPa respectively. It is notable that the value of flexural strength is much higher in weft direction as compared to warp direction. It can be justified with two main reasons, firstly as already mentioned, a 3D orthogonal preform is biased by default, i.e., if there are 'n' layers in warp

direction then there would always be 'n+1' layers in weft direction. Hence in our case there are 5 weft layers and 4 warp layers (

Figure *6-1*). Four layers in warp direction equal a stuffer warp density 29.7 threads per inch and a weft density of 49.4 threads per inch (see Table 2-8). Hence yarn density in weft direction is some 66% higher than in warp direction. Secondly when a sample is subjected to 3-point flexural test, its outer most layers play the most important role. The layer next to the testing machine probe suffers compression and the opposite surface suffers tension. In a weft direction (90°) composite specimen, the outer most layer has weft yarns parallel to the direction of applied tensile force, these weft threads directly bears the surface tensile stress, which in turn, boosts the flexural strength. On the other hand, for testing a 0° warp specimen, these outer most weft threads are at 90° to the direction of the surface tensile stress, these 90° threads do not directly bear the surface tensile stress. In this case the bearing force depends upon the adhesive strength between the resin and fibers of this outer most layer, which in turn weakens the composite resistance against bending force. In such 0° warp specimen, the warp threads which are likely to bear the tensile pull are not present on the surface; rather they are somewhat in the inner layers resulting into weaker flexural strength (

Figure *6-1*). This fact has been verified by the tested results, as the flexural strength in weft direction is a marginal 95% higher than that in weft direction.

On the other hand, in a comparison of bending strain, this outer most surface again plays very important role. In 90° weft specimen, these outer most weft threads, being parallel to the surface stress, offers most resistance against the bending force and hence reducing the strain percent as compared to a 0° warp specimen. This reflects from the measured strain percent which is 5.35% and 6.36% respectively for 90° weft and 0° warp specimens. Hence a 90° weft specimen is 15.9% stiffer than 0° warp specimen. It is interesting to note that apart from the higher amount of crimp in 90° weft specimen, its stiffness is still at the higher side, it

means the outer most position of weft threads in a 90° specimen over comes its inherent weakness of higher amount of crimp. On the other hand, besides lower crimp in stuffer warp, the 0° warp specimen exhibits lower stiffness. This is mainly due to the reason that these lower crimp stuffer warp yarns are in the inner layers of the composite which suffers lower amount of stress/elongation as compared to the outermost layers in a 3-point bending test. In a 3-point bending test the stress/elongation behavior varies among the layers (more stress at outer layers than inner layers), but on the other hand the stress/elongation behavior deals equally in a tensile specimen, which has been verified by the tensile test (see 6.1) where warp direction is 3.8% stiffer than weft.

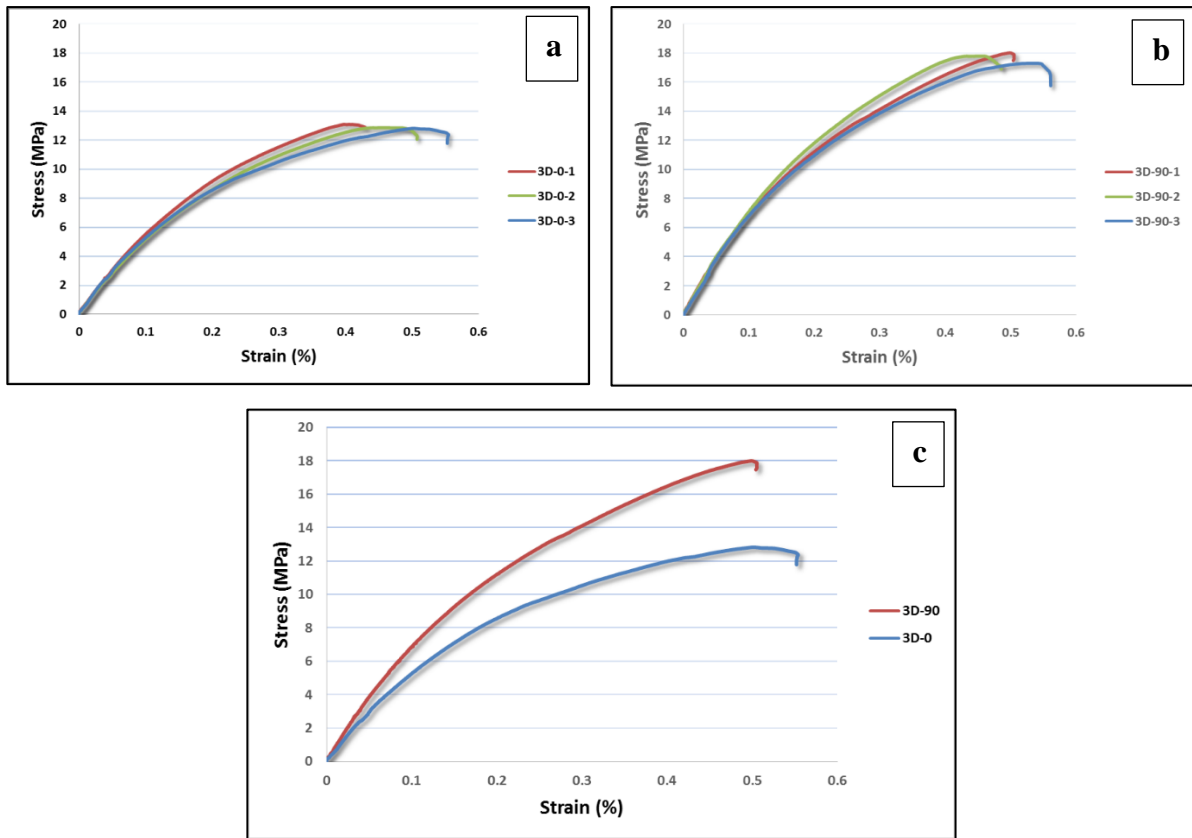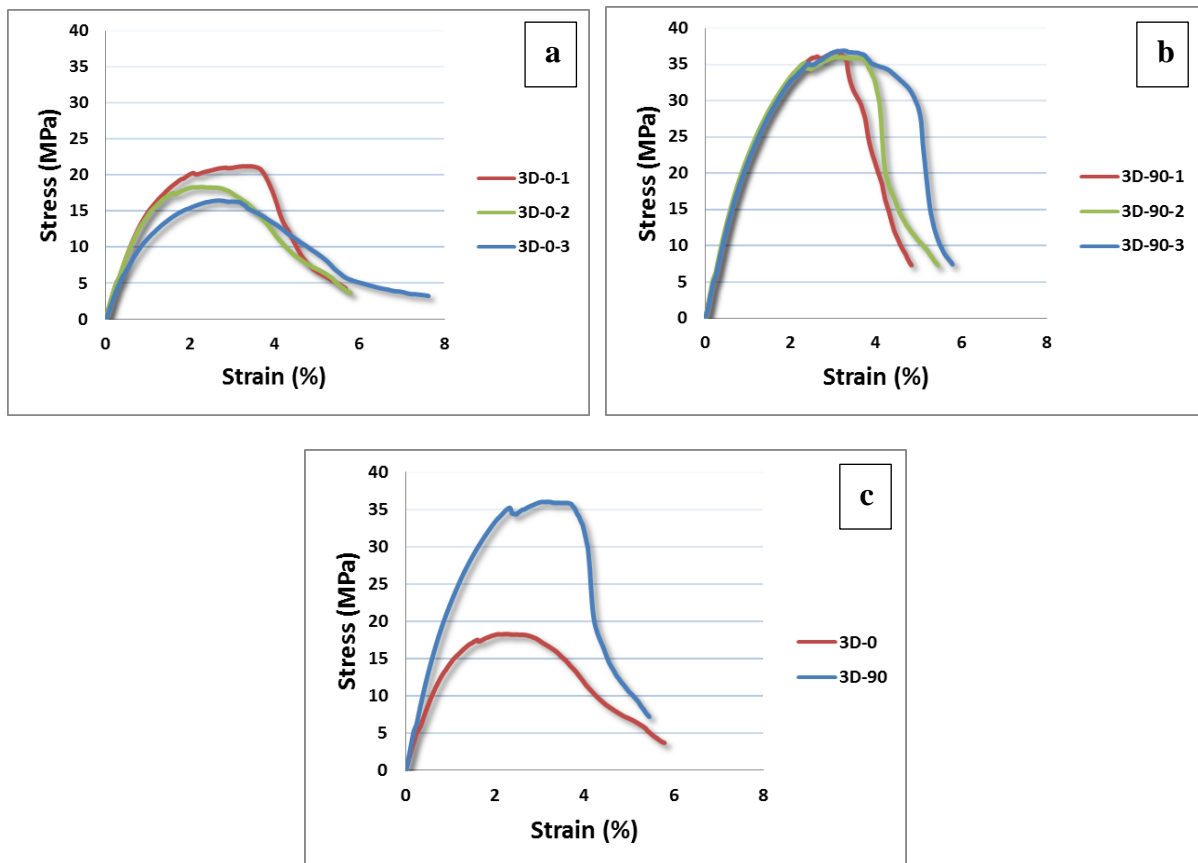*Figure 6-4. Flexural strengths of 3D warp (0^0) and weft (90^0) composite specimens, (a) three curves for 3D warp (0^0), (b) three curves for 3D weft (90^0), (c) average curves of warp and weft specimens, flexural strength in weft direction is 95% higher than warp*

Table 6-2 shows the flexural strength and strain percent values of 3D commingled composite both in warp and weft directions. The flexural strength in weft direction is marginally high at

170

95% as compared to warp direction mainly due to one additional layer (five weft layers verses four warp layers) in weft direction. The strain in warp direction is 18.9% higher than weft direction. The reason for higher flexural strength in weft and higher strain in warp direction has been explained in detail in previous paragraph. The flexural modulus is also marginally 44% higher in weft direction due to higher flexural strength and lower strain in weft direction as compared to warp direction.

Table 6-2. Flexural properties of 3D orthogonal commingled composite in warp and weft directions

	Flexural modulus (GPa)	Flexural strength (MPa)	Strain %
Warp (0°)	1.68±0.06	18.73±3.1	6.36±1.35%
Weft (90°)	2.42±0.09	36.62±0.87	5.35±0.95%
Difference %	44	95.5	18.9

The optical microscope analysis of 3D orthogonal commingled composite specimens against 3-point bending test in weft direction has been shown in Figure 6-5. (a) represents the 3-point specimen before test, (b) represents the 3-point specimen after test, (c) represents the side view showing specimen bending at seven times zoom (d) is representing the side view at forty times zoom (e) represents the tension side of tested specimen at seven times zoom, (f) represents the same at forty times zoom. A yarn dominant breakage is visible. The specimens did not completely break both for warp and weft tests up to 30% of maximum load.
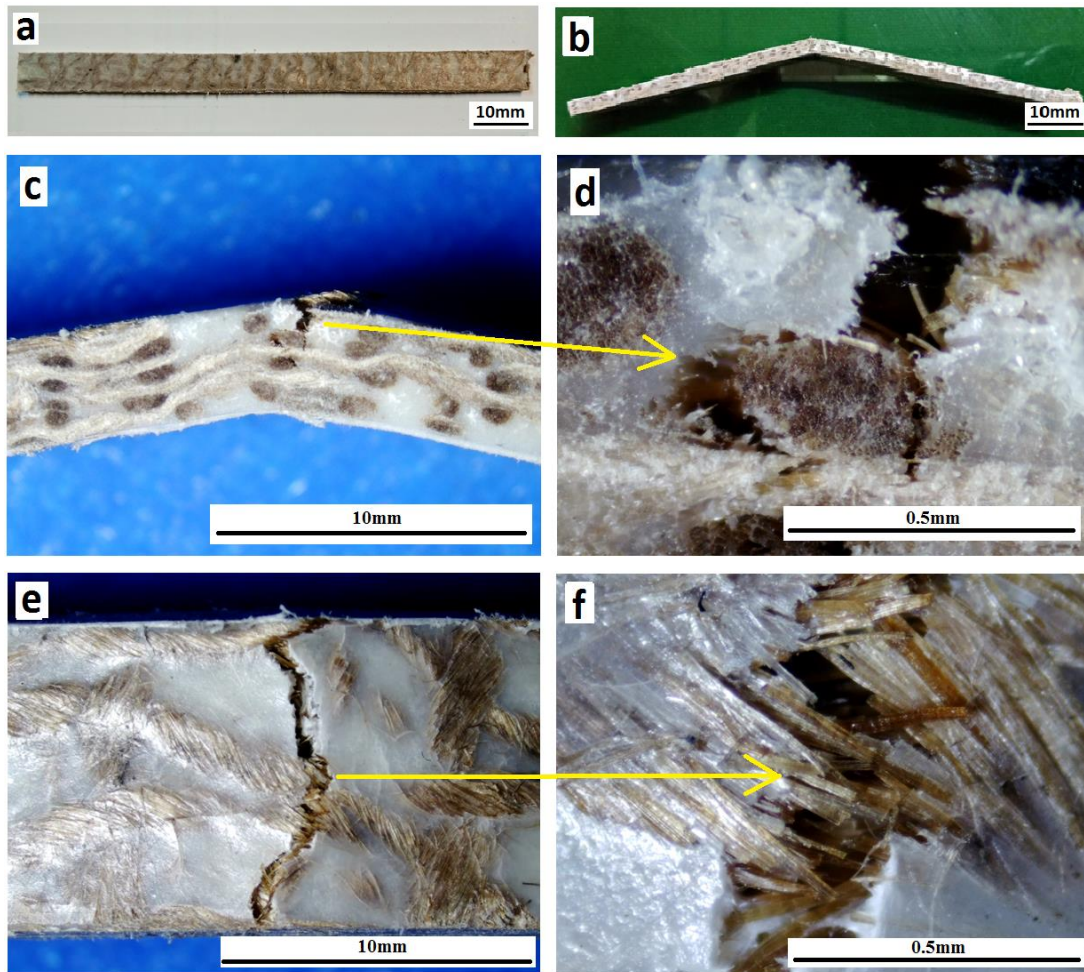
Figure 6-5. 3-point tested samples of non-broken 3D orthogonal commingled specimens (weft direction), (a) 3-point specimen before test, (b) specimen after test, (c) side view at 7x zoom (d) side view at 40x zoom (e) tension side of tested specimen at 7x zoom, (f) tension side at 40x

6.3   Short beam strength of 3D commingled composites

Figure 6-6 shows the short beam strength of 3D orthogonal commingled composite specimens. The short beam strengths of warp (0°) and weft (90°) directions have been compared. The average SBS strength of 3D orthogonal in warp and weft directions is 3.14 and 3.33 MPa respectively. The short beam strength is higher in weft direction as compared to warp direction by 6.1%. On the other hand, the bending displacement is 1.08 mm and 0.8 mm respectively for 0° warp and 90° weft specimens. Hence a 90° weft specimen is 25%

stiffer than 0° warp specimen, the reason of which has been explained in detail at part 6.2 above.
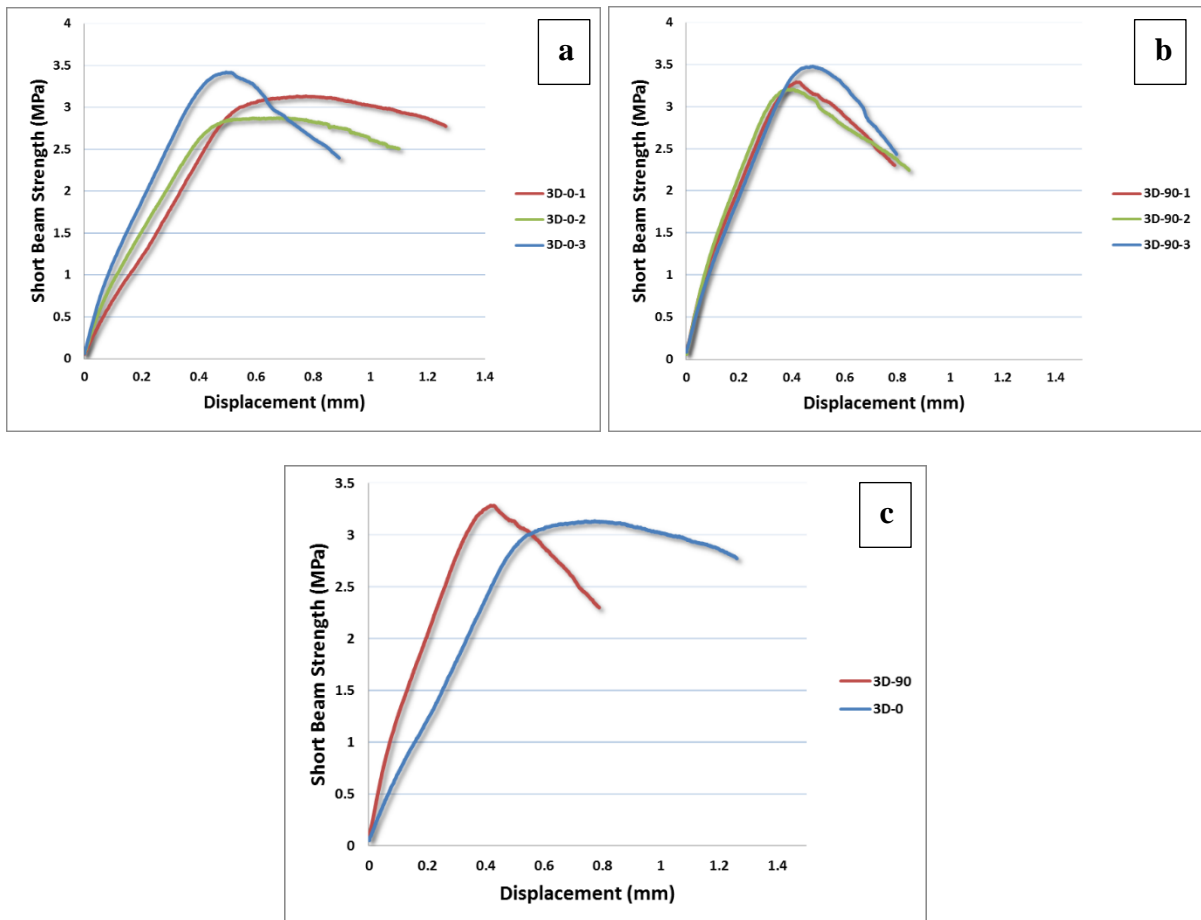
Figure 6-6. Short beam strengths of 3D warp (0^0) and weft (90^0) composite specimens, (a) three curves for 3D warp (0^0), (b) three curves for 3D weft (90^0), (c) average curves of warp and weft specimens

Table 6-3 shows short beam strength and displacement values of 3D commingled composite in warp and weft directions. The short beam strength in weft direction is on the higher side as compared to warp direction mainly due to one additional layer (five weft layers verses four warp layers) in weft direction. However, the displacement for warp is some 33.3% higher, as explained earlier (see 6.2 above)

Table 6-3. Short beam strength (SBS) of 3D orthogonal commingled composite in warp and weft directions

	Short beam strength (MPa)	Displacement (mm)
Warp (0°)	3.14±0.2	1.08±0.19%
Weft (90°)	3.33±0.11	0.81±0.03%

| Difference % | 5.71 | 33.3 |

The optical microscope analysis of 3D orthogonal commingled composite specimens against short beam strength test in weft direction has been explained in Figure 6-7, where (a) represents the SBS specimen before test, (b) represents the SBS specimen after test, (c) represents the side view showing specimen bending at seven times zoom (d) is representing the side view at forty times zoom (e) represents the tension side of tested specimen at seven times zoom, (f) represents the same at forty times zoom. A yarn dominant breakage is visible. The specimens did not completely break both for warp and weft tests up to 30% of maximum load.. It is clear that there are no signs of delamination, which speaks of the presence of z-yarn. Their presence helps fight against delamination, which is a critical property of 3D structures.
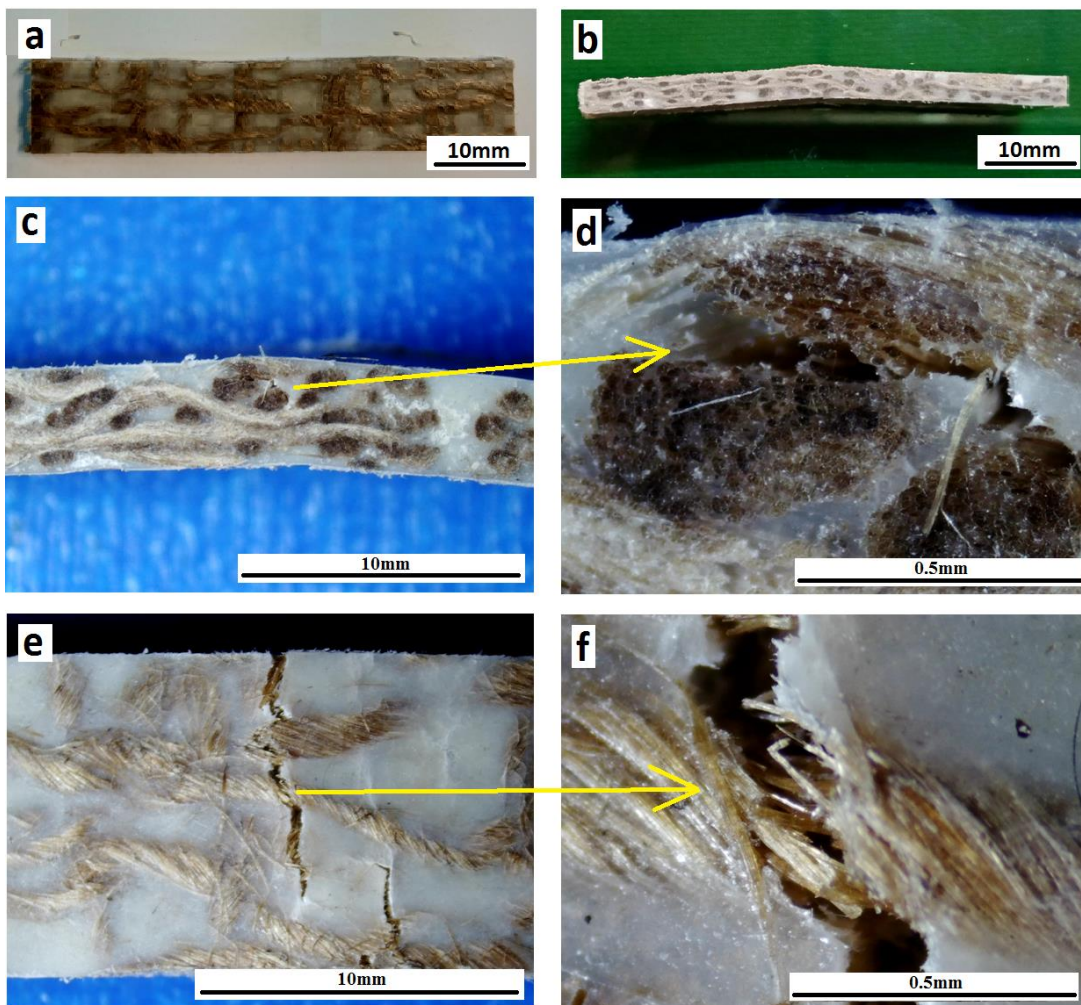
Figure 6-7. SBS tested samples of non-broken 3D orthogonal commingled specimens (weft direction), (a) SBS specimen before test, (b) specimen after test, (c) side view at 7x zoom (d) side view at 40x zoom (e) tension side of tested specimen at 7x zoom, (f) tension side at 40x. A yarn dominant breakage is visible

6.4 Charpy impact properties of 3D commingled composites

Figure 6-8 illustrates the Charpy impact properties of 3D commingled warp (0°) and weft (90°) composite specimens. The impact energy of the warp (0°) and weft (90°) composite specimens are at the order of 87.22mJ and 261mJ respectively, so the impact energy of weft (90°) composite specimens is an unsurpassed 199% higher than the warp (0°) composite specimen. This is a big difference, showing the dominance of weft (90°) composite specimen over warp (0°) composite specimen. A detailed reason has been explained (see 6.2). The same is reflected by the impact strength, which is again a marginal 218% higher (7.38 kJ/mm^2 for weft vs 2.32 kJ/mm^2 for warp). The presence of z-yarns plays an important role in Charpy impact test. As they keep the 3D woven structures in an integrated form due to their presence in through the thickness direction, hence increasing the impact strength.
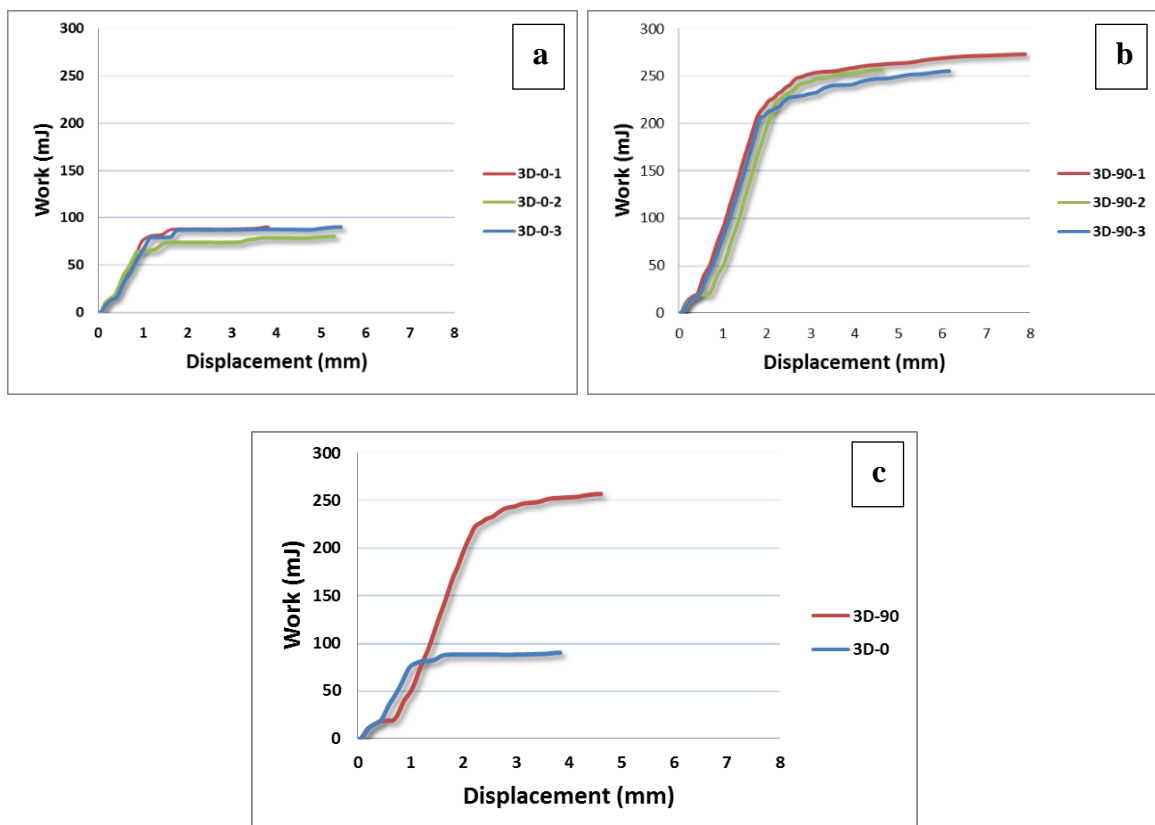
Figure 6-8. Work-displacement curves of 3D orthogonal commingled warp (0°) and weft (90°) composite specimens

Table 6-4 illustrates the impact force, impact energy, impact strength and displacement values of 3D commingled composite in warp and weft directions. The impact energy and strength values of 3D commingled composite in weft direction are 199% and 218% higher than warp direction. Displacement against failure is higher in weft direction at 28%. This in mainly due to higher yarn crimp in weft direction for which the composite lasts longer against the impact force resulting into higher impact values as compared to warp direction.

Table 6-4. Charpy impact energy of 3D orthogonal commingled composite in warp and weft directions

Sample	Impact force (N)	Impact energy (mJ)	Impact strength (kJ/m^2)	Displacement (mm)
Warp (0°)	111	87.22±6.7	2.32±0.4	4.85±0.59%
Weft (90°)	167	261±11.3	7.38±0.5	6.2±1.67%
Difference %	51	199	218	27.8

The optical microscope analysis of 3D orthogonal commingled composite specimens against Charpy impact test in weft direction has been explained in Figure 6-9. The interface line, between the two parts of broken specimens, like the tensile tested specimen, seems following a zigzag path. It seems that the breakage phenomenon goes deep into the body of this 3D commingled specimen which speaks of better adhesion forces between the jute fibers and the polypropylene matrix. The broken specimen has been shown in the Figure 6-9. (a) Represents one of the fractured face of two broken counterparts at fourteen times zoom, (b) represents a thirty times zoomed side view of one of the broken counterparts. The nonlinear/irregular broken surface speaks of a fiber dominant breakage without any signs of delamination due to presence of z-yarns.
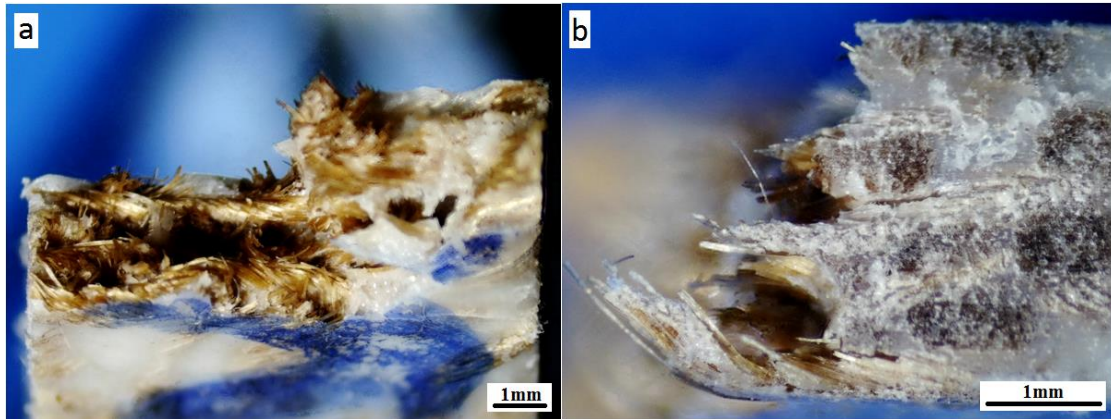
Figure 6-9. Microscopic image of Charpy impact tested samples of 3D orthogonal commingled specimens, (a) fracture face (b) side view

6.5 Summary

The mechanical properties of commingled composites have been proven better over the non-commingled composites for both UD and 2D categories the. However with the introduction of an additional dimension in the fabric, which is the Z direction in 3D fabrics, an extra out of plane reinforcement is provided. This additional dimension further boosts the mechanical properties of the commingled composites to a next level.

Chapter 7. General Conclusions and Future Perspectives

General Conclusions

In this research work, the effect of surface treatment such as singeing of reinforcement on the physical and mechanical properties of jute yarn and associated composites were investigated. The commingling technique for the fabrication of 2D and 3D natural fiber reinforced thermoplastic composites were developed and optimized; and its comparison with composites made with conventional fabrication techniques were established. The commingled composites revealed their overall dominance over the conventional non-commingled composites. The fabrication of composites using commingled yarns technique resulted in impregnation of reinforcement at fiber level, which leads to good adhesion of matrix with fibers, which resulted in the improved mechanical properties such as, the tensile strength and the flexural strength of commingled composites were enhanced up to 57 % and 85% respectively, as compared to the non-commingled composites. The impact energy of commingled composites was found up to 22% higher than non-commingled composites. Furthermore, F*max* value for commingled composites was found up to 88% higher than non-commingled composites with an increment in displacement up to 20%. This shows the high quality and better fiber-matrix adhesion in commingled composites as compared to conventional non-commingled ones. The improvement in mechanical behavior was consistent for thin as well as thick composites. These results demonstrated that the fabrication of thermoplastic composites using the commingled technique is a quick and viable solution resulting in the development of high-quality composites with enhanced properties.

The properties of UD commingled and non-commingled composites, made with the jute yarn and PP matrix, were investigated and their mechanical properties were established. The tensile test results show that the commingled composite has higher tensile strength due to better impregnation of jute yarn within the matrix. The non-commingled composite had high stiffness and low strain due to straighter jute yarns. The flexural results showed the similar trends with the higher flexural strength for commingled composites as compared to non-commingled composites. The flexural strain of non-commingled composite was lower as compared to commingled composite due to straighter jute yarn placement after fabrication. The short beam strength of commingled composite was also higher as compared to non-commingled composites. The Charpy impact strength of commingled composites was higher due to better distribution of matrix and reinforcement in the composite. The overall results

showed that the UD commingled composite has better mechanical properties and can be employed for thermoplastic composites fabrication.

The fiber volume fraction of the commingled composites, as described earlier, was found on the lower side as compared to the non-commingled composites even under the same thermoforming conditions of temperature, pressure, holding time etc. lower value of fiber volume fraction was mainly attributed to a higher diameter of commingled yarn (2mm) as compared to the diameter of jute yarn in non-commingled composites (0.7-0.8mm). The higher diameter of the commingled yarns hinders the close packing of the warp (longitudinal) and weft (transvers) yarns in a woven fabric. However suitable measured can improve the Vf of the commingled composites, such as using finer polypropylene for co-twisting with jute for commingling. This would reduce the commingled yarn diameter to < 2mm, resulting into closer thread spacing in the woven fabric and higher Vf. However there would be a lower threshold for the fineness of polypropylene yarn, as a yarn finer than a certain limit would leave certain regions in the thermoformed composite 'starving' with the matrix.

To put into nutshell, overall, the properties of the commingled composites are better than those of non-commingled composites, but it is important to note that a marginal difference between the Charpy impact properties has been observed which encourages the use of commingled thermoplastic composites for impact applications.

Also, four layer jute/polypropylene commingled composite was subjected to two different type of loading techniques, the instant loading and the gradual loading. It was observed that fibers remained round, without any damage, during gradual loading as compared to elliptical shape of instant loading. Furthermore, the global mechanical properties (tensile, flexural, short beam strength) and Charpy impact properties of composites produced with gradual loading are found significantly better than composites produced with instant loading. It was also noticeable that a higher fiber volume fraction value does not always guarantee a composite with higher mechanical properties. Higher values of fiber volume fractions are related to collapsed lumen of jute fibers in instantaneous compression during thermoforming of the instantly loaded composite. Instant thermoforming pressure is likely to damage the reinforcement fibers and eventually deteriorating the properties of the composites. Since the polypropylene and jute fiber do not have any chemical interlocking, they have just physical interlocking so in that case the even distribution of jute yarn within composite become more important, in spite of the fact the commingled composite was made in both cases, the nature

of loading pressure still effect the yarn distribution and in case of gradual loading we can achieve that goal of even reinforcement distribution.

In the current research work natural fiber 3D commingled composites were developed for the first time. The commingled composites are already proving their grounds in the field of 2D composites, however with the addition of the reinforcement yarns in an additional third dimension (the z dimension) further enhances the mechanical properties of 3D commingled composites to next level. The fabrication time of 2D commingled composite laminates is already faster than the 2D non-commingled composite laminates due to no-use of additional polypropylene sheets during alternate layer stacking, but additionally this composite fabrication time is further shortened by using 3D commingled composites which 'do not' need layers stacking and only a single 3D commingled layers of desired thickness is sufficient.

Future Perspectives

1. To improve the novel technique: this includes improvement and control of fiber volume fraction of jute, fabrication of commingled yarn, study of effect of temperature and effect of pressure, quantification and controlling of voids, study of matrix bleeding.

2. To upscale the developed technique to industrial level.

3. To optimize the development of 3D bio-composites

4. To study in detail the mechanism of deformation and fracture using advanced techniques such as Ultrasound, Digital image correlation etc.

References

References

[1]   Gon D, Das K, Paul P, Maity S. Jute composites as wood substitute. Int J Text Sci 2012;1:84–93.

[2]   Gay D, Hoa S V, Tsai SW. Composite Materials: Design and Applications. 2003.

[3]   Gao C, Peng S, Feng P, Shuai C. Bone biomaterials and interactions with stem cells. Bone Res 2017;5:1–33. https://doi.org/10.1038/boneres.2017.59.

[4]   Mallick PK. Fiber-reinforced composites: materials, manufacturing, and design. CRC press; 2007.

[5]   Campbell FC. Structural Composite Materials. ASM International. New York, USA: ASM International; 2010.

[6]   Wambua P, Ivens J, Verpoest I. Natural fibres: can they replace glass in fibre reinforced plastics? Compos Sci Technol 2003;63:1259–64. https://doi.org/10.1016/S0266-3538(03)00096-4.

[7]   Debnath S, Nguong C, Lee S. A Review on Natural Fibre Reinforced Polymer Composites. World Acad Sci Eng Technol 2013;73:1123–30.

[8]   Joshi S., Drzal L., Mohanty a. ., Arora S. Are natural fiber composites environmentally superior to glass fiber reinforced composites? Compos Part A Appl Sci Manuf 2004;35:371–6. https://doi.org/10.1016/j.compositesa.2003.09.016.

[9]   Natural Fiber Composites Market is expected to augment growth over the forecast period. Glob Mark Res Insight 2016.

[10]   Zaki Abdullah M, Dan-Mallam Y, Megat Yusoff PSM. Effect of environmental degradation on mechanical properties of kenaf/polyethylene terephthalate fiber reinforced polyoxymethylene hybrid Composite. Adv Mater Sci Eng 2013;2013. https://doi.org/10.1155/2013/671481.

[11]   Dittenber DB, GangaRao HVS. Critical review of recent publications on use of natural composites in infrastructure. Compos Part A Appl Sci Manuf 2012;43:1419–29. https://doi.org/10.1016/j.compositesa.2011.11.019.

[12]   Ku H, Wang H, Pattarachaiyakoop N, Trada M. A review on the tensile properties of natural fiber reinforced polymer composites. Compos Part B Eng 2011;42:856–73. https://doi.org/10.1016/j.compositesb.2011.01.010.

[13]   Taj S, Munawar MA, Khan S. Natural Fiber-Reinforced Polymer Composites. Proc Pakistan Acad Sci 2007;44:129–44.

[14]   Zampaloni M. Kenaf natural fiber reinforced polypropylene composites : A discussion

on manufacturing problems and solutions. Compos - Part A Appl Sci Manuf 2007;38:1569–80. https://doi.org/10.1016/j.compositesa.2007.01.001.

[15]   Mohanty AK, Misra M, Hinrichsen G. Biofibres, biodegradable polymers and biocomposites: An overview. Macromol Mater Eng 2000;276–277:1–24.

[16]   Shahzad A. Hemp fiber and its composites - a review. J Compos Mater 2011;46:973–86. https://doi.org/10.1177/0021998311413623.

[17]   Li X, Tabil LG, Panigrahi S. Chemical Treatments of Natural Fiber for Use in Natural Fiber-Reinforced Composites: A Review. J Polym Environ 2007;15:25–33. https://doi.org/10.1007/s10924-006-0042-3.

[18]   Hashim MY, Roslan MN, Amin AM, Mujahid A, Zaidi A. Mercerization Treatment Parameter Effect on Natural Fiber Reinforced Polymer Matrix Composite : A Brief Review. World Acad Sci Eng Technol 2012;6:1638–44.

[19]   Zhu J, Zhu H, Njuguna J, Abhyankar H. Recent Development of Flax Fibres and Their Reinforced Composites Based on Different Polymeric Matrices. Materials (Basel) 2013;6:5171–98. https://doi.org/10.3390/ma6115171.

[20]   Zafeiropoulos NE, Baillie CA, Matthews FL. A study of transcrystallinity and its effect on the interface in flax fibre reinforced composite materials. Compos - Part A Appl Sci Manuf 2001;32:525–43.

[21]   Chabba S, Netravali AN. 'Green' composites Part 1: Characterization of flax fabric and glutaraldehyde modified soy protein concentrate composites. J Mater Sci 2005 4023 2005;40:6263–73. https://doi.org/10.1007/S10853-005-3142-X.

[22]   Andersons J, Joffe R. Estimation of the tensile strength of an oriented flax fiber-reinforced polymer composite. Compos Part A Appl Sci Manuf 2011;42:1229–35. https://doi.org/10.1016/j.compositesa.2011.05.005.

[23]   Notta-Cuvier D, Lauro F, Bennani B. An original approach for mechanical modelling of short-fibre reinforced composites with complex distributions of fibre orientation. Compos   Part   A   Appl   Sci   Manuf   2014;62:60–6. https://doi.org/10.1016/j.compositesa.2014.03.016.

[24]   Oksman K, Skrifvars M, Selin J-F. Natural fibres as reinforcement in polylactic acid (PLA)   composites.   Compos   Sci   Technol   2003;63:1317–24. https://doi.org/10.1016/S0266-3538(03)00103-9.

[25]   Kumar R, Yakabu MK, Anandjiwala RD. Effect of montmorillonite clay on flax fabric reinforced poly lactic acid composites with amphiphilic additives. Compos Part A Appl Sci Manuf 2010;41:1620–7. https://doi.org/10.1016/j.compositesa.2010.07.012.

[26]   Assarar M, Scida D, El Mahi A, Poilâne C, Ayad R. Influence of water ageing on mechanical properties and damage events of two reinforced composite materials: Flax-fibres and glass-fibres. Mater Des 2011;32:788–95. https://doi.org/10.1016/j.matdes.2010.07.024.

[27]   Paynel F, Pavlov A, Colasse L, Rihouey C, Follain N, Duriatti D, et al. Preparation and characterization of flax biocomposites made of seed mucilage reinforced by fibers. Compos Part A Appl Sci Manuf 2014;69:299–305. https://doi.org/10.1016/j.compositesa.2014.11.021.

[28]   Gassan J, Bledzki AK. Possibilities for improving the mechanical properties of jute / epoxy composites by alkali treatment of ® bres. Compos Sci Technol 1999;59:1303–9.

[29]   Pinto MA, Chalivendra VB, Kim YK, Lewis AF. Effect of surface treatment and Z-axis reinforcement on the interlaminar fracture of jute/epoxy laminated composites. Eng Fract Mech 2013;114:104–14. https://doi.org/10.1016/j.engfracmech.2013.10.015.

[30]   Seki Y, Sever K, Sarıkanat M, Şen İ, Aral A. Jute / Polyester Composites : The Effect of Water Aging on The Interlaminar Shear Strength. 6th Int Adv Technol Symp 2011:16–8.

[31]   Munikenche Gowda T, Naidu ACB, Chhaya R. Some mechanical properties of untreated jute fabric-reinforced polyester composites. Compos Part A Appl Sci Manuf 1999;30:277–84. https://doi.org/10.1016/S1359-835X(98)00157-2.

[32]   Ali Azam , Shaker Khubab , Nawab Yasir AM, Basit Abdul SS and UM. Impact of Hydrophobic Treatments of Jute on Moisuture Regain and Mechanical Properties of Composites. Jpurmal Reinf Plast Compos 2014.

[33]   Mishra A. Strength and Corrosion Testing of Jute / Glass- Epoxy Hybrid Composite Laminates. Plast Polym Technol 2013;2.

[34]   Ray D, Sarkar BK, Bose NR. Impact fatigue behaviour of vinylester resin matrix composites reinforced with alkali treated jute fibres. Compos - Part A Appl Sci Manuf 2002;33:233–41. https://doi.org/10.1016/S1359-835X(01)00096-3.

[35]   Plackett D, Andersen TL, Pedersen WB, Nielsen L. Biodegradable composites based on L-polylactide and jute fibres. Compos Sci Technol 2003;63:1287–96. https://doi.org/10.1016/S0266-3538(03)00100-3.

[36]   Rana AK, Mitra BC, Banerjee AN. Short jute fiber-reinforced polypropylene composites: Dynamic mechanical study. J Appl Polym Sci 1999;71:531. https://doi.org/10.1002/(sici)1097-4628(19990124)71:4<531::aid-app2>3.3.co;2-9.

[37]   Ali A, Shaker ZR, Khalina a., Sapuan SM. Development of Anti-Ballistic Board from

Ramie Fiber. Polym Plast Technol Eng 2011;50:622–34. https://doi.org/10.1080/03602559.2010.551381.

[38] Teja TR, Venkata RD, Naidu AL, Bahubalendruni MVA. Mechanical and chemical Properties of Ramie reinforced composites and manufacturing techniques...A Review Article. Int J Res Dev Technol 2017;8:2349–3585.

[39] Zhang Y, Wen B, Cao L, Li X, Zhang J. Preparation and properties of unmodified ramie fiber reinforced polypropylene composites. J Wuhan Univ Technol Sci Ed 2015;30:198–202. https://doi.org/10.1007/s11595-015-1125-6.

[40] Xu H, Wang L, Teng C, Yu M. Biodegradable composites: Ramie fibre reinforced PLLA-PCL composite prepared by in situ polymerization process. Polym Bull 2008;61:663–70. https://doi.org/10.1007/s00289-008-0986-7.

[41] Lodha P, Netravali AN. Characterization of stearic acid modified soy protein isolate resin and ramie fiber reinforced "green" composites. Compos Sci Technol 2005;65:1211–25. https://doi.org/10.1016/j.compscitech.2004.12.036.

[42] Paiva Júnior CZ, De Carvalho LH, Fonseca VM, Monteiro SN, D'Almeida JRM. Analysis of the tensile strength of polyester/hybrid ramie-cotton fabric composites. Polym Test 2004;23:131–5. https://doi.org/10.1016/S0142-9418(03)00071-0.

[43] Gehring F, Bouchart V, Dinzart F, Chevrier P. Microstructure, mechanical behaviour, damage mechanisms of polypropylene/short hemp fibre composites: Experimental investigations. J Reinf Plast Compos 2012;31:1576–85. https://doi.org/10.1177/0731684412464089.

[44] Thwe MM, Liao K. Effects of environmental aging on the mechanical properties of bamboo-glass fiber reinforced polymer matrix hybrid composites. Compos - Part A Appl Sci Manuf 2002;33:43–52. https://doi.org/10.1016/S1359-835X(01)00071-9.

[45] Conzatti L, Giunco F, Stagnaro P, Patrucco A, Marano C, Rink M, et al. Composites : Part A Composites based on polypropylene and short wool fibres. Compos Part A 2013;47:165–71. https://doi.org/10.1016/j.compositesa.2013.01.002.

[46] Herrera-Franco PJ, Valadez-González A. A study of the mechanical properties of short natural-fiber reinforced composites. Compos Part B Eng 2005;36:597–608. https://doi.org/10.1016/j.compositesb.2005.04.001.

[47] Luo CJ, Wightman R, Meyerowitz E, Smoukov SK. A 3-dimensional fibre scaffold as an investigative tool for studying the morphogenesis of isolated plant cells. BMC Plant Biol 2015;15:1–15. https://doi.org/10.1186/s12870-015-0581-7.

[48] Hanselka H, Herrmann AS, Prömper E. Automobil-Leichtbau durch den Einsatz von

(biologisch abbaubaren) Naturfaser-Verbundwerkstoffen. VDI Bericht 1235 (1995)," Neue Werkstoffe Im Automob 1995:159–85.

[49] Wool RP. Hurricane-Resistant Houses from Soybean Oil and Natural Fibers. Bio-Based Polym Compos 2005:448–82. https://doi.org/10.1016/B978-012763952-9/50013-7.

[50] Opportunities in Natural Fiber Composites. Las Colinas: 2011.

[51] Ahmad F, Choi HS, Park MK. A review: Natural fiber composites selection in view of mechanical, light weight, and economic properties. Macromol Mater Eng 2015;300:10–24. https://doi.org/10.1002/mame.201400089.

[52] Bledzki A. Composites reinforced with cellulose based fibres. Prog Polym Sci 1999;24:221–74. https://doi.org/10.1016/S0079-6700(98)00018-5.

[53] Wambua P, Vangrimde B, Lomov S, Verpoest I. The response of natural fibre composites to ballistic impact by fragment simulating projectiles. Compos Struct 2007;77:232–40. https://doi.org/10.1016/j.compstruct.2005.07.006.

[54] Da Luz FS, Monteiro SN, Lima ES, Lima ÉP. Ballistic application of coir fiber reinforced epoxy composite in multilayered armor. Mater Res 2017;20:23–8. https://doi.org/10.1590/1980-5373-MR-2016-0951.

[55] Etherington T. The versatile bamboo. Non-Wood News 2007;14.

[56] Mohammed L, Ansari MNM, Pua G, Jawaid M, Islam MS. A Review on Natural Fiber Reinforced Polymer Composite and Its Applications. Int J Polym Sci 2015;2015. https://doi.org/10.1155/2015/243947.

[57] Li Y, Mai Y-W, Ye L. Sisal fibre and its composites: a review of recent developments. Compos Sci Technol 2000;60:2037–55. https://doi.org/10.1016/S0266-3538(00)00101-9.

[58] Xiao Z, Zhao L, Xie Y, Wang Q. Review for development of wood plastic composites. J Northeast For Univ 2003;31:39–41.

[59] Omrani E, Menezes PL, Rohatgi PK. State of the art on tribological behavior of polymer matrix composites reinforced with natural fibers in the green materials world. Eng Sci Technol an Int J 2016;19:717–36. https://doi.org/10.1016/j.jestch.2015.10.007.

[60] Liu X, Cheng L. Influence of plasma treatment on properties of ramie fiber and the reinforced composites. J Adhes Sci Technol 2017;31:1723–34. https://doi.org/10.1080/01694243.2016.1275095.

[61] Luo S, Netravali AN. Mechanical and thermal properties of environment-friendly "green" composites made from pineapple leaf fibers and poly(hydroxybutyrate-co-

valerate) resin. Polym Compos 1999;20:367–78. https://doi.org/10.1002/pc.10363.

[62] Djafari Petroudy SR. Physical and mechanical properties of natural fibers. Elsevier Ltd; 2016. https://doi.org/10.1016/B978-0-08-100411-1.00003-0.

[63] Cristaldi G, Latteri A, Recca G, Cicala G. Composites Based on Natural Fibre Fabrics. 2010.

[64] Cook JG. Handbook of textile fibres. 1968.

[65] Cai Y, David SK, Pailthorpe MT. Dyeing of jute and jute/cotton blend fabrics with 2:1 pre-metallised dyes. Dye Pigment 2000;45:161–8. https://doi.org/10.1016/S0143-7208(00)00019-X.

[66] Faruk O, Bledzki AK, Fink HP, Sain M. Biocomposites reinforced with natural fibers: 2000-2010. Prog Polym Sci 2012;37:1552–96. https://doi.org/10.1016/j.progpolymsci.2012.04.003.

[67] Jabbar A. Sustainable Jute/Based Composite Materials: Mechanical and Thermomechanical Behaviour. 2017.

[68] Yan L, Chouw N, Jayaraman K. Flax fibre and its composites – A review. Compos Part B Eng 2014;56:296–317. https://doi.org/10.1016/j.compositesb.2013.08.014.

[69] Lu Y, Weng L, Cao X. Morphological, thermal and mechanical properties of ramie crystallites - Reinforced plasticized starch biocomposites. Carbohydr Polym 2006;63:198–204. https://doi.org/10.1016/j.carbpol.2005.08.027.

[70] A. Ajith Kumar K, S. Sreekala M, Arun S. Studies on Properties of Bio-Composites from Ecoflex/Ramie Fabric-Mechanical and Barrier Properties. J Biomater Nanobiotechnol 2012;03:396–404. https://doi.org/10.4236/jbnb.2012.33039.

[71] Das S. Jute composite and its applications. Int Work IJSG, Indian Jute Ind 2009.

[72] Alves C, Ferrao PMC, Silva AJ, Reis LG, Freitas M, Rodrigues LB, et al. Ecodesign of automotive components making use of natural jute fiber composites. J Clean Prod 2010;18:313–27. https://doi.org/10.1016/j.jclepro.2009.10.022.

[73] Ammayappan L, Nayak LK, Ray DP, Das S, Roy a. K. Functional Finishing of Jute Textiles—An Overview in India. J Nat Fibers 2013;10:390–413. https://doi.org/10.1080/15440478.2013.824849.

[74] Kozłowski RM. Handbook of Natural Fibres. vol. 1. Elsevier Ltd; 2012.

[75] Awais H, Nawab Y, Amjad A, Anjang A, Md Akil H, Zainol Abidin MS. Effect of comingling techniques on mechanical properties of natural fibre reinforced cross-ply thermoplastic composites. Compos Part B Eng 2019;177:107279. https://doi.org/10.1016/j.compositesb.2019.107279.

[76] Raghavendra G, Ojha S, Acharya SK, Pal SK. Jute fiber reinforced epoxy composites and comparison with the glass and neat epoxy composites. J Compos Mater 2014;48:2537–47. https://doi.org/10.1177/0021998313499955.

[77] M.Tausif, T.Cassidy, I.Butcher. Yarn and thread manufacturing methods for high-performance apparel. In: McLoughlin O, Sabir T, editors. High-Performance Appar., Woodhead Publishing Series in Textiles; 2018, p. 33–73. https://doi.org/https://doi.org/10.1016/C2015-0-01391-0.

[78] Hari PK. Types and properties of fibres and yarns used in weaving. Woven Text Princ Technol Appl 2012:3–34. https://doi.org/10.1533/9780857095589.1.3.

[79] Grishanov S. Structure and properties of textile materials. Handb Text Ind Dye Princ Process Types Dye 2011;1:28–63. https://doi.org/10.1533/9780857093974.1.28.

[80] Wilson J. Fibres, yarns and fabrics: fundamental principles for the textile designer. Text Des 2011:3–30. https://doi.org/10.1533/9780857092564.1.3.

[81] Cook JG. Handbook of textile fibres. 1968.

[82] Linen Traits - Ulster Linen 2021. https://ulsterlinen.com/.

[83] Lord PR. Handbook of yarn production. 2003. https://doi.org/10.1533/9781855738652.

[84] Xia Z, Wang X, ye W, xu W, Zhang J, Zhao H. Experimental Investigation on the Effect of Singeing on Cotton Yarn Properties. Text Res J 2009;79:1610–5. https://doi.org/10.1177/0040517508099389.

[85] Asghar MA, Imad A, Nawab Y, Hussain M, Saouab A. Effect of yarn singeing and commingling on the mechanical properties of jute / polypropylene composites. Polym Compos 2020:1–14. https://doi.org/10.1002/pc.25868.

[86] Crosky A, Soatthiyanon N, Ruys D, Meatherall S, Potter S. 9 - Thermoset matrix natural fibre-reinforced composites. Woodhead Publishing Limited; 2014. https://doi.org/http://dx.doi.org/10.1533/9780857099228.2.233.

[87] Tamboli SM, Mhaske ST, Kale DD. Crosslinked polyethylene. Indian J Chem Technol 2004;11:853–64. https://doi.org/10.1021/cen-v032n014.p1392.

[88] Polypropylene Fiber: Properties, Uses, Products, Structure 2020. https://rilonfibers.com/.

[89] Balkan O, Demirer H, Ezdeşir A, Yildirim H. Effects of welding procedures on mechanical and morphological properties of hot gas butt welded PE, PP, and PVC sheets. Polym Eng Sci 2008;48:732–46. https://doi.org/10.1002/pen.21014.

[90] Shubhra QT, Alam A, Quaiyyum M. Mechanical properties of polypropylene composites. J Thermoplast Compos Mater 2013;26:362–91.

https://doi.org/10.1177/0892705711428659.

[91] Zampaloni M, Pourboghrat F, Yankovich S a., Rodgers BN, Moore J, Drzal LT, et al. Kenaf natural fiber reinforced polypropylene composites: A discussion on manufacturing problems and solutions. Compos Part A Appl Sci Manuf 2007;38:1569–80. https://doi.org/10.1016/j.compositesa.2007.01.001.

[92] Yao SS, Jin FL, Rhee KY, Hui D, Park SJ. Recent advances in carbon-fiber-reinforced thermoplastic composites: A review. Compos Part B Eng 2018;142:241–50. https://doi.org/10.1016/j.compositesb.2017.12.007.

[93] Mallick PK. Thermoplastics and thermoplastic-matrix composites for lightweight automotive structures. Mater. Des. Manuf. Light. Veh., Woodhead Publishing Limited; 2010, p. 174–207. https://doi.org/10.1533/9781845697822.1.174.

[94] Pickering KL, Efendy MGA, Le TM. A review of recent developments in natural fibre composites and their mechanical performance. Compos Part A Appl Sci Manuf 2016;83:98–112. https://doi.org/10.1016/j.compositesa.2015.08.038.

[95] Dilfi K.F. A, Balan A, Bin H, Xian G, Thomas S. Effect of surface modification of jute fiber on the mechanical properties and durability of jute fiber-reinforced epoxy composites. Polym Compos 2018;39:E2519–28. https://doi.org/10.1002/pc.24817.

[96] Ashik KP, Sharma RS. A Review on Mechanical Properties of Natural Fiber Reinforced Hybrid Polymer Composites. J Miner Mater Charact Eng 2015;03:420–6. https://doi.org/10.4236/jmmce.2015.35044.

[97] Hussain M, Imad A, Saouab A, Kanit T, Nawab Y, Herbelot C, et al. Properties and characterization of novel 3D jute reinforced natural fibre aluminium laminates. J Compos Mater 2020. https://doi.org/10.1177/0021998320980044.

[98] Bonten C, Haberstroh E. Processing of Plastics into Structural Components. Polym. Sci. A Compr. Ref. 10 Vol. Set, vol. 10, Elsevier; 2012, p. 355–68. https://doi.org/10.1016/B978-0-444-53349-4.00271-5.

[99] Pratap B, Gupta RK, Yadav A, Nag M. Plastic injection molding and its process parameters. AIP Conf Proc 2020;2273. https://doi.org/10.1063/5.0024291.

[100] Mathur RN. Design Considerations for Successfully Using Long Fiber Thermoplastic Composites as Substitutes for Metals. Plast Inc 2016:8.

[101] Santulli C, Sarasini F, Puglia D, Kenny JM. 8 Injection moulding of plant fibre composites. Adv Compos Mater Prop Appl 2017:420–39. https://doi.org/10.1515/9783110574432-008.

[102] Li J, Yang S, Xu F, Jiang S. Properties and Structure of Fiber-Reinforced Injection-

Molded Part. MATEC Web Conf 2016;67:1–5. https://doi.org/10.1051/matecconf/20166706057.

[103] Mohan M, Ansari MNM, Shanks RA. Review on the Effects of Process Parameters on Strength, Shrinkage, and Warpage of Injection Molding Plastic Component. Polym -Plast Technol Eng 2017;56:1–12. https://doi.org/10.1080/03602559.2015.1132466.

[104] Spohn W. from the SAGE Social Science Collections . Downloaded All Rights. Eur J Soc Theory 2001;4:499–508.

[105] Thermoforming Temperature Measurement With the Pyromini 2021. www.calex.co.uk.

[106] Yallew TB, Kassegn E, Aregawi S, Gebresias A. Study on effect of process parameters on tensile properties of compression molded natural fiber reinforced polymer composites. SN Appl Sci 2020;2:1–8. https://doi.org/10.1007/s42452-020-2101-0.

[107] Ramakrishnan KR, Le Moigne N, De Almeida O, Regazzi A, Corn S. Optimized manufacturing of thermoplastic biocomposites by fast induction-heated compression moulding: Influence of processing parameters on microstructure development and mechanical behaviour. Compos Part A Appl Sci Manuf 2019;124:105493. https://doi.org/10.1016/j.compositesa.2019.105493.

[108] Jaafar J, Siregar JP, Tezara C, Hamdan MHM, Rihayat T. A review of important considerations in the compression molding process of short natural fiber composites. Int J Adv Manuf Technol 2019:3437–50. https://doi.org/10.1007/s00170-019-04466-8.

[109] Rokbi M, Khaldoune A, Sanjay MR, Senthamaraikannan P, Ati A, Siengchin S. Effect of processing parameters on tensile properties of recycled polypropylene based composites reinforced with jute fabrics. Int J Light Mater Manuf 2020;3:144–9. https://doi.org/10.1016/j.ijlmm.2019.09.005.

[110] Memon A, Nakai A. Fabrication and mechanical properties of jute spun yarn/PLA unidirection composite by compression molding. Energy Procedia 2013;34:830–8. https://doi.org/10.1016/j.egypro.2013.06.819.

[111] Saenz-Castillo D, Martín MI, Calvo S, Rodriguez-Lence F, Güemes A. Effect of processing parameters and void content on mechanical properties and NDI of thermoplastic composites. Compos Part A Appl Sci Manuf 2019;121:308–20. https://doi.org/10.1016/j.compositesa.2019.03.035.

[112] Medina L, Schledjewski R, Schlarb AK. Process related mechanical properties of press molded natural fiber reinforced polymers. Spec Issue 12th Eur Conf Compos Mater ECCM 2006 2009;69:1404–11. https://doi.org/10.1016/j.compscitech.2008.09.017.

[113] Xie J, Wang S, Cui Z, Wu J. Process optimization for compression molding of carbon fiber-reinforced thermosetting polymer. Materials (Basel) 2019;12:1–13. https://doi.org/10.3390/ma12152430.

[114] Lebaupin Y, Chauvin M, Hoang TQT, Touchard F, Beigbeder A. Influence of constituents and process parameters on mechanical properties of flax fibre-reinforced polyamide 11 composite. J Thermoplast Compos Mater 2017;30:1503–21. https://doi.org/10.1177/0892705716644669.

[115] Schledjewski R, Medina L, Lahm M, Jungmann H. Thermoset Bonded Natural Fiber Prepregs a New Approach for an Eco-Composite. ECCM, 2004, p. 102–3.

[116] Michaud V, Törnqvist R, Månson J-AE. Impregnation of Compressible Fiber Mats with a Thermoplastic Resin. Part II: Experiments. J Compos Mater 2001;35:1174–200. https://doi.org/10.1177/002199801772662280.

[117] Schweizer RA. Glass fiber length degradation in thermoplastics processing. Polym Plast Technol Eng 1982;18:81–91. https://doi.org/10.1080/03602558208067712.

[118] Kunc V, Frame B, Nguyen BN, Tucker CL, Velez-Garcia G. Fiber length distribution measurement for long glass and carbon fiber reinforced injection molded thermoplastics. SPE Automot Compos Div - 7th Annu Automot Compos Conf Exhib ACCE 2007 - Driv Perform Product 2007;2:866–76.

[119] Lee DJ. Comparison of mechanical properties of compression and injection molded PEEK/carbon fiber reinforced composites. Key Eng Mater 2006;306-308 II:751–6. https://doi.org/10.4028/www.scientific.net/kem.306-308.751.

[120] Awais H, Nawab Y, Amjad A, Anjang A, Akil H, Zainol MS. Composites Part C : Open Access Environmental benign natural fibre reinforced thermoplastic composites : A review. Compos Part C Open Access 2021;4:100082. https://doi.org/10.1016/j.jcomc.2020.100082.

[121] Ameer MH, Nawab Y, Ali Z, Imad A, Ahmad S. Development and characterization of jute/polypropylene composite by using commingled nonwoven structures. J Text Inst 2019;110:1652–9. https://doi.org/10.1080/00405000.2019.1612502.

[122] Weiss R. Fabrication techniques for thermoplastic composites. Cryogenics (Guildf) 1991;31:319–22.

[123] Holbery J, Houston D. Natural-fiber-reinforced polymer composites in automotive applications. Jom 2006;58:80–6. https://doi.org/10.1007/s11837-006-0234-2.

[124] de Arcaya PA, Retegi A, Arbelaiz A, Kenny JM, Mondragon I. Mechanical properties of natural fibers/polyamides composites. Polym Compos 2009;30:257–64.

https://doi.org/10.1002/pc.20558.

[125] Joseph K, Mattoso LHC, Toledo RD, Thomas S, Carvalho LH de, Pothen L, et al. Natural fiber reinforced thermoplastic composites. Nat Polym Agrofibers Compos 2000;159:159–201.

[126] Khondker OA, Ishiaku US, Nakai A, Hamada H. A novel processing technique for thermoplastic manufacturing of unidirectional composites reinforced with jute yarns. Compos Part A Appl Sci Manuf 2006;37:2274–84. https://doi.org/10.1016/j.compositesa.2005.12.030.

[127] Pinto M, Chalivendra VB, Kim YK, Lewis AF. Improving the strength and service life of jute/epoxy laminar composites for structural applications. Compos Struct 2015. https://doi.org/10.1016/j.compstruct.2015.10.005.

[128] Friedrich K. Commingled yarns and their use for composites 1999:81–9. https://doi.org/10.1007/978-94-011-4421-6_12.

[129] Bernet N, Michaud V, Bourban PE, Månson JAE. Commingled yarn composites for rapid processing of complex shapes. Compos - Part A Appl Sci Manuf 2001;32:1613–26. https://doi.org/10.1016/S1359-835X(00)00180-9.

[130] Miller AH, Dodds N, Hale JM, Gibson AG. High speed pultrusion of thermoplastic matrix composites. Compos Part A Appl Sci Manuf 1998;29:773–82. https://doi.org/10.1016/S1359-835X(98)00006-2.

[131] Thermoplastic composites from commingled yarn 2021. https://www.comfil.biz/.

[132] Choi B-D, Diestel O, Offermann P. Commingled CF/PEEK Hybrid Yarns for Use in Textile Reinforced High Performance Rotors. 12th Int Conf Compos Mater 1999:796–806.

[133] Awais H, Nawab Y, Anjang A, Akil HM, Zainol Abidin MS. Effect of fabric architecture on the shear and impact properties of natural fibre reinforced composites. Compos Part B Eng 2020:108069. https://doi.org/10.1016/j.compositesb.2020.108069.

[134] Morshed MM, Alam MM, Daniels SM. Plasma treatment of natural jute fibre by RIE 80 plus plasma tool. Plasma Sci Technol 2010;12:325–9. https://doi.org/10.1088/1009-0630/12/3/16.

[135] Tserki V, Zafeiropoulos NE, Simon F, Panayiotou C. A study of the effect of acetylation and propionylation surface treatments on natural fibres. Compos Part A Appl Sci Manuf 2005;36:1110–8. https://doi.org/10.1016/j.compositesa.2005.01.004.

[136] Haque MM, Hasan M, Islam MS, Ali ME. Physico-mechanical properties of chemically treated palm and coir fiber reinforced polypropylene composites. Bioresour

Technol 2009;100:4903–6. https://doi.org/10.1016/j.biortech.2009.04.072.

[137] Jute yarn count pounds per spyndle - Manufacturing of jute yarns: An overview of Spinning & Weaving Features 2021. https://sargodhajute.com/.

[138] Sargodha Jute Mills Limited 2021. https://sargodhajute.com/.

[139] Del Río JC, Rencoret J, Marques G, Li J, Gellerstedt G, Jesús JB, et al. Structural characterization of the lignin from jute (corchorus capsuiaris) fibers. J Agric Food Chem 2009;57:10271–81. https://doi.org/10.1021/jf900815x.

[140] Physiol JPB, Macmillan CP, Birke H, Bedon F, Pettolino FA. Plant Biochemistry & Physiology Lignin Deposition in Cotton Cells – Where is the lignin ? 2013;1:2–5. https://doi.org/10.4172/jpbp.1000e106.

[141] USTER®. Description of all quality parameters measured by Uster Technologies fiber and yarn testing equipment 2010;3:10–3.

[142] Li D (Xuedong). Fundamental of fibers. 2020. https://doi.org/10.1016/b978-0-12-820039-1.00003-1.

[143] Saiman MP, Wahab MS, Wahit MU. Proceedings of the International Colloquium in Textile Engineering, Fashion, Apparel and Design 2014 (ICTEFAD 2014). Proc Int Colloq Text Eng Fash Appar Des 2014 (ICTEFAD 2014) 2014;2014:25–9. https://doi.org/10.1007/978-981-287-011-7.

[144] Hussain M, Imad A, Saouab A, Kanit T, Nawab Y, Herbelot C, et al. Properties and characterization of novel 3D jute reinforced natural fibre aluminium laminates. J Compos Mater 2021;55:1879–91. https://doi.org/10.1177/0021998320980044.

[145] Nawab Y, Legrand X, Koncar V. Study of changes in 3D-woven multilayer interlock fabric preforms while forming. J Text Inst 2012.

[146] Boussu F. The use of warp interlock fabric inside textile composite protection against ballistic impact. Text Res J 2011;81:344–54. https://doi.org/10.1177/0040517510385170.

[147] Vaidya AS, Vaidya UK, Uddin N. Impact response of three-dimensional multifunctional sandwich composite. Mater Sci Eng A 2008;472:52–8. https://doi.org/10.1016/j.msea.2007.03.064.

[148] Campbell FC, editor. Manufacturing Processes for Advanced Composites. 2003.

[149] ASTM D2344M-16. Standard Test Method for Short-Beam Strength of Polymer Matrix Composite Materials and Their Laminates. vol. 00. 2016. https://doi.org/10.1520/D2344.

[150] Takagi H, Nakagaito A, Liu K. Natural fiber composites with low thermal

conductivity. 8th Aust. Congr. Appl. Mech. (ACAM, 2014), as Part Eng. Aust. Conv., 2014, p. 883–7.

[151] ImageJ 2021. https://www.imagej.nih.gov/.

[152] Feng T, Qin J, Shao Y, Jia L, Li Q, Hu Y. Size-controlled transparent jute fiber for replacing transparent wood in industry production area. Coatings 2019;9:1–12. https://doi.org/10.3390/coatings9070433.

Résumé

Cette thèse porte sur une étude expérimentale visant à analyser le couplage entre les proécdés d'élaboration et les propriétés mécanique des bio-composites à base de fibres en jute et du Polypropylène (Jute/PP). Une nouvelle technique a été développée dans le cadre de ce travail. Il s'agit d'un processus basé sur la réalisation des fils co-torsadés Jute/PP qui servent à la fabrication de tissus 2D et 3D. Ainsi, les composites sont fabriqués à l'aide d'une presse à chaud par compression. Cette méthode contribue à améliorer la qualité de fabrication des biocomposites à base de fibres naturelles en minimisant les défauts d'imprégnation. Pour évaluer cet apport, plusieurs essais mécaniques standardisés ont été rélaisés : des essais monotones de traction, de flexion et de cisaillement et des essais dynamiques du type Charpy. Les résultats on été compares à ceux obtenus par une technique alternant un tissu de jute et une feuille de matrice en polypropylene. Tous les résultats montrent que les biocomposités réalisés par la nouvelle technique des fils co-torsadés présentent une tenue mécanique meilleure par rapport à la seconde méthode.

En effet, la fabrication de composites utilisant la technique des fils co-torasdés jute/PP entraîne une bonne imprégnation du renfort au niveau des fibres, ce qui conduit à une meilleure adhérence entre la matrice et les fibres. On note que les niveaux de l'énergie d'impact Charpy et de la valeur maxiamle de la charge obtenues pour les biocomposites fabriqués avec des fils co-torsadés sont nettement supérieures et démontrent bien que cette technique améliore notablement la qualité de l'adhrérence Fibres de jute/PP. Aussi, des observations microscopiques ont été effectuées sur des échantillons testés pour vérifier et analyser les modes de dommage pour les différents biocomposites analysés dans cette étude. Cette nouvelle technique de fabrication des biocomposites à base de fibres naturelles a été améliorée en ajustant les paramètres opératoires à savoir la pression et la température.

Mots Clés: Propriétés Mécaniques, fibre de jute, technique de thermoformage, fils co-torsadés, composite thermoplastique

Abstract

This thesis focuses on an experimental study aimed at analyzing the coupling between the production processes and the mechanical properties of bio-composites based on jute fibers and Polypropylene (Jute / PP). A new technique has been developed as part of this work. It is a compression hot press based on the commingling of Jute/PP co-twisted threads that are used to manufacture 2D and 3D fabrics. Thus, composites are manufactured using a compression hot press. This method helps to improve the manufacturing quality of biocomposites based on natural fibers by minimizing impregnation defects. To assess this properties, several standardized mechanical tests were carried out: monotonic tensile, bending and shear tests and dynamic tests of the Charpy type. The results were compared to those obtained by a conventional technique based on a jute fabric and a polypropylene matrix sheet. All the results show that the biocomposities achieved by the new technique of commingled yarn have a better mechanical resistance compared to the second method.

Indeed, the manufacture of composites using the technique of jute /PP commingled yarns results in a good impregnation of the reinforcement at the fiber level, which leads to a better adhesion between the matrix and the fibers. It is noted that the levels of the Charpy impact energy and the maximum load value obtained for biocomposites manufactured with commingling technique are significantly higher and demonstrate that this technique significantly improves the quality of the adhesion Jute/PP fibers. Also, microscopic observations were made on samples tested to verify and analyze the damage modes for the different biocomposites analyzed in this study. This new technique for manufacturing biocomposites based on natural fibres has been improved by adjusting the operating parameters of pressure and temperature.